Differential Modulation of Spinal Nociceptive Processing by Aspirin-triggered Resolvin D1 in Rat Pain Models

Pongsatorn Meesawatsom, BPharm

Thesis submitted to the University of Nottingham for the Degree of Doctor of Philosophy

School of Life Sciences
University of Nottingham Medical School
Queen's Medical Centre

November 2017

Abstract

Harnessing the actions of the resolvin pathways has the potential for the treatment of a wide-range of conditions associated with overt inflammatory signalling. Aspirin-triggered resolvin D1 (AT-RvD1) is a potent anti-inflammatory lipid derived from docosahexaenoic acid (DHA). In rodent, the biological effects of AT-RvD1 are mainly mediated by its specific G-protein coupled receptor, formyl peptide receptor 2 (ALX/FPR2). AT-RvD1 has been demonstrated potent anti-inflammatory and tissue resolution promoting (pro-resolving) activities in preclinical model of inflammatory diseases.

Continuous peripheral activity of nociceptive fibres induces neuroinflammatory responses and alters the excitability neurones in both peripheral and central pain pathways. This thesis focused on spinal neuroinflammation which plays important roles in the sensitisation of nociceptive processing of the spinal dorsal horn neurones and contributes to the nociceptive hypersensitivity of the central pain pathway in acute and chronic pain. Since AT-RvD1 possess a potent anti-inflammatory activity, therefore, enhancing AT-RvD1 signalling in the spinal cord may attenuate the spinal nociceptive sensitisation and provide analgesia. AT-RvD1 also has robust antinociceptive effects in behavioural models of pain, however the potential underlying spinal neurophysiological mechanisms contributing to these inhibitory effects *in vivo* are yet to be determined.

The purposes of this thesis were to investigate the differential effects of spinal AT-RvD1 on evoked responses of spinal neurones *in vivo* in well characterised pain models include carrageenan-induced acute inflammatory pain, monosodium iodoacetate (MIA)-induced OA pain and paclitaxel (PCX)-induced peripheral neuropathic pain and to investigate the alterations in the expression of spinal genes relevant

to the resolvin system and neuroinflammation that may underlie the differential effects of AT-RvD1 among these pain models.

Following model induction, pain behaviour was assessed and then rats were prepared for single unit extracellular recordings of dorsal horn wide dynamic range (WDR) neurones on the following day post carrageenan or day 28-32 post MIA or PCX induction. At the time-matched the spinal recording, ipsilateral dorsal quadrants of spinal cord form separate groups of rats were collected for gene expression quantification using TaqMan® Low Density Arrays (TLDA).

AT-RvD1 clearly demonstrated differential inhibition on evoked responses of WDR neurones in the pain models of interest. Low dose AT-RvD1 (15 ng/50ul) selectively produced a robust inhibition of electrical-evoked responses (Aδ-, C-fibre, post-discharge, input, wind-up) of WDR neurones in carrageenan rats but not in control rats. These effects were abolished by spinal pre-administration of a FPR2/ALX antagonist, butoxy carbonyl-Phe-Leu-Phe-Leu-Phe (BOC-2) (50 μg/50μl). In MIA rats, AT-RvD1 given at a high dose (150 ng/50ul) produced only mild inhibition of electrical evoked Aδ responses but not at a low dose (15 ng/50ul). AT-RvD1 (15 and 150 ng/50ul) had no significant effects on electrical evoked responses of PCX rat WDR neurones. Interestingly, AT-RvD1 produced a dose dependent and selective inhibition of low intensity mechanical evoked responses PCX rats whereas it had no effects in control rats. At high dose (150 ng/50ul), the magnitude of inhibition of 8g mechanical evoked responses was comparable to morphine (1 ug/50ul) applied at the end of the experiments. AT-RvD1 produced a dose dependent inhibition of acetone-evoked responses in PCX rats, however WDR neurones in the control rats were also inhibited to a similar degree.

TLDA revealed the distinct alteration of resolvin genes in spinal cord underpinning the differential inhibition of AT-TvD1. Upregulated 5-lipoxygenase activating protein (FLAP) gene, encoding protein determining endogenous resolvin synthesis, in carrageenan and PCX

rats may underlie the robust inhibition of AT-RvD1 on WDR neurones in these two models. The minimal effects AT-RvD1 of MIA rats were associated with upregulated 15-hydroxyprostaglandin dehydrogenase (15-HPGD) gene, encoding a major enzyme responsible for D-series resolvin inactivation. Data presented in this thesis provide for the first time the differential inhibition of AT-RvD1 on spinal nociceptive processing in different types of pain and the evidence of heterogeneous spinal alterations of the resolvin signalling potentially underlie such inhibition. This thesis strongly supports further investigation of AT-RvD1 as a novel analgesic.

Another part of this thesis demonstrated changes in the responses of spinal WDR neurones in PCX rats. Spinal WDR neurones from PCX rats displayed characteristics representing pain sensitisation including: reduced the thresholds for Aβ and C-fibre responses; increased proportion of neurones exhibiting spontaneous activity, acetone responsiveness and post-discharge following low intensity mechanical stimuli and a more convergence in stimulus processing. A remarkable upregulation of multiple genes in proinflammatory signallings, toll-liked receptor 4 (Tlr4), interleukin-1β (Nlrp1a) and tumour necrosis factor-α receptors (Tnfrsf1a and Tnfrsf1b) and chemokines (Cxcl6, Cxcr1, Cxcr5, Ccr1, Cx3cr1), was found in the spinal cord of PCX rats. This suggests that a high inflammatory component in the spinal cord could contribute to the changes in the responses of spinal WDR neurones in the PCX rats. This thesis supports further investigation of targeting neuroinflammation as a promising approach for the treatment of PCX-induced neuropathic pain.

Publications

Research article

Meesawatsom P, Burston J, Hathway G, Bennet A, Chapman V. (2016). Inhibitory effects of aspirin-triggered resolvin D1 on spinal nociceptive processing in rat pain models. *Journal of Neuroinflammation* 13(1): 233.

Xu L, Nwosu LN, Burston JJ, Millns PJ, Sagar DR, Mapp PI, **Meesawatsom P**, Li L, Bennett AJ, Walsh DA, Chapman V. (2016) The anti-NGF antibody muMab 911 both prevents and reverses pain behaviour and subchondral osteoclast numbers in a rat model of osteoarthritis pain. *Osteoarthritis and Cartilage* 24(9):1587-95.

Abstracts

Meesawatsom P, Burston J, Hathway G, Bennet A, Chapman V. Inhibitory effects of Aspirin-triggered resolvin D1 on spinal pain transmission in acute inflammatory pain (2015). Abstract, The International Cannabinoid Research Society; The ICRS2015 Symposium on the Cannabinoids; Wolfville, Canada.

Meesawatsom P, Burston J, Hathway G, Bennet A, Chapman V. (2016). Differential modulation of spinal nociceptive processing by aspirin-triggered resolvin D1 in rat pain models. Abstract, International Association for the Study of Pain, The 16th World Congress on Pain, Yokohama, Japan.

Meesawatsom P, Hathway G, Chapman V (2016). Electrophysiological characterisation of dorsal spinal neuronal responses and the inhibitory effect of aspirin-triggered resolvin D1 in paclitaxel-induced peripheral neuropathy in rats. Abstract, British Pharmacological Society; Annual Meeting, London, UK.

Acknowledgements

I would like to thank my supervisor Professor Victoria Chapman for her excellent supervision throughout my PhD study. I deeply appreciate her endless encouragement and patience. Without her guidance I would not achieve this far. I would also like thank Dr Gareth Hathway, my co-supervisor, who is always full of ideas and provides me different points of view and motivation. My appreciation also extend to Dr Andrew Bennet for his technical support for the molecular work.

Being immersed in this laboratory has been a great experience in my life. Special thanks goes to the former post-docs, Devi Sagar who made me the sense of ephys and James Burston, Mr. Yes, who gave me both academic and emotional support. It has been such a pleasant time to work around amazing labmates, Pete, James S, Andreza, Suvik, Lilian, Adrian, Junting, Tracy, Andy, Emma, Amanda, Lydia, Steve and others I cannot name them all here. I would also like to thank my family for the support and giving me this strength to pass any difficult tasks I have encountered.

I would like to acknowledge Faculty of Pharmacy Mahidol University and Ministry of Science and Technology, Royal Thai Government for giving me the opportunity and funding.

TABLE OF CONTENTS

Chapter 1 General Introduction 1

1.1. An introduction to pain 2

1.2. Peripheral pain processing 3

1.2.1. Primary afferent fibres 3

1.2.1. Ion channels detecting painful stimuli 4

1.2.1. Voltage-gated ion channels in pain conduction 7

1.2.2. Dorsal root ganglion (DRG) 9

1.3. Spinal pain processing 10

1.3.1. Organisation of the dorsal horn 10

1.3.2. Spinal pain transmission 12

1.3.3. Descending pain pathways 16

1.4. Sensitisation of nociceptive pathways under pathological conditions 18

1.4.1. Peripheral sensitisation 18

1.4.2. Central sensitisation 22

1.4.3. Mechanisms of spinal neuroinflammation and contributions to facilitation of nociceptive processing 25

1.5. Resolvins 31

1.5.1. Biosynthesis, metabolism and action of resolvins 34

1.5.1. AT-RvD1 37

1.6. Aim of the thesis 41

Chapter 2 General experimental methods 42

2.1 Animals 43

2.2 Pain model induction 45

2.2.1 Carrageenan model of acute hind paw inflammatory pain 45

2.2.2 Monosodium iodoacetate model of knee arthritic pain 46

2.2.3 Paclitaxel model of chemotherapy-induced peripheral neuropathic pain 47

2.3 Pain behavioural testing 48

2.3.1 Weight bearing asymmetry 48

2.3.2 Mechanical paw withdrawal threshold 49

2.3.3 Nocifensive behaviour evoked by acetone..... 49
2.3.4 Paw withdrawal latency (PWL) evoked by radiant heat50
2.4 *In vivo* single unit spinal electrophysiology..... 50
2.4.1 Equipment for electrophysiology 53
2.4.2 Production of glass-insulated microelectrodes 56
2.4.3 Induction and maintenance of general anaesthesia.... 62
2.4.4 Tracheal cannulation and laminectomy..... 62
2.4.5 Searching for spinal wide dynamic range (WDR) neurones..... 63
2.4.6 Assessing thresholds for C- and Aβ fibre-evoked responses..... 66
2.4.7 Quantification of WDR neurone responses 66
2.4.8 Choice of general anaesthetic 71
2.5 Pharmacological intervention on spinal neurones 71
2.6 Macroscopic assessment of pain pathology..... 72
2.6.1 Paw circumference 72
2.6.2 Macroscopic scoring of knee joint cartilage pathology 73
2.7 Methods for studying of spinal gene expression in pain models 77
2.7.1 Fresh tissue collection..... 77
2.7.2 RNA extraction form fresh tissues using phase separation method 79
2.7.3 RNA extraction form fresh tissues using Direct-Zol® RNA MiniPrep kit 79
2.7.4 Determination of quality and quantity of extracted total RNA 80
2.7.5 Reverse transcription of extracted RNA to cDNA..... 80
2.7.6 Principle of quantitative polymerase chain reaction.... 82
2.8 General statistical analysis..... 82
Chapter 3 *In vivo* investigation of Effects of aspirin-triggered resolvin D1 on spinal Nociceptive processing in Carrageenan-induced acute inflammatory pain.....84
3.1. Introduction..... 85

3.2. Study hypothesis and objectives 88
3.3. Methods 88
3.3.1 Carrageenan-induced inflammatory pain 88
3.3.2 *In vivo* spinal electrophysiology 89
3.3.3 Spinal drug applications 89
3.3.4 Gene expression study 90
3.4. Results 93
3.4.1 Carrageenan mediated hindpaw inflammation resulted in alterations in WDR neuronal responses 93
3.4.2 Spinal AT-RvD1 inhibited responses of WDR neurones in the carrageenan model of hindpaw inflammation 98
3.4.3 Investigating functional roles of FPR2/ALX receptor in spinal cord following overt peripheral inflammation and effects on AT-RvD1 action 101
3.4.4 The impact of peripheral inflammation on the spinal expression of the resolvin receptors and related enzymatic pathways 106
3.5. Discussion 109
3.5.1 The chosen time points for evaluation of the effect of AT-RvD1in inflammatory pain 109
3.5.2 Alteration of WDR neurone responses after carrageenan induction 109
3.5.3 AT-RvD1 selectively inhibits spinal pain processing in inflammatory pain via FPR2/ALX receptor activation 110
3.5.4 Inhibitory effects of AT-RvD1 accompanies altered gene expression in resolvin system 112
Chapter 4 Effects of aspirin-triggered resolvin D1 on spinal Nociceptive processing in monosodium iodoacetate-induced arthritic pain 117
4.1. Introduction 118
4.2. Study Hypothesis and objectives 123
4.3. Methods 123
4.3.1. Animal preparations 123

4.3.2. *In vivo* spinal electrophysiology 124
4.3.3. Spinal drug applications 124
4.4. Results 124
4.4.1. MIA induces pain behaviour and OA pathology 124
4.4.2. AT-RvD1 had minimal effect on WDR neuronal responses in the MIA model 125
4.5. Discussion 131
4.5.1. Validity of the chosen MIA dose and timepoint preforming electrophysiology 131
4.5.2. Comparison of AT-RvD1 to its precursor 17R-HDHA in the MIA model 133
Chapter 5 Electrophysiological characterisation of spinal WDR neuronal responses and the inhibitory effect of aspirin triggered resolvin D1 in paclitaxel-induced peripheral neuropathic pain 137
5.1 Introduction 138
5.2 Study hypotheses and objectives 140
5.3 Methods 141
5.3.1 Animals 141
5.3.2 *In vivo* spinal electrophysiology 142
5.3.3 Spinal drug applications 142
5.3.4 Specific statistical analysis 143
5.4 Results 143
5.4.1 Established paclitaxel-induced CIPNP 143
5.4.2 Baseline characteristics and physiological properties of spinal WDR neurones 146
5.4.3 Correlation of pain behaviour and responses of spinal WDR neurones 151
5.4.4 Correlation of electrical and mechanical evoked responses of spinal WDR neurones 155
5.4.5 Effects of AT-RvD1 on evoked responses of spinal WDR neurones 157
5.5 Discussion 166

5.5.1 Evoked responses of spinal WDR neurones characterised under isoflurane anaesthesia 167
5.5.2 PCX alters physiological properties of spinal WDR neurones..... 168
5.5.3 Spinal AT-RvD1 inhibits evoked responses of WDR neurones in PCX rats 172
Chapter 6 Investigating Spinal Expression of genes relevant to resolvin system and neuroinflammation in rat pain models 177
6.1 Introduction..... 178
6.2 Study hypothesis and objectives..... 180
6.3 Methods 180
6.3.1 Animals and tissue preparation methods 181
6.3.2 Relative quantification of spinal mRNA expression using TLDA 183
6.3.3 Statistical analyses and interpretation of data from TLDA 191
6.4 Results 197
6.4.1 Pain behaviour..... 197
6.4.2 ΔCT with multiple reference genes was chosen to analyse the TDLA data..... 199
6.4.3 Global changes: overview..... 203
6.4.4 Resolvin system 203
6.4.5 Pro-inflammatory cascades..... 207
6.4.6 Anti-inflammatory cascades..... 213
6.4.7 Glial markers 215
6.4.8 Markers for central sensitisation..... 217
6.4.9 Chemokines and chemokine receptors 219
6.5 Discussion 225
6.5.1 Methods of analysing TLDA data affect the significant mRNAs found..... 225
6.5.2 Distinct changes of resolvin system in pain models.. 227

6.5.3 Profound spinal neuroinflammation in the PCX model is associated with central sensitisation 234
6.5.4 PCX-induced neuropathic pain is associated with a dramatic shift in spinal mRNA expression of multiple chemokine families 237
6.5.5 Anti-inflammatory roles of SOCS2 and PPAR-γ in PCX model 242
6.5.6 Site of the input and area of the spinal cord in the MIA study 243
Chapter 7 General discussion.....244
7.1 Summary of key findings 246
7.2 PCX-model is associated with profound spinal neuroinflammation 248
7.3 Potential underlying mechanisms of the differential inhibition of AT-RvD1 in pain models 252
7.4 Comparison of AT-RvD1 and morphine 255
7.5 Reduced morphine sensitivity in chronic pain models 257
7.6 Limitations 257
7.7 Future directions 260
Conclusion 262
References.....263

Chapter 1 GENERAL INTRODUCTION

1.1.An introduction to pain

Pain has been defined by the International Association for the Study of Pain as "an unpleasant sensory and emotional experience associated with actual or potential tissue damage, or described in terms of such damage" (IASP, 1979). Pain is a protective mechanism that alerts living organisms to avoid harmful environments. However, severe pain can be debilitating and chronic pain can result in disabilities. Chronic pain is a major clinical problem worldwide. The estimated prevalence of chronic pain in adults is 20% in Europe (Breivik *et al.*, 2006) and 33% in the low-income and middle-income countries (Jackson *et al.*, 2015), and up to 56% in the elderly (Jackson *et al.*, 2015). In addition, chronic pain is highly associated with psychiatric comorbidities such as depression (21%) (Breivik *et al.*, 2006), anxiety (20%) (Rosemann *et al.*, 2007) and insomnia (11-40%)(Tang *et al.*, 2007).

Peripheral activation of primary afferent fibres triggers a series of neuronal processes leading to the sensation of pain. General processes of pain sensation comprise the processes of transduction, conduction, transmission and perception. Transduction is the conversion of a noxious thermal, mechanical or chemical stimulus into electrical activity in the peripheral terminals of nociceptive sensory fibre. This process is mediated by numerous receptor and ion channels expressed on the peripheral nerve endings. Conduction is the passage of action potentials from the peripheral terminal along axons to dorsal root ganglion and then to the dorsal horn of spinal cord. Transmission is the synaptic transfer of the input from peripheral sensory fibres to the second order neurones in the dorsal horn. Perception is the sensory and emotional experience once the nociceptive information reaches higher brain centres e.g. somatosensory cortex, anterior cingulate cortex, amygdala, etc. Spinal pain transmission can be modulated by descending pathways originating from the brain e.g. periaqueductal grey and rostral

ventromedial medulla. All of these processes can be altered during chronic pain. A better understanding of the changes within the pain pathway following chronic pain will facilitate the development of novel analgesics. This thesis particularly explores the alterations at the spinal level where the sensory input is transmitted from the peripheral nervous system and extensively modulated by various neural circuits.

1.2.Peripheral pain processing

With their peripheral terminals located in outlying tissues, the primary nociceptive neurones transduce and transmit nociceptive input from these sites to the dorsal horn of spinal cord. Several receptors and ion channels play important roles in these process in the physiological state and their activity can be modulated in chronic (pathological) pain states. Some of well-established ion channels are brought into focus here. Temperature-gated and ligand-gated ion channels are essential in transducing noxious stimuli into depolarising currents. Other groups of ion channels are voltage-gated which are essential for action potential propagation through dorsal root ganglion terminating the dorsal horn of spinal cord.

1.2.1.Primary afferent fibres

Primary afferent fibres (PAF) that carry sensory input can be classified into 3 main following categories as shown in **Table 1.1.**

Table 1.1 Types of primary afferent fibres and their characteristics. (West *et al.*, 2015)

	Myelination	Conduction velocity	Diameter
Aβ fibres	thickly myelinated	Fast 30-100	> 10 um
Aδ fibres	thinly myelinated	Intermediate 12–30 m/sec	2-6 um
C-fibres	unmyelinated	Slow 0.5–2 m/sec	0.4-1.2 um

Aβ fibres have the fastest conduction velocity and are responsible for carrying non-noxious input like touch, low intensity temperature and proprioception. Detection of those sensory input is mediated by specialised peripheral nerve endings e.g. Pacinian corpuscle, Merkel disk and Meissner corpuscle. Aδ fibres have a relatively high threshold for activation by nociceptive mechanical and thermal stimuli and are thought to mediate sharp and well localised pain. There are 2 types of A-fibres that respond to pain (A-fibre nociceptor), Type I and Type II which have distinct stimulus responses, electrophysiological and anatomical characteristics (Treede *et al.*, 1995) as shown in **Table 1.2**.

Table 1.2 Comparison of Type I and Type II A-fibre nociceptors. (Treede *et al.*, 1995)

	Type I	Type II
Cutaneous area found	Glabrous skin	Glabrous and hairy skin
Heat activation threshold	~53°C	~46°C
Conduction velocity	~25 /sec	~15 m/s
Peak responses post-stimulus	Several sec	~1-3 sec
Response latency	Several sec	~120 msec
Threshold following intense heat 53°C	Decrease	Increase

C-fibres are unmyelinated, thus, have slow conduction velocity. C-fibres predominantly mediate dull, diffuse, aching, or burning pain. C-fibres contribute 60–90% of all afferent fibres from the skin and the majority of afferent fibres from the internal organs. Peripheral C-fibre terminals are free nerve endings that respond to damaging or potentially damaging stimuli, so called nociceptors. Nociceptors are equipped with ion channels which respond to thermal, mechanical, and chemical nociceptive stimuli, and are therefore polymodal in nature.

1.2.1. Ion channels detecting painful stimuli

Several types of receptor are found at free nerve endings of primary sensory afferent neurones, as shown in **Figure 1.1**. Most of the receptors responsible for detecting acute tissue-damaging stimuli function as nonselective cation ion channels allowing the influx of sodium (Na^+) and calcium (Ca^{2+}).

Figure 1.1 Principle receptors expressed by peripheral terminal of nociceptive fibre that recognise noxious stimuli. Based on Ringkamp et al., 2013.

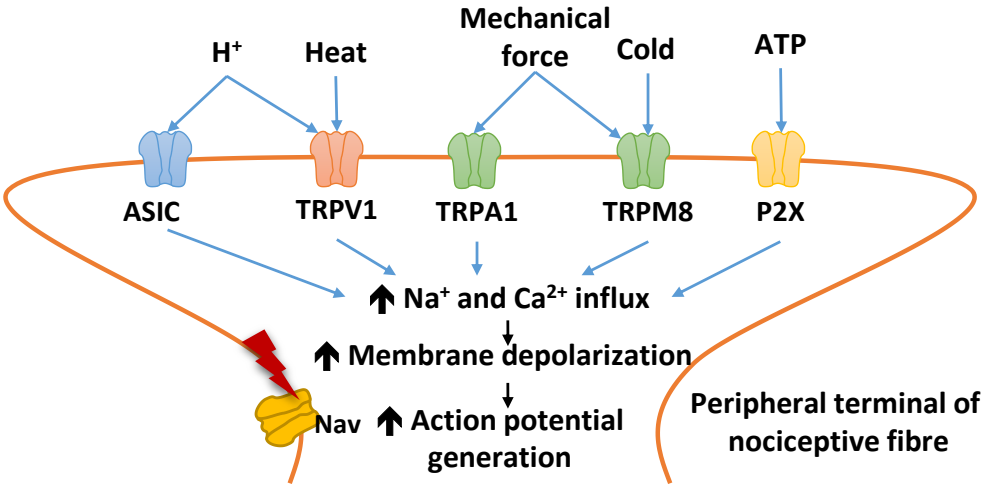

1.2.1.1. Transient receptor potential (TRP) ion channels

TRP ion channels are a vast family of temperature-activated transient receptor potential ion channels. They serve as primary detectors of thermal stimuli in the peripheral nervous system. More than 10 TRP subtypes have been described (Clapham *et al.*, 2001). These channels exhibit distinct thermal activation thresholds: $>43^0$C for TRPV1; $>52^0$C for TRPV2; >34-38^{0}C for TRPV3; >27-35^{0}C for TRPV4; <25-28^{0}C for TRPM8; $<17^0$C for TRPA1(Tominaga *et al.*, 2004). TRPV1 is probably the best characterised TRP with a well characterised role in peripheral pain transduction. TRPV1 normally responds to intense heat over 43^0C, which has the potential to cause

tissue damage. TRPV1 is also activated by low pH <5.9 (Tominaga *et al.*, 1998) and capsaicin (Caterina *et al.*, 1997), and is therefore polymodal. It is a nonselective channel, however the ion of preference is Ca^{2+}(Caterina *et al.*, 1999).

TRPA1 is also activated by many irritants e.g. isothiocyanates (in horseradish, mustard), cinnamaldehyde (in cinnamon) and allicin (in garlic)(Patapoutian *et al.*, 2009). TRPA1 was initially found to be a candidate receptor for noxious cold (Kwan *et al.*, 2006; Story *et al.*, 2003). However, it is still debated since subsequent studies (de Oliveira *et al.*, 2014; Zhou *et al.*, 2013) showed some disagreement with the early studies. TRPV1 and TRPA1 are co-localised on peptidergic DRG neurones (Bautista *et al.*, 2005).

TRPM8, a receptor for menthol and non-noxious and noxious cold, is distinctly expressed by a subpopulation of primary sensory neurones not expressing TRPV1, calcitonin gene-related peptide (CGRP), neurofilament150, or isolectin B4 binding (Peier *et al.*, 2002). TRPM8 is expressed in both Aδ- and C-fibres expressing the receptor tyrosine kinase TrkA, and TRPA1 (Kobayashi *et al.*, 2005). TRPM8 is required for many aspects of cold sensations, including non-noxious (Colburn *et al.*, 2007; Knowlton *et al.*, 2013) and noxious cold (Dhaka *et al.*, 2007; Knowlton *et al.*, 2013). TRPM8 sensitisation has been found in cold allodynia in models of neuropathic pain (Proudfoot *et al.*, 2006; Su *et al.*, 2011; Xing *et al.*, 2007). Acute activation of TRPM8, by cooling or by application of agonists of TRPM8 such as menthol, paradoxically causes cooling analgesia (Dhaka *et al.*, 2007; Knowlton *et al.*, 2013; Proudfoot *et al.*, 2006).

1.2.1.2. Acid-sensing ionic channels (ASICs)

The acid-sensing ionic channel (ASIC) superfamily is composed of sodium channels that are blocked by amiloride, also known as amiloride-sensitive epithelial sodium channels (ENaCs). ASICs (Proudfoot *et al.*, 2006)by protons, an important part of the

inflammatory response (Dawes *et al.*, 2013a). Six subtypes of ASICs have been described, ASIC1a, 1b, 2a, 2b, 3 and 4 (Wemmie *et al.*, 2013). The activation of ASICs by pH is generally below 6.9, a threshold not very distant from physiological pH values. At sites of inflammation, tissue pH values can drop to 5.5 (Lardner, 2001), which is sufficient to activate ASICs. Almost all ASIC subtypes are expressed by primary sensory neurones. ASIC1, ASIC2, and ASIC3 are largely expressed in the small and medium DRG neurones (Ugawa *et al.*, 2005) that mainly respond to noxious chemical, thermal, and high threshold mechanical stimuli (Lingueglia, 2007). ASIC1b and ASIC3 are also expressed in large DRG neurones (Ugawa *et al.*, 2005) that mainly respond to low threshold mechanical stimuli (Lingueglia, 2007).

1.2.1.3. Purinergic P2X receptors

Adenosine triphosphate (ATP) is a potent algogenic agent. Local application of ATP elicited vascular changes in human skin and also caused a persistent sensation of pain (Hamilton *et al.*, 2000). ATP released from damaged or inflamed tissues can interact with P2X receptors expressed on primary afferent neurones (Dawes *et al.*, 2013a; Xiang *et al.*, 1998). P2X receptors function as nonselective cation channels permeable to Ca^{2+} and Na^{+}. Three P2X subtypes have been implicated in pain mechanisms (including P2X3, P2X4 and P2X7), which are expressed by neurones and glial cells in both peripheral and central nervous systems (Donnelly-Roberts *et al.*, 2008).

1.2.1. Voltage-gated ion channels in pain conduction

1.2.1.1. Voltage gated sodium channels

Activation of nonselective cation channels, including TRPs, ASICs and P2X receptors, on the peripheral nerve ending trigger membrane depolarization. These lead to the activation of voltage-gated sodium

channels (VGSCs or Nav) and the generation of action potentials. These action potentials are propagate along the axons to central nerve terminals located in the spinal dorsal horn. There are nine different voltage-gated sodium channels (Nav1.1 to Nav1.9) (Wood *et al.*, 2004). Among these the subtypes are preferentially expressed by nociceptive fibres at relatively high levels include Nav1.7 (Djouhri *et al.*, 2003b; Rush *et al.*, 2006), Nav1.8 (Djouhri *et al.*, 2003a) and Nav1.9 (Fang *et al.*, 2002). These Nav subtypes have different contributions to the excitability of the neurones; NaV1.9 plays a role in setting the resting membrane potential and contributes to continuous firing activity during sustained depolarisations (Momin *et al.*, 2008); NaV1.7 is an important determinant in setting the threshold for generation of action potentials; Nav 1.8 is likely to contribute to continuous firing activity during sustained depolarisations (Momin *et al.*, 2008; Waxman *et al.*, 2014).

In human, single gene mutation of NaV1.7 has been linked to monogenic pain disorders. Genetic mutations of *SCN9A* which encodes the pore-forming (α_1) subunit of NaV1.7 impacts the channel function. In human, the gain-of-function of NaV1.7 by the missense mutations of *SCN9A* (T2573A and T2543C) have been linked to primary erythermalgia, a rare autosomal dominant disease characterised by intermittent burning pain with redness and heat in the extremities (Yang *et al.*, 2004). On the other hand, *SCN9A* nonsense mutations (S459X, I767X and W897X) has been found causing loss-of-function of NaV1.7 and linked to congenital inability to experience pain (Cox *et al.*, 2006).

1.2.1.2. Voltage-gated potassium channels

Voltage-gated potassium channels (VGKC or Kv) are a diverse class of heterotetrameric ion channels, more than 20 subtypes have been described (Alexander *et al.*, 2017; Gutman *et al.*, 2003). Since there are a number of Kv subtypes, it is not surprising that the distribution profile of Kv subtypes in peripheral afferent fibres is complicated, and

they display different distributions in somata, peripheral terminals and tubes which have been extensively reviewed elsewhere (Tsantoulas *et al.*, 2014a). In contrast to Nav1.8 and 1.9, that are selectively located upon nociceptive fibres, nociceptive specific VGKCs have not been identified. The most important function of VGKCs to mention here is Kv conduction typically responsible for repolarisation and inhibit the action potential generation, Kv activity generally inhibits sensory neuron excitability (Busserolles *et al.*, 2016). Kv2.1 is expressed in the vast majority of medium–large neurons and more than half of small nociceptors. (Tsantoulas *et al.*, 2012; Tsantoulas *et al.*, 2014b). Kv9.1 is selectively expressed in myelinated sensory neurons. Since Kv2.1 is also found in the majority of C-fibre neurones (Tsantoulas *et al.*, 2014b) and blocking Kv2.1 augments sensory neurone excitability by allowing greater repeated firing during sustained input (Tsantoulas *et al.*, 2014b) suggesting that Kv2.1 functions as an excitability brake of C-fibre neurones.

1.2.2. Dorsal root ganglion (DRG)

DRG is where the somata of peripheral sensory neurones reside. In addition, other cell types are found in DRG e.g. satellite glial cells and macrophages. DRG neurones can be divided into several subtypes based in their neurochemistry, anatomy and physiology.

Histochemical markers have been used to differentiate primary afferent neurones. Large and medium sized A-fibre neurones express heavy chain neurofilament 200 kDa (Lawson *et al.*, 1984). More recently Toll-like receptor 5 (TLR5) has found to be co-expressed with neurofilament-200 in large-diameter A-fibre neurones (Xu *et al.*, 2015). Medium to large-diameter A-fibre neurones also express transient receptor potential V2 (TRPV2)(Tamura *et al.*, 2005). Some medium sized A-fibre neurones express CGRP which are high threshold mechanosensitive, therefore a type of nociceptor (Djouhri *et al.*, 2004).

Small diameter DRG neurones possessing unmyelinated axons can be divided into 2 main categories based on being neuropeptide positive or negative (Ringkamp *et al.*, 2013). In rats, 50% of C-fibre- and 20% of Aδ fibres (McCarthy *et al.*, 1989) are classified as peptidergic, constitutively expressing neuropeptides such as calcitonin gene-related peptide (CGRP), substance P and may also other neuropeptides(Ju *et al.*, 1987). Many of these peptidergic DRG neurones also express TRPV1 and TRPA1. The second subgroup identified are neurones that express surface carbohydrates (α-D galactose groups of glycol conjugates) that bind the plant lectin isolectin B4 (IB4) from *Griffonia simplicifolia (Alvarez et al., 1991)*. Unlike peptidergic DRG neurones, IB4 neurones do not express neuropeptide CGRP and SP or only express them at low levels (Kashiba *et al.*, 2001) but some IB4 neurones do express other neuropeptide e.g. somatostatin (Michael *et al.*, 1999). IB4 neurones selectively express several distinct molecular markers: purinergic receptor P2X3; bradykinin B1 receptor; TRPC3; Mas-related G protein coupled receptor D (Mrgprd) (reviewed in (Priestley, 2009; Ringkamp *et al.*, 2013). TRPV1 is also expressed by the majority of IB4 neurones. Peptidergic and non- peptidergic DRG neurones innervate distinct central pathways that predominantly mediate sensory (ventral posterior lateral/medial hypothalamus and parabrachial nucleus projections) and affective (amygdala and bed nucleus of the stria terminalis projections) components of pain (Braz *et al.*, 2005).

1.3.Spinal pain processing

1.3.1.Organisation of the dorsal horn

The spinal dorsal horn is the first site of the central nervous system receiving sensory information from the peripheral nervous system. The spinal cord is divided into 10 laminae based on Rexed's definition using cytoarchitectonic (Rexed, 1952). Of these, 5 laminae of the

dorsal horn are distinctly innervated by different primary afferent fibres in a highly organised fashion (Todd *et al.*, 2013), shown as a schematic representation in **Figure 1.2**. The superficial laminae (lamina I and II) are the main termination sites for nociceptive Aδ and C-fibres. Lamina I also contain second order neurones which specifically respond nociceptive stimuli, so called nociceptive specific (NS) neurones which receive input from peptidergic C-fibres. Lamina II, also known as substantia gelatinosa, is divided into 2 sublaminae; the outer part (laminar IIo) receive mixed input from both peptidergic and non-peptidergic C-fibres, and the inner part (laminar IIi) receive input from non-peptidergic C-fibres. The deeper laminae (lamina III and VI) mainly receive sensory input from low threshold Aβ fibres. The superficial and also the deeper laminae are innervated with Aδ fibres. In the deeper lamina, especially lamina V is where the wide dynamic range (WDR) neurones are most concentrated. Unlike NS neurones in the superficial laminae, WDR neurones receive input from all 3 fibre types and respond to a wide range of stimuli from low to intensity mechanical, thermal and chemical stimuli (Dostrovsky *et al.*, 2013).

Figure 1.2 Schematic representation of organisation of dorsal horn laminae and termination sites of different primary sensory fibres. Modified from Todd et al., 2013 and D'Mello et al., 2008

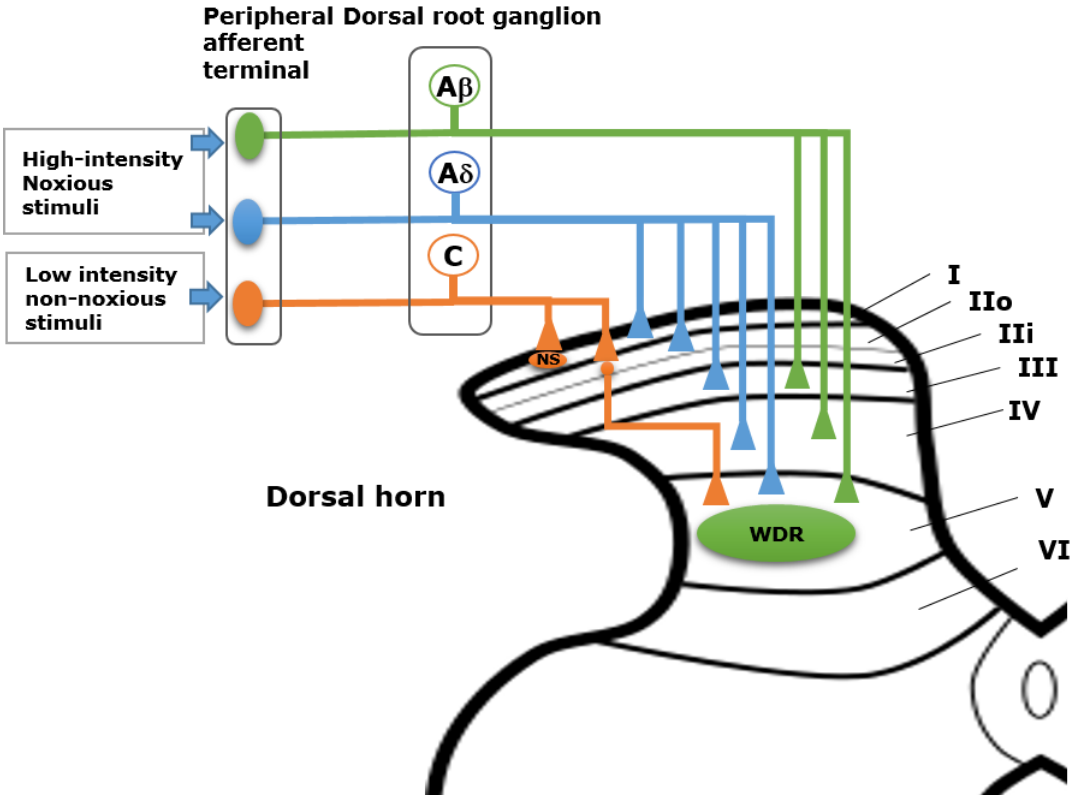

NS= nociceptive specific neurone, WDR=wide dynamic range neurone.

1.3.2. Spinal pain transmission

The nociceptive signal is relayed from the central terminal of primary afferent fibres to second order neurones in the dorsal horn via chemical transmission as shown in **Figure 1.3**.

1.3.2.1. Voltage-gated calcium channels

Voltage-gated calcium channels (VGCC or Cav) are essential for the neurotransmitter release from the central terminals of primary afferent fibres in the dorsal horn. Here, the depolarisation-induced opening of voltage-gated calcium channels results in the release of

neurotransmitters, including glutamate, CGRP and substance P, from the primary afferent fibre terminals (**Figure 1.3**). VGCCs are composed of multiple subunits: $\alpha 1$, β, γ, and $\alpha 2\delta$. The $\alpha 1$ subunit forms the calcium-permeable pore and the other subunits modulate the kinetics of the $\alpha 1$ subunit. VGCCs are classified into 9 subtypes based on the amino acid sequence of the $\alpha 1$ subunit, Cav1.-Cav1.4, Cav2.1-Cav2.3 and Cav3.1-Cav3.3 (Catterall *et al.*, 2005). Cav2.2, also known as N-type calcium channel, is highly concentrated in neurones and the N-type channel has a major role in controlling synaptic transmission in pain pathways (Park *et al.*, 2010).

The $\alpha 2\delta$ subunit is probably considered as the most important auxiliary subunit of VGCC. This subunit plays important role in mediating spinal plasticity during chronic pain especially neuropathic pain. Previous studies has shown that $\alpha 2\delta$ subunit protein level was upregulated in the DRGs and/or the dorsal spinal cords in rodent models of neuropathic pain e.g. sciatic nerve chronic constricting injury, spinal nerve transection, or ligation, and neuropathy induced by streptozotocin-induced diabetes or vincristine (Luo *et al.*, 2002). The $\alpha 2\delta$ subunit enhances the calcium current mediated by the $\alpha 1$ subunit (Gao *et al.*, 2000), therefore, the spinal nociceptive transmission may be enhanced as a result of its upregulation. The $\alpha 2\delta$ subunit was identified as a molecular target of gabapentinoids e.g. gabapentin and pregabalin, drugs commonly used for the treatment of neuropathic pain as demonstrated by ligand binding assay (Gee et al., 1996), transgenic mice (Field *et al.*, 2006; Patel *et al.*, 2013). Subsequent studies has demonstrated that only prolonged but not acute exposure of gabapentin could inhibit direct block $\alpha 1$ subunit seems unlikely to contribute to their neuronal suppressing effect but the intracellular action (Hendrichet al., 2008). Instead, gabapentinoids have been shown to inhibit axonal trafficking of $\alpha 2$ and also the recycling of calcium channel complexes between intracellular compartments and the synaptic membrane (Bauer *et al.*, 2009; Tran-Van-Minh *et al.*, 2010)

1.3.2.2. Glutamatergic neurotransmission

Glutamate is the principal neurotransmitter released by primary afferent fibres. Glutamate can be co-released with CGRP and substance P (**Figure 1.3**). Upon their Ca^{2+}-dependent exocytosis, these neurotransmitters bind to specific receptors in the dorsal horn, glutamate receptors; N-methyl-d-aspartate (NMDA), α-amino-3-hydroxy-5-methyl-4-isoxazolepropionic acid (AMPA), and metabotropic receptors (mGluR); substance P receptor neurokinin 1 (NK1) and CGRP receptor CGRP1.

NMDA receptors play a pivotal role in dorsal horn nociceptive processing. NMDA receptors are heterotetrameric subunit protein complex foaming ligand-gated ion channels permeable to Ca^{2+} and Na^{+}. Seven subunit have been identified; GluN1, GluN2A, GluN2B, GluN2C, GluN2D, GluN3A and GluN3B (Paoletti *et al.*, 2013). NMDA receptor requires a combination of GluN1, an essential channel-forming subunit, and at least one of the GluN2 subunits. The agonist binding site for glutamate is on the GLuN2 subunits and there is a co-agonist binding site for co-agonist glycine on the GLUN1 subunit. GluN1, GluN2A and GluN2C are possibly the most important subunits expressed in spinal cords and essential in pain processing.

In the resting state, the pore of NMDA receptor is blocked by Mg^{2+}. To unblock the Mg^{2+} plug and activate NMDA receptor requires 1) occupancy of both co-agonist sites and 2) prolonged excitatory post synaptic potentials (EPSPs). C-fibre stimulation can create very long EPSPs because of glutamate and neurokinin receptor mediated components (Liu *et al.*, 1997). Temporal summation of the EPSPs generates sufficient depolarisation required to remove the Mg^{2+} block and permit Na^{+} and Ca^{2+} influx into the neurone, which in turn increases neuronal excitability (Urban *et al.*, 1994). The receptors that are thought to mediate slow modulatory effects and underlie the

prolonged EPSPs include, NK1 receptors (coupled to Gq), and CGRP1 (coupled to Gs) (Latremoliere *et al.*, 2009). These G-protein coupled receptors (GPCRs) are highly expressed in superficial dorsal horn suggesting they are crucial in the sensitisation of spinal neurones.

Following the activation of spinal neurons, nociceptive input is transmitted to the higher brain centres. In the absence of tissue damage, the sensation of pain can be transient. On the other hand, if prolonged activation of nociceptive fibres occurs, activation of dorsal horn neurones is subject to plasticity, manifesting as a progressive increase in the response of the system to repetitive stimuli (see references in (Sandkuhler, 2013)) as discussed below (**section 1.4**).

Figure 1.3 Nociceptive neurotransmission in the spinal dorsal horn. Modified from Luo et al., 2014.

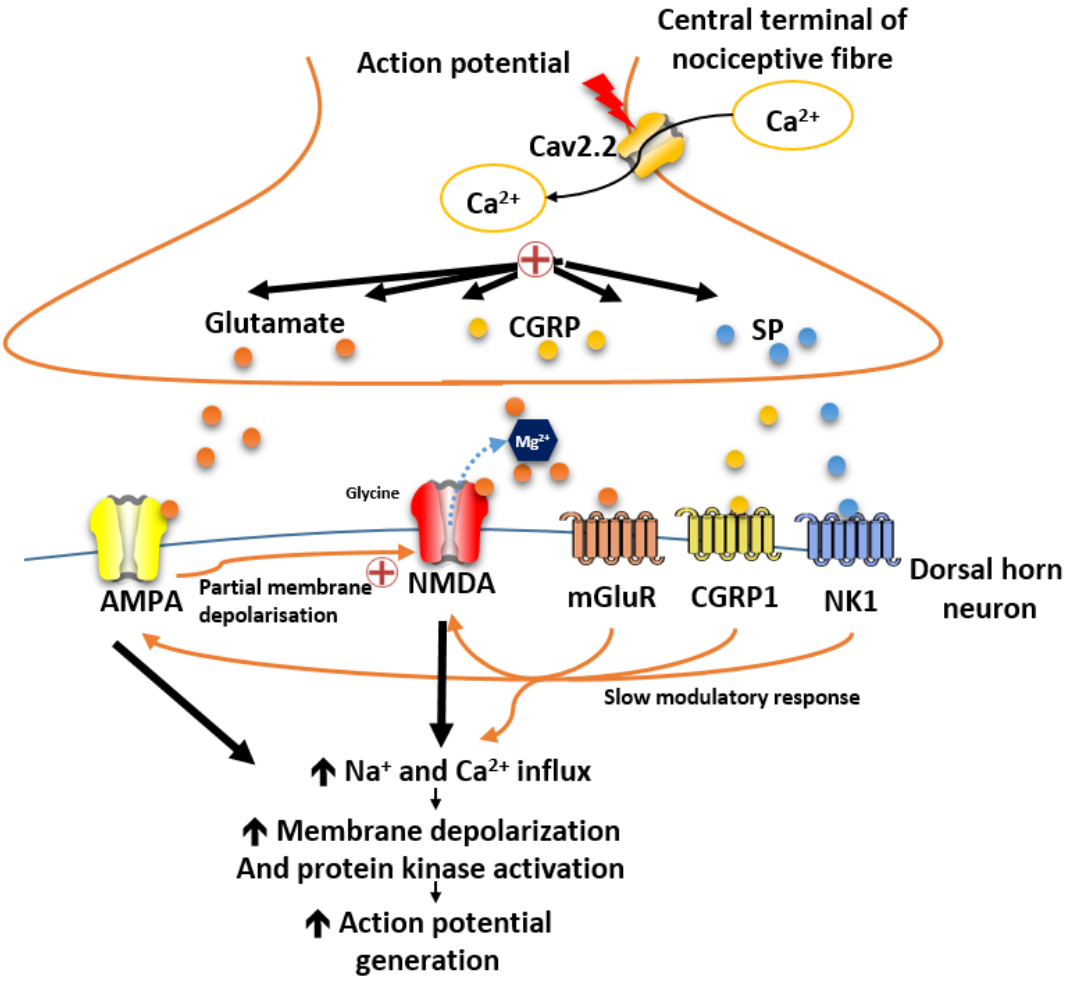

1.3.2.3. Inhibitory circuits in the dorsal horn

Classical inhibitory neurotransmitters γ-aminobutyric acid (GABA) and glycine are also found in dorsal horn interneurons. The vast majority of neurones in laminae I–III are interneurons. In rats, GABA-immunoreactivity is present in ~25%, 30% and 40% of neurones in laminae I, II and III, respectively (Polgar *et al.*, 2003). Glycine is found in similar laminae to GABA, but at high levels in lamina III (Polgar *et al.*, 2003). In addition, it appears that most interneurons containing glycine also contain GABA, suggesting they are co-released (Todd *et al.*, 1996). Activation of GABA and glycine receptors leads to the inhibition of spinal pain transmission since they are coupled with either inhibitory G-protein (Gi) or Cl^- channels, as shown in **Table 1.3**.

The endogenous opioids e.g. enkephalins, dynorphins and endorphins are synthesised in interneurons distributed widely throughout the CNS and are found in laminae I and II of the dorsal horn of the spinal cord. The enkephalinergic interneurons in the dorsal horn produce presynaptic inhibition of primary afferent neurons and postsynaptic inhibition of secondary neurons in ascending pathways. Endogenous opioids bind to several opiate receptor subtypes which coupled with Gi potently hyperpolarise and inhibit pain transmission from primary nociceptive afferents and nociceptive neurones in the dorsal horn of the spinal cord (Dickenson *et al.*, 2013). The major opiate receptor subtypes are μ (mu opioid receptor or MOR), δ (delta opioid receptor or DOR) and κ (kappa opioid receptor or KOR) receptor which are molecular target for classical opioid analgesics such as morphine (Dickenson *et al.*, 2013; Rang *et al.*, 2007).

1.3.3. Descending pain pathways

Spinal dorsal horn output is modulated by descending pathways from several nuclei. The descending pain-inhibitory systems originate in

the periaqueductal grey (PAG) which receives input from many brain regions e.g. central nucleus of amygdala, ventromedial hypothalamus and anterior cingulate cortex and projects to rostroventral medulla (RVM) which release 5-hydroxytryptamine (5-HT or serotonin) (Heinricher *et al.*, 2013). In addition, the PAG and RVM have projections to pontine noradrenergic cell groups A5, A7 and the locus coeruleus (LC) which release norepinephrine (NE). RVM and LC project to the dorsal horn and thereby modulate spinal nociceptive transmission via the release of 5-HT and NE which act on different postsynaptic receptors, as shown in **Table 1.3**. 5-HT receptor activation has bidirectional modulation to either inhibit or facilitate spinal pain transmission depending on the subtypes (Bannister *et al.*, 2017) which are coupled with different signalling pathways as shown in **Table 1.3**.

Table 1.3 Modulatory effects of different receptors on nociceptive fiber-dorsal horn synapses. Based on Sorokin et al., 2013.

Neurotransmitter	Receptor	Signaling	Synaptic transmission after activation
Endogenous opioids	μ, δ and κ	Gi	↓
GABA	$GABA_A$	Ionotropic (Cl^-)	↓
	$GABA_B$	Gi	↓
Glycine	GlyR	Gi	↓
5-HT	$5\text{-}HT_{1A}$	Gi	↓
	$5\text{-}HT_2$	Gq	↑
	$5\text{-}HT_3$	Ionotropic ($Na^+$and Ca^{2+})	↑
	$5\text{-}HT_7$	Gs	↑
NE	α_2	Gi	↓

1.4. Sensitisation of nociceptive pathways under pathological conditions

In pathological pain states such as following tissue injury, there are complex alterations in pain pathway in response to continuous nociceptive activation, mostly in the way that nociceptive inputs are amplified, so called sensitisation. Sensitisation is defined by IASP as "increased responsiveness of nociceptive neurones to their normal input, and/or recruitment of a response to normally subthreshold inputs" (IASP, 1994). This phenomenon can occur at the level of the peripheral nervous and central nervous systems. Clinically the sensitisation may manifest as hyperalgesia (increased pain from a stimulus that normally provokes pain) or allodynia (pain due to a stimulus that does not normally provoke pain)(Woolf, 2011). As part of sensitisation, expansion of the receptive field size (spreading of the area of hypersensitivity) can be found (Arendt-Nielsen *et al.*, 2010; Cook *et al.*, 1987). Mechanisms underlying the increased responsiveness of pain pathway following nociceptor activation are complicated involving time-dependent changes ranging from molecular, cellular and structural levels throughout the peripheral and central nervous systems.

1.4.1. Peripheral sensitisation

Following tissue injury, there are a number of mediators released from injured cells, e.g. cellular contents (H^+ and ATP) from recruited leukocytes e.g. prostaglandins (PGs), bradykinin, histamine, serotonin (5-HT), pro-inflammatory cytokines; tumour necrosis factor (TNF)-α, interleukin (IL)-1β, and IL-6 etc. Protons and ATP are detected by TRPV1/ASIC and P2X receptors, resulting in increases in Ca^{2+} and Na^+ influx into the neurones. Primary afferent fibres not only express those ion channels sensing painful stimuli, but also express a number of membrane receptors (see **Table 1.4**) which are

activated / sensitised by the mediators released during tissue damage (Dawes *et al.*, 2013a). Activation of these receptors induces complex cellular changes leading to the peripheral sensitisation which is defined as "increased responsiveness of nociceptive neurons to their normal input, and/or recruitment of a response to normally subthreshold inputs" (IASP, 1994).

Activation of an array of receptors by pro-inflammatory mediators triggers a series of intracellular signalling pathways to be activated, for example activation of protein kinases (PK) A, PKC and calcium-dependent calmodulin kinase II (CaMKII). These kinases phosphorylate nociceptive ion channels TRPs, ASICs and P2X and also voltage-gated ion channels Nav (**Figure 1.4)**.

Prostaglandins (PGs) are a pivotal group of pro-inflammatory mediators, which are derived from arachidonic acid. Tissue inflammation is associated with a rapid upregulation of cyclooxygenase-2 (COX-2), which increases the local production of prostanoids, especially PGE2 and PGI2. The roles of prostaglandins in peripheral sensitisation is well documented (Marchand *et al.*, 2005; Ren *et al.*, 2010; Samad *et al.*, 2002). In the presence of PGE2 or PGI2, the temperature threshold for TRPV1 activation decreases to below 35°C via a PKA dependent mechanism (Moriyama *et al.*, 2005). Phosphorylation-mediated sensitisation of TRPA1 via PKA (Meents *et al.*, 2017) and PKC (Wang *et al.*, 2008), and ASIC sensitization via PKA (Chai *et al.*, 2007) has been demonstrated. Both activation of PKC or PKA increases Nav-mediated currents (Gold *et al.*, 1998), suggesting increased responsiveness of these channels.

Nerve growth factor (NGF) is produced and released by various non-neuronal cell types present at peripheral sites such as mast cells (Leon *et al.*, 1994) and keratinocytes (Groneberg *et al.*, 2005). Activation of tropomyosin receptor kinase A (TrkA), the high affinity receptor for NGF results potentiates TRPV1-mediated Ca^{+} current via CaMKII and PKC (Bonnington *et al.*, 2003). Prolonged accumulation

of intracellular calcium and activation of TrkA also leads to changes in gene expression in the primary afferent neurones e.g. TRPV1, ASIC3 and bradykinin receptor B2, Nav and substance P (Hefti *et al.*, 2006; Wang *et al.*, 2011). Following peripheral inflammation, TRPV1 upregulation appears to occur at peripheral terminals of primary afferent sensory neurones, leading to pre-synaptic augmentation of glutamatergic transmission in the spinal cord (Lappin *et al.*, 2006). Changes in gene expression could induce further sensitisation and are likely to induce long term changes in the peripheral nervous system resulting chronic pain.

Table 1.4 Pro-inflammatory receptors expressed by peripheral afferent fibres. Based on Dawes *et al.*, 2013.

Receptors	Proinflammatory mediators
EP1-4	Prostaglandin E2
IP2	Prostaglandin I2
BK1 and BK2	Bradykinins
H1	Histamine
5-HT2A	5-HT
TrkA	Nerve growth factor
IL-1RI	Interleukin-1β
IL-6R	Interleukin-6
TNR1, TNFR2	TNF-α

Figure 1.4 Intracellular events leading to peripheral sensitisation of primary afferent fibres. Modified from Marchand *et al*., 2005 and Dawes *et al.*, 2013.

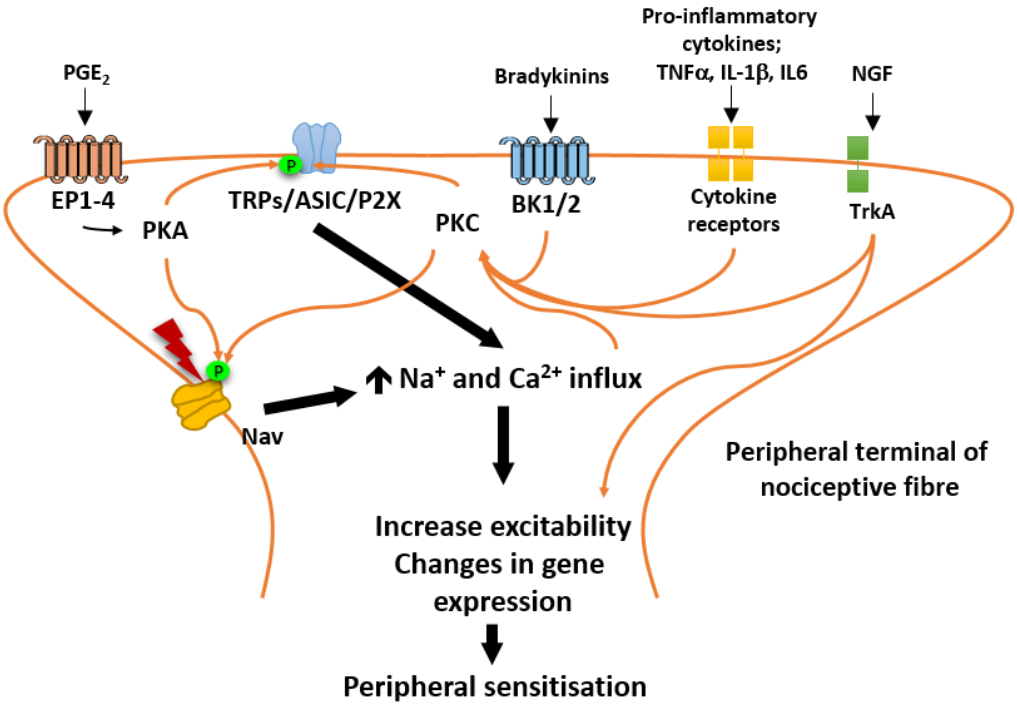

1.4.2. Central sensitisation

Central sensitisation is an enhancement in the functional status of neurones and circuits in the central nociceptive pathway. Central sensitisation is implicated in the manifestations of pain hypersensitivity such as hyperalgesia and allodynia. Primary hyperalgesia is limited to the area of injury and is characterized by enhanced pain to both mechanical and heat stimuli and secondary hyperalgesia occurs in undamaged skin adjacent to the injured tissue and is characterised by enhanced pain, often to mechanical stimuli (Raja *et al.*, 1984; Treede *et al.*, 1992) and also thermal stimuli (Xu *et al.*, 2007). Sensitisation of C-fibres has been implicated as an underlying mechanisms of primary hyperalgesia whereas sensitisation A-fibres in case of secondary hyperalgesia (Hsieh *et al.*, 2015). Blocking of the peripheral sensory fibres using local anaesthetic applied or injected at the primary site has been found did not reverse the pain hypersensitivity in the secondary area both in rodent (Haywood *et al.*, 2018) and human (Torebjork *et al.*, 1992) pain models suggesting that secondary hyperalgesia was not mediated only by peripheral changes. Therefore, secondary hyperalgesia likely depends on the alterations in the central nervous system, particularly in the dorsal horn. Plasticity of the dorsal horn following a nociceptive barrage can be seen at many levels ranging from molecular (e.g. gene/protein expression and protein phosphorylation), functional (e.g. wind-up representing excitability) and structural (e.g. spinal gliosis) levels (Kuner *et al.*, 2017; Latremoliere *et al.*, 2009).

Similar to peripheral sensitisation, activity of ion channels in the dorsal horn neurones particularly NMDA and AMPA receptors can be modulated by numerous receptors expressed by neurones. Previous research has shown that co-activation of NK1 receptor substance P, VGCCs, NMDA receptors and mGluR1 and mGluR5 all contribute to a steep rise in postsynaptic Ca^{2+} levels in lamina I neurones (Ikeda *et*

al., 2003). Again, Ca^{2+} can trigger a series of signal transduction events such as PKA, PKC, CaMKII, and neuronal nitric oxide synthase (nNOS) activation. (Latremoliere *et al.*, 2009). Binding of BDNF to TrkB receptor can increase NR2B NMDA receptor phosphorylation via Src family kinase (Chen *et al.*, 2014). Collectively these signalling pathways ultimately lead to potentiation of AMPA and NMDA receptor-mediated responses, either by phosphorylation of the existing receptors or by recruitment of additional receptors to the cell membrane (Ji *et al.*, 2003; Luo *et al.*, 2014), as summarised in **Figure 1.5**

Figure 1.5 Summary of the major events underlying central sensitisation mechanisms in the dorsal horn of the spinal cord. Modified from Ji et al., 2003 and Luo et al., 2014.

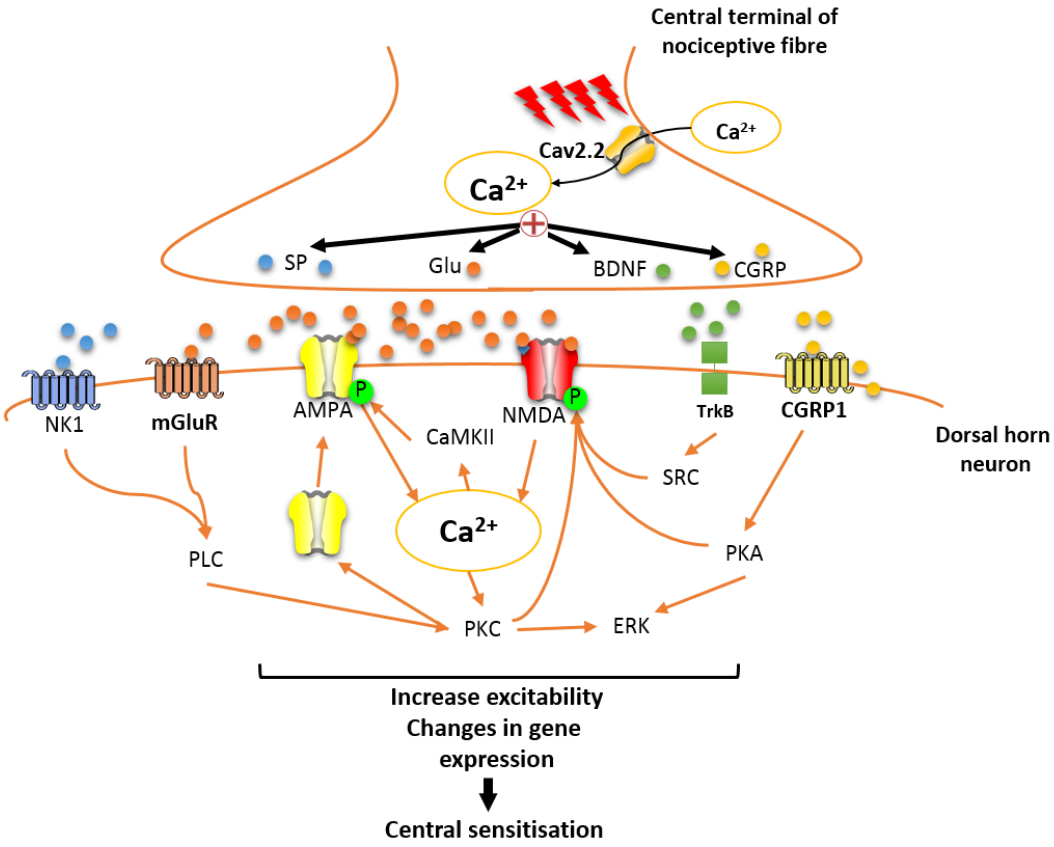

There are two main forms of activity-dependent synaptic plasticity of sensitised dorsal horn neurones following repetitive stimulation, homosynaptic (such as wind-up) and heterosynaptic facilitation.

Wind-up is a form of short-term, reversible homosynaptic activity dependent plasticity whereby only the efficiency of the activated synapse is changed (Latremoliere *et al.*, 2009). Wind-up can be studied electrophysiologically, neuronal discharge is progressively increased following repetitive low-frequency (0.5-5Hz) C-fibre stimulation (Mendell, 1966). Sustained NMDA receptor-mediated excitatory postsynaptic potential following repetitive stimulation thought to be a major underlying mechanism. Blocking of NMDA receptor produce a robust inhibition of mediated by C-fibre wind-up,

but not Aβ-fibre evoked responses (Dickenson *et al.*, 1987), suggesting that wind-up occurs predominantly in nociceptive synapse. Thus wind-up may be considered as a mechanism contributing to the initial early-onset central sensitisation (Ji *et al.*, 2003) and responsible for primary hyperalgesia (Latremoliere *et al.*, 2009).

Heterosynaptic facilitation is an activity-dependent phenomenon in which the activity of the activated synapses augments the subsequent activity of the neighbouring non-activated synapses. The putative mechanisms underlying the spreading of the facilitation are the Group I mGluR receptor-mediated release of Ca^{2+} from the endoplasmic reticulum (Fagni *et al.*, 2000) and the release of nitric oxide which diffuse and activate the downstream signallings (e.g. guanylyl cyclase and PKG) at a distance from the activated synapse (Meller *et al.*, 1993). Heterosynaptic facilitation is responsible for secondary hyperalgesia and allodynia (Latremoliere *et al.*, 2009).

1.4.3. Mechanisms of spinal neuroinflammation and contributions to facilitation of nociceptive processing

Following tissue injury, inflammation may not be limited only at the site of injury but also in the central nervous system. Accumulating evidence suggests that spinal neuroinflammation, which is characterised by activation of glial cells and production of pro-inflammatory mediators in the spinal cord, has an important role in the induction and maintenance of chronic pain.

A classic example of peripheral inflammation-induced spinal neuroinflammation is the rapid increase in COX-2 and microsomal prostaglandin E2 synthase-1 (mPGES-1) expression in the spinal cord a few hours following intra-plantar injection of the inflammogens

complete Freund's type adjuvant (CFA)(Beiche *et al.*, 1996; Hay *et al.*, 1997; Samad *et al.*, 2001) or carrageenan (Guay *et al.*, 2004). COX-2 and mPGEs-1 generate PGE2 in the spinal cord, contributing to inflammatory hyperalgesia and allodynia (Bazan, 2001; Beiche *et al.*, 1996; Guay *et al.*, 2004; Hay *et al.*, 1997; Samad *et al.*, 2001). PKA-dependent phosphorylation following EP2 receptor activation by PGE2 leads to the inhibition of glycine receptor subtype (GlyRα2/3) (Ahmadi *et al.*, 2002; Hosl *et al.*, 2006), which in turn sensitises dorsal horn neurones. There are numerous pro-inflammatory mediators produced within the spinal cord following sustained nociceptive input, including those released from local activated microglia and astrocytes.

1.4.3.1. Microglia and astrocytes

Sustained activation of nociceptive fibres not only induces changes of the excitability of neurones in the dorsal horn, but also the function of the surrounding cells specifically, microglia and astrocytes (Beggs *et al.*, 2013; Milligan *et al.*, 2009; Tawfik *et al.*, 2009). These cells are not quiescent as originally thought, but have a great contribution in the modulation of spinal nociceptive processing. Microglia and astrocytes are activated by glutamate and other mediators released following nociceptive stimulation, central terminals of primary nociceptive fibres release ATP and chemokines such as CCL2 (Van Steenwinckel *et al.*, 2011), CX3CL1 (Zhang *et al.*, 2013b)and CCL21 (Ji *et al.*, 2013). Activated microglia change their shape from ramified to amoeboid and up-regulate microglial markers e.g. CCR3/CD11b, major histocompatibility complex II (MHC II), and ionized calcium-binding adaptor molecule-(IbA1)(Beggs, 2009). Activated astrocytes increase their surface markers such as glial fibrillary acidic protein (GFAP)(Tawfik *et al.*, 2009). Gliopathy could represent a structural change in there spinal cord in response to nociceptive barrage.

Spinal microglia express receptors for ATP (P2X4, P2X7, P2Y6, P2Y12), and chemokines (CX3CR1, CCR2); astrocytes express

receptors for glutamate (AMPA, NMDA, mGluR5), ATP (P2Y1 and P2Y2, 4) (Burnstock, 2008; Ji *et al.*, 2013). Activation of these receptors leads to the activation of nuclear factor (NF)-κB and the enhanced production and release of proinflammatory cytokines (TNF-α and IL-1β), and brain-derived neurotrophic factors (BDNF) (Burnstock, 2008; Grace *et al.*, 2014; Ji *et al.*, 2013). TNF-β, IL-1β and CCL2 are capable of enhancing glutamate release from presynaptic terminals (Gao *et al.*, 2009; Kawasaki *et al.*, 2008). TNF-α also activates p38 MAPK (Jin *et al.*, 2003), ERK (Zhuang *et al.*, 2005) and PKA (Wigerblad *et al.*, 2017) resulting in the phosphorylation sensitisation of AMPA (Wigerblad *et al.*, 2017) and NMDA receptors (Jara *et al.*, 2007). In addition, TNF-α and IL-1β increase surface expression of AMPA subunit GluR1 (Stellwagen *et al.*, 2005), leading to sensitised glutamatergic transmission. BDNF, acting through TrkB receptors, decreases expression of the potassium-chloride cotransporter 2 (KCC2) resulting in a rise in intracellular chloride (Coull *et al.*, 2005). This shift in the neuronal anion gradient attenuates the inhibitory response to GABA or in some cases the response to GABA becomes excitatory rather than inhibitory (Coull *et al.*, 2005). Therefore, BDNF attenuates the intrinsic inhibitory mechanism in the dorsal horn.

Astrocytes play a major role in the reuptake of synaptic glutamate via excitatory amino acid transporters e.g. glutamate transporter-1 (GLT1) and glutamate-aspartate transporter-1 (GLAST) (Gegelashvili *et al.*, 2014). Clearance of synaptic glutamate is also disrupted in activated astrocytes in chronic pain. Animal models of neuropathic pain have shown the down regulation in GLT1 and of GLAST such as neuropathic pain induced by chronic constriction nerve injury (Sung *et al.*, 2003) or by the chemotherapeutic agent paclitaxel (Cata *et al.*, 2006). This can lead to sustained elevation of glutamate concentration in the synaptic cleft and thus contribute to aberrant glutamate transmission.

Evidence suggests distinct profiles in the activation of microglia and astrocytes in animal models of acute and chronic pain. For instance, spinal IbA1 (a marker for microglia) immunofluorescence was increased following paw incision model of acute pain (Romero-Sandoval *et al.*, 2008). In contrast, IbA1 and GFAP (a marker for astrocytes) immunofluorescence were increased in L5 nerve exposure or L5 nerve transection surgery models of neuropathic pain (Romero-Sandoval *et al.*, 2008). In a chemical model of osteoarthritic pain spinal IbA1-positive activated microglia were increased at early time points, and declined at later timepoints, whereas the significant increase in GFAP immunofluorescence was only detected at the late time points (Sagar *et al.*, 2011). Therefore, the patterns of activation of microglia and astrocytes in response to painful stimuli are injury specific and time dependent.

1.4.3.2. Cytokines

Cytokines are small regulatory proteins that are released in a wide variety of cells to modulate cell–cell interaction and other functions especially important for inflammation and immune responses. In the spinal cord, microglia and astrocytes are importance sources of pro-inflammatory cytokines which are produced and released upon the activation of microglia and/or astrocytes.

Major pro-inflammatory cytokines that have been well documented for their role in sensitising spinal pain processing include, TNF-α and IL-β. TNF-α is not expressed by spinal neurones but expressed in DRG neurones (Berta *et al.*, 2014; Schafers *et al.*, 2003). The majority of microglia (>90%) and some astrocytes (40%) express TNF-α (Berta *et al.*, 2014; Xu *et al.*, 2006). Neurones in the dorsal horn express TNF receptor 1 (TNFR1) and TNFR2. Studies in TNFR1- and TNFR2-knockout (KO) mice revealed that heat hyperalgesia after intraplantar injection of CFA was decreased in the early phase in TNFR2-KO mice, but reduced in both the early and later phase in TNFR1-KO mice. Lamina II spinal neurons from TNFR1-KO mice have

attenuated NMDA currents evoked by TNF-α (Zhang *et al.*, 2011). These data suggest distinct roles of TNFR1 and TNFR2, and the greater contribution of TNFR1 in inflammatory pain.

IL-1β is expressed by both spinal microglia (Clark *et al.*, 2010) and astrocytes (Zhang *et al.*, 2005). There are two IL-1 receptors, IL-1 type 1 receptor (IL-1RI) essential for IL-1β signal transduction and IL-1 RII a decoy receptor (Rothwell *et al.*, 2000). Activated IL-1RI recruits adaptor proteins myeloid differentiation primary responses (MyD88), IL-1R-associated kinase-4 (IRAK4) and TNF-receptor-associated factor (TRAF6) which ultimately activate p38 MAPK, ERK and NF-κB (Braddock *et al.*, 2004). IL-1β enhances nociceptive activity in the dorsal horn through some of the same mechanisms as TNF-α discussed above, enhancing neurotransmitter releases from primary afferent fibres (Kawasaki *et al.*, 2008) and NMDA GluN1 subunit phosphorylation (Guo *et al.*, 2007). In addition, IL-1β influences inhibitory neurotransmission by suppressing inhibitory post-synaptic current and GABA- and glycine-induced currents in lamina II spinal neurones (Kawasaki *et al.*, 2008). In addition, IL-1β up-regulates COX-2 in spinal cord which increases the PGE2 production as discussed above (Samad *et al.*, 2001).

The anti-inflammatory cytokine IL-10 also has a role in controlling spinal nociceptive processing. Spinal neurones do not express IL-10 receptors (Ledeboer *et al.*, 2003), which are expressed by microglia and astrocytes (Ledeboer *et al.*, 2002). Intrathecal injection of plasmid DNA encoding for rat interleukin-10 (pDNA-IL-10) produced long lasting reversal of mechanical allodynia in paclitaxel model of neuropathic pain (Ledeboer *et al.*, 2007). The putative mechanism (s) underlying this effect was a blockade of the action of IL-1β (Ledeboer *et al.*, 2007) and possibly other pro-inflammatory mediators released in the spinal cord.

1.4.3.3. Chemokines

Chemokines are a large family of small proteins (8–14 kDa), similar to cytokines, but possess chemotactic activity; more than 50 chemokine ligands and 19 functional receptors have been described (Bachelerie *et al.*, 2014). Chemokines are classified into three main subfamilies: CC, CXC, and CX3C based on the number amino acids present between the first and the second cysteine at the N-terminal (Bachelerie *et al.*, 2014).

Chemokines play crucial role in mediating glial-neurone interactions. All chemokine receptors are 7-transmembrane receptors coupled with various G-proteins (Gs, Gi or Gq) depending on the subtypes to the receptors. Activation of chemokine receptors can activate specific kinase enzymes leading to the sensitisation of dorsal horn neurones. For example CCL2 is synthesised and released by primary neurones and astrocytes and binds to CCR2 on neurones and microglia. CCR2 receptor activation increases spontaneous excitatory postsynaptic currents, NMDA and NMDA-induced current and inhibits GABA-induced currents in dorsal horn neurones (Gao *et al.*, 2009). Pharmacological studies in neuropathic pain models have revealed that dampening down chemokine signalling using antibodies or receptor antagonists of several chemokines e.g. CCL2 (Thacker *et al.*, 2009), CCL7 (Imai *et al.*, 2013), CCL21 (Biber *et al.*, 2011), CX3CL1 (Sun *et al.*, 2013) and CXCL1 (Zhang *et al.*, 2013b) not only alleviate pain behavioural measures, but also markers for spinal neuroinflammation. Contributions of other chemokines to central sensation in chronic pain models has been extensively reviewed (Grace *et al.*, 2014; Ji *et al.*, 2014).

Table 1.5 Examples of chemokine-chemokine receptors mediating glial-neurone interactions, their source and target cells. Modified from Ji et al., 2014

Chemokine	Source	Receptor	Target cells
CCL2	Neurons	CCR2	Microglia
	Astrocytes	CCR2	Neurons
CCL7	Astrocytes	CCR2	Microglia
CCL21	Neurons	CXCR3	Microglia
CX3CL1	Neurons	CX3CR1	Microglia
CXCL1	Astrocytes	CXCR2	Neurons

1.5.Resolvins

Biological responses to tissue injury are dynamic, involving not only inflammation but also anti-inflammatory responses which promote tissue resolution. Healing processes after tissue injury were thought to be passive, but there is now strong evidence that this is an active process (Damazo *et al.*, 2006; Gilroy *et al.*, 1999; Levy *et al.*, 2001). Many recruited immune cells and locally produced mediators are involved. Pro-inflammatory lipid mediators derived from arachidonic acid, PGE2 and PGI2 have firmly established roles in pain pathway sensitisation at the site of injury and in the spinal cord region as elaborated earlier, so called pro-algesic lipids. However, recent research suggested that diverse families of anti-inflammatory or pro-resolution mediators is also generated (Bannenberg *et al.*, 2005; Serhan *et al.*, 2008b) (**Figure 1.6**). New families of specialised proresolving mediators (SPMs) have been identified, includes essential fatty acid–derived lipoxins, resolvins, protectins, and, maresins (Serhan, 2014; Serhan *et al.*, 2008b; Serhan *et al.*, 2004). The diverse biological effects of the resolvins and other SPMs have been extensively reviewed, for example inhibition of leukocyte infiltration and the production of pro-inflammatory cytokines (Ariel *et al.*, 2007; Serhan, 2007; Serhan *et al.*, 2008b), as well as shortening the resolution interval (Schwab *et al.*, 2007; Serhan *et al.*, 2011) and

attenuation of pain behaviour in preclinical pain models (Ji *et al.*, 2011).

Resolvins, the lipid family of interest in this thesis, was originally found in exudates from mice treated with aspirin and docosahexaenoic acid (DHA) (C22:6) produce a novel family of bioactive 17R-hydroxy-containing di- and tri-hydroxy-docosanoids (Serhan *et al.*, 2002). As the lipids were found in the exudate obtained in the resolution phase of inflammation, thus they were termed resolvins (Serhan *et al.*, 2002). Resolvins are broadly divided into 2 families on the basis of the polyunsaturated fatty acid (PUFA) precursors, D-series resolvins (RvD1-RvD6) derived from docosahexaenoic acid (DHA) and E-series resolvins (RvE1 and RvE 2) derived from eicosapentaenoic acid (EPA). Some resolvins are produced following the modulation of COX-2 enzymes by aspirins, so called aspirin-triggered resolvins (AT-Rvs).

Figure 1.6 A time course of acute inflammatory response. At the initiation, acute peripheral inflammation, e.g. peritonitis, induces the release of proinflammatory lipids resulting in tissue edema, platelet activation and chemotaxis. Polymorphonuclear (PMN) neutrophils, the first leukocyte responder, are capable to synthesis specialised proresolving mediators (SPMs). SPMs are generated during inflammation that block vasodilatation/edema formation and limit further chemotaxis and enhance the phagocytic activity of recruited monocyte and macrophage thus promoting tissue resolution and allowing for the return to homoeostasis. Modified from Serhan, 2014.

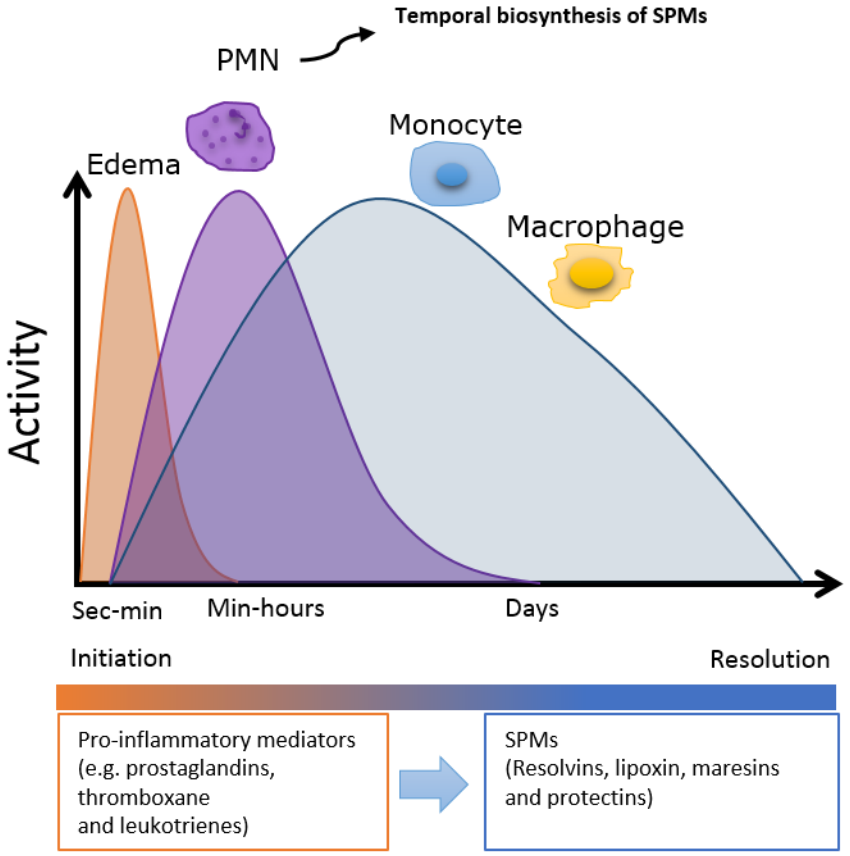

1.5.1. Biosynthesis, metabolism and action of resolvins

The biosynthesis of resolvins is complex involving several enzymes catalysing sequential reactions (Norling *et al.*, 2013; Serhan, 2014), as shown in **Figure 1.6A**. D-series resolvins are endogenously synthesised by 2 sequential reactions, firstly the conversion of DHA to 17S- or 17R-hydroperoxy docosahexaenoic acid (17S- or 17R-HDHA) intermediates. In the case of RvD1, the conversion of DHA to 17S-HDHA is catalysed by 15-lipoxygenase (15-LOX). 5-lipoxygenase (5-LOX) catalyses the final step reaction which generates RvD1, RvD2 and D-series resolvins. In contrast to aspirin-triggered resolvinD1 (AT-RvD1) which can be selectively synthesised after the administration of aspirin. Acetylation of a serine residue on cyclooxygenase-2 (COX-2) enzyme modulates its activity, permitting the enzyme to convert DHA to 17R-HDHA (Serhan *et al.*, 2002) which then undergoes the last 5-LOX-mediated AT-RvD1 formation (Sun *et al.*, 2007). In the case of E-series resolvins, EPA is first converted to 18R-hydroxy eicosapentaenoic acid (18S-HEPE) either by acetylated COX-2 or cytochrome P450 (CYP) enzyme. Then 18S-HEPE is subsequently converted to RvE1 by 5-LOX and leukotriene A4 hydrolase (LTA4H) (Arita *et al.*, 2005a; Oh *et al.*, 2011). Note that activity of 5-LOX is controlled by 5-LOX activating protein (FLAP) (Lehmann *et al.*, 2015).

D-and E-series resolvins are metabolised by 2 main enzymes leukotriene B4 12-hydroxydehydrogenase (LTB4DH) and hydroxyprostaglandin dehydrogenase (HPGD). D-series resolvins are mainly metabolised by HPGD (Sun *et al.*, 2007) whereas E-series resolvins are mainly metabolised both LTB4DH and HPGD (Arita *et al.*, 2005a; Arita *et al.*, 2006).

Resolvins exert their biological activities by activating specific GPCRs (Chiang *et al.*, 2017). Despite being lipophilic molecules, resolvins do not activate common intracellular nuclear receptors for endogenous lipids such as peroxisome proliferator-activated receptors

(PPARs)(Krishnamoorthy *et al.*, 2010). Four GPCRs have been identified as targets for resolvins, as shown in **Figure 1.6B**. RvD1 and AT-RvD1 activate G protein-coupled receptor 18 (GPR32) and formyl peptide receptor 2 (FPR2/ALX) (Mori *et al.*, 2014; Seretny *et al.*, 2014; Ye *et al.*, 2009) Both receptors are expressed in human tissue but GPR32 receptor has not been identified in rodents (Abdelmoaty *et al.*, 2013). RvE1 acts as an agonist for chemerin receptor23 (ChemR23)(Arita *et al.*, 2005a), but as an antagonist of leukotriene B4 receptor1 (BLT1)(Arita *et al.*, 2007). More recently, RvD2 has shown to act at GPR18 (Chiang *et al.*, 2015). All of these receptors utilise Gi/Go as a primary signal transduction (Back *et al.*, 2014; Chiang *et al.*, 2006). ChemR23 and FPR2/ALX, the receptor for RvE1 and (AT-)-RvD1 has been known known to be expressed in DRGs and the dorsal horn of the spinal dorsal cord (**Table 1.6**).

Figure 1.6 D-and E series resolvin system. (**A**) D-and E series biosynthesis and metabolism. (**B**) Known resolvin target receptors. Modified from Norling et al., 2013 and Serhan, 2014

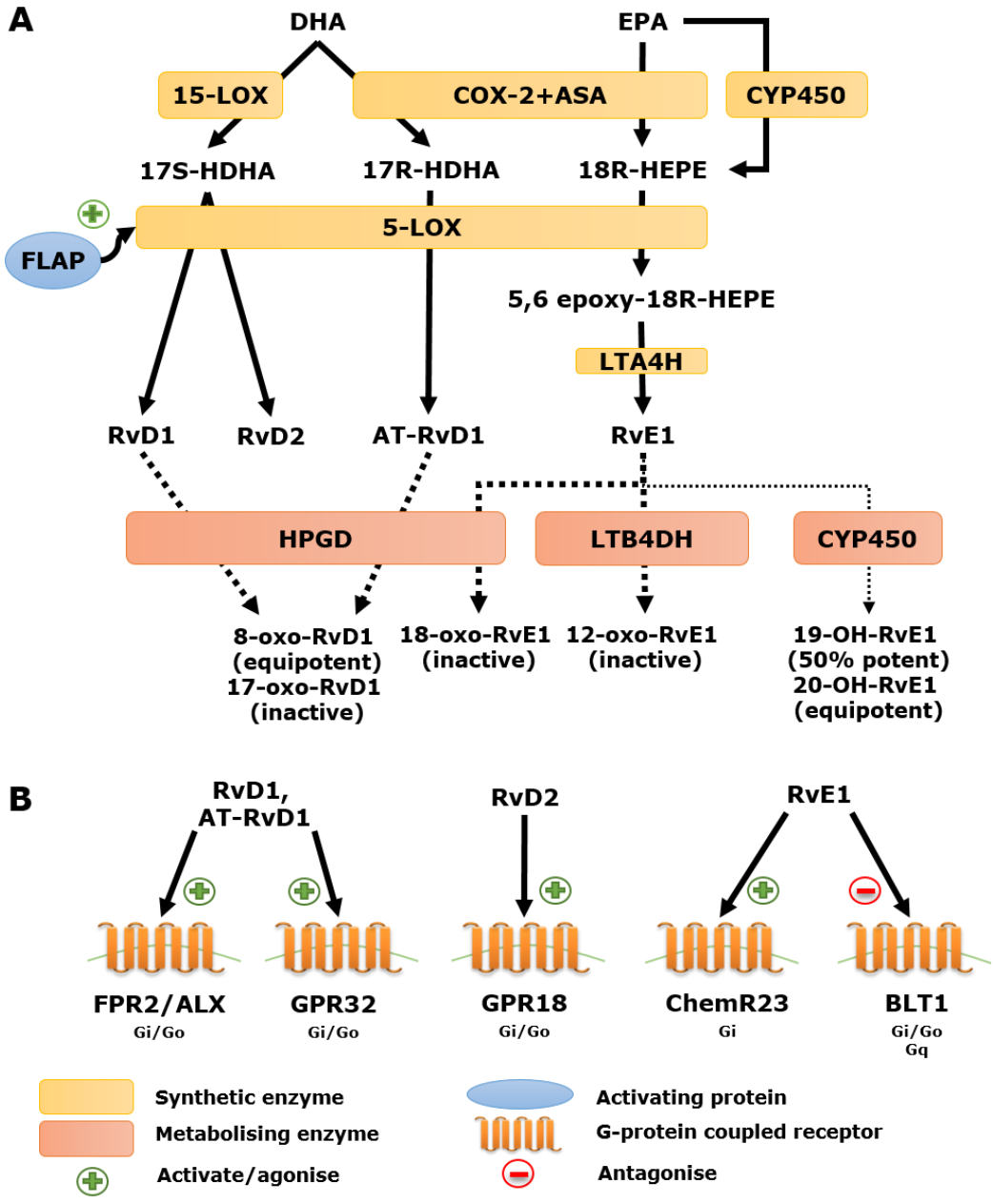

Abbreviations; ASA: acetyl salicylic acid or aspirin, BLT1: leukotriene B4 receptor1, ChemR23: chemerin receptor23, COX-2:cyclooxygenase, CYP450:cytochrome P450, DHA: docosahexaenoic acid, EPA: eicosapentaenoic acid, FLAP: 5-LOX activating protein, FPR2/ALX: formyl peptide receptor 2, GPR18 or 32: G protein-coupled receptor 18 or 32, HPGD: hydroxyprostaglandin dehydrogenase, LTA4H:leukotriene A4 hydrolase, LTB4: leukotriene B4, LTB4DH: leukotriene B4 12-hydroxydehydrogenase, LXA4: lipoxin A4, 17-R-HDHA:17-R-hydroperoxy docosahexaenoic acid, 17S-HDHA:17S-hydroperoxy docosahexaenoic acid, 15-LOX:15-lipoxegenase, 5-LOX:5-lipoxegense, 5,6-epoxy-18R-HEPE:5,6-epoxy,18R-hydroxy eicosapentaenoic acid, 8-oxo-RvD1or E1: 8-oxo-resolvin D1 or E1, 19-OH-RvE1: 19- or 20-hydroxy-RvE1: 19- or 20-hydroxy-resolvin E1.

Table 1.6 Known tissue distribution of FPR2/ALX and ChemR23 receptors in pain pathway

Receptors	DRG	Spinal dorsal horn
FPR2/ALX	Primarily in satellite glial cells and some neurones (Pei *et al.*, 2011).	Expressed primarily in astrocyte, and some neurones but not in microglia (Wang *et al.*, 2014b)
ChemR23	45% of ChemR23 expressing neurones also express TRPV1 and ~60% of TRPV1 expressing (TRPV1+) neurons also express ChemR23 (Xu *et al.*, 2010)	Expressed on the central terminals of primary sensory fibres containing substance P and spinal neurones at superficial lamina (Xu *et al.*, 2010)

1.5.1.AT-RvD1

AT-RvD1 is a stereoisomer of RvD1. The configuration of the hydroxyl group at position 17 chiral carbon is S- for RvD1 and R- for AT-RvD1, as shown in **Figure 1.7**. (Sun *et al.*, 2007) . This difference lead to the stereoselective features AT-RvD1 and RvD1. The most important difference between AT-RvD1 and RvD1 is the resistance to HPGD-mediated inactivation. Whereas RvD1 is rapidly metabolised by HPGD, AT-RvD1, is essentially resistant to the enzyme (Sun *et al.*, 2007). Because of the metabolic stability, AT-RvD1 was therefore chosen to be used in this thesis. The differences in pharmacodynamics of AT-RvD1 and RvD1 are less clear. Ligand-receptor interaction using EC 50 for human FLR2/ALX receptor activation of RvD1 was slightly lower than AT-RvD1 ($4.5x\ 10^{-11}$ M versus $1.8x10^{-10}$ M) whereas EC50 of both for human GPR32 were not very different ($3.6x10^{-12}$ nM versus $4.8x10^{-10}$ M) (Krishnamoorthy *et al., 2012)*. However, polymorphonuclear leukocyte (PMN) migration assay revealed that both RvD1 and AT-RvD1 demonstrated a similar degree inhibiting PMN migration (Sun *et al.*, 2007) suggesting they possess the same targets in PMN.

Figure1.7 Comparison of RVD1 and AT-TvD1 chemical structures

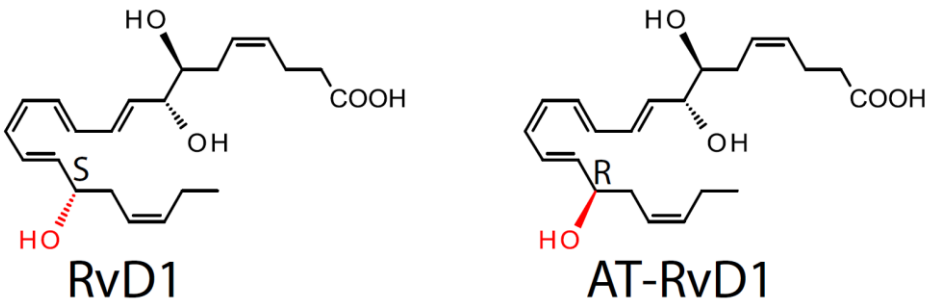

The initial pain behavioural studies have shown that either local or intrathecal injection of RvE1 or RvD1 could attenuated pain behaviour in rodent models of inflammatory pain (induced by either formalin, CFA or carrageenan) suggesting peripheral or central sites of action (Xu et al., 2010).

1.5.1.1. Effects on ion channels in pain pathway

In vitro and *in vivo* evidence indicates that D-series resiolvins are capable to modulate several peripheral nociceptive ion channels. Whole cell calcium imaging and electrophysiological studies have shown AT-RVD1 at 3 uM blocked TRPV3-mediated responses (Bang *et al.*, 2012). Subsequent behavioural studies have confirmed that AT-RVD1 30 uM (intraplantar injection) antagonise licking time and thermal hypersensitivity induced by TPPV3, agonist farnesyl pyrophosphate (Bang *et al.*, 2012). The evidence for RvD1 using the same techniques have also revealed RvD1 at nanomolar concentrations (100 and 300 nM) inhibited TRPV3 and TRPV4-mediated increase in intracellular calcium in cultured human embryonic kidney 293 (HEK293) cells and DRG neurones cultures whereas inhibited TRPA1 at a higher concentration (1uM) (Bang *et al.*, 2010). However, RvD1 had no significant effects on calcium

responses elicited by TRPV1, TRPV2 and TRPM8 activation. In addition, a previous report investigating NMDA receptor phosphorylation in a rat model of chronic pancreatitis has shown that intrathecal injection of RvD1 10 and 500ng dose-dependently reduced phosphorylated NMDA receptor subunit NR1 and NR2B levels in spinal cord especially the dorsal horn (Quan-Xin *et al.*, 2012). This was in accordance with the alleviation of mechanical hypersensitivity (Quan-Xin *et al.*, 2012), suggesting that RvD1 could modulate NMDA receptor activity and influence spinal nociceptive transmission.

1.5.1.2. Effects on spinal neuroinflammation and pain behaviour in pain models

AT-RvD1 and RvD1 have been investigated in different animal models representing both acute and chronic pain (summarised in **Table 1.7**), including acute inflammatory pain following intraplantar injection of inflammogens (carrageenan or CFA) or hind paw incision, chronic inflammatory pain following retraction surgery, chronic visceral pain following trinitrobenzene sulfonic acid injection and chronic neuropathic pain compressive lumbar disc herniation. These behavioural studies have shown the analgesic potential of AT-RvD1 and RvD1 intrathecal injection in reducing mechanical or thermal hypersensitivity. Most studies used AT-RvD1 or RvD1 at very low concentrations in nanogram range, indicating AT-RvD1 and RvD1 are very potent. AT-RvD1/RvD1 mediated analgesia in some studies appears concurrently with the reduction in markers for spinal neuroinflammation in models of acute (Abdelmoaty et al., 2013) and chronic pain (Liu *et al.*, 2016b; Quan-Xin *et al.*, 2012) such as TNF-α, IL-1β, IL-6 and NF-κB subunit p65. These suggests that AT-RvD1/RvD1 may affect spinal neuroinflammation which in turn inhibit spinal nociceptive processing.

As anti-nociceptive of intrathecal RvD1 have been reported in different pain models, it suggests that RvD1 can possibly target

spinal neuroinflammation and modulate spinal nociceptive processing in pathological pain from different underlying mechanisms.

Table 1.7 Summary of the effects of AT-RvD1 and RvD1 on pain behaviour and markers for spinal neuroinflammation in the preclinical pain models.

Models	Tested drugs	Behavioural effects	Reference
Acute pain models			
■ Carrageenan i.plantar	AT-RvD1 0.3, 3 and 300 ng i.t.	↓ paw mechanical hypersensitivity (3 and 300 ng), dose-dependent	(Abdelmoaty *et al.*, 2013)
■ Lateral paw incision	RvD1 10, 20 and 40 ng i.t.	↓ paw mechanical hypersensitivity, dose-dependent	(Huang *et al.*, 2011)
■ Complete Freund's adjuvant, i.plantar	RvD1 10 ng, i.t.	↓ paw thermal hypersensitivity	(Xu *et al.*, 2010)
Chronic pain model			
■ Skin/muscle incision and retraction surgery (hind limb)	RvD1 10, 20 and 40 ng i.t.	↓ paw mechanical hypersensitivity, dose-dependent	(Huang *et al.*, 2011)
■ Non-compressive lumbar disc herniation	RvD1 10 and 100 ng, i.t.	↓ mechanical hypersensitivity, dose-dependent	(Liu *et al.*, 2016b)
■ Trinitrobenzene sulfonic acid-induced chronic pancreatitis	RvD1 10, 100 and 500ng, i.t.	↓ abdominal mechanical hypersensitivity (100 and 500 ng)	(Quan-Xin *et al.*, 2012)

i.plantar=intraplantar injection, i.t.=intrathecal injection

1.6. Aim of the thesis

The aim of the thesis is to investigate the effects of AT-RvD1 on spinal nociceptive processing and spinal alterations of the resolvin system and neuroinflammation in models of acute and chronic pain mimicking different pain mechanisms. The outcomes of this research should provide a preclinical basis for the development of novel analgesic targets.

Investigations of the effects of spinal AT-RvD1 on evoked responses of spinal neurones *in vivo* in well characterised pain models were performed in carrageenan-induced acute inflammatory pain (**Chapter 3**), monosodium iodoacetate (MIA)-induced osteoarthritic pain (**Chapter 4**) and paclitaxel (PCX)-induced peripheral neuropathic pain (**Chapter 5**). The hypothesis of the 3 beginning chapters is whether spinally applied AT-RvD1 can inhibit spinal nociceptive processing when compared to baseline responses in each particular model. The final part (**Chapter 6**) is a question-based experiment to investigate the alterations in the expression of spinal genes relevant to resolvin system and neuroinflammation that may underlie the differential effects of AT-RvD1 among these pain models.

Chapter 2 GENERAL EXPERIMENTAL METHODS

2.1 Animals

Male Sprague-Dawley rats were purchased from Charles River, UK. The initial weight ranges were 200-250 g and 150-175 g on the day of model induction for acute pain model and chronic pain model, respectively. Studies were carried out in accordance with UK Home Office Animals (Scientific Procedures) Act (1986) and followed the guidelines of the International Association for the Study of Pain (Zimmermann, 1983) and were approved by local ethical review board at the University of Nottingham.

Rats were group housed (3-4/cage) at the BioSupport Unit, University of Nottingham, in open cages, fed *ad libitum* and in a 12 hr light-dark cycle. In accordance with the ARRIVE guidelines (Kilkenny *et al.*, 2012) full details of the group sizes for the different studies and experimental endpoints are in **Table 2.1**. Rats were acclimatised in the home cage for 3-7 days prior to induction of pain model. Rats received 1-2 sessions of habituation in the test environment to minimise stress interference 1-2 days prior to behavioural pain assessment. On the day of pain behavioural testing, rat were acclimatised 15-30 min before testing.

Table 2.1 Group sizes of animals in the studies

	Method	Model	Spinal treatment	Group Size
Chapter 3	Electro-physiology	Intraplantar saline	PBS	5
		Intraplantar saline	AT-RvD1	10
		Intraplantar carrageenan	PBS	10
		Intraplantar carrageenan	AT-RvD1	10
		Intraplantar carrageenan	BOC-2	9
		Intraplantar carrageenan	BOC-2-AT-RvD1	9
		Intraplantar carrageenan	BOC-2 vehicle	6
	Gene expression using Taqman	Intraplantar saline	NA	6
		Intraplantar carrageenan	NA	5
Chapter 4	Electro-physiology	Intra-articular saline	AT-RvD1-Morphine	9
		Intra-articular MIA	AT-RvD1-Morphine	11
Chapter 5	Electro-physiology	Intraperitoneal	AT-RvD1-Morphine	16
		Intraperitponeal PCX	AT-RvD1-Morphine	15
Chapter 6	Gene expression suing TLDA	Intraplantar saline	NA	6
		Intraplantar carrageenan	NA	7
		Intra-articular saline	NA	7
		Intra-articular MIA	NA	6
		Intraperitoneal vehicle	NA	7
		Intraperitponeal PCX	NA	7

NA=not applicable

2.2 Pain model induction

The injections for pain model induction were carried out in a blinded fashion.

2.2.1 Carrageenan model of acute hind paw inflammatory pain

Carrageenan (2%) solution was prepared by weighing the required amount of λ-carrageenan (Sigma Aldridge, UK) into a glass container. A half of the required volumes of sterile 0.9% sodium chloride was added and left overnight for hydrating λ-carrageenan. Once λ-carrageenan was hydrated, the volume was adjusted and mixed thoroughly by vigorous shaking. The solution was left for at least 24 h before use.

Intraplantar injection of 2% carrageenan or 0.9% sodium chloride as a vehicle was performed as previously described (Hargreaves *et al.*, 1988; Jhaveri *et al.*, 2008; Morris, 2003) under brief inhalation anaesthesia (isoflurane 2.5–3 % in O_2 1 l/min). Once areflexic, the rat was placed on it chest and the left hindpaw was disinfected using chlorhexidine gluconate 4% surgical scrub (Hydrex®). Carrageenan solution was first drawn into a 1 ml sterile syringe, a 25 gauge (5/8”) needle was attached and the volume was adjusted to 100 ul. Injection was perform by placing the tip of the needle parallel to the paw. The needle was inserted into the subcutaneous of the plantar surface, then carrageenan/saline was slowly injected. Injected rats were placed back in to the home cages for recovery. Severe limping and spontaneous vocalisation were monitored for 24 h. I lost 1 animal during carrageenan injection when the rat was anaesthetised (at 2.5 % isoflurane) due to sudden respiratory arrest without any specific course. Post-mortem investigation found no internal organ abnormality. The death was reported according to standard protocol of the Biosupport Unit. None of the rats developed severe adverse effect following carrageenan injection.

Following carrageenan injection, the hind paw thickness representing the inflammation peaks generally at 2.5-6 h and then reduced toward baseline whereas the hind paw thermal and mechanical hypersensitivity peak at 2.5-4 h but last longer, at least 24-48 (Hargreaves *et al.*, 1988). Spinal electrophysiology recordings were performed and spinal cords were collected following a 24 hour-period of peripheral inflammation of the hindpaw. I extended the period following carrageenan injection to allow the characterisation of spinal events at timepoints more relevant to injuries associated with acute inflammation and pain seen clinically, and the expected timecourse of the activation of the endogenous resolution pathways (Bannenberg *et al.*, 2005).

2.2.2 Monosodium iodoacetate model of knee arthritic pain

Monosodium iodoacetate (MIA) (Sigma-Aldrich, Germany) was dissolved in sterile 0.9% sodium chloride to obtain 1 mg/50 ul final concentration. Under inhalation anaesthesia (isoflurane 2.5–3 % in O_2 1 l/min), once areflexic, the rat was then placed on its back and both hind limbs were shaved from the toe to groin with a hair clipper. The knees and paws was wiped clean with chlorhexidine gluconate 4% surgical scrub (Hydrex®). The ipsilateral paw was then extended and the base of the patella was located. Either 50ul of the MIA solution or vehicle was injected in to the left knee joint using a 0.5 ml microsyringe via infra-patella ligament perpendicular to the knee joint. Only 2/3 the length of the needle was inserted into the knee joint to prevent posterior leakage. Injected rats were placed back in to the home cages for recovery. For animal welfare, injected rats were closely monitored at 1 h, 3h, 24h and then once daily for 3 days following the injection. Humane endpoints were severe joint swelling (>2 folds increased in knee joint diameter), severe limping more than 3 days post-injection and spontaneous vocalisation. In the studies,

injected animals displayed only temporary joint swelling and limping which resolved with 3 days.

I have chosen the timepoint of 28 days following MIA injection to perform electrophysiological and spinal gene expression studies based on previous model characterisations. At this timepoint, MIA-injected develop OA pathology (Guingamp et al., 1997; Guzman et al., 2003) al well a pain behaviour (Arendt-Nielsen et al., 2010; Sagar et al., 2011) including the shifting in weight bearing to the contralateral hind limb and the reduction in distal mechanical paw withdrawal threshold of the ipsilateral hind limb. The electrophysiological characterisation of spinal WDR neuronal responses at this timepoint shows the correlation of mechanical evoked responses and weight bearing asymmetry (Sagar *et al.*, 2010) and there is an increase in spinal astrocyte activation (Sagar *et al.*, 2011). In addition, this dose has produced consistent pain behaviour and OA pathology in a series of studies in this laboratory (Burston *et al.*, 2013; Huang *et al.*, 2017; Nwosu *et al.*, 2016; Sagar *et al.*, 2010).

2.2.3 Paclitaxel model of chemotherapy-induced peripheral neuropathic pain

Paclitaxel (PCX) (Tocris, UK) solution was prepared in a safety cabinet. Since the aqueous solubility of PCX powder is very low, PCX was first dissolved in absolute ethanol then stepwise added Cremophore as the following method. This was prepared as a stock solution, kept at -20 °C and used within 5 days. On the day of injection sterile normal saline (0.9 % sodium chloride) was added to the stock solution to give the final concentration of 2 mg/ml in 10% Cremophore, 5% ethanol in normal saline. Rats received a intraperitoneal injection with either PCX (cumulative dose of 8 mg/kg) or vehicle on 4 alternate days (Flatters et al., 2006; Polomano et al., 2001). Following the injection, rats were closely monitored at 1, 3 and 6 hours. Loose stool indicating the miss

injection into the gastrointestinal tracts was monitored once daily in the first week. Severe limping, spontaneous vocalisation, bodyweight change, the appearance of the hind limb and sign of severe stress were monitored throughout the study. Human endpoints were the rat displayed severe weight loss (>20% of initial weight). PCX and vehicle treated rats appeared similar in the weight gain rate and general health conditions. All rats did not display any signs of severe adverse effects e.g. post-injection diarrhoea and weight lost.

The timepoint of 28 day-post the first dose of PCX injection was chosen to characterise the spinal neuronal responses, perform pharmacological studies and investigate spinal gene expression. This timepoints has been reported that PCX-injected rats develop robust hindpaw thermal, mechanical and cold hypersensitivity (Flatters *et al.*, 2004; Pascual *et al.*, 2005a; Polomano *et al.*, 2001; Xiao *et al.*, 2007). In addition, it has been consistently reported to produce pain behaviour which coincides with the reduced PGP9.5 positive intraepidermal nerve fibre density (Bennett *et al.*, 2011; Boyette-Davis *et al.*, 2011; Jin *et al.*, 2008; Ko *et al.*, 2014; Liu *et al.*, 2010; Siau *et al.*, 2006) suggesting the existence of peripheral neuropathy.

2.3 Pain behavioural testing

All behavioural tests performed in this thesis were carried out in a blinded fashion.

2.3.1 Weight bearing asymmetry

Weight bearing asymmetry, reflecting the altering of weight bearing from the ipsilateral hind limb to the contralateral hind limb was assessed as previously described (Bove *et al.*, 2003; Sagar *et al.*, 2011; Sagar *et al.*, 2010) using an incapacitance tester (Linton Instrument, UK) calibrated with 50 g brass weight before testing. Rats were placed in an angled plexiglass chamber, positioned each hind limb on to separate weighing pans. When acclimatised and

leaning toward the front, the hindpaw weight bearing was recorded over the period of 3 seconds. Three readings were taken at each timepoint and then averaged. Data were as percentage of weight bearing asymmetry from the formula;

Weight bearing asymmetry $=[(Wt_{Cont}-Wt_{Ipsi}) / (Wt_{Cont}+Wt_{Ipsi})] \times 100$

$Wt_{Con}t$ = weight bearing the contralateral hind limb

Wt_{Ipsi} = weight bearing the ipsilateral hind limb

2.3.2 Mechanical paw withdrawal threshold

Rats were acclimatised in Perspex chambers with metal mesh floor for at least 15 min before test commencing. Mechanical paw withdrawal thresholds (PWT) of both hindpaws were assessed using the up-down method (Chaplan *et al.*, 1994) with von Frey monofilaments with a range of bending forces (1, 1.4, 2, 4, 6, 8, 10, 15 and 26 g) starting at 4 g. A filament was gently applied to the plantar surface of either hindpaw until slightly bent then held for a period of 3 sec starting from 4 g. Three different areas of each hind paw were tested. A positive response is a brisk paw withdrawal from the stimulus. If there is no response from the given monofilament the ascending filament was then applied. Once a withdrawal reflex was observed, the next descending monofilament was applied to retest until no response elicited. The lowest force of monofilament which evoked a paw withdrawal reflex was recorded as PWT. A 3-5 minutes interval was allowed between stimulus applications to minimise sensitisation.

2.3.3 Nocifensive behaviour evoked by acetone

Acetone-evoked nocifensive behaviour has been described as a method to test for cold allodynia (Choi *et al.*, 1994). The test was performed in Perspex chambers with metal mesh floors. A single

droplet of acetone (~100 ul) was formed at the end of a polystyrene tubing attached to a 5ml syringe. The syringe was gently moved upward until the droplet contacted to the plantar surface of the hindpaw. The test was carried out alternately of either hindpaw 3 times, with 3-5 min interval. Nocifensive behaviour, including brisk foot withdrawal, flinching, shaking, licking the plantar surface was observed and timed in sec. The total time of nocifensive behaviour in responses to acetone applications (3 times/paw) was calculated. Rats received 1-2 sessions of acetone test habituation prior to the experiment to minimise the confounding effect of acetone odour.

2.3.4 Paw withdrawal latency (PWL) evoked by radiant heat

Heat hyperalgesia was tested using the plantar test (Hargreaves) apparatus, as previously described (Hargreaves *et al.*, 1988; Yeomans *et al.*, 1994). The rat was placed into the test chamber for 15-20 minute for acclimation. Then the infrared beam which used as a radiant heat stimulus was applied to the left hind paw. Time of the paw withdrawal latencies (PWL) to radiant heat stimuli were recorded 3 times, and a 5-minute interval was maintained between trials to avoid sensitisation. The exposure time was limited by 40 sec to prevent tissue damage. The PWL of each rat was calculated as the mean of 3 trials.

2.4 *In vivo* single unit spinal electrophysiology

Single unit *in vivo* electrophysiology recording of deep dorsal horn wide dynamic range (WDR) neurones was performed, as previously described (Chapman *et al.*, 1998; Urch *et al.*, 2003). The method records the activity of single WDR neurones by using a glass coated tungsten electrode connected to a head stage measuring the signal generated by the neurone with subtraction of the signal form the

animal (skin) grounded a stereotaxic frame. The electrical activities were amplified, filtered by Neurolog system (Digitimer, U.K.), digitised by CED Micro1401 (Cambridge Electronic Design, Cambridge, U.K.) and captured/analysed by Spike 2 version 6.05 software (Cambridge Electronic Design, U.K.). An overview of the animal setup is shown in **Figure 2.1.**

Figure 2.1 Overview of the animal setup on stereotaxic frame for single unit spinal electrophysiology. Electrodes for differential recording connected to the head stage include, recording (black), reference (blue) and ground (green) electrodes.

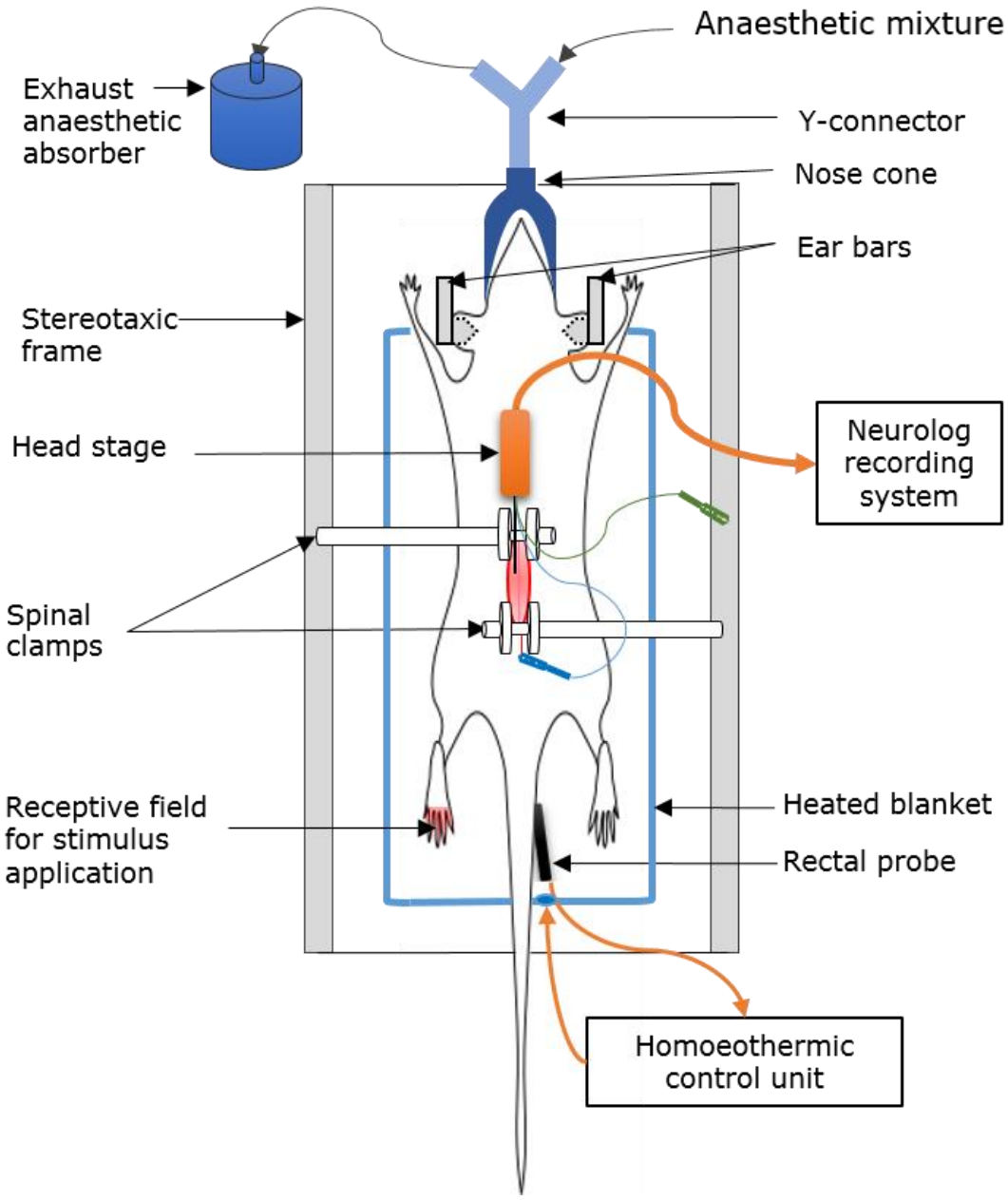

2.4.1 Equipment for electrophysiology

2.4.1.1 Anaesthetic unit

An anaesthetic unit comprised of N_2O and O_2 gases (BOC gases, UK) delivered to a vaporiser (Burtons Medical Equipment Ltd, UK) for isoflurane (Abbott, UK). The flow rate was controlled by separate flow meters and deliver to the rat via Y-tube connecter. The excess anaesthetic gases were absorbed by Aldasorber® (Sherley Aldred, UK)

2.4.1.2 Electrophysiology rig

Electrophysiological recording *in vivo* were on a stereotaxic frame, magnetically fixed to a vibration-dampened metal table (Medical Engineering Unit, University of Nottingham) to stabilise the preparation. Animal core body temperature was monitor with a rectal probe, maintained via a heat blanket and homoeothermic control unit (Harvard Apparatus, UK).

2.4.1.3 Electrode depth controlling unit

Recording electrode was attached to a set of headstage fixed with a micromanipulator. This allows manual control of the electrode in order to change searching locations. The micromanipulator was also connected to SCAT-01 microdrive D301 and Epson HX-20 computer (Digitimer, UK) for fine adjustment of the depth of electrode tip from the spinal surface.

2.4.1.4 Neurolog recording system

Neurolog recording system and related components are shown in **Figure 2.2**. Neuronal signal was amplified (Neurolog NL104 x 1K, Neurolog 106 x 69) and filtered through low and high-pass filters (Neurolog NL125; bandwidth 0.8-1.5 KHz). Signals of >300Hz correlate to field potentials, electromyograms etc., whereas single

unit spikes produce signals of <500Hz. The filtered signal was fed into 1) an oscilloscope (Tektronix TDS210) for visualisation of the neuronal responses, 2) an audioamp (NL120s) connected to a speaker providing an auditory cue and 3) Neurolog NL201a as a window discriminator which adjusted to count action potentials (spikes) of a specified height, separating responses of the target neurone from background noise. Only spikes having amplitude crossing a threshold were counted. The neuronal signal was digitised by CED Micro1401 (Cambridge Electronic Design, UK) and captured/analysed by Spike 2 version 6.05 software (Cambridge Electronic Design, UK).

Modules NL304 (Period Generator), NL603 (Counter), NL401 (Digital Width), and NL510 (Pulse Buffer) were utilised to generate electrical impulses, which were delivered to the rat by a NL800 (Current Stimulus Isolator) via 2 stimulating electrodes (**Figure 2.2**).

Figure 2.2 Neurolog system and related components used for recording neuronal responses and generating electrical stimulation.

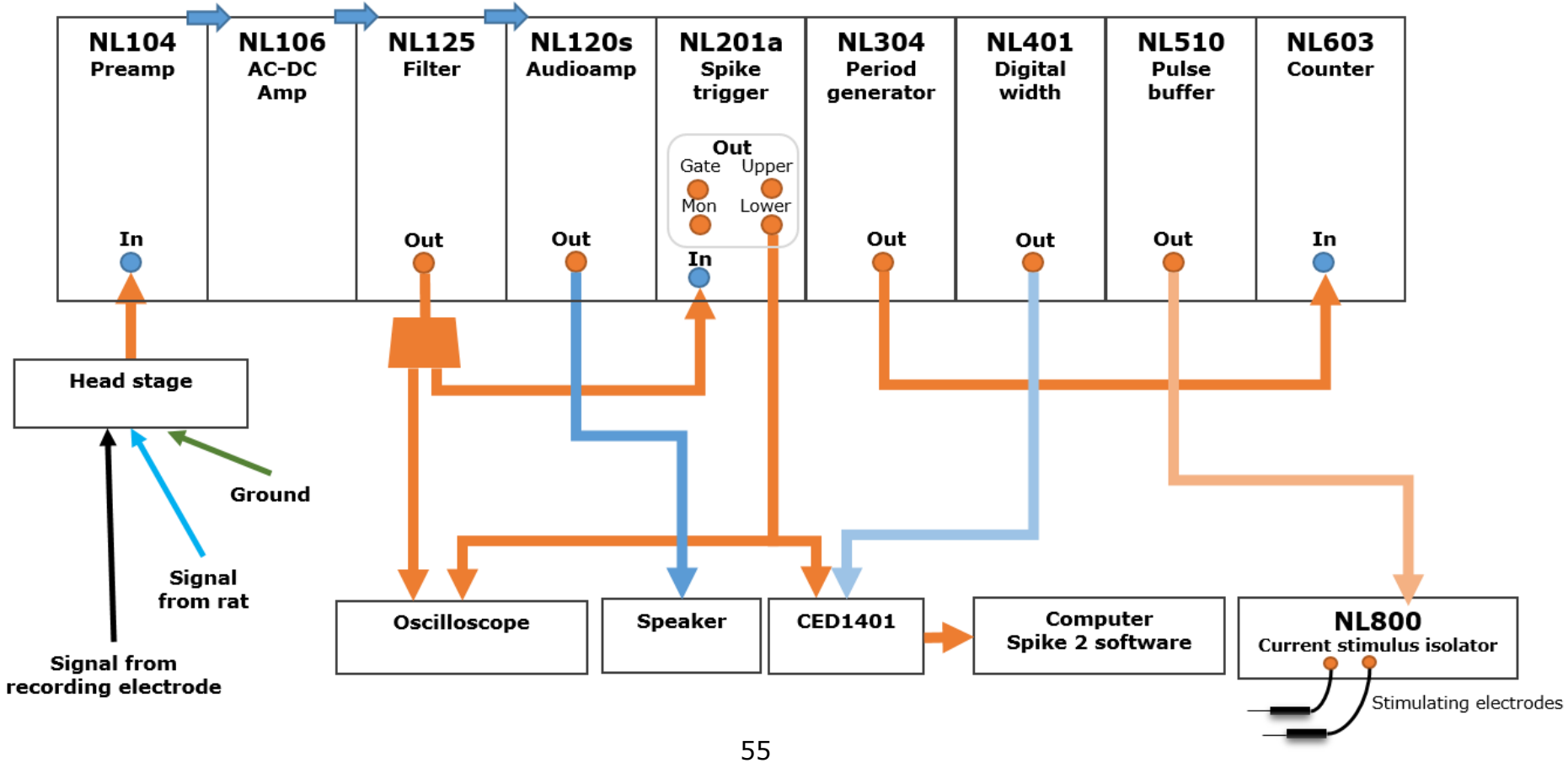

2.4.2 Production of glass-insulated microelectrodes

Glass-insulated electrodes were in-house manufactured as previously described (Bullock *et al.*, 1988). Electrode workstation comprises of 1) an etching unit, 2) a heating unit for electrode glass coating and glass tip removal and 3) a simple light microscope for glass tip removal.

2.4.2.1 Electrode etching

Thirty straightened tungsten electrodes (Harvard Apparatus, Kent, UK) were loaded into a clean (with 100% acetone) Perspex jig (75 x 50mm (Medical Engineering Unit, University of Nottingham) (**Figure 2.3A**). One end of the electrodes were taped using sellotape. A brass barrel was cleaned thoroughly with sandpaper to ensure a good contact between the barrel and electrodes prior to attaching the electrodes. The length of the sellotape containing electrodes was then transferred to the barrel by wraping the tape around the barrel leaving 3-4 cm of the lengths of wire protruding beyond the edge of the barrel (**Figure 2.3B**). Affixed pressure was applied to ensure a good contact between the barrel and electrodes. The loaded barrel was then connected to the rotatable arm of the etching unit (Medical Engineering Unit, University of Nottingham) (**Figure 2.3C**). The arm of the etching unit was adjusted until only 10 electrodes were immersed under the surface of the etching solution (**Figure 2.3D**) containing 90 g potassium nitrate (KNO_2, Sigma Aldridge, UK) in 80 ml distilled water. A carbon electrode connected to the etching unit was placed in the solution to complete the circuit and allow current flow. Current was initially set to 250 mA while the barrel was rotated (5 rpm). The etching was deemed to finish once the current dropped to 200 mA, approximately 17-20 minutes.

Figure 2.3 Microelectrode etching process. (see text for explanation)

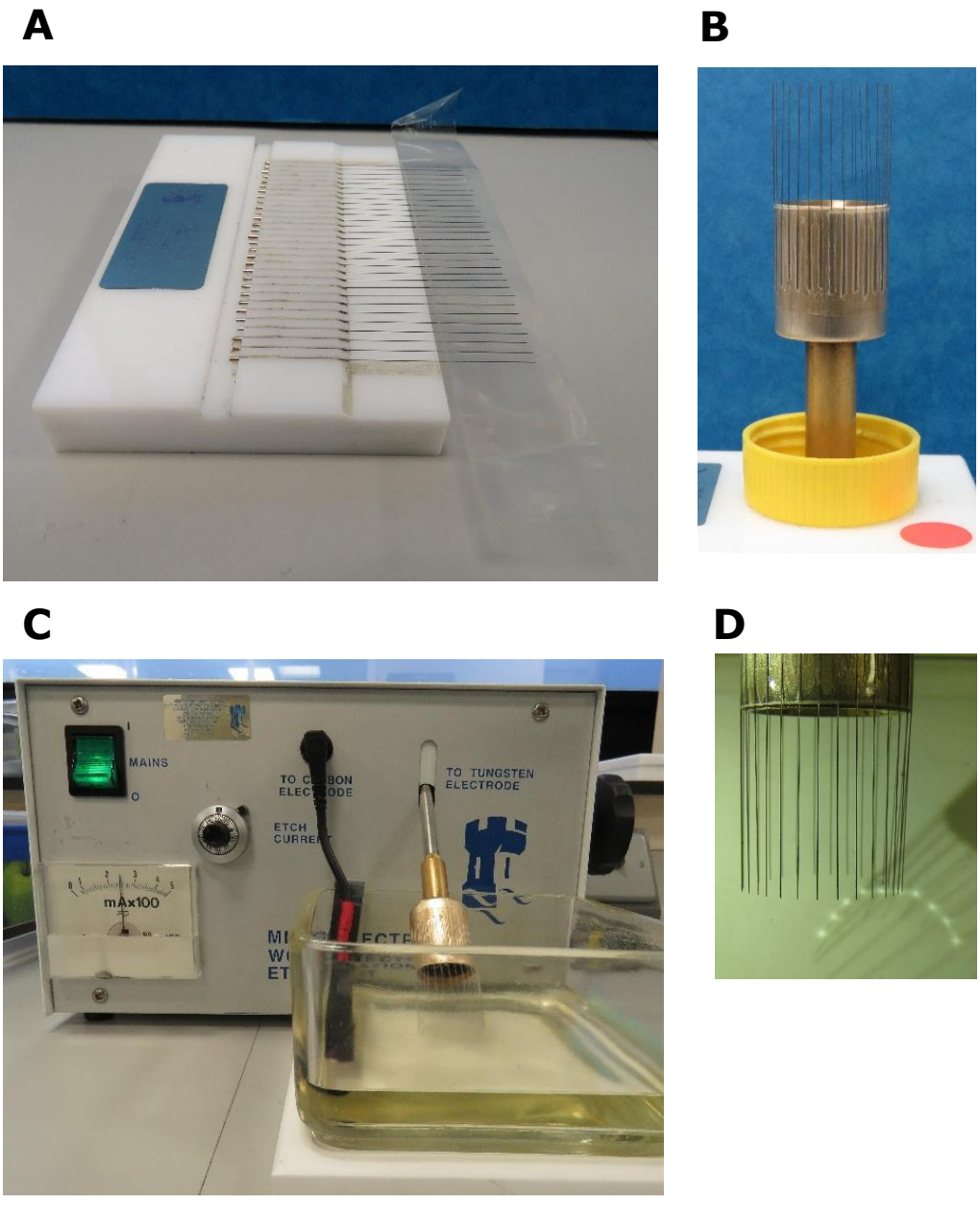

2.4.2.2 Electrode glass coating and removing glass tip

A borosilicate glass capillary (1.5 mm outer diameter x 0.86 mm inner diameter, Harvard Apparatus) were stoppered at one end with plasticine. An etched electrode was removed from the barrel by cutting out the sellotape at its base, passed through a flame to remove residual sellotape and loaded into the stoppered capillary putting the blunt end first. The electrode was transferred to the puller unit (**Figure 2.4A**). The electrode loaded capillary was passed through the upper jaw of an electrode puller (University of Nottingham, Medical Faculty Workshop) until the lower part reach the level lover than a heating coil and then was clamped (**Figure 2.4B**). The lower jaw of the electrode puller was lifted and clamped around the lower part of the capillary. Current was applied through the coil to melt the glass (**Figure 2.4C**) and the lower jaw containing the etched wire dropped by gravity, coating the electrode wire with glass.

Figure 2.4 Microelectrode glass coating process (see text for explanation)

A



B



C



2.4.2.3 Removing the glass tip from coated electrode

The glass tip was removed from the coated electrode under a microscope (**Figure 2.5A**) installed with a cauterising wire with borax bead (**Figure 2.5B**). The coated electrode was place in the microscope by securing the stoppered end with a V-clamp (**Figure 2.5B**). The heating wire with borax crystals and the electrode tip were placed into the visual field, shown as schematic presentation in **Figure 2.5C**. A current was passed through the cauterising wire melting the borax bead. The electrode tip was slowly advanced towards the molten borax bead (**Figure 2.5D**). When the tip was slightly inserted in to the borax bead, the current was turned off. As the borax bead cooled down, it retracted and removed the glass tip from coated electrode exposing the tungsten below (**Figure 2.5E**).

Figure 2.5 Process in removing the glass tip from coated electrode. (see text for explanation)

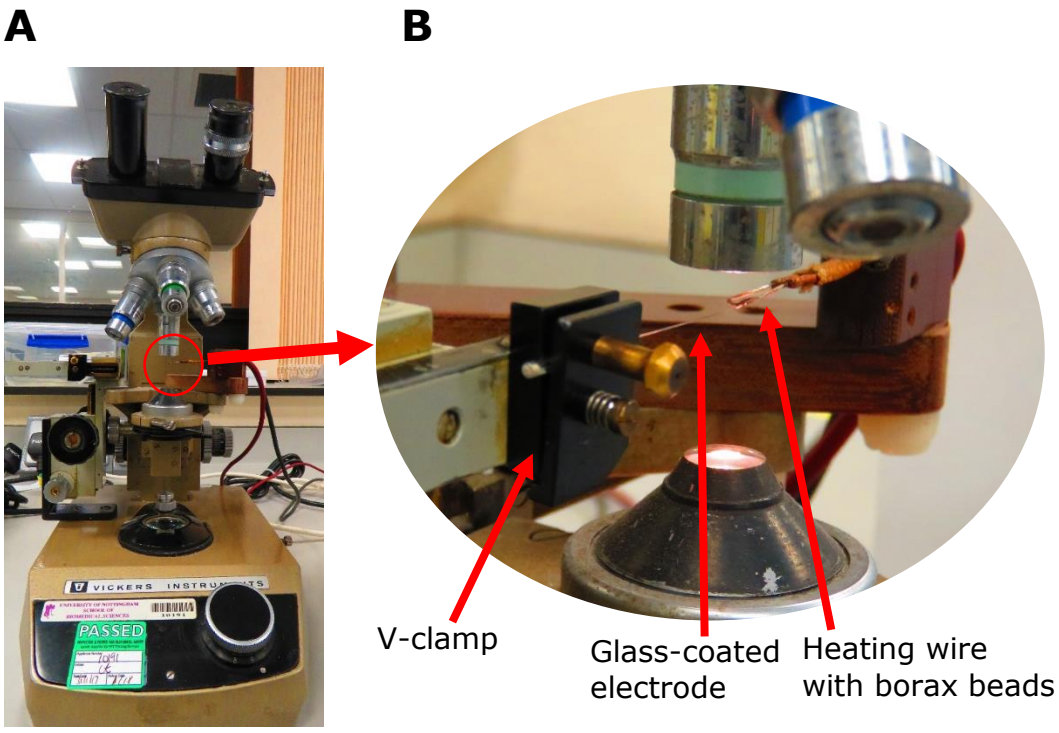

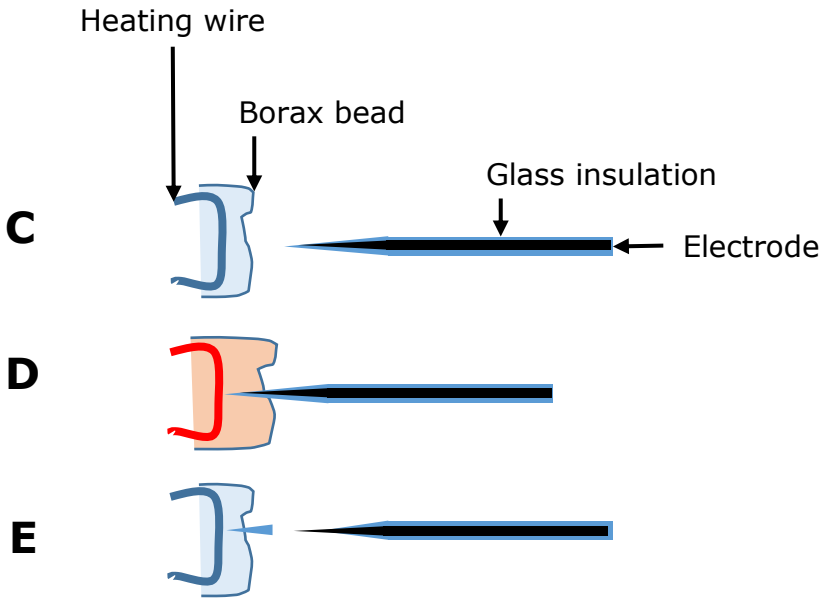

2.4.3 Induction and maintenance of general anaesthesia

A mixture of inhalation anaesthetic isoflurane (3% induction, 2% surgery, 1.5-1.75% maintenance) in 0.6 l/min N_2O and 0.3 l/min O_2 was used. Rats were first received anaesthetic induction with 3% isoflurane in a clear plastic chamber until righting reflex loss (tested by tilting the chamber). The rat were transferred to a nose cone connected with the anaesthetic system for tracheal cannulation. After completion of the cannulation, the anaesthetics were delivered via the tube cannulated. Isoflurane was stepwise reduced to 2% for further surgery and 1.5-1.75% to maintain anaesthetic depth and areflexia throughout the experiment. Core body temperature was maintained (36.5-37°C) using a homoeothermic heated blanket linked to a rectal probe (Harvard Instruments, U.K.).

2.4.4 Tracheal cannulation and laminectomy

Once the rat lost nociceptive and corneal reflexes, skin overlaying the throat was shaved and vertically incised using iris scissors. The trachea was exposed by blunt dissection of surrounding connective tissues and muscle using toothed forceps. Fine forceps were slipped under the trachea in order to isolate the trachea from surrounding tissue. Aided by curved forceps, a piece of ligature (suture silk, 20 cm folded half) was passed through the space underneath the trachea, cut in 2 halves, then loosely secured the top and bottom ends of the exposed trachea, approximately 1 cm apart. A horizontal incision was made using a scalpel blade (15-guage) at 1/3 from the top suture, taking care not cutting through the trachea. A 5 cm tracheal cannula (Portex nylon tubing internal diameter 1.50 mm, external diameter 2.10 mm), black marked at 5 mm from bevelled end) was cannulated into the lower trachea until the black mark levelled was below the bottom suture, taking care not entering the bronchus. The tracheal cannula was tightly secured using the placed sutures, black marked along the length as a visual aid, and connected

to the anaesthetic system via a Y-connector. The rat was transferred into the ear bars of a stereotaxic frame and the rectal probe was inserted. A vertical midline incision was made along the length of the vertebrae using a scalpel blade and connective fascia was removed. Paraspinal incisions at either sides of spine were made from just above T12 (identified by locating the base of the rib cage) down to approximately L2-L3. The rostral end of the paraspinal incision was secured using a metal spinal clamp, then slightly elevated to allow normal expansion of the rib cage for assisting breathing. A vertical tear shape incision was made at the midline of the spine from inside the jaws of the spinal clamp extending down approximately 1.0-1.5 cm. A narrow strip of connective tissue was removed using rongeurs, leaving surrounding tissue to form a natural well. A laminectomy was made by removing spinal processes and vertebrae overlaying the L4-6 region of spinal cord, taking care not to damage the cord and the central vessel. The caudal end of the laminectomy was secured using another spinal clamp. In some preparations, dura, appearing in dull rough membrane, might need peeling off using fine forceps. The spinal surface was kept moist using 0.9% saline, 50 ul applied occasionally. The isoflurane was reduced and maintained at 1.5-1.75% throughout the experiment. A 15-20 min interval was allow for anaesthetic stabilisation prior to further procedure.

2.4.5 Searching for spinal wide dynamic range (WDR) neurones

A glass-coated tungsten microelectrode attached to the head stage was inserted into the ipsilateral side of the spinal cord adjacent to the central vessel. The depth was controlled by SCAT-01 Microdrive (Digitimer, UK). Neurones were searched by slowly lowering the electrode whist the ipsilateral foot was gently tapped. Signals from neurones was isolated aided by means of an oscilloscope and a speaker as visual and auditory cues, respectively. The surface of the cord was determined once electrode slightly dimpled the surface,

then the electrode was slowly withdrawn until the signal became silent giving the surface depth (0 um). The electrode was then advanced to the depth of 500-1000 um from the surface corresponding to laminae V-VI. The recording electrode was advanced to give distinguishable (signal to noise ratio at least 4:1, **Figure 2.6**) and uniform spikes, indicating it was just close to an adjacent neurone. WDR neurones will respond upon non-noxious (tapping or 8-10g von Frey filaments) and noxious (pinching or 15-26 g von Frey filaments) stimuli applied to the cutaneous receptive field and display constant firing upon the noxious stimuli. The neurones that had a graded response to mechanical stimulation and responses in Aβ, Aδ and C-fibres and post-discharge latencies were deemed wide dynamic range.

Figure 2.6 Spike 2 trace example showing evoked neuronal action potentials (spikes) of a recorded spinal neurone and signal to noise ratio. Two spikes were counted since they have a high amplitude (~1.5 mV) which could be separated from the background noise (~0.25 mV) by setting up the threshold in NL201. These two spikes demonstrate the similar amplitude and wave form implying that they were generated by a single unit.

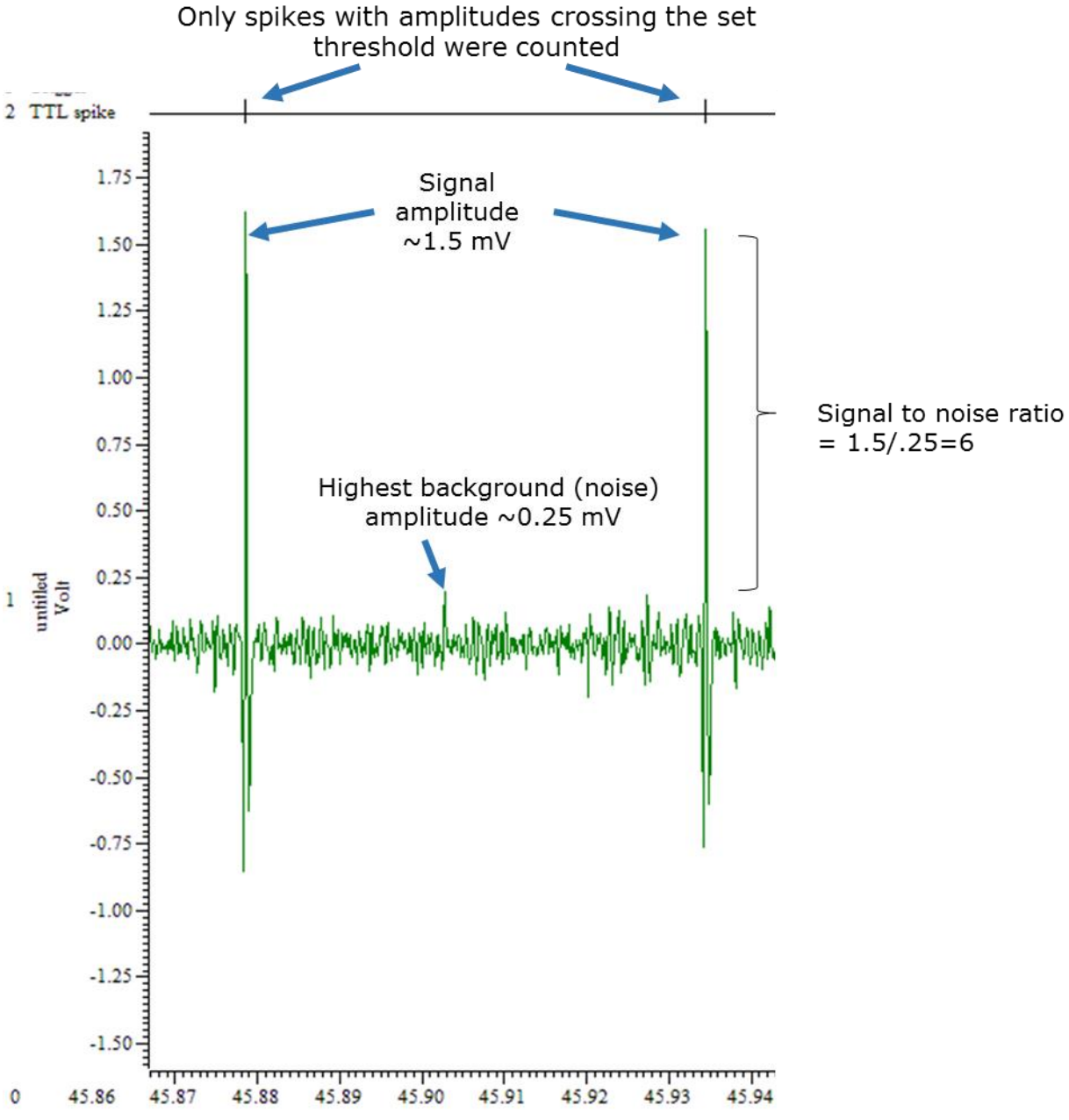

2.4.6 Assessing thresholds for C- and Aβ fibre-evoked responses

A single electrical stimulus (2-ms pulse width) was applied at increasing amplitude in 0.1-mA steps; when a single action potential was elicited in a 90–300-ms post-stimulus range, the stimulus amplitude was taken as the C-fibre threshold and the latency were recorded. Aβ-fibre threshold and latency were measured in the same manner but with a 0.01-mA amplitude increment and in a 0–20-ms post-stimulus latency.

2.4.7 Quantification of WDR neurone responses

2.4.7.1 Responses evoked by electrical stimulation

Electrical stimulation was delivered using 2 stimulation pins connected to NL800 Current Stimulus Isolator. Trains of 16 (0.5 Hz, 2-ms pulse width) consecutive transcutaneous electrical stimulation were delivered at the centre of the hind paw receptive field. Evoke action potential were captured (**Figure 2.7A**) and analysed by Spike 2 version 6.05 software (Cambridge Electronic Design, UK). Responses were elicited at three times (3×) the threshold for C-fibres and then 3×the threshold for Aβ fibres. Note that C-fibre stimulus intensity also activates Aβ and Aδ fibres which will modulate WDR neuronal responses. Post-stimulus time histograms (PSTH) were built on the basis of response latency as shown in **Figure 2.7B**. The Aβ-fibre-evoked responses were taken as the action potential number recorded 0–20 ms after the electrical stimulus, Aδ-fibre-evoked responses were taken as the action potential number recorded 20–90 ms after the electrical stimulus, and C-fibre-evoked responses were taken as the action potential number recorded 90–300 ms after the electrical stimulus. The remaining neuronal response (300–800 ms post stimulus) was defined as the post-discharge (PD) of the neurone. The input (non-potentiated response) was calculated as the

number of action potentials in C-fibre and PD bands produced by the first stimulation (initial baseline response) multiplied by the total number of stimuli. Wind-up (WU, potentiated response) was calculated as the difference between the total number of action potentials in C-fibre and PD bands produced by the train of 16 stimuli minus the input.

It is worth to note that these latencies bands are based on rats weighing 200-250g (Stanfa *et al.*, 2004). The chronic pain models studied (MIA and PCX) in this thesis have been carried out with a slight different weight range which may affect the latencies because of the difference in size/length and conduction velocity of the neurone and the degree of myelination. For example, in rats weighing 350 g the C-fibre latency may extend to 350 ms with the PD between 350-800 but C-fibre latency and PD may be 50-250 ms and 250-800 ms, respectively in rat pup weighing 100 g (Stanfa *et al.*, 2004). The initial rat weight for carrageenan study when received the pain model induction in this thesis was 200-250, similar to that in the original protocol (Stanfa *et al.*, 2004). Whereas in the chronic pain studies (MIA and PCX), the initial weight was 150-175 g (considers as late peri-natal) and the final weight range was approximately 350-425 g. Neuronal activities and pain behaviour may be affected by the immature development of nervous system in the case induction pain model in too young rats. On the other hand, pain model induction in older rats, particularly for the chronic pain model, may decrease the success rats, of the spinal electrophysiology. The well-ossified vertebrae in the older rat may increase the chance of bleeding during performing laminectomy and interfere the recoding neuronal activities and spinal drug application. Therefore, the weight ranges mentioned earlier was chosen.

However, I did not adjust the latency because it may need further characterisation and to be able to compare the results with previous characterisation, for MIA model in particular. In addition, the baseline

firing results of each latency band were analysed by comparing to the appropriate vehicle control with the same age.

In carrageenan (**Chapter 3**), MIA (**Chapter 4**) and PCX (**Chapter 5**) studies, cycles of the electrical stimulations at 3×C-fibre threshold followed by and then 3×Aβ fibre threshold were carried out in 15-min intervals.

Figure 2.7 Spike 2 trace examples showing neuronal responses following electrical stimulation. (**A**) Evoked action potential recorded from a SDR neurone evoked by a train of 16 consecutive electrical stimulation at 3xC-fibre threshold. (**B**) Post-stimulus time histogram (PSTH) of the responses from (**A**) was built on the basis of response latency.

A Evoked action potentials following electrical stimulation

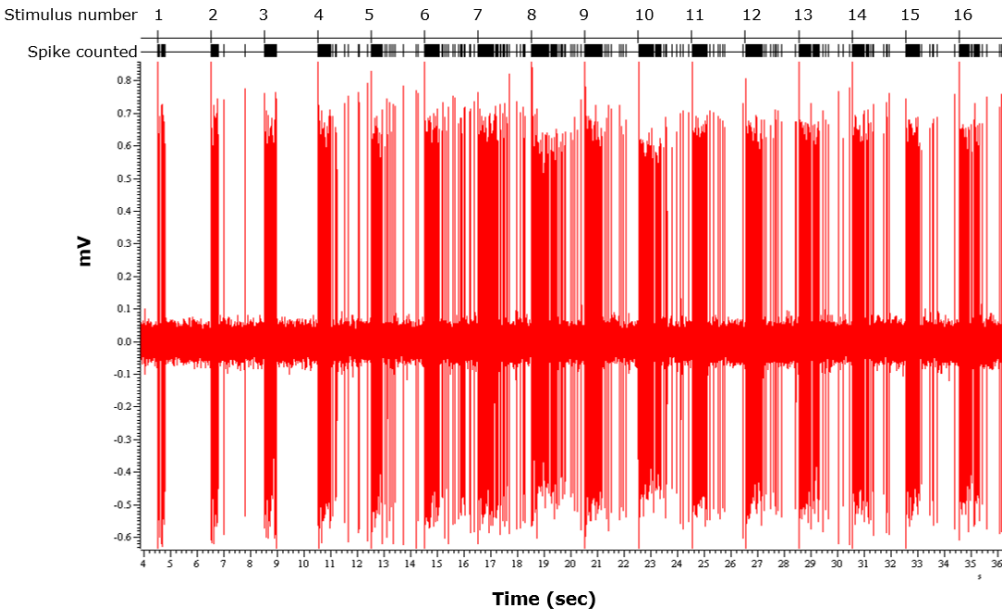

B Post-stimulus time histogram

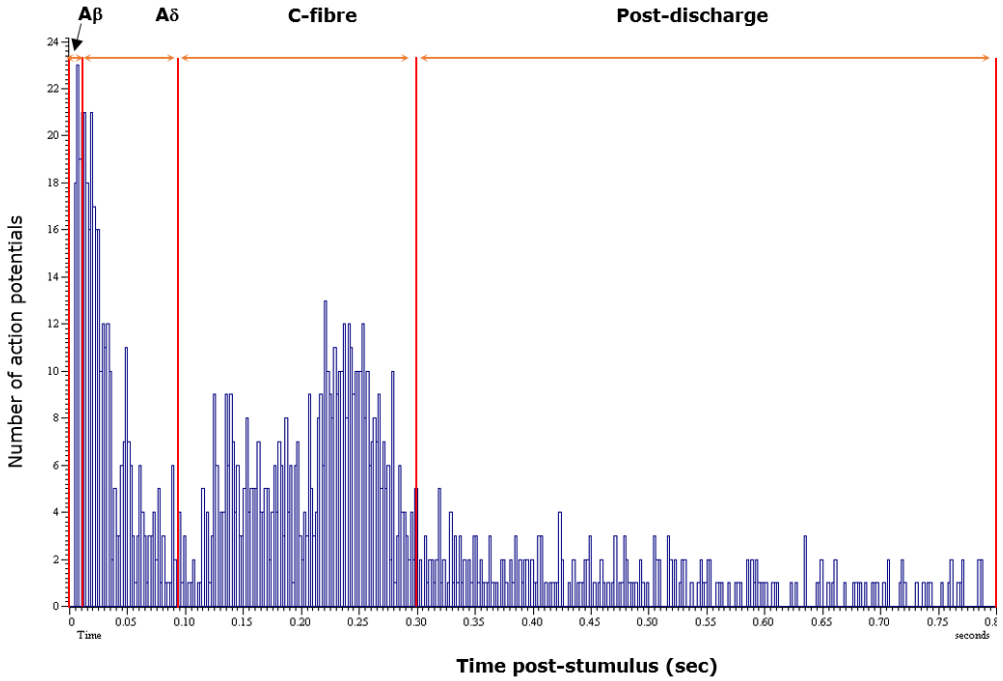

2.4.7.2 Responses evoked by natural stimuli

Neuronal action potentials in spikes/sec evoked by mechanical (von Frey filaments) cold (acetone) stimulations were recorded using rate meter in Spike 2 software.

In paclitaxel study (**Chapter 5**), 3 stimulus modalities were applied to the receptive field. Trains of 4 von Frey filaments (8, 10, 15 and 26g) were applied for 10 sec with 10 sec interval between each filament followed by a drop of acetone (~100 ul) 10-30 sec after mechanical stimulation. The neurones were left for a minimum of 5 min before stimulating with the electrical stimulation at 3×C-fibre threshold followed by and then 3×Aβ fibre threshold similar to **Section 2.4.7.1**. Cycles were carried out in 15-min intervals. An example of trace acquired by rate meter from Spike 2 software is shown in **Figure 2.8.**

Figure 2.8 Rate meter trace example from Spike 2 showing neuronal responses following a train of natural stimuli.

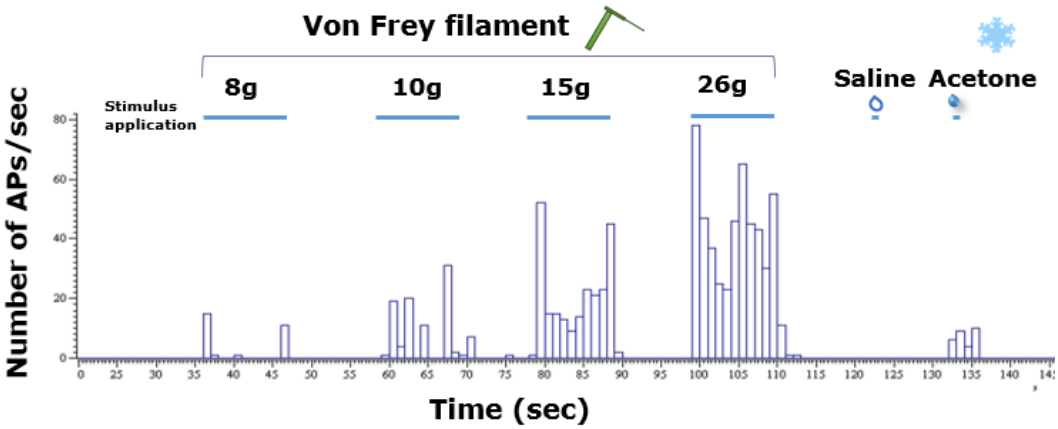

2.4.8 Choice of general anaesthetic

General anaesthesia has been known to suppress the dorsal horn neuronal responses (Collins *et al.*, 1995). Therefore, the anaesthetic was carefully chosen to minimise the impact on the neuronal responses. The use of volatile anaesthetics allows a rapid induction of general anaesthesia and the experimenter full control the anaesthetic depth. Halogenated hydrocarbon halothane and isoflurane have been widely used for *in vivo* electrophysiology recordings. The putative mechanism of actions of halogenated hydrocarbon are augmenting the effects of GABA on $GABA_A$ receptor (Orser *et al.*, 2002) and possibly blocking voltage-gated ion channels (Herold *et al.*, 2009; Shiraishi *et al.*, 2004). The use of halothane has declined due to potential hepatotoxicity. Previous studies has shown that both halothane and isoflurane suppressed the C-fibre and wind-up responses of WDR neurones (Cuellar *et al.*, 2005; Jinks *et al.*, 2004). However, such effects were greater by halothane (Cuellar *et al.*, 2005). Therefore, isoflurane was chosen to use.

2.5 Pharmacological intervention on spinal neurones

Following stable control-evoked neuronal responses (<10 % variation of C-fibre responses and/or responses to natural stimuli), drugs were applied topically to the surface of the exposed L4-5 segments of the spinal cord via a Hamilton syringe in 50-ul volume. Concentrations of AT-RvD1 and butoxy carbonyl-Phe-Leu-Phe-Leu-Phe (BOC-2), a FPR2/ALX receptor antagonist (Stenfeldt *et al.*, 2007), were based on previous studies (Abdelmoaty *et al.*, 2013; Wang *et al.*, 2014b; Xu *et al.*, 2010).

In the carrageenan study (**Chapter 3**), saline or carrageenan rats received one of the following spinal treatments:

- AT-RvD1 (Cayman Chemical, USA) 15 ng in 50 µl PBS (phosphate-buffered saline);
- PBS 50 µl as a vehicle for AT-RvD1;
- BOC-2 (Phoenix Pharmaceuticals, Inc., USA) 50 µg in 50 µl 3 % Tween 80 + 0.5 % ethanol in saline;
- BOC-2 50 µg in 50 µl 3 % Tween 80 + 0.5 % ethanol in saline for 15 min and then AT-RvD1 at 15 ng;
- 3 % Tween 80 + 0.5 % ethanol 50 µl as a vehicle for BOC-2.

In the MIA (**Chapter 4**) and paclitaxel (**Chapter 5**) studies, MIA, paclitaxel or their appropriate vehicle control rats received spinal AT-RvD1 cumulatively (15 ng and 150 ng /50 µl) and then spinal morphine sulphate (Queen's Medical Centre Pharmacy, Nottingham, UK) 1 µg/50 µl in PBS vehicle.

Previous drug solution was removed from the spinal cord between treatments. Effects of treatments on electrically evoked responses of neurones were followed for 60 min post treatment.

2.6 Macroscopic assessment of pain pathology

2.6.1 Paw circumference

The circumference of ipsilateral paw was measured at baseline and 24 h post carrageenan injection as previously described (Jhaveri *et al.*, 2008; Morris, 2003). A piece of suture was horizontally wrap around the widest part of the hindpaw and carefully cut without damaging paw skin. The length (mm) of the cut suture was taken as a paw circumference.

2.6.2 Macroscopic scoring of knee joint cartilage pathology

Ipsilateral knee joints of rats in MIA study were collected at the end of the study and were disarticulated. Macroscopic scoring of knee joint pathology was based on a previously reported scoring system (Guingamp *et al.*, 1997). The severity of the pathology of the cartilage surface was graded as follows; 0 = normal appearance, 1 = slight yellowish discoloration of the chondral surface or swelling, 2 = little cartilage erosions in load-bearing areas, 3 = large erosions extending down to the subchondral bone, 4 = large erosions with large areas of subchondral bone exposure. Six compartments were scored including, medial femoral condyle, lateral femoral condyle, medial tibial plateau, lateral tibial plateau, femoral groove and patella; then were combined to give a total score (possible maximum score 24). Abnormal growth of bone was recorded as osteophyte presentation. The experimenter was blinded for the induction procedure. Image examples of knee joint for macroscopic scoring are shown in **Figure 2.9**.

Figure 2.9 Image examples of rat knee joints at 28 days following saline and MIA injection. (A) Anatomical alignment of the rat knee joint used in the macroscopic scoring. Six areas of cartilage surface were score 0-4 based on the pathology including **(B)** femoral groove and femoral condyles (medial and lateral), **(C)** tibial plateaus (medial and lateral) and **(D)** patella. In saline group, cartilage surface in all area was smooth and intact, total score =0. MIA induced cartilage pathology in most area evaluated including erosion at tibial plateaus, femoral condyles, and patella and swelling at femoral groove, total score = 15 (1+3+3+3+3+2). Osteophytes (OP) were present at tibial plateaus in MIA rats

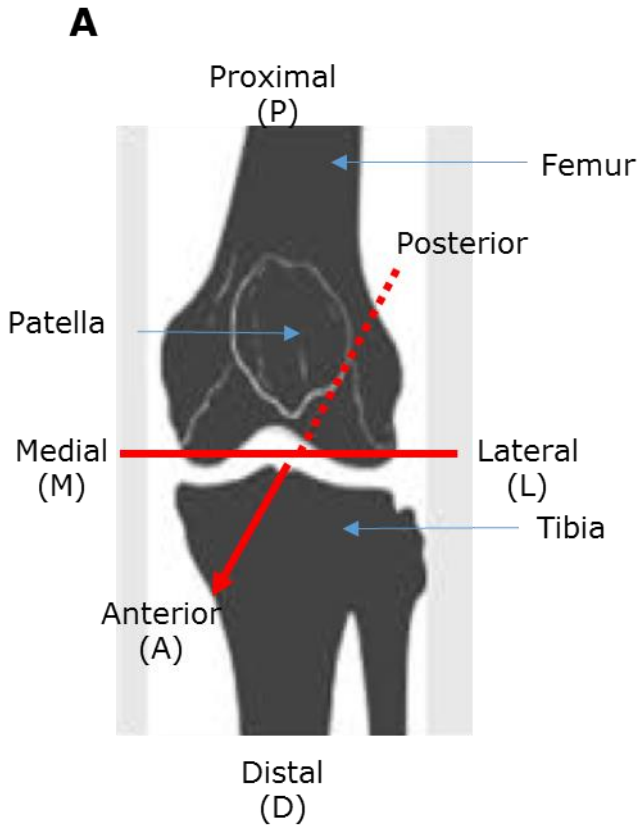

Figure 2.9 - continue

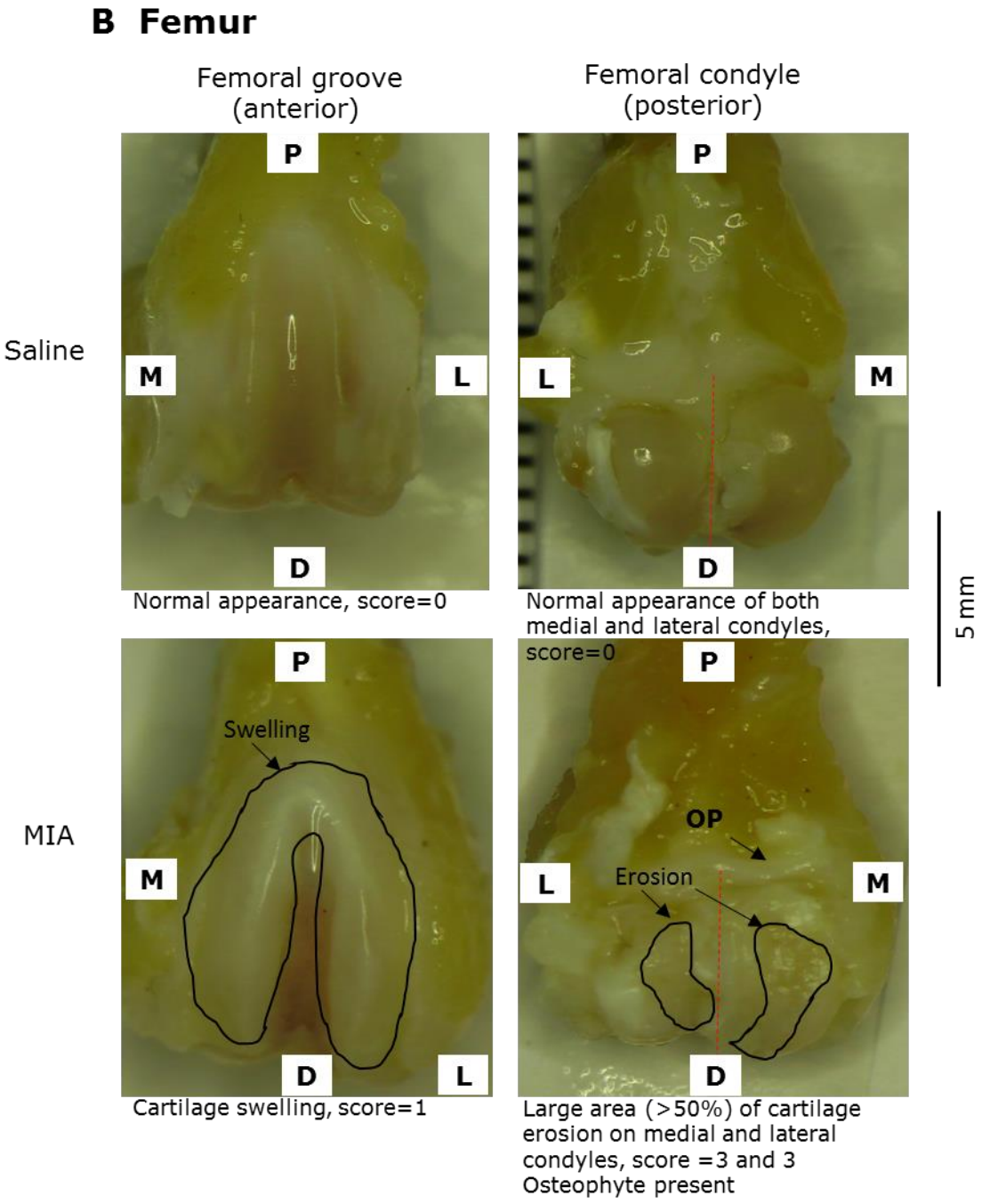

Figure 2.9 - continue

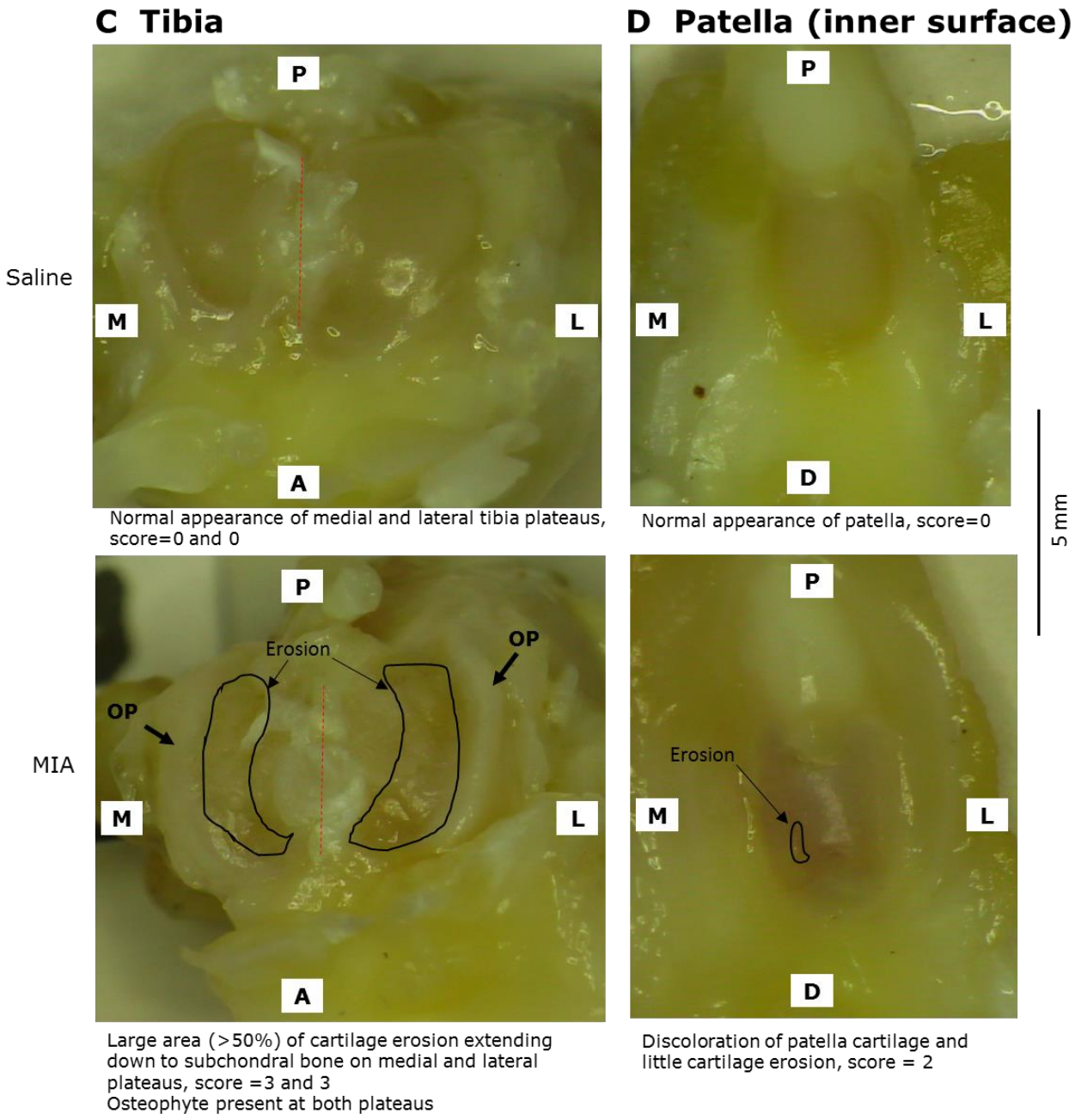

Normal appearance of medial and lateral tibia plateaus, score=0 and 0

Normal appearance of patella, score=0

Large area (>50%) of cartilage erosion extending down to subchondral bone on medial and lateral plateaus, score =3 and 3
Osteophyte present at both plateaus

Discoloration of patella cartilage and little cartilage erosion, score = 2

2.7 Methods for studying of spinal gene expression in pain models

2.7.1 Fresh tissue collection

Rats were sacrificed by cranial concussion and decapitated (Schedule 1 of the Animal (Scientific Procedure) Act 1996) at 30 h post carrageenan or day 28 post either MIA or PCX induction. The lumbar enlargement (L4–L6) of the spinal cord was dissected free. The ipsilateral dorsal quadrant was separated using the method shown in **Figure 2.10**. The dissected lumbar enlargement was placed straight on a clean metal plate facing the ventral horn upward. The ipsilateral and contralateral sides were separated using a scalpel blade cutting longitudinally along the central groove (**Figure 2.10A**). Each hemisection was flipped facing the lateral surface upward and cut again to separate the dorsal quadrant apart from the ventral quadrant (**Figure 2.10B**). Only the ipsilateral dorsal and contralateral dorsal quadrants were collected and immediately frozen on dry ice and stored at -80°C in separate cryotubes until use. Note that the collected samples are a mixture of all cell types e.g. neurones, microglia and astrocytes.

Figure 2.10 Method of isolating ipsilateral dorsal quadrants of rat spinal cord for studying gene expression. CD=contralateral dorsal, CI= contralateral ventral, ID=ipsilateral dorsal, and IV= ipsilateral ventral.

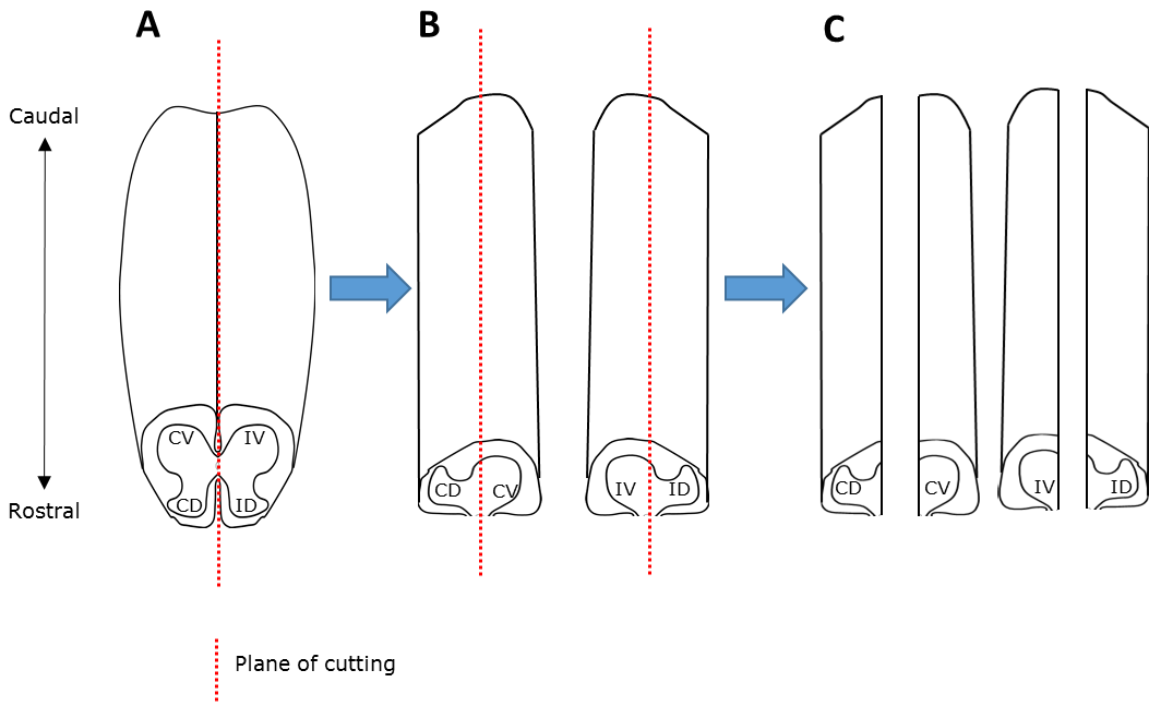

2.7.2 RNA extraction form fresh tissues using phase separation method

This method was used to prepared spinal cord tissue in Chapter 3. Ipsilateral spinal cord samples was treated with 2 ml ice cold Tri reagent (Sigma Aldridge, UK), then homogenised. A 5 min incubation at room temperature was allow to permit a complete dissolution of nucleoprotein complexes. 1-Bromo-3-Chloro-propane (BCP) 0.4 ml was added, vigorously mixed by vortexing. Following centrifugation at 10,000g for 25 min at 4°C, aqueous supernatant containing RNA was collected, treated thoroughly with 0.25 ml sodium acetate (2M, pH 4, 0.25 ml) and 0.7 ml isopropanol and centrifuged at maximum speed for 10 min 4°C to precipitate RNA. Supernatant were discarded and precipitated RNA was wash twice with 70% ethanol and centrifuged at maximum speed for 10 min 4°C. Remaining solvent was carefully removed and left ethanol to evaporated for 2-3 min. RNA pellets were reconstitute with DNase/RNase free water.

2.7.3 RNA extraction form fresh tissues using Direct-Zol® RNA MiniPrep kit

This method was used to prepared spinal cord tissue in Chapter 6. Ipsilateral spinal cord samples were homogenised with 600 ul ice-cold Tri reagent (Sigma Aldridge, UK). Then, total RNA was extracted by Direct-Zol® RNA MiniPrep kit according to manufacturer instructions. Homogenised samples were mixed with 600 ul ethanol, transferred to Zymo-Spin columns and centrifuge at 14,000 g for 30 sec. RNA trapped by the column was washed twice using RNA prewash followed by RNA wash buffers. Residual DNA was decontaminated by treating the column with DNAase I and its digestion buffer. Finally total RNA was eluted with 40 ul DNase/RNase

free water. All reagents above were provided by Direct-Zol® RNA MiniPrep kit except Tri reagent.

2.7.4 Determination of quality and quantity of extracted total RNA

Concentration and purity of extracted RNA were determined using a NanoDrop 2000 spectrophotometer (Thermo Scientific, USA). RNA concentration was quantified by measuring UV absorbance of samples at wave length 260 nm. Wave lengths at 230 and 280 nm were used to measure remaining solvent and protein impurities. Sample with ratios of 1.8 - 2.0 for 260nm/280nm and 260nm/230 nm were considered acceptable (Becker *et al.*, 2010). RNA solution was stored at -80°C until use.

2.7.5 Reverse transcription of extracted RNA to cDNA

Complimentary DNA (cDNA) was synthesised by reverse transcription from 500 ng total RNA using SuperScript III reverse transcriptase (Invitrogen, UK) according to the manufacturer's instructions. Reaction components are shown in **Table 2.2**. Samples were mixed with deoxynucleotide triphosphates (dNTPs) mixture (consists of 10nM each of deoxyadenosine triphosphate (dATP), deoxyguanosine triphosphate (dGTP), deoxycytidine triphosphate (dCTP) and deoxythymidine triphosphate (dTTP)) (Promega, UK), random primers (Promega, UK) and RNase free water and incubated at 65 °C for 5 min. Affinity Script buffer (Agilent Technologies, USA), dithiothreitol (DTT) (Invitrogen, UK), recombinant RNase inhibitor (40U/µl) (Invitrogen, UK) and SuperScript III reverse transcriptase enzyme (Invitrogen, UK) were then added. Samples were further incubated at 25°C for 10 min, 37°C for 50 min and followed by 70°C for 15 min to terminate the reaction. cDNA samples were kept at -80°C until use.

Table 2.2 Reaction components for the reverse transcription of extracted RNA to cDNA

	Volume (ul)	Final concentration
RNA samples 20 ng/ul	1	0.0769 ng/ul
Random primers 100 ng	1	3.842 ng/ul
dNTP mixture 10 nM	1	0.3 nM
RNase free water	17	
Affinity Script buffer 5x	2	
DTT 0.1 M	2	0.0077 nM
Recombinant RNase inhibitor 40 unit	1	1.5385 unit/ul
SuperScript III reverse transcriptase 200 unit	1	7.6923 unit/ul
Total	26	

2.7.6 Principle of quantitative polymerase chain reaction

Gene expression quantification was performed using Taqman® quantitative polymerase chain reaction (qPCR) (Giulietti *et al.*, 2001; Nolan *et al.*, 2006). This technique utilises the temperature-dependent denaturation of cDNA and activity of Taq polymerase enzyme from *Thermus aquaticus*. The cycles of PCR starts, the template cDNA is denatured from double strand to 2 separate single strands at high temperature 90-954°C. Taqman probes containing fluorophore and quencher also bind to the single strand cDNA after denaturation. Next, the temperature is lowered to 40-60°C, this allows forward and reverse primers to bind to specific regions on the template cDNA. In the third step (extension), temperature is raised to 70-75°C permitting Taq polymerase activity to elongate the primers using the dNTP from 5'->3'. During the extension step the probe is cleaved by the 5'->3' enzymatic activity of Taq polymerase. Thereby quencher and fluorophore are separated, allowing fluorescence emission from the reporter dye. These steps repeat 40-45 cycles. The PCR products are exponentially increased each cycle. The most common quencher in Taqman assay is 6-carboxyfluorescein (FAM) and dye is 6-carboxytetramethylrhodamine (TAMRA). The quantitative endpoint of the method is the threshold cycle ($C_{T,}$ between 0-40) which the fluorescence of the reporter dye reaches the placed threshold. The numerical value of C_T is inversely related to the amount amplicon amplified. Specific protocol for Taqman® qPCR are detailed in **Chapter 3** for classical Taqman® qPCR and **Chapter 6** for Taqman® Low Density Array (TLDA).

2.8 General statistical analysis

GraphPad Prism 6.05 (GraphPad Software, USA) was used for statistical analyses and graphical presentation. Data were excluded from the statistical analysis where outliers were identified by Grubb's

tests at $\alpha = 0.05$. Results were expressed as mean ± standard error of mean (SEM) unless otherwise specified. Kolmogorov-Smirnov tests were used to determine whether data were normally distributed. Statistical significance was considered where p value <0.05.

Pain behaviour: Pain behaviour data of rats injected with either carrageenan, MIA or PCX were compared with the respective control rats using two-way analysis of variance (ANOVA) with Sidak post hoc tests. Where differences in behaviour at a time point pain between a treatment and its respective control were compared using either unpaired t-test or Mann Whitney U test.

Macroscopic assessments: Differences in paw circumference between carrageenan and saline and chondropathy scores between MIA versus saline were analysed using a Mann-Whitney U test.

Electrophysiological data: Baseline evoked responses of spinal WDR neurones in rats injected with either carrageenan, MIA or PCX were compared with the respective control rats using unpaired test or Mann Whitney U test. Evoked responses following spinal AT-RvD1 15ng/50ul application in the carrageenan study were compared to baseline using paired t tests or Wilcoxon tests. In the MIA and PCX studies, evoked responses following application of either spinal AT-RvD1 (15 and 150 ng/50 ul) and by morphine 1 ug/50ul application were compared to baseline using repeated measure ANOVA followed by Sidak post hoc test or Friedman statistics followed by Dunn's post hoc test. Percentages of maximal inhibition were calculated versus baseline (pre-drug responses) and were compared between groups using Kruskal-Wallis test with Dunn's post hoc test.

Chapter 3 *IN VIVO* INVESTIGATION OF EFFECTS OF ASPIRIN-TRIGGERED RESOLVIN D1 ON SPINAL NOCICEPTIVE PROCESSING IN CARRAGEENAN-INDUCED ACUTE INFLAMMATORY PAIN

DECLARATION

Contents presented in this chapter have been published recently in Journal of Neuroinflammation. (Meesawatsom *et al.*, 2016). Figures and tables reproduced or amended from the published article are indicated.

3.1. Introduction

During acute inflammation, there is a large number of pro-inflammatory mediators released e.g. arachidonic acid derivatives (e.g. prostaglandins and leukotrienes), pro-inflammatory cytokines (interleukin (IL)-1β, IL-6 and tumour necrosis factor-α (TNF-α) and cellular components (e.g. H^+ and ATP) which are capable of directly activating and/or sensitising pain pathway both at the peripheral and central level (Marchand *et al.*, 2005). Lipid mediators derived from arachidonic acid, for example prostaglandin E2 (PGE2) and prostacyclin (PGI2) have firmly established roles in pain pathway sensitisation at the site of injury and in the spinal cord region corresponding to the sensory input from periphery (Latremoliere *et al.*, 2009; Vardeh *et al.*, 2009), so called pronociceptive lipids.

However, recent research has shown that not only pro-inflammatory mediators are generated but also anti-inflammatory or specialised proresolving mediators (SPMs). SPM, such as the essential fatty acid–derived lipoxins, resolvins, protectins and maresins (Recchiuti *et al.*, 2012; Serhan, 2014) have robust inhibitory effects on inflammatory signalling pathways. This has been particularly well evidenced for the D-series resolvins, specifically resolvin D1 (RvD1 or 17S-RvD1) and its isomer, aspirin-triggered-RvD1 (AT-RvD1 or 17R-RvD1), which are SPMs derived from the polyunsaturated fatty acid docosahexaenoic acid (DHA) (Serhan *et al.*, 2002). SPMs are generated after an overt inflammatory insult to promote resolution (Recchiuti *et al.*, 2012), this is achieved by the inhibition of pro-

inflammatory cytokine production, enhance anti-inflammatory cytokine production e.g. IL-10 and shortening of the interval between inflammation and resolution by inhibiting neutrophil infiltration and stimulating macrophage phagocytosis (Recchiuti *et al.*, 2012; Wang *et al.*, 2014a).

Endogenous synthesis of the D-series resolvins is via the 15-lipoxygenase (15-LOX) mediated conversion of DHA to hydroperoxy intermediates (see also **Chapter 1**). Synthesis of AT-RvD1 is enhanced by aspirin (Serhan *et al.*, 2002) via the acetylation of a serine residue on cyclooxygenase-2 (COX-2), to permit enzymatic conversion of DHA to 17R-hydroperoxy intermediate. Finally, hydroperoxy intermediates undergo 5-LOX-mediated RvD1/AT-RvD1 formation. Recent research has shown that 5-LOX (Lehmann *et al.*, 2015) synthetic is controlled by 5-LOX activating protein (FLAP). RvD1 and AT-RvD1 are rapidly metabolised, predominantly by hydroxyprostaglandin dehydrogenase (HPGD) to 8-oxo- and 17-oxo-metabolites (Sun *et al.*, 2007). AT-RvD1 and RvD1 are different in their metabolic inactivation pathways and pharmacodynamics (see also **Chapter 1**). However, the most important difference between AT-RvD1 and RvD1 is the resistance to HPGD-mediated inactivation. Whereas RvD1 is rapidly metabolised by HPGD, AT-RvD1, is essentially resistant to the enzyme (Sun *et al.*, 2007).Recently, a metabolically more stable analogue of resolvin D1 has been developed with similar potency in reducing neutrophil infiltration and increasing macrophage phagocytosis (Orr *et al.*, 2015).

The biological effects of RvD1 and AT-RvD1 have been attributed to the G-protein coupled receptors GPR32 and formyl peptide receptor 2 (FPR2/ALX) receptor, whereas RvE1 activates chemerin receptor 23 (ChemR23). All of these receptors utilise Gi and possibly Gq as signal transductions (Arita *et al.*, 2005a; Back *et al.*, 2014; Chiang *et al.*, 2006). FPR2/ALX and GPR32 receptors are expressed in human tissue but GPR32 is not yet identified in rodents (Abdelmoaty

et al., 2013). FPR2/ALX receptor is possibly the most important site of action of RvD1/AT-RvD1 since in ALX/FPR2 knockout mice, RvD1 neither significantly reduced leukocyte infiltration in zymosan-induced peritonitis nor regulated anti-inflammatory IL-10 in these mice (Krishnamoorthy *et al.*, 2012). In pain pathway, FPR2/ALX is primarily expressed by satellite gial cells in DRG and astrocytes in the spinal dorsal horn but expressed in only small population of DRG and spinal neurones (Pei *et al.*, 2011; Wang *et al.*, 2014b).

Despite their rapid degradation, locally administered RvD1 and AT-RvD1 have analgesic effects in various animal models of pain (Abdelmoaty *et al.*, 2013; Huang *et al.*, 2017; Huang *et al.*, 2011; Lima-Garcia *et al.*, 2011; Xu *et al.*, 2013; Xu *et al.*, 2010). In carrageenan-induced inflammatory pain, intraplantar administration of RvD1 attenuated paw oedema and heat hyperalgesia (Xu *et al.*, 2010). Single intrathecal administration of RvD1 or AT-RvD1 rapidly decreased thermal pain thresholds and reduced mechanical hypersensitivity in behavioural tests in the carrageenan model (Abdelmoaty *et al.*, 2013; Xu *et al.*, 2010). The spinal neuronal mechanisms underlying these neurophysiological effects on pain behaviour have yet to be elucidated.

An *ex vivo* study investigating the roles of resolvins in nociceptive processing using isolated spinal cord slices indicates that RvD1 reduces presynaptic glutamate release (only in the presence of TNF-α) and postsynaptic NMDA receptor mediated currents (Xu *et al.*, 2010). However, spinal nociceptive transmission in pathological conditions can be modulated by several neuronal networks i.e. excitatory and inhibitory interneurones, ascending input from the periphery and descending input from the higher centres of the central nervous system including the rostral ventral medial medulla and periaqueductal grey (Hunt *et al.*, 2001; West *et al.*, 2015).

To understand putative mechanisms of AT-RvD1 on spinal nociceptive processing following acute inflammation *in vivo*, this

chapter applied an electrophysiological approach to study spinal nociceptive processing in a carrageenan-induced inflammatory pain model, at a late time point (>24 h. post model induction), allowing a certain degree tissue resolution. Spinal gene expressions of receptors and enzymes involved in the resolvin signalling system were also investigated.

3.2. Study hypothesis and objectives

The study hypothesis is spinally applied AT-RvD1 inhibits the evoke responses of spinal WDR neurones following a period of overt peripheral inflammation and this event is accompanied by the plasticity of the resolvin system in the spinal cord.

The objectives of these studies were to;

- investigate acute effects of spinal administration of AT-RvD1 on evoked spinal WDR neuronal responses in carrageenan-induced acute inflammatory pain model, at a late time point
- examine alteration in expression of genes relevant to resolvin system in spinal cord following extended period of overt inflammation

3.3. Methods

3.3.1 Carrageenan-induced inflammatory pain

Under brief anaesthesia, male Sprague-Dawley rats weight ranged 200-250 g, were injected with either intraplantar 2% γ-carrageenan 100 μl or control vehicle (0.9 % saline) into the glabrous surface of the left hind paw (detailed in **Chapter 2 Section 2.2**). Paw withdrawal threshold and weight bearing asymmetry were assessed

in a blinded fashion at baseline, 2 and 8 h post carrageenan injection (detailed in **Chapter 2 Section 2.3**). Note that, in this chapter the pain behaviour at 24 h was not measured due to the limitation of the time management with the persons who could provide supervision for electrophysiology recording since I injected carrageenan to a rat and set up the recording of the same rat on the next day. To maintain the best practice for animal welfare, when I began training (in the first 3-4 months), I avoided performing the recording alone but did under close supervision from competent colleagues/supervisor. The circumference of the ipsilateral paw was measured at baseline and 24 h post carrageenan injection as previously described (Jhaveri *et al.*, 2008; Morris, 2003) (detailed in **Chapter 2 Section 2.6**). Paw circumference was measured prior to and approximately 24 h post intraplantar injection.

3.3.2 *In vivo* spinal electrophysiology

At 24 h following intraplantar injection, rats were prepared for in *vivo* spinal electrophysiology (detailed in **Chapter 2 Section 2.4**).

3.3.3 Spinal drug applications

Saline and carrageenan pre-treated rats received one of the following spinal treatments;

- Phosphate buffered saline (PBS) as a vehicle 50 μl (saline n=5, carrageenan n=10);
- AT-RvD1 (Cayman Chemical, USA) 15 ng in 50 μl PBS (saline n=10, carrageenan n=10);
- Butoxy carbonyl-Phe-Leu-Phe-Leu-Phe (BOC-2) (Phoenix Pharmaceuticals, Inc., USA) 50 μg in 50 μl 3% Tween80+0.5% ethanol in saline (carrageenan n=9);
    - BOC-2 is a peptide that acts an FPR2/ALX receptor antagonist with EC50 2.5 x10^{-7}M in inhibiting neutrophil

superoxide production (Stenfeldt *et al.*, 2007) and has been used as a tool to probe the function of A PR2/ALX receptor (Hayhoe *et al.*, 2006; Machado *et al.*, 2006; Walther *et al.*, 2000). The data for the selectivity of BOC-2 are very limited. The peptide itself had no effect on the release of β-glucuronidase from rabbit peritoneal neutrophils suggesting the limited action where there is no agonist (Day *et al.*, 1980). This peptide has, however, been reported to be a nonselective antagonist for both FPR1 and FPR2/ALX in some studies (Babbin *et al.*, 2006; Hayhoe *et al.*, 2006). The concentration (50 μg/50 μl) was chosen based on a previous pain behavioural studied using intrathecal injection of BOC-2 (Pei *et al.*, 2011)

- BOC-2 50 μg in 50 μl 3% Tween80+0.5% ethanol in saline for 15 min and followed by AT-RvD1 15 ng in 50 μl PBS (carrageenan n=9);
- 3% Tween80+0.5% ethanol in saline 50 μl as a vehicle for BOC-2 (carrageenan n=6);

Responses of the spinal WDR neurones were evoked using trains of 16-electrical stimulation every 15 minute and then quantified as described (**Chapter 2 Section 2.4.7**). Effects of the treatments were followed for 60 min post-treatment. Because of the difficulty to obtain consistent evoked neuronal responses following the application of mechanical stimulation (using von Frey filaments), therefore, only the electrical stimulus was applied. This might be due to the slippery of the inflamed skin following the period of inflammation (24 h).

3.3.4 Gene expression study

RNA extraction, cDNA synthesis and analysed of data in this section were carried out with assistance from Dr. James Burston.

In separate cohorts of intraplantar saline (n=6) and carrageenan (n=5) injected rats, pain behaviour was assessed as previously described. Carrageenan-inflammed rats displayed significant elevation of weight bearing asymmetry and reduction in PWT compared to control rats, as shown in **Supplementary Figure 1**. At 30 h post carrageenan induction. The lumbar enlargement (L4-L6) of the spinal cord was dissected free. The ipsilateral quadrants of spinal dorsal horn were collected. RNA was extracted using the phase separation method and assessed the quantity and quality (detailed in **Chapter 2 Section 2.7**). Complimentary DNA (cDNA) was synthesised by reverse transcription from 500 ng total RNA using SuperScript III reverse transcriptase (Invitrogen, UK) (detailed **in Chapter 2 Section 2.7**)

Gene expression quantification was performed using Taqman® qPCR as previously described (Erhuma *et al.*, 2007; Sagar *et al.*, 2011). cDNA from all samples was pooled to obtain a super neat source. Four serial 1 in 4 dilutions (in RNase free water) specifically, 1:4, 1:16, 1:64 and 1:256 were then made up. These were used for the production of a 5 point standard curve. cDNA samples were diluted to 1:16, a mid point of the standard curve. Diluted pooled cDNA and each sample were mixed with reagents shown in **Table 3.1A** and leaded into Taqman® RNase P 96-well plates (Applied Biosystem, USA) in triplicate. The plates were then incubated at 95°C for 20 sec, then 40 cycles at 95°C for 1 sec and 60°C for 20 sec in Step OnePlus® Thermal cycler (Applied Biosystem, USA). Cycle thresholds (C_T) were recorded and used for further calculation. The quantity target of genes was calculated by constructing a standard curve of C_T versus quantity then calculating quantity of target genes using recorded C_T. Expression levels of target genes were then normalised relative to β-actin. Genes examined were FPR2/ALX, ChemR23, 5-LOX, 15-LOX,

COX-2, 5-lipoxygenase activating protein (FLAP) and interleukin-10 (IL-10). Primers and probes were based on a previous study (Okine *et al.*, 2012) or designed by PrimerExpress 3.0 software and synthesised by MWG Biotech (Germany); sequences shown in **Table 3.1B**.

Table 3.1 Reagents and master formulae used in gene expression study. (**A**) Master formula for qPCR and (**B**) sequences of primers and probes of genes of interest.

A

Component	Volume (ul) /reaction	Concentration
cDNA sample 100 ng/ml	3	23 ug/ml
Taqman gene expression Fast Master Mix	6.5	
Forward primer 10 pM	0.375	0.2885 pM
Reverse primer 10 pM	0.375	0.2885 pM
Taqman Probe 10 pM	0.25	0.1923 pM
RNase free water	2.5	
Total volume	13	

B

Gene	Forward primer	Reverse primer	Taqman probe
Beta actin	AGGCCATGTACGT AGCCATCCA	TCTCCGGAGTCCAT CACAATG	TGTCCCTGTATGCC TCTGGTCGTACCAC
ALX	CTTGGACCGCTGC ATTTGT	CCTTCCTAGCCAG GCTCACA	CAGTCTGGGCTCA GAACCACCGC
ChemR23	AGGACCTACCCTC GAGTTCTATTCT	CGTAGATGCTGGA GTCGTTGTAA	TCCAAAGAGATGG AGTACGA
COX-2	GGCACAAATATGAT GTTCGCA	CTCGCTTCTGATCT GTCTTGA	TCTTTGCCCAGCAC TTCACTCATCAGTT T
FLAP	CCCCACTTTCCTTG TGGTACTC	TGCCTCACGAACA GATACATCAG	AGCCAAGTCCCCG CCGCCT
IL-10	GAAGCTGAAGACC CTCTGGATACA	CCTTTGTCTTGGAG CTTATTAAAATCA	CGCTGTCATCGATT TCTCCCCTGTGA
5-LOX	TGGTGTCTGAGGT GTTCGGTAT	GGCAATGGTGAAC CTCACATG	CCCTTTTCAAGCTG CTG
15-LOX	TGATGCCTGATGG ACAACTCTT	CCG AGG GCG TGA AAA TAG G	CCATAGCCATCCAG CTTGAACTTC CCA

3.4. Results

3.4.1 Carrageenan mediated hindpaw inflammation resulted in alterations in WDR neuronal responses

Baseline paw circumferences of control and carrageenan rats were comparable, 25 ± 0.3 mm and 26 ± 0.2 mm, respectively. Carrageenan rats exhibited robust weight bearing asymmetry and lowered PWTs at 2 and 8 h post injection, compared to control rats ($p< 0.0001$, two-way ANOVA with Sidak's post hoc test; **Figure 3.1 A, B**). Intraplantar injection of carrageenan also produced a profound paw swelling, evident at 1-2 h and significant at 24 h post-injection, compared to saline treated rats ($p< 0.0001$, two-way ANOVA with Sidak's post hoc test, **Figure 3.1C**).

WDR neurones (n=59) were characterised in a total of 59 rats (control n=15 and carrageenan n=44) at 24 h after intraplantar injection of saline or carrageenan (**Table 3.2**). The mean depths of neurones of all groups were within the 500-1000 μm range, corresponding to laminae V-VI. Comparison of thresholds of evoked responses of WDR neurones revealed significantly higher thresholds for Aβ ($p<0.01$ Mann Whitney U test) and C-fibre ($p<0.05$ unpaired t-test) evoked responses in the carrageenan group, compared to control. Aβ and C-fibre latencies were not altered. Aδ-fibre evoked responses of WDR neurones were significantly facilitated in carrageenan ($p<0.01$ Mann Whitney U test, corresponding to 163% of baseline) compared to control rats (see also in **Figure 3.3 A**). There was a trend towards an increase in the input response in carrageenan rats, but significance was not reached. There were no differences in the magnitudes of the other evoked responses of the WDR neurones in the carrageenan group compared to saline controls. Twenty two neurones (58%) in carrageenan rats displayed higher C-

fibre responses than the mean of control rats (431 ± 49 APs, **Table 3.2** and **Figure 3.3 B**).

Analyses of post-stimulus histograms of action potentials (PSTH, **Figure 3.3C and D**) revealed that neurones in carrageenan rats had significantly greater area under the curve (AUC, $p<0.05$ Mann Whitney U test) and higher peak responses in Aβ and Aδ ranges (0-90 msec post-stimulus) compared to control ($p<0.01$ Mann Whitney U test) whereas time to peak responses were comparable.

Figure 3.1 Figure 1 Carrageenan evoked pain behaviour and paw inflammation. Intraplantar injection of 2% λ-carrageenan significantly increased weight bearing asymmetry **(A)** and decreased mechanical PWT **(B)** from 2 to 8 h post injection and produced a profound paw swelling **(C)** at 24 h. ****p<0.0001 vs versus saline-treated group, two-way repeated measure ANOVA with Sidak post hoc test. Saline n=15 and carrageenan n=44. Modified from Meesawatsom P. *et al* 2016.

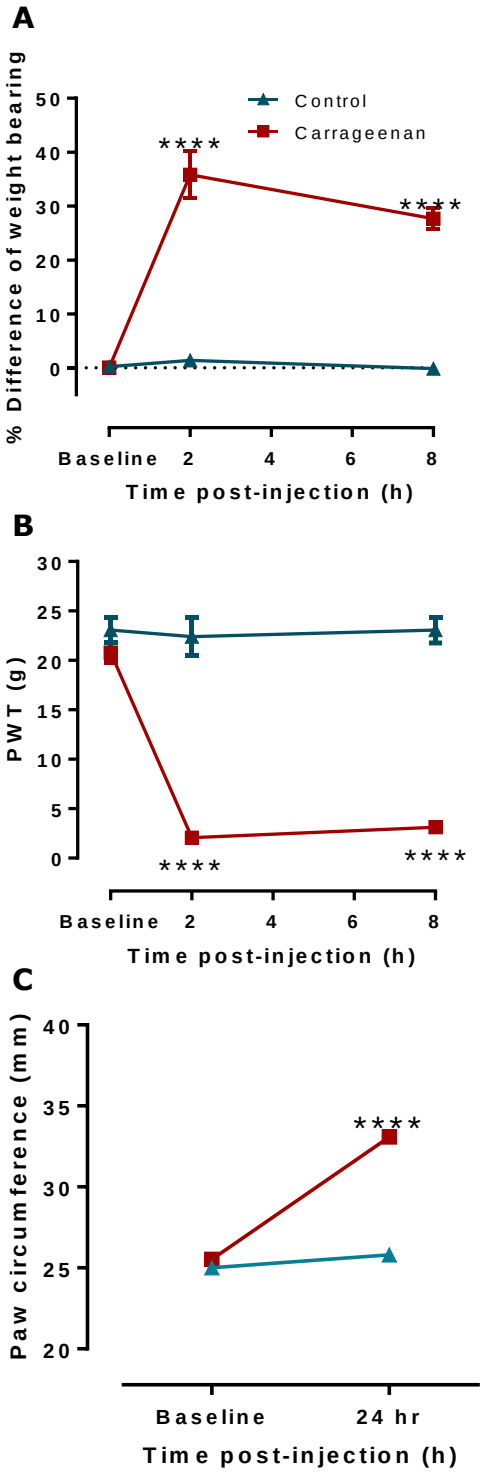

Table 3.2 Comparison of characteristics of WDR neurones in carrageenan versus saline-treated rats.

	Control (n=15)	Carrageenan (n=44)	Carrageenan (% control)
Depth (μm)	677 ± 31	747 ± 21	NA
Threshold (mA)			
Aβ	0.14 ± 0.01	0.19 ± 0.01##	130
C	1.47 ± 0.08	1.81 ± 0.10*	124
Latency (ms)			
Aβ	7.6 ± 0.79	7.3 ± 0.40	96
C	182.3 ± 8.76	191.0 ± 8.50	105
Electrical-evoked responses (number of APs)			
Aβ[a]	121 ± 10	126 ± 8	104
Aβ[b]	143 ± 10	145 ± 8	101
Aδ[b]	91 ± 16	148 ± 17##	163
C[b]	431 ± 49	497 ± 41	114
PD[b]	352 ± 49	381 ± 37	106
Input[b]	271 ± 51	368 ± 60	136
WU[b]	505 ± 60	502 ± 46	100

Characteristics of spinal WDR neurones recorded at approximately 30 h. following intraplantar injection of 2% λ-carrageenan or saline. *p<0.05 unpaired t-test, ##p<0.01 Mann Whitney U test, [a] Responses electrically evoked by 3xAβ fibre threshold, [b] Responses electrically evoked by 3xC-fibre threshold, APs; action potentials, NA; not applicable. Modified from Meesawatsom P. *et al* 2016.

Figure 3.3 Alteration of WDR neuronal responses after carrageenan induction. Comparison of Aδ (**A**) and C-fibre (**B**) responses. Dotted lines in (**A**) and (**B**) indicate mean responses in control rats. **(C and D)** Post-stimulus histograms of action potentials generated by spinal WDR neurons upon 16 electrical stimulations delivered to the hind paw in carrageenan compared to control rats. Neurones in carrageenan rats had significantly greater area under the curve (AUC) and higher peak responses in Aβ and Aδ ranges (0-90 msec post-stimulus) compared to control. Responses were evoked by 3XC-fibre threshold and recorded in 2 msec bins. $^{\#}p<0.05$, $^{\#\#}p<0.01$ Mann-Whitney U test. Control n= 15, Carrageenan n=44.

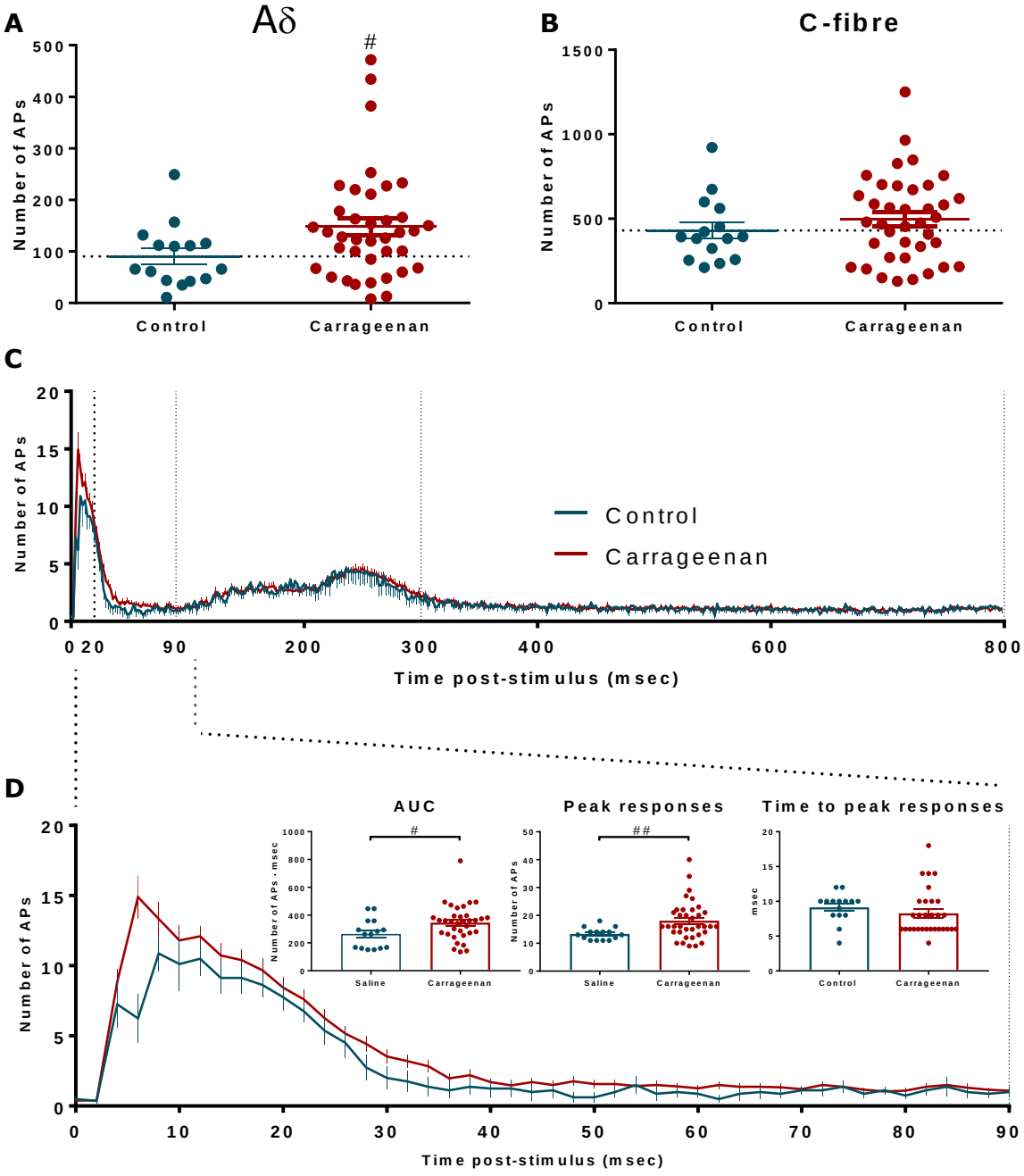

3.4.2 Spinal AT-RvD1 inhibited responses of WDR neurones in the carrageenan model of hindpaw inflammation

The mean time of spinal administration of AT-RvD1 was 29.2±0.2 h (ranged 26.3-32.2 h) post intraplantar injection of carrageenan / saline. Effects of AT-RvD1 versus PBS on evoked responses of spinal neurones were determined for 60 min after application to the surface of the spinal cord. Spinal administration of PBS did not alter any parameters in either control or carrageenan rats. In the carrageenan treated group, responses of 9 out of 10 neurones were inhibited by spinal administration of AT-RvD1. Maximal inhibition of evoked responses was observed between 25-39 min post-treatment. Spinal administration of AT-RvD1 (15 ng) did not significantly alter Aβ-fibre evoked responses in carrageenan-treated rats (**Figure 3.4A**). This treatment did however significantly attenuate Aδ- and C-fibre, PD and WU responses of WDR neurones in carrageenan rats, but not control rats (**Figure 3.4 B, C, D, F** and **Table 3.3**). There was a significant increase in input responses following treatment with spinal administration of AT-RvD1 in control rats (Figure 3.4E). Comparison of AUC of the stimulus-response curve of WU following 16 electrical stimulations in carrageenan-treated rats received AT-RvD1 versus PBS was significantly different (**Figure 3.4G**, $p<0.05$ Wilcoxon test). An example of evoked responses of a WDR neurone following AT-RvD1 administration in a carrageenan rat is shown in **Figure 3.4H**.

Figure 3.4 Effect of spinal administration of AT-RvD1 on evoked responses of WDR neurons. (A-F) Spinal administration of AT-RvD1 selectively inhibited nociceptive fibre-evoked responses of spinal WDR neurones in carrageenan-treated rats. In saline-treated rats (teal bars), electrically evoked responses were not altered by PBS (n=5) vehicle or AT-RvD1 (n=10), except the input response which was slightly facilitated by AT-RvD1 (third and fourth bars). AT-RvD1 (15 ng/50μl) resulted in a non-significant decrease in Aβ fibre-evoked responses (p=0.0781) in carrageenan-treated rats (red bars, n=9). **(B-F)** Spinal AT-RvD1 significantly supressed WDR neurone responses evoked by electrical stimulation of Aδ and C-fibres as well as PD, input and WU responses, when compared to pre-drug responses. **(G)** An illustration of the effects of AT-RvD1 on WU of WDR neurones following 16 electrical stimulations in carrageenan-treated rats. At 15 min post AT-RvD1, the AUC was significantly lowered when compared to baseline (**G inset**). **(H)** An example of the electrically-evoked responses of a WDR neurone recorded for 60 min following AT-RvD1 application in a carrageenan-treated rat.
Data in **Figure A-F** are mean maximal number of action potentials post drug application. *p<0.05, **p<0.01 paired t-test, #p< 0.05, #p<0.001 Wilcoxon test, n=8-10 group, except for Saline-PBS n=5. APs; action potentials. Reproduced from Meesawatsom P. *et al* 2016.

Figure 3.4

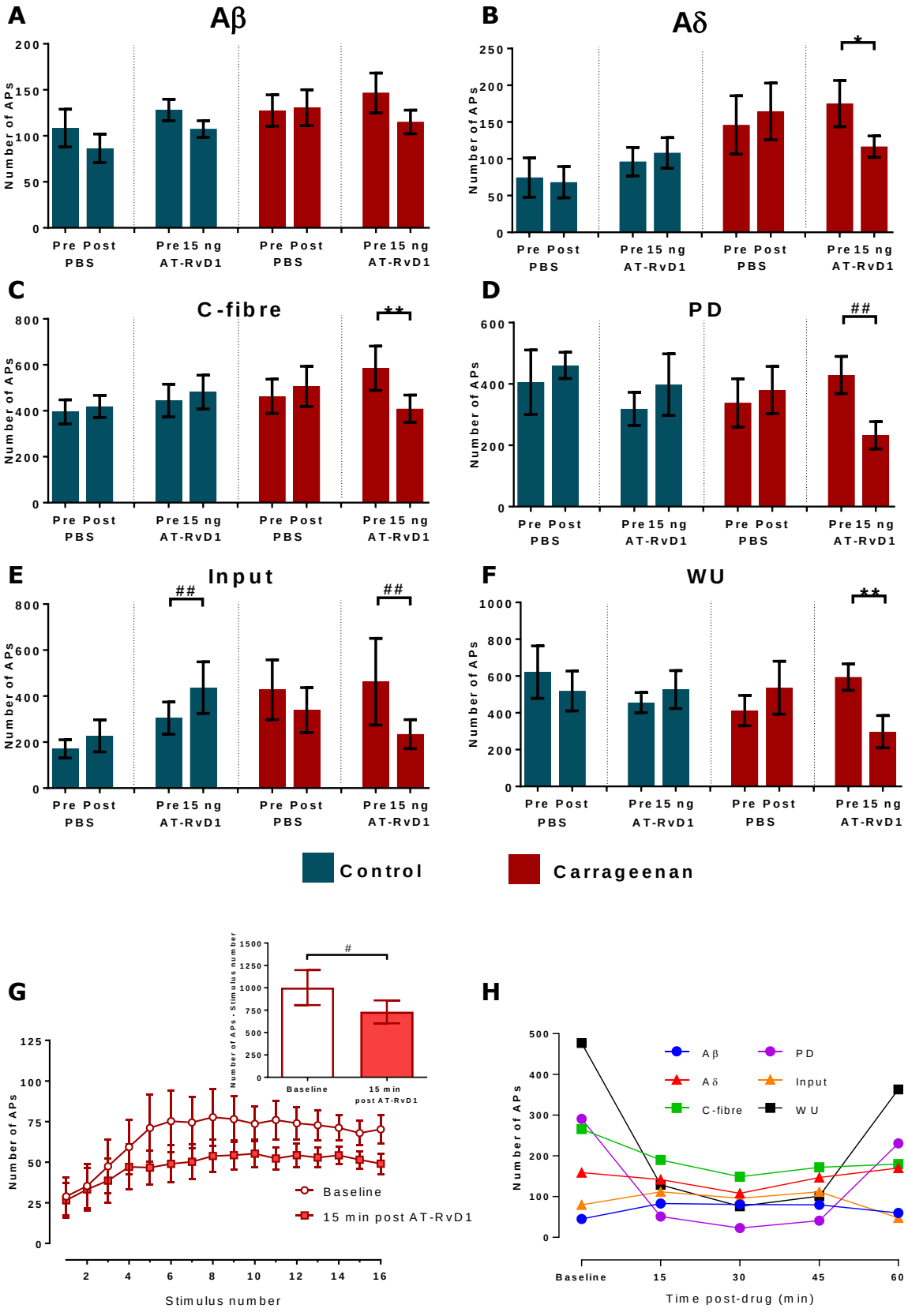
A
Aβ
Number of APs
Pre Post PBS
Pre 15 ng AT-RvD1
B
Aδ
*
C
C-fibre
**
D
PD
##
E
Input
##
##
F
WU
**
Control
Carrageenan
G
Number of APs - Stimulus number
#
Baseline
15 min post AT-RvD1
Stimulus number
H
Aβ
Aδ
C-fibre
PD
Input
WU
Time post-drug (min)

3.4.3 Investigating functional roles of FPR2/ALX receptor in spinal cord following overt peripheral inflammation and effects on AT-RvD1 action

To investigate the functional roles of the spinal FPR2/ALX receptor in overt inflammation and the effects of AT-RvD1 on evoked responses of spinal neurones, the effects of spinal administration of BOC-2 (50 μg/50 μl) alone or with AT-RvD1 15 μl/50 μl were tested in carrageenan rats. Spinal administration of either vehicle of BOC-2 (n=6, data shown in **Figure 3.5**) or BOC-2 alone did not alter the evoked firing of spinal neurones compared to pre-drug responses after following up to 60 min (n=9, **Figure 3.6** blue bars and **Figure 3.7** blue lines). In contrast to AT-RvD1 alone, AT-RvD1 15 ug administered following a 15 min pre-treatment with BOC-2 did not alter evoked neuronal responses in carrageenan rats (n=8, **Figure 3.6** red bars, **Figure 3.7** red lines and **Table 3.3**). The mean maximal percentage inhibition of Aδ, C-fibre, input and WU responses of WDR neurones produced by AT-RvD1 alone were significantly higher than those produced by AT-RvD1 in the presence of BOC-2 ($p < 0.05$ Kruskall-Wallis test with Dunn's post hoc test, **Table 3.3**) suggesting FPR2/ALX receptor dependent action of AT-RvD1.

Figure 3.5 Effect of 3% Tween80 +0.5% ethanol in saline, a vehicle for BOC-2 on evoked responses of WDR neurone in carrageenan rats. The vehicle had no significant effect on WDR neurones when compared responses of pre versus post spinal administration. n=6.

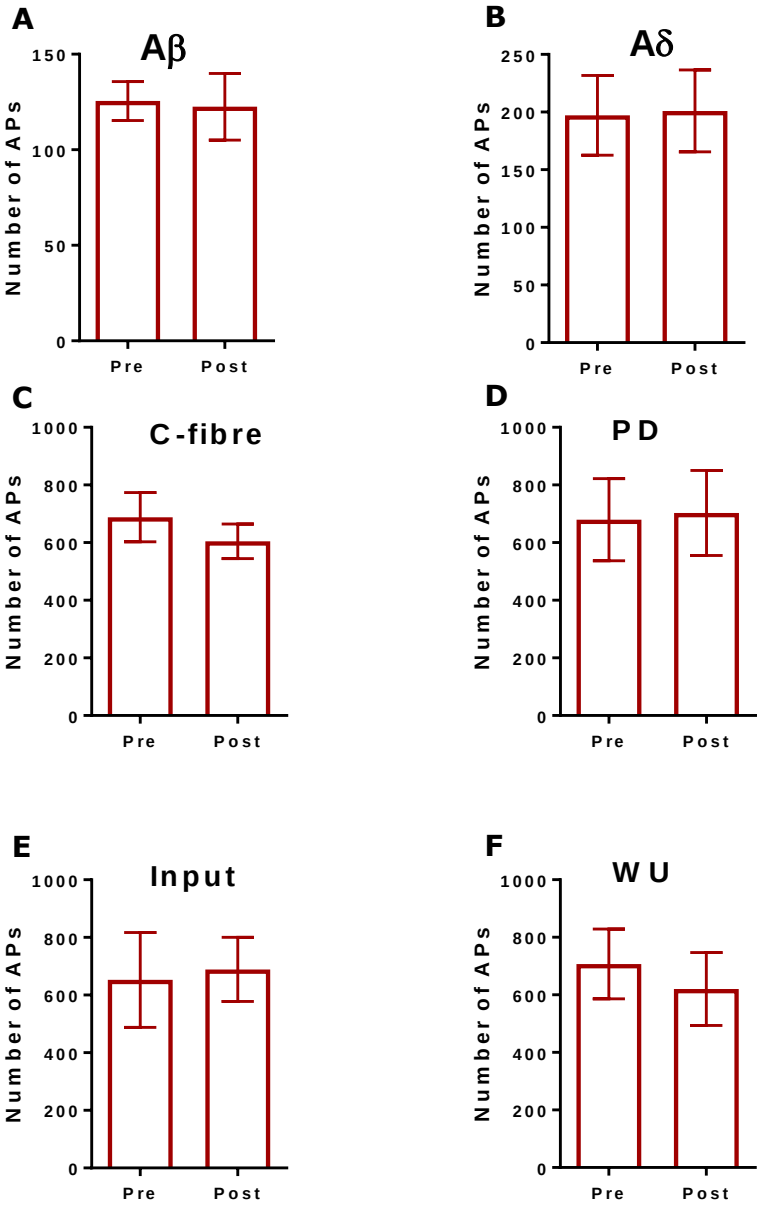

Figure 3.6 Effects of an FPR2/ALX receptor antagonist, BOC-2 on spinal WDR neuronal responses when administered alone and prior to AT-RvD1 in carrageenan rats. Spinal administration of BOC-2 50 ug 50/ul alone (blue bars, n=9) did not alter electrical evoked responses of WDR neurones in carrageenan rats when compared to pre-drug responses (shown as maximal changes within 60 min post administration). A 15 min pre-administration of BOC-2 abolished inhibitory effects of AT-RvD1 15ng/50ul in carrageenan rats (red bars, n=9).

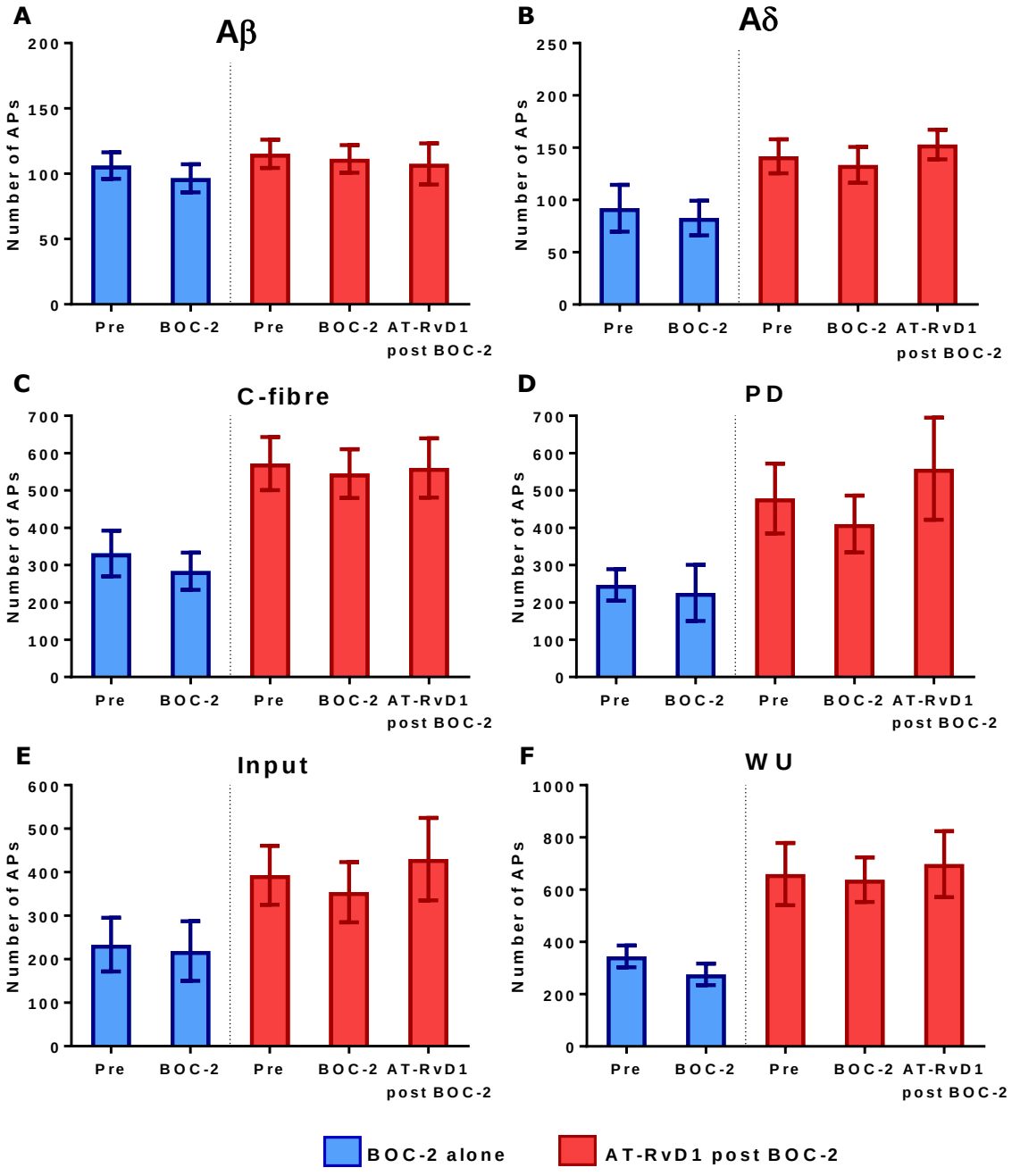

Figure 3.7 Time course of the inhibitory effects of AT-RvD1 on WDR neuronal responses in carrageenan rats when administered alone or post BOC-2. AT-RvD1 15 ng/50ul alone (n=9) inhibited Aδ, C-fibre, PD, input and WU responses of WDR neurones; maximal effect observed at 15-30 min post-administration. Such effects were abolished by pretreatment of BOC-2 (n=9).

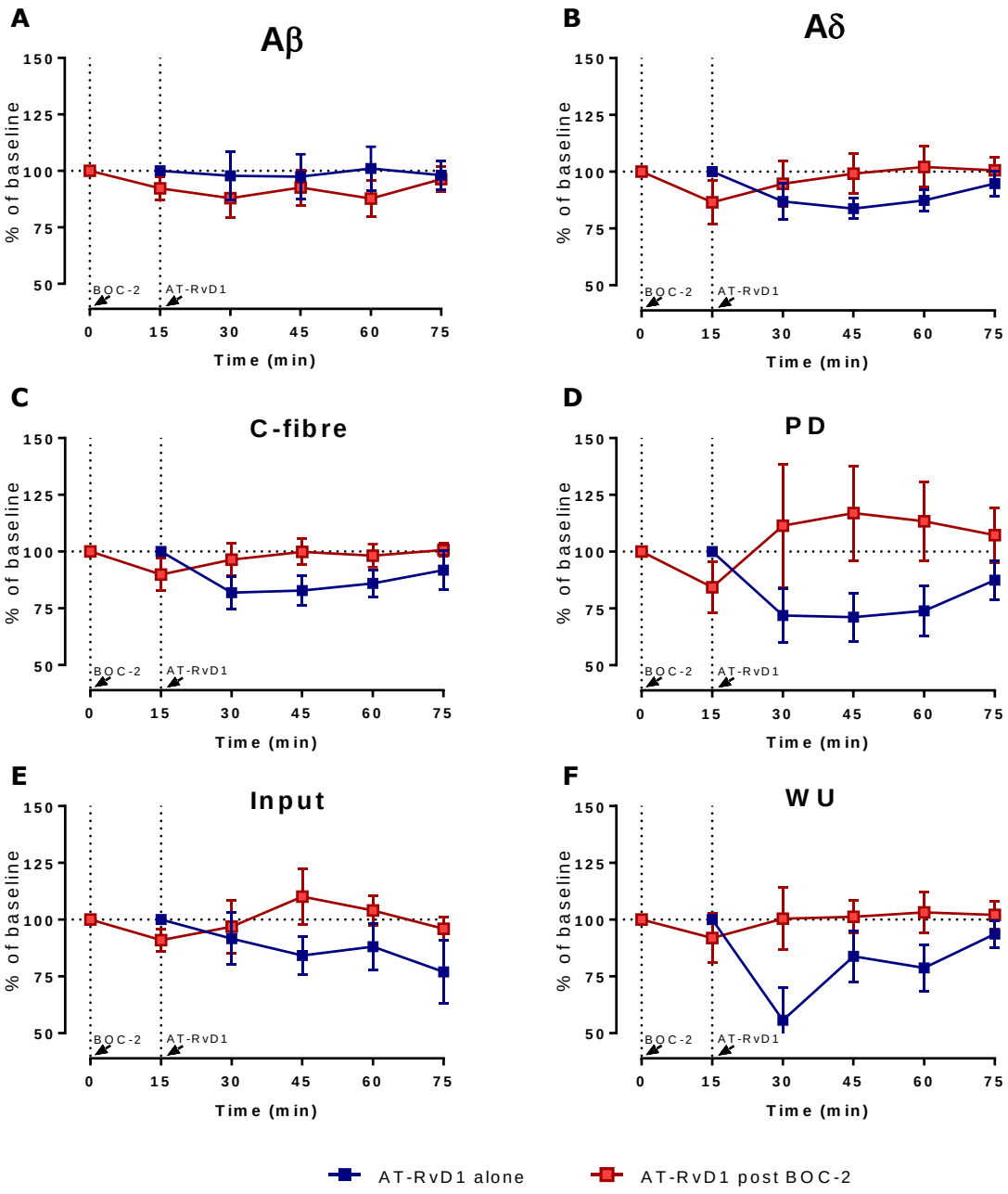

Table 3.3 Mean maximal percentage inhibition of evoked responses by AT-RvD1 in control and carrageenan rats.

	Group effect (% maximal inhibition)		
	Control	Carrageenan	
	AT-RvD1 (n=10)	AT-RvD1 (n=9)	AT-RvD1 post BOC-2 (n=8)[a]
Aβ	2±9	11±13	5±9
Aδ	-14±12	27±7[$]	-13±8[#]
C	-10±10	29±5[$$]	-1±6[#]
PD	-19±23	46±8	-9±14[#]
Input	-19±15	41±8[$]	-9±14
WU	-10±15	53±12[$$]	-1±7[#]

Comparison of group effects of AT-RvD1 (15 ng/50μl) on electrically evoked responses of spinal WDR neurones in carrageenan-treated rats versus saline-treated rats and the effect of pre-treatment with BOC-2 50μg/50μl (expressed as % maximal inhibition). AT-RvD1 significantly inhibited a number of evoked parameters in carrageenan-treated-rats but not saline-treated rats. Pretreatment with BOC-2 significantly prevented the inhibitory effects of AT-RvD1 for most of parameters. Note that negative values indicate facilitation. [$]$p<0.05$, [$$]$p<0.01$: compared to AT-RvD1 in saline-treated group; [#]$p<0.05$: compared to AT-RvD1 in carrageenan-treated group without BOC-2, Kruskall-Wallis test with Dunn's post hoc test. [a]One neurone was inhibited by BOC-2, and was excluded from further analysis. Reproduced from Meesawatsom P. *et al* 2016.

3.4.4 The impact of peripheral inflammation on the spinal expression of the resolvin receptors and related enzymatic pathways

In separate groups of inflamed rats with developed pain behaviour (**Figure 3.8)**, ipsilateral dorsal horns of the spinal cord were collected at 30 h following intraplantar carrageenan injection for gene expression studies. β-actin mRNA expression was comparable in both groups of rats (control 0.3068 ± 0.013 versus carrageenan 0.2965 ± 0.016, **Figure 3.9A**) serving as a suitable reference gene for relative comparisons. Following intraplantar injection of carrageenan, levels of FPR2/ALX mRNA remained stable in the dorsal horn of the spinal cords, compared to control rats (**Figure 3.9B**). Carrageenan treatment was associated with a significant increase (1.5 fold, $p<0.05$, Mann Whitney U test) in ChemR23 mRNA expression (**Figure 3.9C**). Focusing on enzymes involved in resolvin biosynthesis, 5-LOX mRNA expression in the dorsal horn of the spinal cord was similar in carrageenan and saline-treated rats (**Figure 3.9D**). However expression of the 5-LOX activating protein FLAP was significantly higher (1.3 fold increase, $p<0.05$, Mann Whitney U test) in the dorsal horn of the spinal cord of carrageenan rats, compared to control (**Figure 3.9F**). Expression of 15-LOX mRNA level was significantly lower in carrageenan rats when compare to control rats ($p<0.05$, Mann Whitney U test; **Figure 3.9E**).

Figure 3.8 Pain behaviour and paw inflammation of rats used in spinal gene expression study. ****p<0.0001, **p<0.01 vs versus saline-treated group, two-way repeated measure ANOVA with Sidak post hoc test. Control (saline) n=6 and carrageenan n=5.

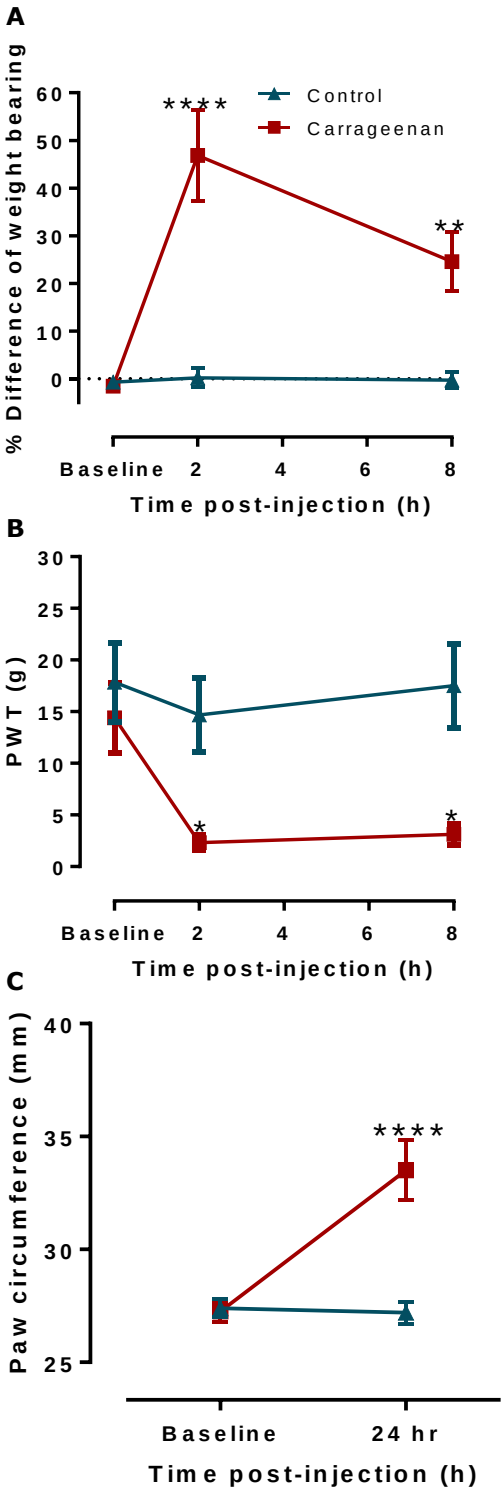

Figure 3.9 Changes in gene expression in spinal cord post intraplantar injection of saline or carrageenan. The ipsilateral dorsal horn of spinal cords were collected at 30 h post injection; mRNA levels are relative to (**A**) β-actin. (**B** and **C**) mRNA levels of receptors for resolvin D and resolvin E – FPR2/ALX and ChemR23 , respectively, (**D-F**) enzymes involved in resolvin biosynthesis-5-LOX and 15-LOX, activating protein for 5-LOX – FLAP, (G) pro-inflammatory enzyme – COX-2 and (H) anti-inflammatory cytokine – IL-10. Data expressed as mean ± S.E.M. *p<0.05 Mann Whitney U test. Control n=6, carrageenan n=5. Reproduced from Meesawatsom P. *et al* 2016.

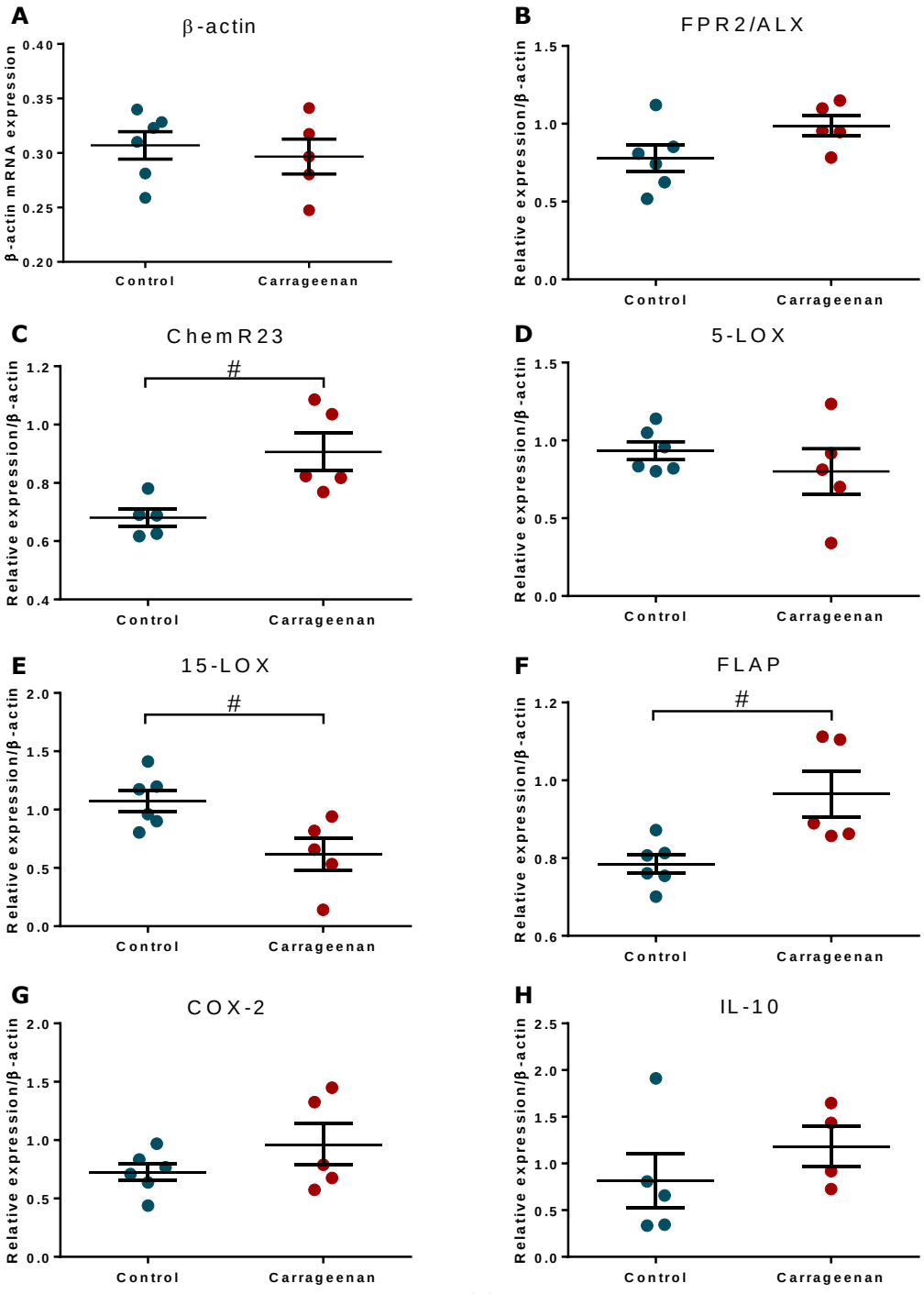

3.5. Discussion

Previous studies reported acute inhibitory effects of spinal resolvins on behavioural responses to painful stimuli (Abdelmoaty *et al.*, 2013; Huang *et al.*, 2011; Xu *et al.*, 2010). The results reported here demonstrate that spinal administration of AT-RvD1 did not alter physiological spinal nociceptive responses, but significantly attenuated evoked nociceptive responses of dorsal horn spinal neurones following a 24 hour-period of peripheral inflammation of the hindpaw. At the timepoint of the novel effects of spinal AT-RvD1, we demonstrate that the model of hindpaw inflammation is associated with changes in the dorsal horn gene expression of enzymes related to resolvin pathways.

3.5.1 The chosen time points for evaluation of the effect of AT-RvD1in inflammatory pain

The carrageenan model was associated with robust pain behaviour, altered weight bearing and decreased PWT, consistent with previous studies at early timepoints (Hargreaves *et al.*, 1988; Jhaveri *et al.*, 2008). In the present study, we extended the period following carrageenan injection to allow the characterisation of spinal events at timepoints more relevant to injuries associated with acute inflammation and pain seen clinically, and the expected timecourse of the activation of the endogenous resolution pathways (Bannenberg *et al.*, 2005).

3.5.2 Alteration of WDR neurone responses after carrageenan induction

At the timepoint of spinal neuronal recordings, carrageenan treatment was associated with a significant increase in neuronal responses in myelinated fibre latencies, including enhanced Aδ-evoked responses and higher AUC and peak responses in Aβ and Aδ latencies.

A-fibre nociceptors are classified into 2 categories, Type I and II, based on the nature of responses to stimulus modalities (heat, mechanical), electrophysiological properties (responses peak, latency and conduction velocity) anatomical locations and sensitisation upon heat injury. The properties of type I A-fibre nociceptor are conduction velocity (25-55 m/sec) falling into a category between both Aβ and Aδ fibres (35-75 and 5-35 m/sec) (Ringkamp *et al.*, 2013), prevalent in glabrous skin (Treede *et al.*, 1995) and becoming sensitised to heat injury. The findings that enhanced responses expanded across Aβ and Aδ bands revealed in PSTH alongside with the anatomical location therefore provide a suggestion that sensitisation of type I A-fibre nociceptors may be involved in the facilitated responses in this latency window in the carrageenan model at this timepoint. All other evoked responses of WDR neurones were similar in saline and carrageenan rats. Clearly a limitation of quantifying the responses of WDR neurones at this later timepoint was that baseline neuronal responses pre-carrageenan injection could not be characterised, and therefore only population changes in response can be reported. Previously, WDR neuronal responses characterised before and at 3 h. post carrageenan injection were reported to exhibit increased C-fibre evoked responses in around half the group, and the rest had decreased responses (Stanfa *et al.*, 1992). In my study, 58% of neurones in carrageenan rats had higher baseline C-fibre responses compared to the mean of in non-inflamed rats. Despite the neuronal characterisation performed using a different approach, the proportion of facilitated neurones is similar to previously reported (Stanfa *et al.*, 1992).

3.5.3 AT-RvD1 selectively inhibits spinal pain processing in inflammatory pain via FPR2/ALX receptor activation

Spinal administration of AT-RvD1 attenuated C-fibre evoked responses of spinal neurones in carrageenan rats, but not in saline controls. The magnitudes of the inhibitory effects of AT-RvD1 were comparable for both non-facilitated (input) and facilitated (post-discharge and WU) C-fibre evoked responses of WDR neurones. WU was the most sensitive to the effects of AT-RvD1 (53% inhibited). These data provide for the first time a neurophysiological basis for the effects of a resolvin molecule on spinal nociception *in vivo*, and reveal that these inhibitory effects are only evident under certain conditions. My results are in agreement with other *ex vivo* spinal cord slice studies which demonstrated that RvE1 selectively reduces excitatory post synaptic potentials in the presence of the pro-inflammatory cytokine tumour necrosis factor-α (TNF-α), by inhibiting N-methyl-D-aspartate (NMDA) receptor activation (Xu *et al.*, 2010) and RvD2 selectively attenuates long- term potentiation of spinal neurones from inflamed animals (Park *et al.*, 2011). To date the reported analgesic and anti-inflammatory effects of resolvins in animal pain models (Abdelmoaty *et al.*, 2013; Lima-Garcia *et al.*, 2011; Xu *et al.*, 2013; Xu *et al.*, 2010) were hypothesised to be mediated by both peripheral and central nervous system sites of action (Xu *et al.*, 2010). The demonstration of a direct spinal effect on neuronal responses *in vivo* provides a neuronal basis for the behavioural evidence that spinal AT-RvD1 reduces carrageenan-induced mechanical hypersensitivity at earlier timepoints (Abdelmoaty *et al.*, 2013). Time-course analysis of the effects of AT-RvD1 revealed 15 min onset and peak at 30 min post-administration, with responses returning to control levels within the hour. The rapid onset of the inhibition suggests the immediate effect is independent of changes in gene expression. Although AT-RvD1 is more resistant to metabolism compared to RvD1 (Sun *et al.*, 2007), the short-lived nature of action of these bioactive lipids is a disadvantage that needs to be overcome if they are to be harnessed as analgesics (Arita *et al.*, 2006; Orr *et al.*, 2015).

FPR2/ALX is crucial for the immediate inhibitory effects of AT-RvD1 on nociceptive processing *in vivo*. The inhibitory effects of AT-RvD1 on evoked responses of WDR neurones were blocked by BOC-2, an antagonist for FPR2/ALX receptor, supporting an essential role of the receptor in spinal analgesic action of AT-RvD1 as presented here and also several anti-inflammatory mediators such as annexin1 (Pei *et al.*, 2011), lipoxin A4 (Martini *et al.*, 2016). Several mechanisms can be postulated for the inhibitory effects of AT-RVD1 via FPR2/ALX activation. FPR2/ALX is thought to be coupled to Gi (Chiang *et al.*, 2006; Fredman *et al.*, 2014). In principle, FPR2/ALX-mediated signalling is capable of reducing neuronal excitability by attenuating TRPA1, TRPV3 and TRPV4 activation (Bang *et al.*, 2012; Bang *et al.*, 2010). Potential inhibition on PKA mediated by AT-RvD1-activated signalling via Gi may also counteract the glycinergic dysfunction and result in immediate inhibitory effects on neuronal responses.

The findings of unaltered spinal of FPR2/ALX mRNA level and unaltered evoked neuronal responses following spinal administration of BOC-2 alone in inflamed rats suggest that FPR2/ALX has limited tonic inhibition of spinal neuronal activity in the presence of overt inflammation. These findings are in line with unaltered FPR2/ALX protein level in previous reports using the carrageenan model (Svensson *et al.*, 2007) and other pain models (Hu *et al.*, 2012; Wang *et al.*, 2014b). However, the possibility that there are changes in FPR2/ALX receptor downstream signalling molecule (s) is conceivable.

Although it is possible that higher spinal doses of AT-RvD1 may alter physiological spinal nociception in control rats, the greater inhibitory effects of spinal AT-RvD1 following peripheral inflammation suggests that treatments targeting this mechanism may have a window of selectivity for inflammatory pain.

3.5.4 Inhibitory effects of AT-RvD1 accompanies altered gene expression in resolvin system

The differential effect of AT-RvD1 on spinal nociceptive transmission following a period of overt peripheral inflammation is suggestive of changes in the resolvin system, compared to control. Significant changes are summarised in **Figure 3.10**.

Figure 3.10 Summary of the carrageenan model-induced significant changes in the expression of the resolvin genes in the spinal dorsal horn. The genes of interest indicated in red, ⬆ significantly increased, ⬇ significantly decreased. Values in brackets indicates the expression fold changes relative to saline injected rats.

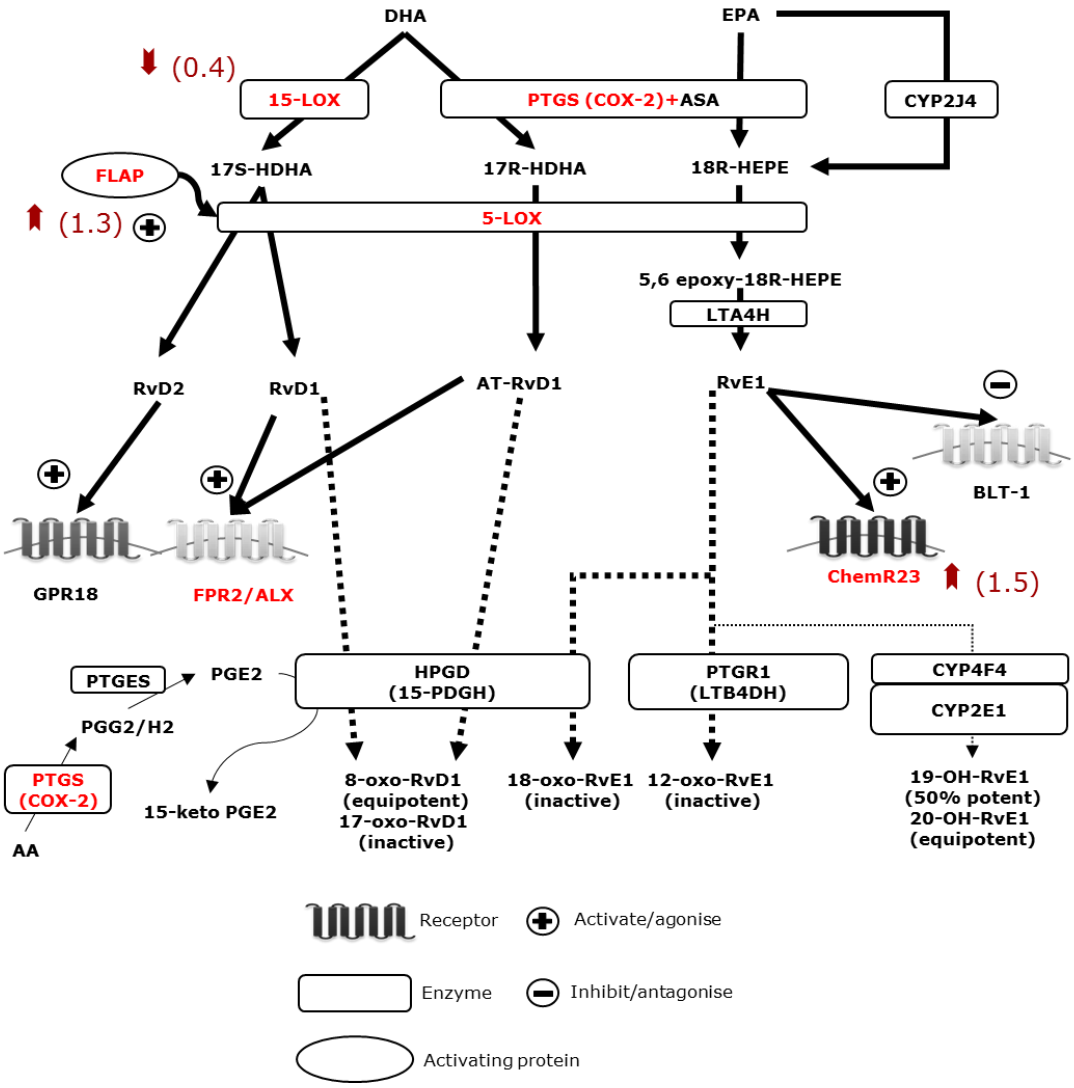

Spinal expression of two well characterised resolvin receptors FPR2/ALX and ChemR23 was quantified in the dorsal horn of the spinal cord in carrageenan and control rats. FPR2/ALX, activated by RvD1 and AT-RvD1, is predominantly localised with GFAP, an astrocyte marker (Abdelmoaty *et al.*, 2013; Wang *et al.*, 2014b). ChemR23 is expressed by neurones (Xu *et al.*, 2010) and localised with substance P in the central terminals of primary afferents in the superficial dorsal horn (Xu *et al.*, 2010). There was no change in FPR2/ALX receptor mRNA level at 30 h post carrageenan injection, compared to controls. There was however a significant elevation in spinal expression of ChemR23 mRNA in the carrageenan model of inflammatory pain compared to controls. This observation is consistent with the report that ChemR23 gene expression is increased in chronic constriction model of neuropathic pain, but not in CFA-induced paw inflammation, at day 3 and 14 post model induction (Rodriguez Parkitna *et al.*, 2006). The observation that spinal expression of ChemR23 is increased, while FPR2/ALX was unaltered, in the carrageenan model does not necessarily account for the increased effect of AT-RvD1 in this group of rats. Previous studies have reported that RvD1 (structurally very similar to AT-RvD1 (Sun *et al.*, 2007) has negligible effect at ChemR23, whereas resolvin E1 (RvE1) has an EC_{50} $\sim 1.3\times10^{-11}$ M for ChemR23 (Krishnamoorthy *et al.*, 2010). On this basis, it is unlikely that the increased effectiveness of AT-RvD1 arises as a result of an increased expression of ChemR23 in the spinal dorsal horn in the carrageenan model of inflammation.

In parallel with these studies, evidence for potential changes in the spinal gene expression of enzymes involved with resolvin biosynthesis following the period of hindpaw inflammation was also sought. There was a significant decrease in the gene expression of 15-LOX, the first step enzyme converting DHA to 17S-hydroxy DHA (Serhan *et al.*, 2011), in the dorsal horn of the spinal cord in the model of carrageenan inflammation. Expression of 5-LOX, the final

enzyme in the biosynthesis of RvD1 and RvE1, was unaltered in the carrageenan model. Recent research has shown that cellular localisation of 5-LOX determines the substrate and product selectivity of the enzyme leading to local eicosanoid generating either anti-inflammatory LXA4 (from cytosolic 5-LOX) or proinflammatory LTB4 (from nuclear membrane 5-LOX) (Fredman *et al.*, 2014; Norris *et al.*, 2014). Collectively these data support further investigation of the role of changes in cellular distribution of 5-LOX in spinal pain processing following peripheral inflammatory insult.

Concomitantly there was a significant increase in the expression of FLAP mRNA, in the dorsal horn of the spinal cord in carrageenan treated rats compared to controls. I hypothesise that FLAP plays important roles in controlling endogenous tone of resolvin system in spinal cord of inflamed rats as it has been shown as a key enzyme mediating RvD1 and AT-RvD1 biosynthesis in polymorphonuclear cells (Lehmann *et al.*, 2015). Resolvins are endogenously generated during the resolution phase of inflammation (Serhan, 2014), which is consistent with the timing of our electrophysiological and gene expression studies. Although not proven, increased expression of 15-LOX and FLAP in the dorsal horn of the spinal cord is likely to increase baseline synthesis of endogenous resolvins, which may directly enhance the inhibitory effects of exogenous AT-RvD1, or reduce the rate of catabolism of exogenous AT-RvD1, leading to an increased inhibitory effect on evoked neuronal responses. Interrogation of this proposal is not readily achievable as spinal blockade of LOXs and COX-2 has analgesic effects (Gregus *et al.*, 2012; Trang *et al.*, 2004) or inhibits neuronal firing (Staniaszek *et al.*, 2010) per se. Collectively these data provide new evidence for complex changes in key enzymes involved in the biosynthesis of the resolvins in the spinal cord under specific conditions, which require further interrogation.

In summary, spinal administration of AT-RvD1 only reduced peripheral nociceptive fibre-evoked responses of spinal WDR neurones *in vivo* in the presence of peripheral hindpaw inflammation, with minimal effects on physiological spinal nociception. The ability of AT-RvD1 to selectively target inflammatory driven spinal hyperexcitability of nociceptive pathways was associated with pathway specific changes in the gene expression of enzymes known to mediate the generation of the resolvins. The data presented here support the further investigation of the analgesic potential of this class of molecules.

Chapter 4 Effects of aspirin-triggered resolvin D1 on spinal Nociceptive processing in monosodium iodoacetate-induced arthritic pain

4.1. Introduction

Osteoarthritis (OA) is a chronic degenerative joint disease affecting a number of people worldwide (Woolf *et al.*, 2003). The estimates of symptomatic OA in people at age of 60 years or older are 9.6% of men and 18.0% of women (Woolf *et al.*, 2003). Typical symptoms of OA include joint pain, brief morning stiffness, and functional limitation (Zhang *et al.*, 2010). OA pain is the major chief complaint and factor driving patients to seek medical treatment. Chronic OA pain results in reduced quality of life (Dominick *et al.*, 2004) and is also a major determinant of functional impairment and disabilities in patients with knee OA (Creamer *et al.*, 2000; McAlindon *et al.*, 1993).

Current available analgesics for symptomatic management of OA pain offer mild to moderate pain reduction or have some limitations. Paracetamol and topical non-steroidal anti-inflammatory drugs (NSAIDs), the initial treatments for OA pain, are generally well tolerated, however, provide only modest analgesia (Derry *et al.*, 2016; Zhang *et al.*, 2004). Classical NSAIDs and selective cyclooxygenase-2 (COX-2) inhibitors demonstrate superior analgesic efficacy than paracetamol in clinical trials (Bannuru *et al.*, 2015; da Costa *et al.*, 2016). However, they are associated with end organ damages in long term use such as increasing risk of gastrointestinal bleeding from classical NSAIDs (Sostres *et al.*, 2013), and increasing risk of developing cardiovascular diseases especially, myocardial infarction (Kearney *et al.*, 2006; Motsko *et al.*, 2006) from selective COX-2 inhibitors. Moreover, both classes possess the similar risk of kidney injury (Brater *et al.*, 2001) which is largely concerned in the elderly, the majority of patients with OA. Opioids may provide additional pain relief or may be used as alternatives in patients having contraindication of NSAIDs (Zhang *et al.*, 2008). However, unwanted side effects may limit the use of opioids such as drowsiness, constipation, nausea, sedation, cognitive disturbance and tolerance in long term use. These lead to the need for developing

of novel analgesics with different mechanisms of action and that are safer to treat OA pain.

OA has been considered as a disease affecting articular cartilage. Under normal conditions, there is a balance of extracellular matrix synthesis and catabolism of the articular cartilage. However, in OA joints, both genetic and environmental factors may predispose a patient to OA by changing biochemical pathways of chondrocyte function, leading to the disruption of the balance and causing progressive cartilage degeneration.

OA has been reported to induce numerous changes in the affected joint and adjacent structures (Loeser *et al.*, 2012), including changes in the cartilage, subchondral bone, synovium, menisci and ligaments. Examples of such important changes include progressive cartilage degradation, abnormal formation of subchondral bone (osteophytes), inflammation of the synovium (synovitis) and increasing osteochondral space. With disease progression, a number of proinflammatory mediators, for example, proinflammatory cytokines, matrix degradation enzymes, peptides, prostanoids and nitric oxide, are excessively released in the affected joint (Kapoor *et al.*, 2011; Lories *et al.*, 2011; Zhang *et al.*, 2013a) and finally lead to joint destruction.

Changes in structure and function of somatosensory system both at peripheral and central levels have been found in chronic OA pain (Zhang *et al.*, 2013a). Normal cartilage is an avascular and aneural tissue. However, neurovascular invasion into articular cartilage has been reported in human OA knee joints (Suri *et al.*, 2007), suggesting an alteration in peripheral nerve innervation. Inflammation, particularly synovitis, has more correlation to OA pain than overall radiographic scoring (Hill *et al.*, 2007). There are numerous proinflammatory mediators released from inflamed synovium including tumour necrosis factor-α (TNF-α), interleukin-1β (IL-1β), IL-6 and IL-17; nerve growth factor (NGF), vasoactive

intestinal peptide (VIP) and vascular endothelial growth factor (VEGF) and prostaglandins (Sokolove *et al.*, 2013). Binding of these mediators to their receptors on peripheral nociceptive terminals can lead to the activation and sensitisation of nociceptors (Schaible *et al.*, 2011). Thus, synovitis may be considered as an important source of inflammatory mediators activating/sensitising peripheral sensory fibres in OA pain.

A chemical model using intra-articular injection of monosodium iodoacetate (MIA) has been widely used for investigating OA pain mechanism in rats. MIA is an inhibitor of glyceraldehyde-3-phosphate dehydrogenase, an essential enzyme in chondrocyte glycolysis (Grossin *et al.*, 2004), causing chondrocyte apoptosis. MIA induces rapid development of OA-like pathology in rats; at one week after injection there are changes to the joint similar to characteristics of human OA, for example, osteophytes, cartilage damage, subchondral bone remodelling (Guingamp *et al.*, 1997; Pomonis *et al.*, 2005; Sagar *et al.*, 2015; Sagar *et al.*, 2010). This model results in a shift of the weight bearing to contralateral limb (Bove *et al.*, 2003; Pomonis *et al.*, 2005; Sagar *et al.*, 2011) resembling abnormal gait in OA patients. There are 2 phases of the weight bearing asymmetry induced by MIA. The first phase (0-3 days) is thought to be driven by acute inflammatory mechanisms whereas the second phase (from 5-7 days onward) correlates with the onset of OA pathology (Guingamp *et al.*, 1997; Guzman *et al.*, 2003). MIA also elicits a more gradual reduction in distal hindpaw mechanical withdrawal thresholds, representing centrally mediated receptive field expansion in OA patients (Arendt-Nielsen *et al.*, 2010; Sagar *et al.*, 2011), which reaches a plateau approximately by a week post injection (Sagar *et al.*, 2011; Sagar *et al.*, 2010). Although it can be argued that MIA causes a too rapid development of OA-like pathology, the features are clinically relevant and this timecourse limits the need to maintain animals for longer periods. The efficacy of clinical analgesics in inhibiting MIA-induced OA pain indicate that this model has

clinically utility to investigate pain mechanisms in OA (Zhang *et al.*, 2013a).

A number of studies have investigated the underlying mechanisms of pain in this model. Within the MIA-treated joints, levels of TNF-α and interleukin-6 (IL-6) are elevated earlier from day 1 and highest at day 4-7, then gradually decline but are still different from control at day 28 (Orita *et al.*, 2012). NGF is gradually upregulated from day 7 and continuously increased to day 28, in association with mechanical allodynia of the ipsilateral hind paw (Orita *et al.*, 2012). This suggested that different mediators contribute to the pain behaviour at different timepoints. This model has been shown to lead to increases in spontaneous firing rate of mechanosensitive C-fibres and decreased mechanical threshold and increased mechanical-evoked firing rate of mechanosensitive A-fibres, suggesting fibre specific contributions to OA pain (Kelly *et al.*, 2012). In addition, this model is also associated with changes in gene expression and function of sensory fibres and DRGs. An increase in TrkA mRNA expression in lumbar (L) 3, 4 and 5 dorsal root ganglia (DRG) was associated with an increase in weight bearing asymmetry and a decrease in paw mechanical threshold (Ashraf *et al.*, 2014).

Association of mechanical hypersensitivity in MIA model and changes in the central nervous system, particularly gliosis in spinal dorsal horn has been reported (Sagar *et al.*, 2011). The total numbers of ionised calcium binding adaptor molecule 1 (Iba1) positive activated microglia in the ipsilateral side of the dorsal horn was increased from as early as week 1, and then peaked at 2 weeks and decreased at week 4 following MIA injection, suggesting a limited role of microglia in the late phase mechanisms of OA pain (Sagar *et al.*, 2011). On the contrary, spinal GFAP immunofluorescence, reflecting activated astrocytes, was increased at the later timepoint (day 28), but not at the early timepoints in the MIA model. Repeated treatment by either oral nimesulide, a classical NSAID or oral minocycline, an inhibitor of

microglia, attenuated pain behaviour as well as those molecular markers (Sagar *et al.*, 2011) in spinal cord. Previous evidence from animal models of pain e.g. inflammatory and neuropathic pain states (Hains *et al.*, 2006; Svensson *et al.*, 2003; Zhou *et al.*, 2008) strongly supports a contribution of spinal gliosis to longer-term pain responses. These data suggest that spinal neuroinflammation is likely to contribute to the pain behaviour in the MIA model.

Resolvins have been studied in models of arthritis e.g. inflammatory arthritis induced by CFA (Lima-Garcia *et al.*, 2011) or K/BxN serum transfer (Arnardottir *et al.*, 2016; Norling *et al.*, 2016), and osteoarthritis induced by MIA (Huang *et al.*, 2017) . Most of the studies used systemic administration of RvD1/AT-RvD1 and investigated at the peripheral tissues e.g. articular cartilage, synovium and bones. RvD1 levels was higher in the synovial fluid of OA dogs compared to control suggesting that this system is enhanced in OA (Benabdoune *et al.*, 2016). Lipidomic analysis of the synovial fluid in a mouse model of RA has shown that D-series resolvins RvD1, RvD2 and RvD3 increased in arthritic joints during the resolution phase (Arnardottir *et al.*, 2016). AT-RvD1 (100 ng/day, ip.), attenuated arthritis severity, cachexia, hindpaw edema, and paw leukocyte infiltration and shortened the remission interval (Norling *et al.*, 2016). The proposed mechanisms underlying such effects were the inhibition of PGE2 and pro-inflammatory cytokine (TNF-α and IL-1β) syntheses, attenuation of leucocyte infiltration, enhancing of protectin D1(an anti-inflammatory lipid) and prevention of the loss of cartilage matrix glycosaminoglycans in the inflamed joints (Benabdoune *et al.*, 2016; Lima-Garcia *et al.*, 2011; Norling *et al.*, 2016). In the MIA model of OA, FPR2/ALX gene expression in the synovium was unaltered whereas ChemR23 gene expression was reduced at day 14 and 35 post MIA induction (Huang *et al.*, 2017). In the same study spinal dorsal horn expression of FPR2/ALX gene was transiently upregulated at day 14 while ChemR23 expression was upregulated at the late time point (day 35) (Huang *et al.*, 2017).

Repeated administration of 17R-HDHA, a precursor for D-series resolvin (300 ng/day, ip., from day 14-28 post MIA) was found to alleviate weight bearing asymmetry and hindpaw mechanical hypersensitivity in the MIA model (Huang *et al.*, 2017).

Clinical evidence indicates that both FPR2/ALX and ChemR23 are present in synovium and medial tibial plateau bone obtained from patients with knee OA (Huang *et al.*, 2017). The expression of FPR2/ALX and 15-LOX is positively correlated with expression of IL-6, which is a clinically relevant knee pain biomarker in patients with early OA and those with advanced-stage knee OA (Huang *et al.*, 2017).

To advance the understanding of the antinociceptive effects of resolvins, this chapter investigated the effects of AT-RvD1 at the spinal level in a model of OA.

4.2. Study Hypothesis and objectives

The study hypothesis is spinally applied AT-RvD1 inhibits the evoke responses of spinal WDR neurones in rats established chronic osteoarthritic pain.

The objective of this study was to;

- investigate the potential effects of the acute spinal administration of AT-RvD1 on evoked spinal WDR neuronal responses in MIA rats, compared to control rats

4.3. Methods

4.3.1. Animal preparations

Male Sprague-Dawley rats 150-175g received intra-articular injection of either 1 mg monosodium iodoacetate (MIA) in 50 ul saline (n=11) or 50 ul saline (n=9) under brief isoflurane anaesthesia (detailed in

Chapter 2 Section 2.2). Paw withdrawal threshold (PWT) and weight bearing asymmetry were assessed at baseline and twice weekly for 28 days post MIA injection (detailed in **Chapter 2 Section 2.3**). On day 28-32, rats were prepared for spinal electrophysiology (see section 4.3.2 and 4.3.3). At the end of the experiment, rats were humanely killed by overdosing with 5% isoflurane, then ipsilateral knee joints were collected for post mortem macroscopic scoring of articular chondropathy as previously described (Guingamp *et al.*, 1997) (detailed in **Chapter 2 Section 2.6**).

4.3.2. *In vivo* spinal electrophysiology

On day 28-32 following model induction, rats were prepared for *in vivo* spinal electrophysiology recording under anaesthesia (detailed in **Chapter 2 Section 2.4**). WDR neuronal responses were evoked by electrical stimulations at 3xC-fibre threshold followed by 3xAβ fibre threshold in 15-min cycles.

4.3.3. Spinal drug applications

Following stable control evoked responses (<10% variation of C-fibre responses) AT-RvD1 (Cayman Chemicals, UK) 15 ng and 150 ng/50 ul and then spinal morphine sulphate (Queen's Medical Centre Pharmacy, Nottingham, UK) 1 ug/ 50 ul in PBS vehicle were cumulatively applied onto the exposed spinal cord. Previous drug solution was removed from the spinal surface between treatments. Responses of the spinal WDR neurones were evoked using trains of 16-electrical stimulation every 15 minute and then quantified as described (**Chapter 2 Section 2.4.7**). Effects of the treatments were followed for 60 min post-treatment.

4.4. Results

4.4.1. MIA induces pain behaviour and OA pathology

Following intra-articular injection of MIA (n=11) rats had a significantly higher weight bearing asymmetry from 2±2 versus 15±2% ($p<0.01$, Mann-Whitney U test) and a decrease in punctate mechanical threshold from 17±2.7 to 6±2 0.8 g ($p<0.01$, Mann-Whitney U test) compared to saline injected control rats (n=9) (Table 4.1). Post mortem macroscopic score of articular chondropathy of the knee joints from MIA rats was significantly higher than control rats ($p<0.0001$, Mann-Whitney U test) (**Table 4.1**). Osteophytes were observed in 10/11 of MIA injected knees, whereas none were evident in saline injected rats (**Table 4.1**).

4.4.2. AT-RvD1 had minimal effect on WDR neuronal responses in the MIA model

On day 28-32 following model induction, rats were prepared for spinal recordings. Two rats from each group were excluded from the analysis due to incomplete data sets (not receiving morphine) or identified as outliers by Grubb's tests. The baseline characteristics of spinal WDR neurones in MIA (n=9) and control (n=7) rats are shown in **Table 4.1**. Neurone depths, thresholds and latencies of Aβ and C-fibre responses of WDR neurones in MIA were comparable to those in saline injected control rats. No significant change in electrical evoked responses of WDR neurones was observed between those 2 groups similar to a previous study characterising the neuronal responses using the same protocol for stimulation (Staniaszek, 2010).

In general spinal administration of AT-RvD1 (15 ng) did not alter electrically-evoked responses of WDR neurones in either MIA or control rats (**Fig. 4.1A-F**). To ascertain whether there was a shift in the efficacy of treatment, a higher dose of AT-RvD1 (150 ng) was also studied. This dose produced a small but significant inhibition of Aδ-fibre evoked responses of WDR neurones in MIA rats, compared to baseline (**Fig. 4.1B**), but did not alter other responses. Spinal administration of morphine (1 μg/50μl) significantly attenuated Aδ-

and C-fibre evoked responses of spinal neurones in both MIA and saline injected control rats (**Figure 4.1 B-F**). Morphine also produced a small but significant inhibition of Aβ-fibre evoked responses of WDR neurones in control rats (**Figure 4.1A**). Comparison of the maximal effect of morphine on evoked responses of WDR neurones (**Table 4.2**) revealed that the inhibitory effect of morphine against Aβ-evoked responses in MIA rats was significantly less than in saline injected control rats (2±7 versus 28±6 % inhibition, $p<0.05$ Mann-Whitney U test).

Table 4.1 Comparison of pain behaviour, joint pathology and characteristics of WDR neurones in MIA model of OA pain.

	Saline-treated (n=9)	MIA-treated (n=11)	MIA (% control)
Pain behaviour day 28			
% Weight bearing difference	2 ± 2	15 ± 2$^{\#\#}$	
PWT (g)	17 ± 2.7	6 ± 0.8$^{\#\#}$	
Knee joint pathology			
Macroscopic score	0 ± 0.14	14 ± 1.5$^{\#\#\#\#}$	
Presence of osteophytes	0/9	10/11	
Number of analysed neurones	7	9	
Depth (μm)	780 ± 48	720 ± 47	
Threshold (mA)			
Aβ	0.14 ± 0.01	0.14 ± 0.01	100
C	1.41 ± 0.12	1.54 ± 0.14	109
Latency (ms)			
Aβ	7.4 ± 1.04	7.5 ± 0.73	101
C	187.6 ± 24	141.1 ± 15	75
Electrical-evoked responses (number of APs)			
Aβ[a]	129 ± 14	121 ± 14	94
Aβ[b]	151 ± 12	135 ± 12	89
Aδ[b]	146 ± 16	118 ± 19	81
C[b]	384 ± 52	419 ± 49	109
PD[b]	394 ± 42	365 ± 67	93
Input[b]	280 ± 52	362 ± 61	129
WU[b]	502 ± 63	426 ± 56	85

Pain behaviour (weight bearing difference and hindpaw withdrawal thresholds) was assessed at day 28 following intra-articular injection of MIA. Spinal WDR neurones were recorded at 28-32 days following intra-articular injection of MIA or saline. Knee joint pathology was assessed following electrophysiological recordings. ##p<0.01, ####p<0.0001 Mann Whitney U test, [a]Responses electrically evoked by 3xAβ fibre threshold, [b]Responses electrically evoked by 3xC-fibre threshold, APs; action potentials. Reproduced from Meesawatsom P. *et al* 2016.

Figure 4.1 Minimal effects of AT-RvD1 on spinal WDR neurones in MIA-treated rats. On day 28-32 post model induction (intra-articular 1 mg MIA or saline control), AT-RvD1 15 and 150 ng/50ul applied spinally did not alter spinal WDR neurone firing in control rats (teal bars). In MIA-treated rats (orange bars), even at the higher dose AT-RvD1 significantly inhibited only Aδ responses (**B**). However, WDR neurone firing in both groups were markedly suppressed following 1 ng/50ul morphine (Mor) application. Data expressed as mean maximal number of action potentials post drug application. *p<0.05, **p<0.01, ***p<0.0001 repeated measure ANOVA with Sidak post hoc test, $^{\#}$p<0.05 Friedman test with Dunn's post hoc test. Saline n=7, MIA n=9. Note that 2 neurones from each group were excluded due to incomplete data sets (not receiving morphine) and identified as outliers. Reproduced from Meesawatsom P. *et al* 2016.

Figure 4.1

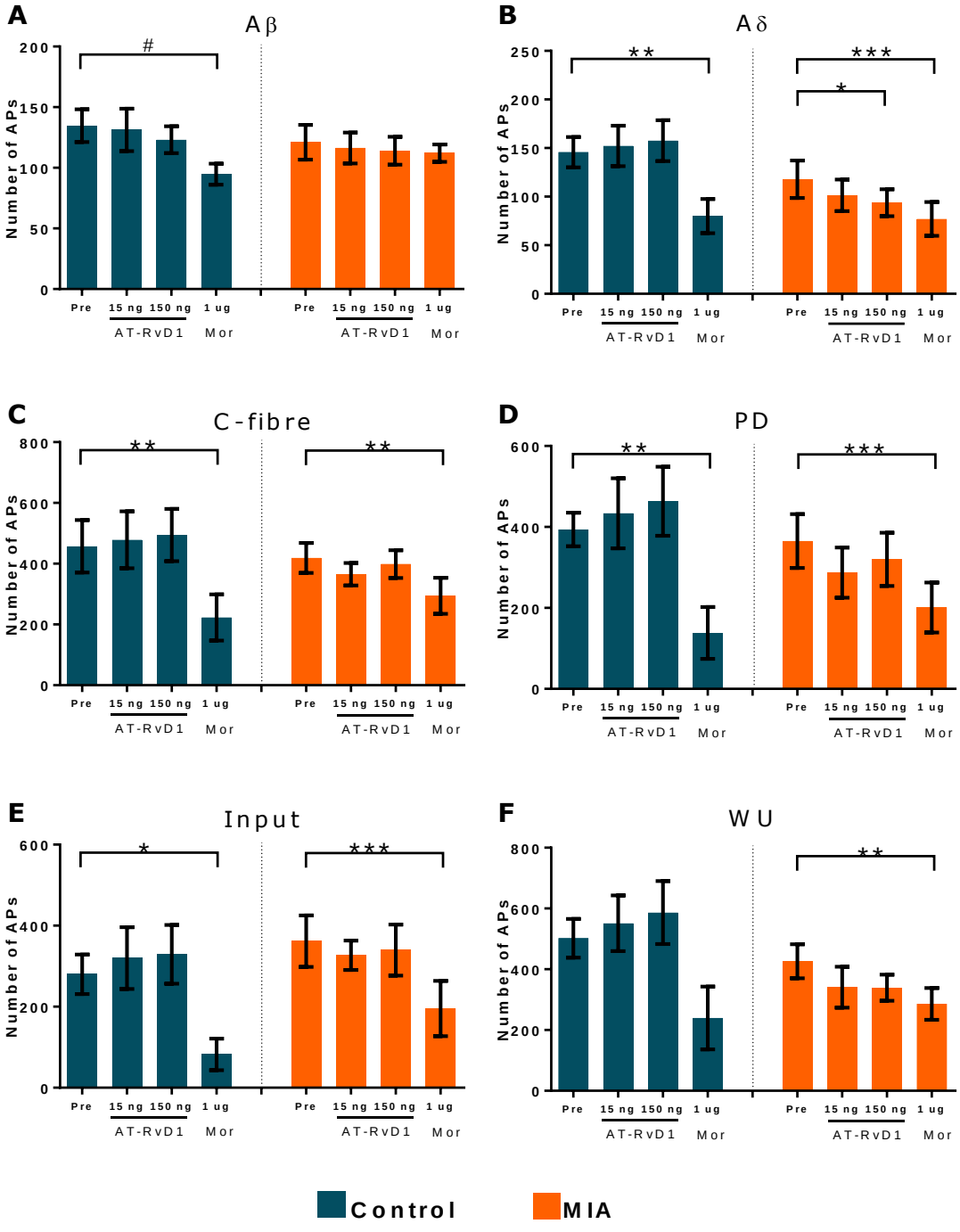
A
Aβ
#
Number of APs
200
150
100
50
0
Pre
15 ng
150 ng
1 ug
AT-RvD1
Mor
B
Aδ
**
***
*
250
C
C-fibre
D
PD
E
Input
F
WU
Control
MIA

Table 4.2 Mean maximal percentage inhibition of evoked responses by AT-RvD1 in control and MIA rats

	Control (n=7)			MIA (n=9)		
	AT-RvD1		Morphine	AT-RvD1		Morphine
	15 ng	150 ng	1 μg	15 ng	150 ng	1 μg
Aβ	5±7	6±5	28±6	1±8	1±9	2±7[#]
Aδ	-5±10	-10±13	47±7	11±8	14±10	40±6
C	-4±7	-13±9	60±14	10±7	3±8	35±8
PD	-6±14	-16±15	70±12	16±24	9±14	55±9
Input	-5±15	-19±21	71±12	-2±12	2±14	58±11
WU	-12±13	-20±16	62±13	17±19	12±12	34±6

Comparison of group effects of AT-RvD1 (15, 150 ug/50 ul) and morphine (1ug 50/ul) on electrically evoked firing of spinal WDR neurones in MIA rats versus saline control rats, expressed as % maximal inhibition. Note that negative values indicate facilitation. [#]$p<0.05$ Mann-Whitney U test effect of morphine on responses in MIA versus control rats. Reproduced from Meesawatsom P. *et al* 2016.

4.5. Discussion

Intra-articular injection of MIA produced a shift in weight bearing from the ipsilateral hindlimb to the contralateral hindlimb and a reduction in paw withdrawal threshold, similar to previous studies (Bove *et al.*, 2003; Pomonis *et al.*, 2005; Sagar *et al.*, 2011). Post mortem macroscopic assessment of the rat knee joints confirmed that all MIA rats developed pathological features reminiscent of OA, including cartilage damage/osteophytes (Guingamp *et al.*, 1997; Sagar *et al.*, 2015). Spinal administration of AT-RvD1, at the higher dose, produced modest (14%) inhibition of Aδ-fibre evoked responses of WDR neurones in MIA-treated rats, all other evoked responses of WDR neurones were unaltered. Nevertheless, the positive control, spinal morphine given at the end of the experiment clearly inhibited the evoked responses of WDR neurones, consistent with many previous studies.

4.5.1. Validity of the chosen MIA dose and timepoint preforming electrophysiology

In this study, 1 mg MIA was used as it produced consistent pain behaviour and knee joint pathology and has previously been widely characterised. The concentrations of MIA used in previous studies typically ranged from 0.1-3 mg (Ashraf *et al.*, 2014; Bove *et al.*, 2003; Guingamp *et al.*, 1997; Kelly *et al.*, 2013; Nwosu *et al.*, 2016; Sagar *et al.*, 2011; Schuelert *et al.*, 2009; Thakur *et al.*, 2012), all of which induce different mechanistic features and varying extents of joint damage. As well as variations in the dose of MIA used, this model is studied at differing timepoints. For example, 0.1 mg MIA is sufficient to induce chondropathy (Guingamp *et al.*, 1997), but produces only hindpaw mechanical hypersensitivity and not weight bearing asymmetry (Nwosu *et al.*, 2016). MIA (1 and 2 mg) produces similar degree of weight bearing asymmetry and articular proteoglycan loss at day 14 following the injection (Thakur *et al.*,

2012). However the distal mechanical threshold reduction is more robust with MIA 2 mg (Thakur *et al.*, 2012). Increasing the dose of MIA is not only associated with more robust pain behaviour, but also underlying pain mechanisms. A dose-dependent upregulation of activating transcription factor (ATF)-3, a selective marker for peripheral neuronal injury (Tsujino *et al.*, 2000) was previously reported following 0.3-3 mg MIA injection (Ferreira-Gomes *et al.*, 2012; Thakur *et al.*, 2012). ATF-3 immunoreactivity in L5 DRG was previously found to be transiently increased at 8 and 14 days following 1 mg MIA and then returned towards the normal level at the later timepoints (Ivanavicius *et al.*, 2007). The higher dose (2 mg) of MIA lead to a more substantial proportion of ATF-3 positive DRG neurones in the L4/L5 DRG at day 3, 7 and 14 compared to 1 mg MIA (Thakur *et al.*, 2012). Increased ATF-3 immunoreactivity was maintained until day 28 in L4 DRG neurones innervating the knee joints (Orita *et al.*, 2011). These reports suggest an increase in the neuropathic component underlying MIA evoked pain behaviour as the MIA dose increased, especially at more than 1 mg. A previous characterisation of evoked responses of spinal WDR neurones in rats at 14 days following 2 mg MIA compared to saline control has shown enhanced evoked responses and after discharge following application of von Frey filament 8, 26 and 60 g, which was sensitive to antineuropathic agent pregabalin (Rahman *et al.*, 2009; Thakur *et al.*, 2012). The enhanced spinal neuronal responses and pregabalin sensitivity were not seen following 1 mg MIA (Thakur *et al.*, 2012), supporting distinct spinal mechanisms of MIA at different doses.

The timepoint of 28-day post 1 mg MIA pain was chosen to perform pharmacological studies. In fact, the OA pathology, specifically cartilage damage, is apparent as early as 7 days post-MIA. Pain behaviour is associated with the early surge of proinflammatory cytokines (TNF-α and IL-6) during day 4-7 and followed by the gradual elevation of NGF from day 7 to day 28 (Orita *et al.*, 2011). Therefore, the pain mechanisms following MIA induction evolve over

time. An electrophysiological characterisation of the spinal WDR neuronal responses at this timepoint (day 28) has shown a positive correlation between mechanical evoked WDR neuronal responses and weight bearing and an increase in spinal astrocyte activation (Sagar *et al.*, 2010). In addition, this dose has produced consistent pain behaviour and OA pathology in a series of studies in this laboratory (Burston *et al.*, 2013; Huang *et al.*, 2017; Nwosu *et al.*, 2016; Sagar *et al.*, 2010).

4.5.2. Comparison of AT-RvD1 to its precursor 17R-HDHA in the MIA model

Previous studies have shown that resolvins given via the spinal route alleviate pain behaviour in numerous pain models which have different underlying mechanisms, such as acute paw inflammation-induced by formalin, carrageenan or complete Freund's adjuvant (CFA) (Abdelmoaty *et al.*, 2013; Xu *et al.*, 2010), lateral paw incision (Huang *et al.*, 2011), chronic pancreatitis (Quan-Xin *et al.*, 2012), neuropathic pain from mechanical nerve injury (Xu *et al.*, 2013) and lumbar disc herniation (Liu *et al.*, 2016a). However in the current study AT-RvD1 had minimal inhibitory effects on the electrical evoked responses of WDR neurones.

Previous work investigating systemic administration of 17R-hydroxy docosahexaenoic acid (17R-HDHA or 17R-HDoHE), an AT-RvD1 precursor in rats with CFA-induced inflammatory arthritis has shown analgesic potential of 17R-HDHA (300 ng or 600 ng, ip) in the prevention and treatment of mechanical hyperalgesia (Lima-Garcia *et al.*, 2011). Treatment with 17R-HDHA for 6 days reduced arthritic pain and joint stiffness, but not paw and joint edema suggesting the resolvin may mainly act as an analgesic in this model. However, the structural modifying effects of AT-RvD1 (100 ng/day, ip.) have been reported in K/BxN serum transfer, another model of inflammatory arthritis (Norling *et al.*, 2016). A behavioural study from the group in Nottingham reported antinociceptive potential of 17R-HDHA in the

MIA model (Huang *et al.*, 2017). Single intraperitoneal injection of 17R-HDHA (300 ng) rapidly normalised weight bearing asymmetry and partially reversed the reduced PWT in MIA rats, with effects sustained for at least 6 h (Huang *et al.*, 2017). These results clearly suggest an acute antinociceptive effect of 17R-HDHA but the major sites of action whether peripheral, spinal or supraspinal were not differentiated. The partial reversal of PWT by 17R-HDHA suggests the potential of inhibiting secondary allodynia. Interestingly, the antinociceptive effects from repeated administration of 17R-HDHA at the same dose from day 14 to day 28 had no effect on chondropathy, synovial inflammation and subchondral bone structure (Huang *et al.*, 2017). This suggests that 17R-HDHA antinociceptive effects in OA, where the OA pathology has already developed, are possibly mediated by its actions on other target tissues e.g. peripheral nerves and CNS, particularly spinal cord.

In the present study, the delivery of the electrical stimulation at the hindpaw, rather than the knee joint, was used in order to investigate whether AT-RvD1, an active metabolite of 17R-HDHA could inhibit evoked responses of WDR neurones from the secondary receptive field. AT-RvD1 applied spinally produced only a mild inhibition of the hindpaw evoked responses of WDR neurones. This limited effect differs from the robust inhibitory effect of spinal AT-RvD1 on hindpaw-evoked responses of WDR neurones in carrageenan-induced hindpaw inflammation (**Chapter 3**). This is possibly due to the differences in the areas of the primary pathology occurs. In the carrageenan study, the electrical stimulation was applied directly to the inflamed hindpaw which considered as the main site of the pathology and the evoked responses of the spinal WDR neurones receiving the input form the same area were recorded. In the current MIA study, the stimulation was applied to the ipsilateral hindpaw of the affected knee, thus the hindpaw is a secondary site. This design was in order to investigate whether AT-RvD1 could inhibit the evoked responses in the spinal recoding which may resemble the alleviation

of distal hypersensitivity seen in the previous study (Huang *et al.*, 2017). Since the neural mechanisms of primary and secondary hyperalgesia differ, e.g. the types of primary sensory fibres that are sensitised (see **Chapter 1 Section 1.4.2**), these may therefore underlie the different effects of AT-RvD1 in the carrageenan and the MIA studies.

Data presented in this chapter suggests that the D-series resolvin augmentation may have a limited immediate inhibition on spinal nociceptive responses in the MIA model of OA. Overall, it is accepted that articular and systemic inflammation is relatively low in OA, compared to other forms of inflammatory arthritis (Robinson *et al.*, 2016; Sokolove *et al.*, 2013) and this is also the case for the MIA model (Finn *et al.*, 2014). It is feasible that the differences in the effects of systemic 17-HDHA and spinal AT-RvD1 on pain responses in this model, may reflect the differences in the stimulus used (electrical versus mechanical). Alternatively it may be that the active compound leading to the inhibitory effects of 17R-HDHA is something other than AT-RvD1. For example 17R-HDHA can be converted to other 17R-RvD series such as 17-R-RvD2-6 (Hong *et al.*, 2003; Norling *et al.*, 2013), protectin D1 (Hong *et al.*, 2007) and 17-oxoDHA (Egawa *et al.*, 2016), which could bind to different molecular targets to AT-RvD1. For example, GPR18 has been recently identified as a receptor for RvD2 (Chiang *et al.*, 2015). In addition, RvD1 and RvD2 have distinct inhibitory profiles on TRPV1/TRPA1 channels (Park *et al.*, 2011). Thus, the antihypernociception of systemic 17R-HDHA on pain behaviour (Huang *et al.*, 2017) may be as a result of multiple 17-R-HDHA-derived lipids acting in concert or targeting multiple sites of action or both. In addition, recent research has shown that plasma levels of 17-HDHA was associated with increased heat pain thresholds and with lower pain scores in OA patients but not those of RvD1, D2, D3, D5 and E1 (Valdes *et al.*, 2017).

Alteration in enzymes essential in inactivation of AT-RvD1, may also contribute to the minimal effects of AT-RvD1 in the MIA model. Spinal upregulation of these enzymes may reduce the availability and abrogate the effects of the exogenous AT-RvD1. Despite AT-RvD1 being more metabolically stable than RvD1 to leukotriene B4 12-hydroxydehydrogenase (LTB4DH) and 15-hydroxyprostaglandin dehydrogenase (15-HPGD)-mediated inactivation (Sun *et al.*, 2007), this property may overcome the possible increased of those enzymes.

Another possible factor affecting the action of AT-RvD1 is drug exposure time. The single spinal administration of AT-RvD1 demonstrated a short duration (<1 h) in inhibiting evoked responses of spinal WDR neurones in the carrageenan model of inflammatory pain (presented in **Chapter 3**) while the reversal of PWT post single intraperitoneal injection of 17R-HDHA lasted up to 6 h (Huang *et al.*, 2017). Spinal neurones in this circumstance may require a longer time of exposure to the drug to be inhibited. Systemic 17R-HDHA may be gradually converted to D-series resolvins creating longer exposure time than the single spinal administration and contribute to longer analgesic duration. This, however, needs further pharmacokinetics studies to confirm.

In summary, this chapter has demonstrated that spinal AT-RvD1 15 and 150 ng/50ul had modest suppression of evoked responses of spinal WDR in MIA rats. The higher dose 150 ng/50ul produced a slight but significant (~14%) inhibition on Aδ evoked responses whereas other electrical evoked responses were not altered. Therefore the spinal cord may not the primary site of the immediate analgesia of AT-RvD1. Morphine applied at the end of the experiment consistently produced a robust inhibition on the electrical evoked responses in MIA and control rats confirming the access of AT-RvD1. AT-RvD1 had no significant effect in control rats supporting the state dependent action of AT-RvD1.

Chapter 5 ELECTROPHYSIOLOGICAL CHARACTERISATION OF SPINAL WDR NEURONAL RESPONSES AND THE INHIBITORY EFFECT OF ASPIRIN TRIGGERED RESOLVIN D1 IN PACLITAXEL-INDUCED PERIPHERAL NEUROPATHIC PAIN

5.1 Introduction

Chemotherapy-induced peripheral neuropathic pain (CIPNP) is a common adverse effect of antineoplastic agents which may limit the tolerability of chemotherapeutic regimens. Several anticancer treatments often associate with CIPNP e.g. taxanes, platinum-based compounds, vinca alkaloids and borzetomib. Among these, paclitaxel (PCX, also known as taxol), a taxane derivative, is of interest as it has a high estimated prevalence of CINP at 70%, assessed at 1-6 months after the course of chemotherapy (Seretny *et al.*, 2014). The primary mechanism of action of PCX is acting as a tubulin-stabilizing factor and inhibiting tumour cell proliferation. This mechanism simultaneously affects neuronal function by disrupting axonal transport (Jordan *et al.*, 2004), and causes demyelination leading to length-dependent neuropathy, often impacting on sensory nerves. The sensory neuropathy manifests predominantly at distal sites e.g. palms and feet; symptoms include, numbness, burning, allodynia upon mechanical and cold stimuli (Dougherty *et al.*, 2004). Current treatments for other types of neuropathic pain e.g. gabapentin, pregabalin, venlafaxine, and duloxetine also have efficacy in treating PCX-induced CIPNP (Hershman *et al.*, 2014); however, there are currently no approved pharmacologic agents.

Experimental models of PCX-induced CIPNP in rats have been shown to cause pain behaviour resembling pain symptoms found in humans. A previous behavioural characterisation of PCX-induced CIPNP in male Sprague–Dawley rats has shown that PCX (0.5, 1.0, or 2.0 mg/kg) injected intra-peritoneal on 4 alternate days, cumulative 2, 4 and 8 mg/kg respectively) caused sensory abnormalities, including heat hyperalgesia, mechanical allodynia and cold allodynia starting from day 3 following the first dose and sustained until day 35 without affecting motor function (Polomano *et al.*, 2001). Following the cumulative dose of 8 mg/kg of PCX, pain behaviour was associated with of peripheral nerve pathology such as atypical (swollen and

vacuolated) mitochondria in both sensory C-fibres and myelinated axons at days 7 and 27 (Flatters *et al.*, 2006) and reduced the number of PGP9.5-positive intraepidermal nerve fibres (IENF) in the hind paw glabrous skin at day 31 (Siau *et al.*, 2006). Levels of ATF3-positive dorsal root ganglion (DRG) neurones, indicating nerve injury, were normal following the cumulative dose of 8 mg/kg (Flatters *et al.*, 2006) but increased following for higher cumulative doses of 18 and 24 mg/kg (Liu *et al.*, 2010; Peters *et al.*, 2007a).

Underlying mechanisms implicated in pain pathway sensitisation in PCX-induced CIPNP are complicated (Sisignano *et al.*, 2014). The disruption of mitochondrial function of primary afferent neurones mentioned earlier leads to the release of Ca^{2+} from the mitochondria (Flatters *et al.*, 2006). Previous studies have shown that the PCX model is associated with sensitisation of ion channels, TRPV1, TRPv4 (Materazzi *et al.*, 2012), voltage gated calcium channel (Xiao *et al.*, 2007) and NMDA receptor (Xie *et al.*, 2016). Importantly, profound neuroinflammation in both peripheral and central nervous systems has been consistently found in the PCX model and the degree is considered to be higher than other well characterised vincristine and oxaliplatin models (Sisignano *et al.*, 2014). At the peripheral level, a marked infiltration of OX-6 positive Langerhan cells to the paw skin has been reported (Peters *et al.*, 2007a). In DRG, ~500 fold increased in GFAP-immunoreactivity in DRGs versus control (Peters *et al.*, 2007a) and pronounced CD68-positive macrophage infiltration were previously reported (Zhang *et al.*, 2016b). DRG TNF-α and IL-1β mRNA expression was found to be up-regulated 3-6 fold (Ledeboer *et al.*, 2007). In the spinal cord, PCX treatment is associated with increased GFAP positive astrocyte immunoreactivity in rat dorsal horn as soon as 4 hr after the first PCX injection and is maintained at least 28 days (Zhang *et al.*, 2012). The spinal inflammatory response which is likely to lead enhanced spinal nociceptive transmission including: increased release of proinflammatory cytokines such as TNF-α, IL-1β, IL-6 (Burgos *et al.*, 2012; Deng *et*

al., 2015) and chemokines such as CX3CL1 (Li *et al.*, 2015a), CCL3 (Ochi-ishi *et al.*, 2014) and MCP (Deng *et al.*, 2015)); upregulation of chemokine receptors CCR5 (Ochi-ishi *et al.*, 2014). The role of microglia in the spinal pathophysiology of PCX-induced CIPNP is controversial as reported to be increase (Burgos *et al.*, 2012) or no change (Zhang *et al.*, 2012; Zheng *et al.*, 2011) in microglia activation at a comparable time point (28-29 days).

Prior studies have shown the analgesic potential of targeting neuroinflammation in PCX-induced-CIPNP. Minocycline, a selective micro-glia/macrophage inhibitor, given systemically was found to alleviate mechanical allodynia (Cata *et al.*, 2008; Liu *et al.*, 2010; Zhang *et al.*, 2012) as well as surrogate pain molecular markers such as the loss of IENFs (Liu *et al.*, 2010), the increases in DRG ED-1-positive macrophages (Liu *et al.*, 2010) and the increase in spinal GFAP-positive astrocyte (Zhang *et al.*, 2012). Intrathecal delivery of plasmid DNA encoding IL-10 or intrathecal IL-1 receptor antagonist (IL-1ra) has been shown to diminish reduced paw withdrawal threshold in the PCX model (Ledeboer *et al.*, 2007).

Given the robust inflammatory mechanisms associate with this model of CIPNP, the effects of AT-RvD1 in PCX-induced CIPNP was investigated in this chapter. Previous research has shown therapeutic potential of resolvins in prevention (Xu *et al.*, 2013) and treatment (Xu *et al.*, 2010) of neuropathic pain behaviour following nerve injury. As described herein, AT-RvD1 has a distinct inhibitory effect on evoked responses of spinal wide dynamic range (WDR) neurones in models of inflammatory and arthritic pain (Meesawatsom *et al.*, 2016).

5.2 Study hypotheses and objectives

The study hypotheses were;

- the PCX model induces nociceptive hypersensitivity in rats following the PCX induction (since this was the first time that this PCX model was characterised in this laboratory)

- PCX model induces alteration in the evoked responses of the spinal WDR neurones in rats with established nociceptive hypersensitivity

- spinally applied AT-RvD1 inhibits the evoked responses of spinal WDR neurones in PCX model

The objectives of this study were to;

- characterise pain behaviour and evoked spinal WDR neuronal responses in the PCX model of chemotherapy induced pain

- investigate the potential effects of the acute spinal administration of AT-RvD1 on evoked spinal WDR neuronal responses PCX rats, compared to control rats

5.3 Methods

5.3.1 Animals

Male Sprague-Dawley rats 175-250 g received intraperitoneal injection of paclitaxel (Tocris, UK) 2 mg/kg (n=11) or vehicle (10% Cremophor, 5% ethanol in saline) (n=9) on 4 alternate days (cumulative dose of 8mg/kg) (Flatters *et al.*, 2006; Polomano *et al.*, 2001) (detailed in **Chapter 2 Section 2.2**). Baseline and then for 28 days, paw withdrawal threshold (PWT) was measured twice a week; acetone challenges (Choi *et al.*, 1994) evoked nocifensive duration and paw withdrawal latency were assessed once a week following PWT test (detailed in **Chapter 2 Section 2.3**). Weight gain and general behaviour of the PCX and control rats was monitored over the course of the study.

5.3.2 *In vivo* spinal electrophysiology

In separate groups of rats, on day 28-32 following model induction, rats were prepared for *in vivo* spinal electrophysiology (detailed in **Chapter 2 Section 2.4**). Responses of wide dynamic range (WDR) neurones were evoked by 3 stimulus modalities. A train of von Frey filaments (8, 10, 15 and 26 g applied for 10 sec each) followed by a drop of saline as a control, and then a drop of acetone, gently applied by polystyrene tubing attached to a 1ml syringe to the hindpaw receptive field. Following a 5-7 min interval, then electrical stimulation at 3xC-fibre threshold followed by 3xAβ fibre threshold were delivered to the same receptive field. This set of stimuli were delivered in 15-min cycles.

Spontaneous activity (SA) was defined as any activity more than 0.05 APs/sec recorded during 1 min prior to the first stimulus presentation. Due to the variability in the literature on the criteria to distinguish SA from random firing, the cut-off at 0.05 APs/sec was set in this thesis based on following reasons. Previous studies have shown that C-fibre in control animal could generate a very low level of SA at 0.06 ± 0.08 APs/sec (Hulse *et al.*, 2010) and spinal dorsal horn neurones exhibited spontaneous activity 5-6 spike/min (0.08-1 APs/sec) under the isoflurane concentration that produced immobility (Kawamata *et al.*, 2005).

Neurones generating action potentials after the cessation of 8g von Frey filament presentation were deemed as 8g post-discharge (8gPD) neurones. Neuronal responses to acetone were normalised to the saline control response (acetone-saline), and those generating action potential upon acetone application were deemed as acetone responsive (AR). One to three spinal WDR neurones per rat were characterised. Only the last neurone found from each animal received pharmacological interventions (see next section)

5.3.3 Spinal drug applications

Pharmacological studies were performed to the last spinal WDR neurone found from each animal. Following stable control evoked responses (<10% variation of C-fibre and natural stimulus responses), AT-RvD1 (Cayman Chemicals, UK) 15 ng and 150 ng /50 ul and then spinal morphine sulphate (Queen's Medical Centre Pharmacy, Nottingham, UK) 1 ug/50 ul in PBS vehicle were cumulatively applied on to the exposed spinal cord. Responses of the spinal WDR neurones were evoked by mechanical, cold and electrical stimuli and then quantified as described (**Chapter 2 Section 2.4.7**). Effects of the treatments were followed for 60 min post-treatment.

5.3.4 Specific statistical analysis

General statistical analyses are detailed in **Chapter 2 Section 2.8**. For analysing correlations between evoked responses of spinal WDR neurones and pain behaviour, when >1 neurone from an animal was characterised, the evoked responses from those neurones were averaged. The correlations of pain behaviour and evoked responses were performed using two-tailed Spearman's rank tests. Differences in proportion of neurones between PCX and control were analysed using Fisher's exact tests. Evoked responses following spinal morphine application were compared to baseline using paired-t tests or nonparametric Wilcoxon tests.

5.4 Results

5.4.1 Established paclitaxel-induced CIPNP

Prior to model induction, there was no difference in PWT, nocifensive duration after acetone challenges or PWL (baseline in **Fig 5.1A-C**) between groups of rats. PCX-treated rats (n=15) exhibited robust mechanical hypersensitivity and cold allodynia evident by a significant lowering of PWT and higher nocifensive duration after acetone challenges from day 3 after the first dose onward, compared to control rats (n=16). At the last test session, on day 28 for PWT

and day 24 for cold allodynia (**Figure 5-1A** and **B**), those 2 parameters in PCX rats reached significance (two-way ANOVA with Sidak's post hoc test), compared to control rats. PWL remained comparable between groups throughout 28 days (**Figure 5.1C**).

Figure 5.1 PCX evoked pain behavior. Intraperitoneal injection of PCX 2 mg/kg on 4 alternate days significantly decreased paw withdrawal threshold (**A**) and increased nocifensive duration after acetone challenges (**B**) from day 3 post-first dosing onward compared to control (10% Cremophor, 5% ethanol in saline vehicle). PCX had no effect on paw withdrawal latency (PWL) (**C**). *p<0.05, **p<0.01, ****p<0.001, ****p<0.0001, Two-way repeated measure ANOVA with Sidak's post hoc test. Control n=15 and PCX n=16 rats.

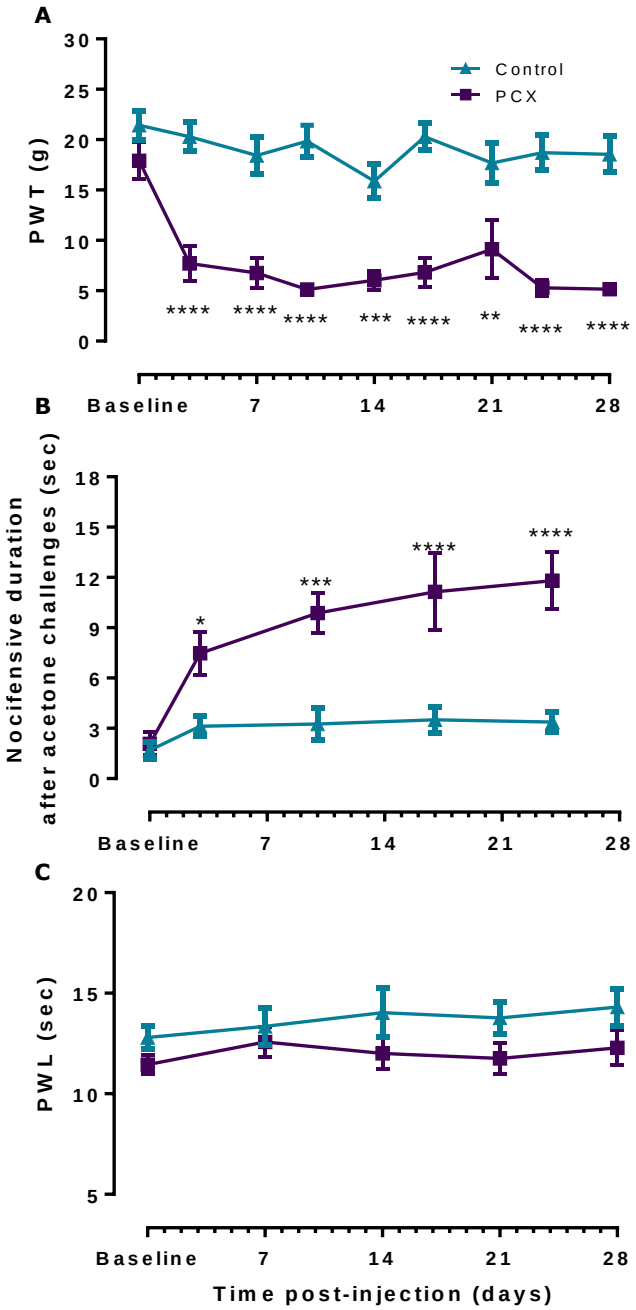

5.4.2 Baseline characteristics and physiological properties of spinal WDR neurones

Spinal WDR neurones (n=51) were characterised on day 28-32 post model induction from a total of 31 rats (PCX n=16 and vehicle control n= 15), neuronal characteristics shown in **Table 5.1**. All neurones had comparable depths of location, between 500-1000 μm, corresponding to laminae V–VI. Compared to control rats, electrical thresholds for Aβ and C-fibre (AT and CT) activation were significantly lower in PCX rats ($p<0.01$, Mann-Whitney U test), whereas the latencies of the Aβ- and C-fibre evoked responses were unaltered.

The magnitude of baseline electrical or acetone evoked responses of WDR neurones were comparable between groups. However, baseline mechanical evoked responses in the PCX group tended towards a lower magnitude. In the case of the 15 g von Frey hair evoked responses, this was significantly lower in PCX rats, compared control rats (26±2 APs/sec versus 47±6 APs/sec, $p=0.02$). Although the number of APs evoked by electrical stimulation were generally similar, analyses of PSTH revealed that neuronal response patterns in PCX rats were significantly altered (**Figure 5.2A**). AUC analysis of responses in Aβ-fibre and Aδ-fibre latencies in PCX rats were significantly larger ($p<0.05$, unpaired t-test, **Figure 5.2B** inset) compared to controls. Neuronal responses in C-fibre-PD latency reached the peak significantly faster ($p<0.05$ Mann-Whitney U test, Figure 5.2C inset) in PCX rats, compared to control rats.

A further characterisation of features which may imply hyperexcitability were studied in the two groups of rats: spontaneous activity (SA); generation of post-discharge after low intensity mechanical stimulation by 8 von Frey hair (8gPD) and acetone responsiveness (AR) (**Figure 5.3**). For each component, a significantly larger proportion of WDR neurones in PCX rats displayed either 8gPD, AR or SA, compared to control ($p<0.05$, Fisher's exact test) whilst neurones lacking all of those properties (**Figure 5.3**

shown as None) were significantly less common ($p<0.05$, Fisher's exact test). Further analyses showed that a specific subset of neurones exhibiting only 8gPD (orange subset) was more common (13%) in control rats whereas none were recorded in PCX rats ($p<0.0001$, Fisher's exact test). However, neurones exhibiting multiple properties specifically, 8gPD + AR and 8gPD+AR+SA, were significantly higher in PCX rats than in control rats (41% versus 21% and 30% versus 17%, respectively, $p<0.05$, Fisher's exact test).

Table 5.1 Comparison of characteristics of WDR neurones in PCX versus vehicle control rats.

	Control	PCX	PCX (% control)
Number of rats	16	15	NA
Number of analysed neurones	24	27	NA
Depth (μm)	780 ± 48	720 ± 47	NA
Threshold (mA)			
Aβ	0.15 ± 0.009	0.12 ± 0.006##	80
C	1.4 ± 0.07	1.2 ± 0.08##	86
Latency (ms)			
Aβ	8.3 ± 0.43	9.3 ± 0.54	112
C	201.3 ± 3.5	195.2 ± 11.6	97
Electrical-evoked responses (number of APs)			
Aβ[a]	146 ± 7	142 ± 4	97
Aβ[b]	160 ± 9	146 ± 7	91
Aδ[b]	165 ± 12	154 ± 11	93
C[b]	436 ± 37	435 ± 28	100
PD[b]	561 ± 59	434 ± 39	77
Input[b]	551 ± 70	460 ± 41	83
WU[b]	456 ± 59	409 ± 37	90
Mechanical-evoked responses (number of APs/sec)			
8g	16 ± 4	9 ± 1	56
10g	25 ± 5	14 ± 2	56
15g	47 ± 6	26 ± 3#	55
26g	57 ± 6	42 ± 3	74
Acetone -evoked responses (number of APs/sec)[c]	5 ± 0	6 ± 2	120
Spontaneous activity (number of APs/sec)[d]	0.4 ± 0.13	0.5 ± 0.31	125

Characteristics of spinal WDR neurones recorded on day 28-32 following intraperitoneal injection of PCX 2 mg/kg on 4 alternate days or control. #p<0.05, ##p < 0.01 Mann-Whitney U test, [a]Responses electrically evoked by 3xAβ fibre threshold, [b]Responses electrically evoked by 3xC-fibre threshold, APs; action potentials

Figure 5.2 Post-stimulus histograms of action potentials generated by spinal WDR neurons upon 16 electrical stimulations delivered to the hind paw. (**A**) Post-stimulus histograms. Neurones in PCX rats had significantly greater area under the curve (AUC) of responses in Aβ and Aδ latencies (0-90 msec post-stimulus) (**B**) and earlier time to peak response in C-fibre and PD latencies (90-800 msec post-stimulus) (**C**) compared to control. Responses were evoked by 3X C-fibre threshold and recorded in 2 msec bins. *p<0.05 unpaired t-test, #p<0.05 Mann-Whitney U test. Control n=24 and PCX n=27 neurones.

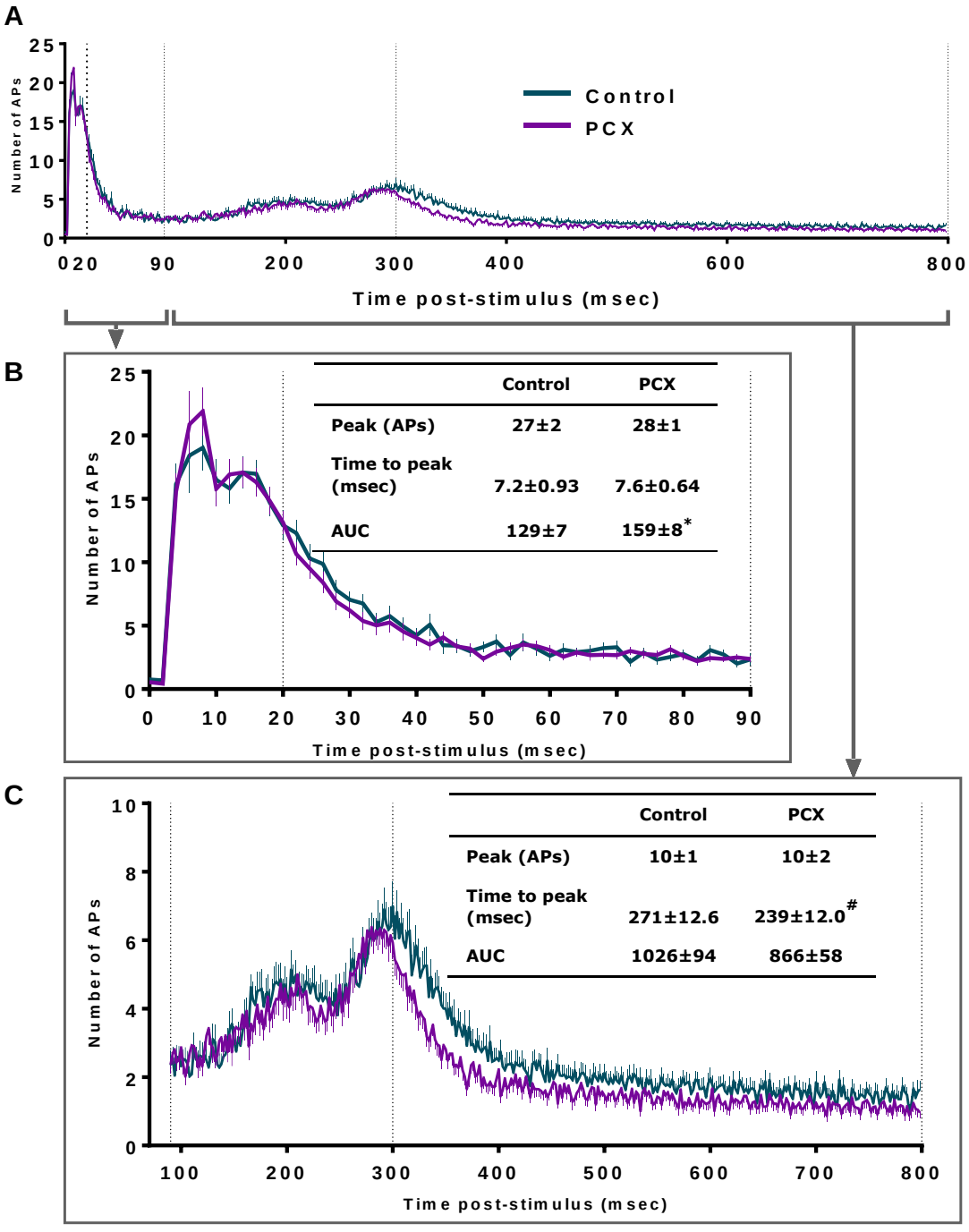

Figure 5.3 Venn diagrams comparing subgroups of WDR neurones from control and PCX rats. Spinal WDR neurones were classified by response properties including generating post discharge following 8g von Frey hair stimulation (8gPD), acetone responsive (AR) and generating spontaneous activity (SA). PCX treatment associated with altered neuronal populations. $^{\#}p<0.05$, $^{\#\#\#}p<0.01$, $^{\#\#\#\#\#}p<0.0001$ Fisher's exact test. Control n=24 and PCX n=27 neurones.

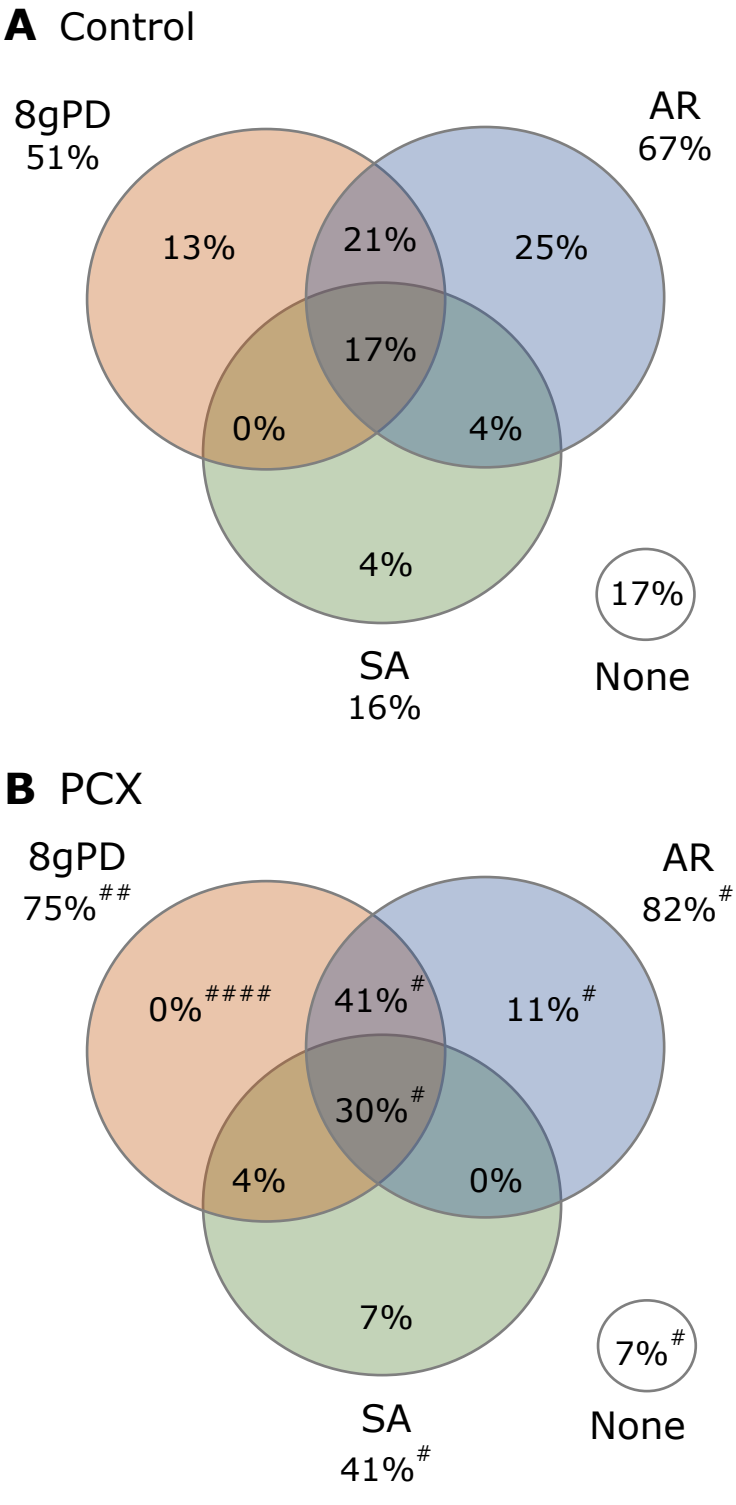

5.4.3 Correlation of pain behaviour and responses of spinal WDR neurones

To test for potential correlations between pain behaviour and evoked responses of spinal WDR neurones, PWT and nocifensive duration after acetone challenges versus evoked responses recorded during spinal electrophysiology were analysed. Results are shown in **Figures 5.4-5.6**.

The correlation of day28 PWT and electrical threshold and WDR neuronal responses evoked by electrical stimulation is shown in **Figure 5.4**. There was no correlation of PWT and Aβ fibre threshold (**5.4A**, orange axis) of neurones from control and PCX rats. However, PWT positively correlated with C-fibre threshold (r^2 0.2874, $p<0.05$, Spearman's rank two-tailed correlation, **Figure 5.4A**, green axis) in PCX rat, but not in control.

Correlation of PWT and electrical evoked responses in Aβ and C-fibre latencies in control and PCX rats are shown in **Figure 5.4B**. There was a negative correlation of PWT with electrical evoked responses in C-fibre range in control (n=16) rats, but not in PCX rat (n=15) ($r^2=0.2477$, $p<0.05$, Spearman's rank two-tailed correlation). There was no correlation of PWT and electrical evoked responses in the Aβ range in either group. Similarly, there was no significant correlation of PWT and mechanical evoked responses of WDR neurons in either group (**Figure 5.5**), and no correlation between nocifensive duration after acetone challenges versus acetone evoked responses of WDR neurons in either group (**Figure 5.6**).

Figure 5.4 Correlation of day 28 pain behavior and electrical threshold or WDR neuronal responses evoked by electrical stimulation recorded by spinal electrophysiology. In PCX rat (n=15), day 28 paw withdrawal threshold (PWT) was positively correlated with C-fiber threshold but not in control rats (n=16) (**A green axis**). PWT was negatively correlated with responses in C-fiber range in control (n=16) rats but not in PCX rat (n=15) (**B**). No correlation for PWT and Aβ threshold (**A orange axis**) or responses in Aβ **(B)**. Responses in (**B**) were evoked at 3x of the threshold of Aβ or C-fibre and quantified at 0-20 ms (Aβ) or 90-300 ms (C-fibre) post-stimulus, respectively. Spearman's rank two-tailed correlation tests were employed for the analyses.

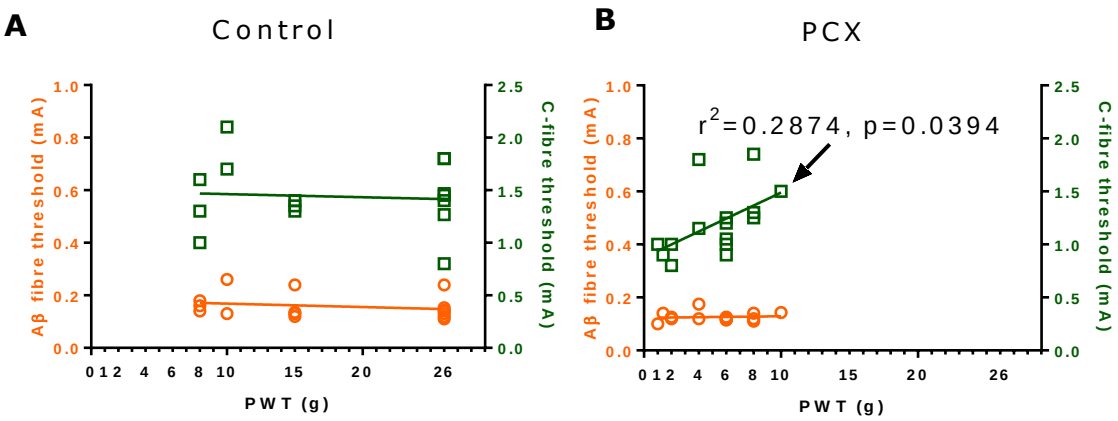

Figure 5.5 Correlation of day 28 paw withdrawal threshold (PWT) and mechanical evoked responses of spinal WDR neurons recorded by spinal electrophysiology. No significant correlations between PWT and mechanical evoked neuronal responses in control (n=15) or PCX (n=16) rats were identified.

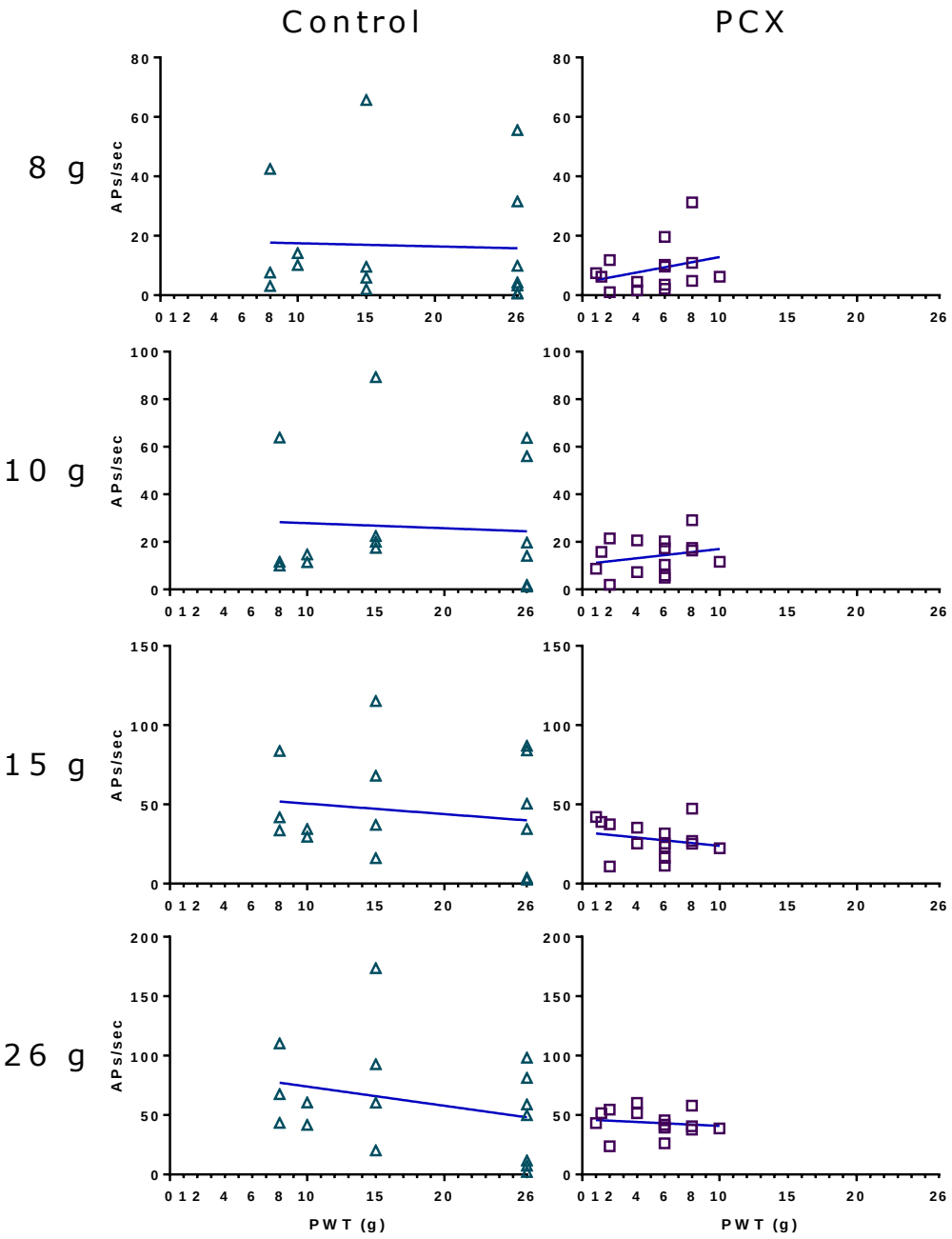

Figure 5.6 Correlation of acetone evoked pain behavior (day 24) and WDR neuronal responses recorded by spinal electrophysiology. No significant correlations between nocifensive duration following acetone challenges and acetone evoked neuronal responses in control (n=15) or PCX (n=16) rats were identifies.

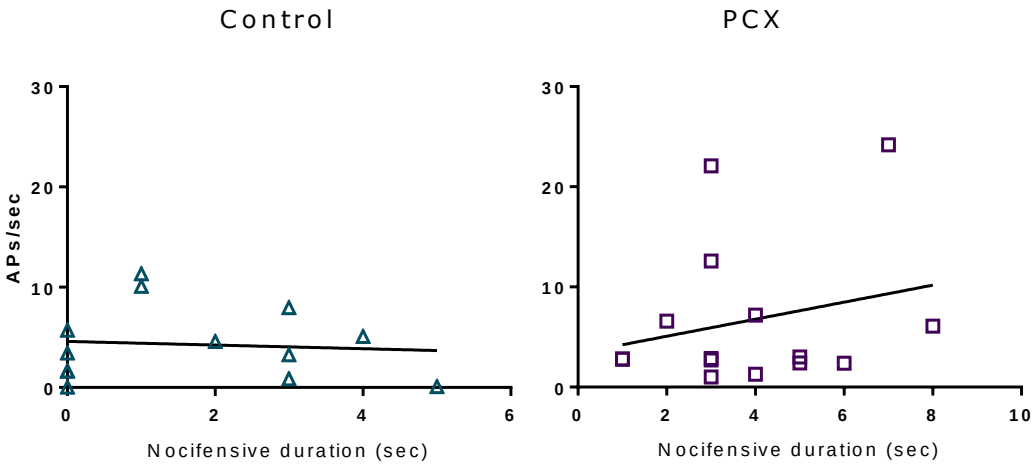

5.4.4 Correlation of electrical and mechanical evoked responses of spinal WDR neurones

To examine differences in nociceptive information from artificial (electrical) and natural (mechanical) noxious stimuli encoded by spinal WDR neurones, paired evoked responses from electrical (in Aδ and C-fibre ranges) and noxious mechanical (15 and 26g) stimuli were analysed (**Figure 5.7**). Electrical evoked responses of neurones in the Aδ fibre latency range of control rats (n=16) were positively correlated with 15g and 26g mechanical evoked responses (r^2=0.2531 and 0.2769, $p<0.05$, Spearman's rank two-tailed correlation, **Figure 5.7A**). This was also the case, but stronger, for the correlation between electrical evoked responses of neurones in C-fibre latency range and 15g or 26g mechanical evoked responses of WDR neurones (r^2=0.4798 and 0.6432, $p<0.05$, Spearman's rank two-tailed correlation, **Figure 5.7B and G**). Interestingly, these correlations were absent in PCX rats (n=15) (**Figure 5.7A** and **B** right panels). There was no correlation between responses in the Aβ fibre latency range and 8g or 10g evoked responses of WDR neurones (data not shown) in any group.

Figure 5.7 Correlations of electrical and mechanical evoked responses of WDR neurones in PCX and control rats. In control rats (n=16, left panels) electrical evoked responses in (**A**) Aδ and (**B**) C-fibre ranges significantly correlated with von Frey filaments 15 and 26 g evoked responses. However, such correlations were absent in PCX rats (n=15, right panels). Responses were evoked at 3xC-fibre threshold and quantified at 20-90 msec (Aδ) and 90-300 msec (C-fibre) post-stimulus. Analysed using Spearman's rank two-tailed correlation test. The low- and high- responsive neurones are indicate in green and orange boxes, respectively.

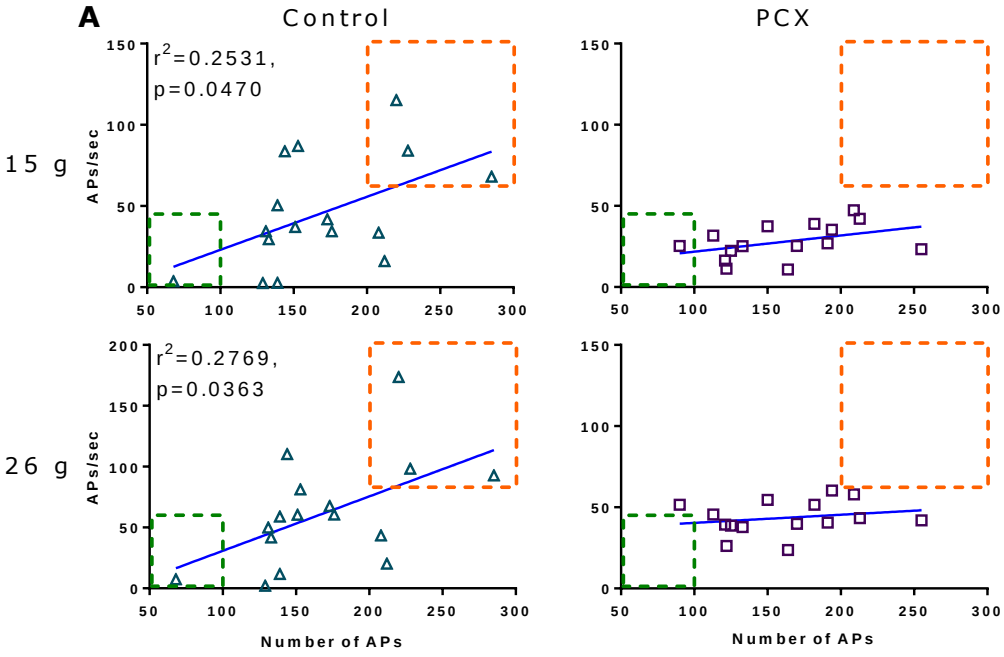

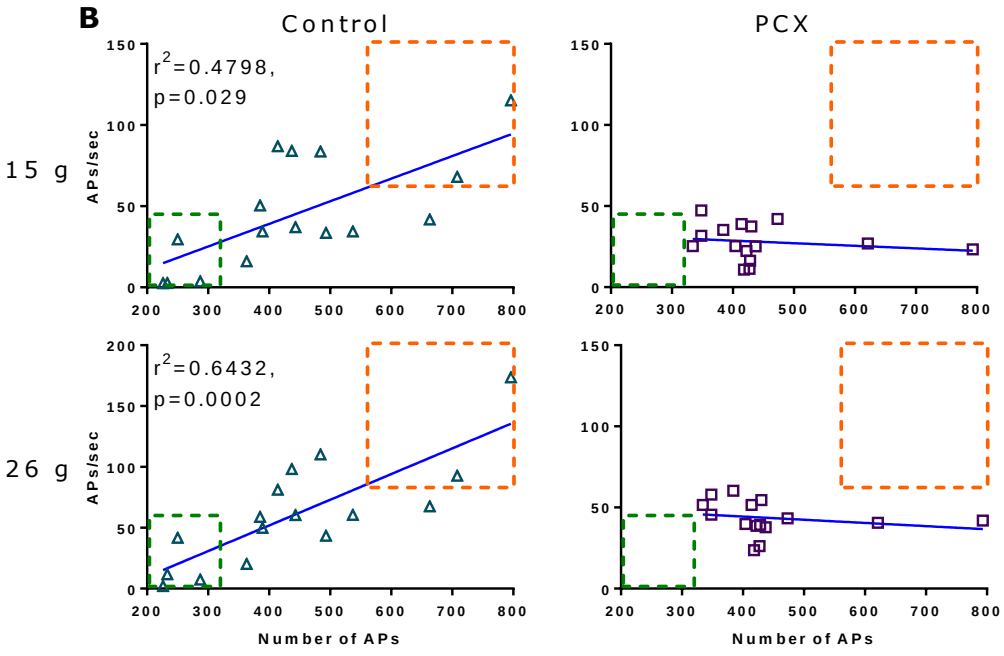

In summary, electrophysiological responses of spinal WDR neurons were distinct in PCX rats compared to control rats. PCX treatment was associated with a significant reduction in thresholds for Aβ and C-fibre responses, greater responses in Aβ-Aδ latency, shorter time to peak response in C-fibre-PD latency. Electrical and acetone evoked responses and spontaneous activity of PCX neurones were not significantly altered compared to control neurones whereas mechanical evoked responses were generally reduced and were significantly lower following 15 von Frey filament. A significantly greater proportion of neurones in PCX rats displayed spontaneous activity, acetone responsiveness and post-discharge following 8 g von Frey filament. Correlation analyses revealed that the thresholds of C-fibre in PCX but not control rat correlated with day 28 PWT and the correlations of evoked responses between noxious electrical (in Aδ and C-fibre latencies) and noxious mechanical (15 and 26 g) stimuli were found in control but not PCX rats.

5.4.5 Effects of AT-RvD1 on evoked responses of spinal WDR neurones

Following stable baseline responses, effects of spinal application of AT-RvD1 (15 and 150 ng/50ul) and morphine (1 ug/50ul) on electrical evoked responses of spinal WDR neurones were examined (**Figure 5.8-5.10**), **Table 5.2** compares effects between control and PCX rats.

For electrical-evoked responses in control rats (n=9), AT-RvD1 produced mixed effects both facilitation and inhibition of C-fibre evoked responses, these effects were not dose-related. Overall, electrical evoked C-fibre responses were unaffected by 15 ng of AT-RvD1 whereas the higher dose (150 ng) produced a mild but significant inhibition of responses in the Aβ latency ($p<0.05$, Friedman test with Dunn's post hoc test), compared to baseline.

In PCX rats (n=9), AT-RvD1 (15 and 150 ng) facilitated C-fibre evoked responses in 2 different neurones. In the remaining 7 neurones, neither dose of AT-RvD1 (15 nor 150 ng) inhibited the electrical evoked responses in PCX rats.

At the end of the AT-RvD1 study, the effect of spinal administration of morphine was studied. The majority of electrically evoked responses of WDR neurones were markedly inhibited by spinal administration of 1 ug of morphine in control and PCX rat ($p<0.05$ versus baseline, paired-t tests or Wilcoxon tests, **Figure 5.8B**) except WU in control rats.

Effects of AT-RvD1 on mechanical evoked responses of WDR neurones in control rats were modest, changes corresponding to -7-23% and effects were not dose related (**Figure 5.9A** and **Table5.2**). In PCX rats, spinal administration of AT-RvD1 (15 and 150ng) produced a significant dose-dependent inhibition of low intensity (8g and 10g) evoked responses of WDR neurones ($p<0.001$ Friedman test with Dunn's post hoc test), (n=6-8, excluded neurones with low baseline responses upon filament presentation or >20% facilitated). The magnitude of inhibition of the 8g evoked responses following exposure to AT-RvD1 was significantly larger than the effect of the same treatment in control rats (**Figure 5.9A**, and **Table 5.2**). The magnitude of the effects of AT-RvD1 15 and 150 ng on 8g evoked responses was comparable to 1ug of morphine (73±5% and 73±7% versus 84±4%, $p>0.05$ Friedman test with Dunn's post hoc test). Spinal AT-RvD1 had less effect on higher intensity mechanically evoked responses of WDR neurones in PCX rats. AT-RvD1 (15 and 150ng) produced 35±18 and 46±11% inhibition of 10 g evoked responses (**Table 5.2**), which was considered a half of morphine potency (84.4%). Spinal AT-RvD1 did not significantly alter 15 and 26g evoked responses of WDR neurones in PCX rats (Figure 5.9A). Morphine dramatically supressed all mechanically evoked responses

of WDR neurones in both control and PCX rats ($p<0.05$, **Figure 5.9B**).

In this pharmacological cohort, control neurones (n=7) exhibited low baseline acetone evoked responses which were not different from baseline acetone evoked responses in PCX rats (n=8) (control 2±1 versus PCX 8±5 APs/sec). AT-RvD1 (15 and 150 ng) produced a profound and dose-related inhibition of acetone evoked responses of WDR neurones (68-83% inhibition) in both PXC and control rats (**Figure 5.9A**, **5.10** and **Table5.2**). Spinal morphine also produced a dramatic suppression of acetone evoked responses of WDR neurones, corresponding to ≥90% inhibition in both groups of rats (Figure 5.9A, 5.10 and Table5.2).

AT-RvD1 inhibited mechanical evoked responses predominantly in PCX rats, shown as a higher degree of inhibition (**Table 5.2**). The peak inhibitory effects of AT-RvD1 on mechanical or cold evoked responses occurred in the range of 15-30 min post application.

The effects of spinal AT-RvD1 on the properties of the tested neurones, specifically, SA, 8gPD and AR are shown in **Table 5.3**. AT-RvD1 had inhibitory effects against these properties in all groups. In control rats, SA in 1 neurone was partially inhibited by 15 ng and facilitated by 150 ng; 1 neurone was facilitated by all doses and none was completely inhibited. The ability of AT-RvD1 to reverse those properties was more robust in PCX rats. AT-RvD1 partially reduced 8gPD and AR in most of neurones (6/8 neurones) and SA, 8gPD and AR were completely diminished in 2/8 neurones.

Figure 5.8 Effects of spinal AT-RvD1 (15 ng, 150 ng) and morphine (1 ug/50 ul) on electrical evoked responses of WDR neurons in PCX-treated vs vehicle-treated rats. (A) AT-RvD1 150 ng produced a significant inhibition on Aβ-evoked responses in control. In PCX-rats, AT-RvD1 15 ng significantly inhibited Aδ-evoked responses. **(B)** Neuronal response were generally inhibited by morphine. *p<0.05, **p<0.01, ***p<0.001 repeated measure ANOVA with Dunnett's post hoc test for AT-RvD1 15 and 150 ng vs pre-drug responses or paired-t test for morphine versus pre-drug responses. #p<0.05, ##p<0.01, ###p<0.001 Friedman test with Dunn's post hoc test for AT-RvD1 15 and 150 ng versus pre-drug responses or Wilcoxon test for morphine versus pre-drug responses. n=6-9/group for AT-RvD1 and 6-7/group for Morphine. APs: action potentials.

Figure 5.8

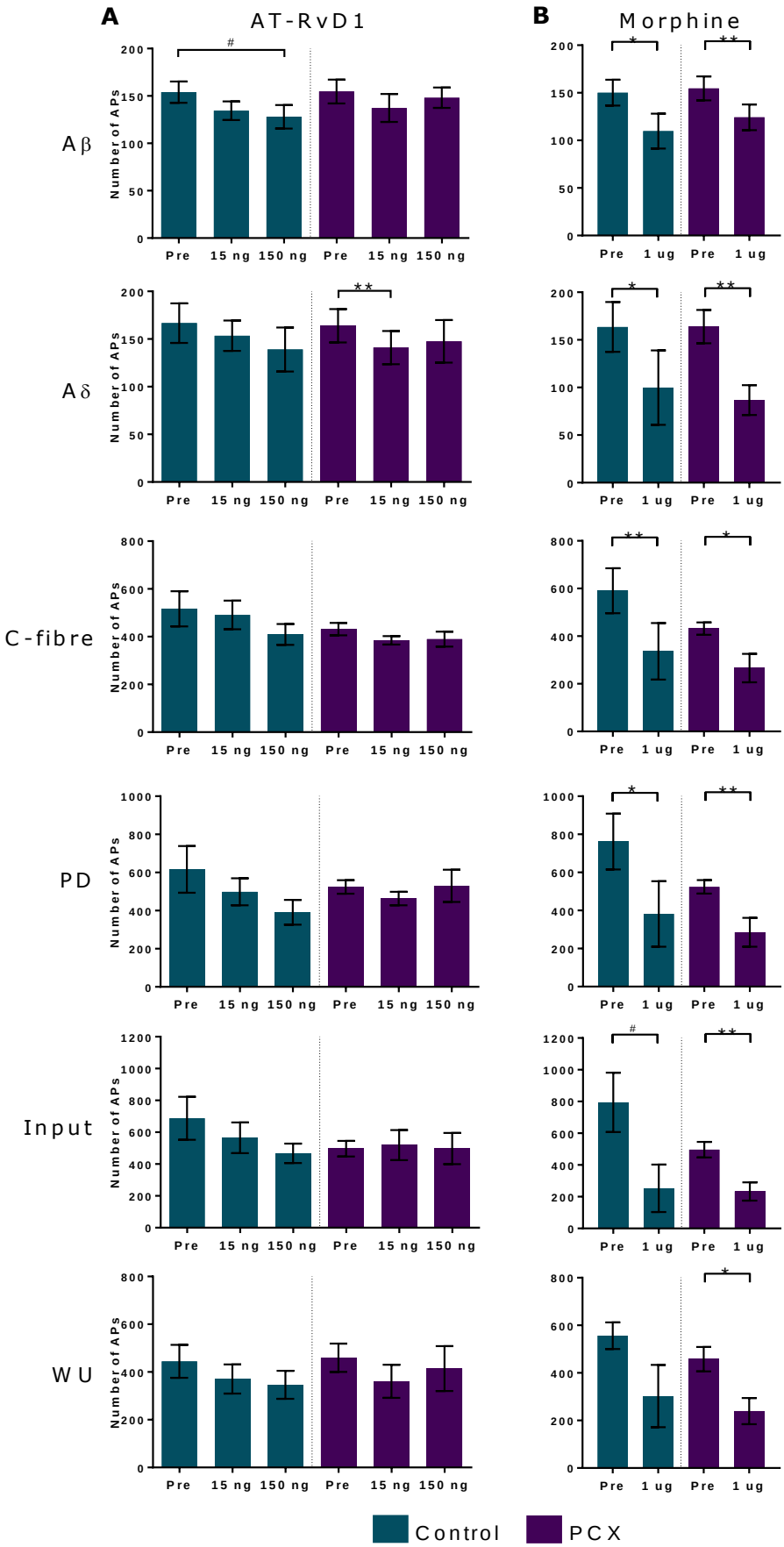
A
AT-RvD1
B
Morphine
Aβ
Aδ
C-fibre
PD
Input
WU
Number of APs
Pre
15 ng
150 ng
1 ug
Control
PCX

Figure 5.9 Effects of spinal AT-RvD1 (15 ng, 150 ng) and morphine (1 ug/50 ul) on mechanical evoked responses of WDR neurons in PCX-treated vs vehicle-treated rats. (A) In PCX rats, AT-RvD1 15 and 150 ng dose-dependently inhibited 8 g and 10 g but not 15 g and 26 g evoked responses compared to pre-drug responses (pre). AT-RvD1 had no significant effect on mechanical evoked responses in control rats. Acetone evoked responses were significantly inhibited by all doses of AT-RvD1 both in control and PCX rats. **(B)** Morphine produced dramatically suppressed both mechanical and acetone evoked responses. *p<0.05, **p<0.01, ***p<0.001 repeated measure ANOVA with Dunnett's post hoc test for AT-RvD1 15 and 150 ng versus pre-drug responses or paired-t test for morphine versus pre-drug responses. #p<0.05, ##p<0.01, ###p<0.001 Friedman test with Dunn's post hoc test for AT-RvD1 15 and 150 ng versus pre-drug responses or Wilcoxon test for morphine versus pre-drug responses. n=6-9/group for AT-RvD1 and 6-7 for Morphine. APs: action potentials.

Figure 5.9

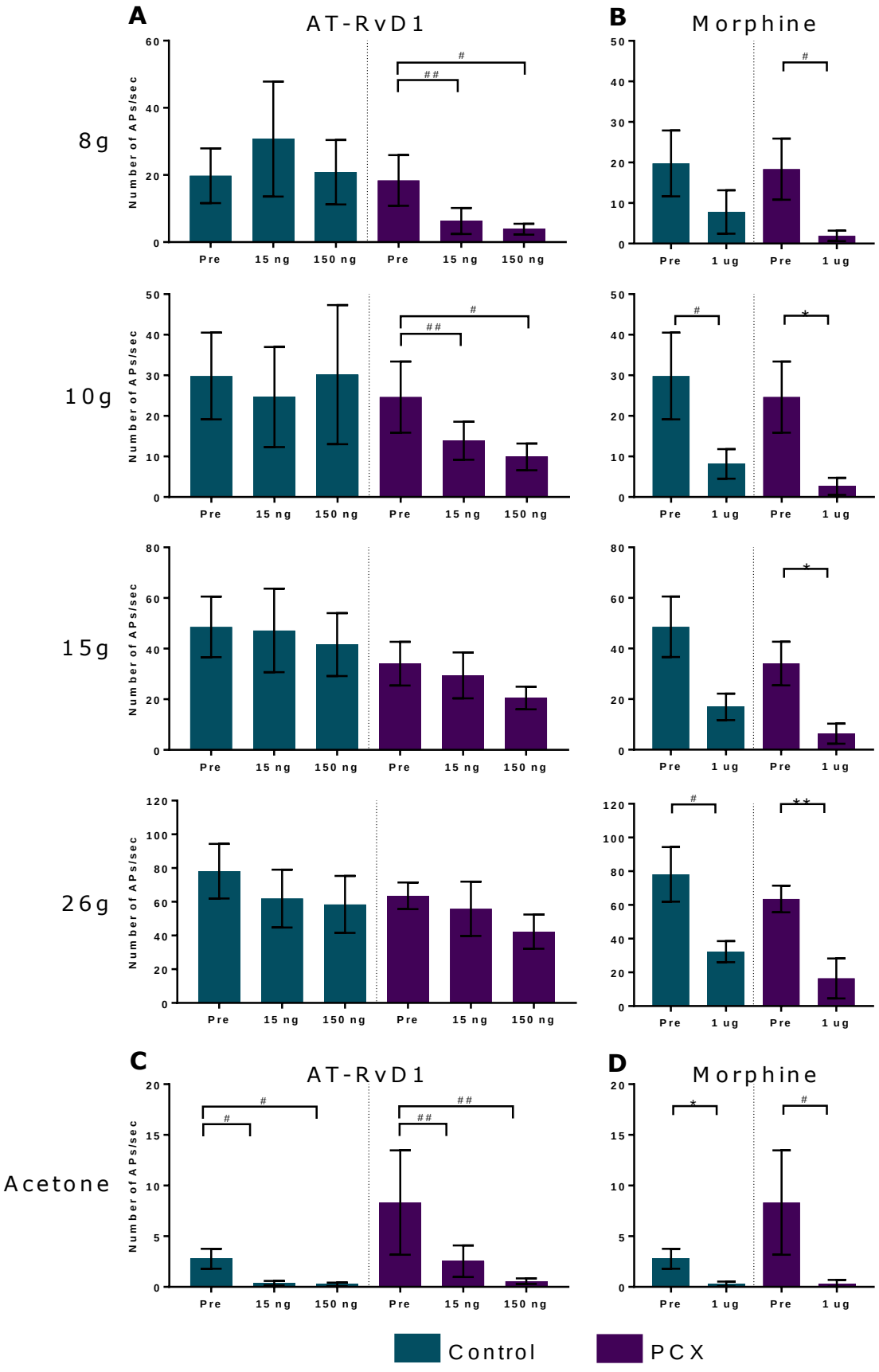
A
AT-RvD1
B
Morphine
8g
10g
15g
26g
Number of APs/sec
Pre
15 ng
150 ng
1 ug
C
AT-RvD1
D
Morphine
Acetone
Control
PCX

Table 5.2 Mean maximal % inhibition of evoked responses by AT-RvD1 and morphine in PCX and control rats.

Stimulus modality	Control (n=9)			Paclitaxel (n=9)		
	AT-RvD1		Morphine 1 μg	AT-RvD1		Morphine 1 μg
	15 ng	150 ng		15 ng	150 ng	
Mechanical						
8g	-7±25	-3±31	66±22	**73±5#**	**73±7#**	84±4
10g	20±20	-1±37	73±15	35±18$$	46±11$	84±4
15g	-9±27	-7±26	72±9	14±14	24±21	77±4
26g	23±19	7±35	60±9	19±15	25±23	73±8
Cold						
Acetone	83±7	81±12	96±4	68±13	82±9	90±7
Electrical						
Aβ	12±4	17±4	44±11	10±7	0±11	19±8
Aδ	3±8	17±9	59±13	15±3	11±8	47±7
C	0±8	15±10	63±13	10±4	7±9	39±12
PD	-3±20	12±24	70±12	10±6	-4±17	47±12
Input	0±17	18±18	82±8	-7±19	-6±23	**54±11#**
WU	8±15	12±17	45±22	20±16	14±25	51±14

Comparison of group effects of spinal AT-RVD1 (15 and 150 ng/50ul) and morphine 1 ug/50ul on spinal WDR neuronal responses evoked by mechanical, cold and electrical stimuli in PCX versus control rats (expressed as % maximal inhibition). AT-RVD1 15 and 150 ng/50ul predominantly inhibited low intensity mechanical (8g and 10g) evoked responses in PCX rats compared to control.
Note that negative values indicate facilitation. #$p < 0.05$ Mann-Whitney U test versus the corresponding control groups. $ $p < 0.05$, $$ $p < 0.01$ versus morphine 1 μg Friedman test with Dunn's post hoc tests. One to three neurones from each group were excluded due to incomplete data sets (not receiving morphine) or identified as outliers.

Table 5.3. Effects of AT-RvD1 on the different properties of WDR neurones.

	Presence (number of neurone)	Effects of AT-RvD1		
		Reduced[a]	Completely reversed[b]	Facilitated[c]
Vehicle (n=8)				
• SA	1	1[d]		1[d]
• 8gPD	4	3		1
• AR	6	6		
PCX (n=9)				
• SA	2		2	
• 8gPD	8	6	2	
• AR	8	6	2	

Note that not all tested neurones displayed such characteristics. [A]Maximal response post application < 20% of predrug responses, [b]Absence of a particular property, [C]Maximal response post application > 20% of pre-drug responses, [d]The same neurones inhibited by 15 ng and facilitated by 150 ng AT-RvD1, SA= spontaneous activity, 8gPD= post-discharge following 8g mechanical stimulation, AR=acetone responsive.

5.5 Discussion

I have characterised evoked responses of spinal WDR neurones in PCX rats with established pain behaviour and investigated the effects of spinal AT-RvD1 on nociceptive processing in the PCX compared to control rats.

Rats in the present study developed robust hindpaw mechanical and cold hypersensitivity similar to other reports (Flatters *et al.*, 2004; Polomano *et al.*, 2001; Xiao *et al.*, 2007). Hindpaw heat hyperalgesia was previously reported, but was not as robust as other pain behaviour (Pascual *et al.*, 2005a; Polomano *et al.*, 2001). My data confirm this previous finding as in the present study PCX rats did not exhibit a reduction in PWL to thermal stimulation. The dose of PCX used (cumulative 8mg/kg) has been consistently reported to produce mechanical hypersensitivity which coincides with the reduced intraepidermal nerve fibre density (Bennett *et al.*, 2011; Boyette-Davis *et al.*, 2011; Jin *et al.*, 2008; Ko *et al.*, 2014; Liu *et al.*, 2010; Siau *et al.*, 2006) suggesting electrophysiological characterisation and pharmacological studies (day 28) were performed at a valid timepoint when peripheral nerve pathology occurs. PCX and control rats were prepared for spinal electrophysiology recoding. The current study assessed only the pain behaviour but did not provide anatomical evidence for peripheral neuropathy. Immunohistochemistry of intraepidermal nerve fibre density using PGP9.5 antibody (Boyette-Davis *et al.*, 2011) can be performed in the future experiment to provide anatomical evidence that PCX-associated peripheral nerve pathology has been developed.

Since this was the first electrophysiological study of PCX model in this laboratory, I first performed the characterisation of the evoked responses of spinal WDR neurones from PCX compared to control rats and then test the effect of spinal AT-RvD1 on some of those neurones. PCX is associated with a functional switch of WDR

neurones in the dorsal horn; reduced threshold for Aβ and C-fibre responses and altered responses of neuronal subsets.

5.5.1 Evoked responses of spinal WDR neurones characterised under isoflurane anaesthesia

Previously, characterisation of evoked responses of spinal WDR neurones in PCX rats (14 day following the induction with similar dose of PCX) using urethane as an anaesthetic agent has shown that the neurones displayed higher spontaneous activity, post discharge following brush and high intensity mechanical stimuli and wind-up following electrical stimulation (Cata *et al.*, 2006) suggesting spinal sensitisation. The spontaneous activity in PCX neurones in the current study was comparable to control which is not in line the previous report (Cata *et al.*, 2006). The main contributor may be the anaesthetic agents used, as they are known to influence the characteristics and drug responses of WDR neurones (Cuellar *et al.*, 2005; Hirsch *et al.*, 2014). Volatile halogenated hydrocarbon anaesthetics are capable of enhancing $GABA_A$ receptor-mediated inhibition on neurones and also block voltage-gated sodium channel subtypes Na1.2, Nav1.6, Na1.7 and Nav1.8 (Herold *et al.*, 2009; Shiraishi *et al.*, 2004). Among these Nav1.7 is, in particular, upregulated in DRG in the PCX model (Xia *et al.*, 2016). The effects of the isoflurane on this channel could reduce spontaneous ectopic input from peripheral nerves and/or activity of spinal neurones. Urethane modestly modulates multiple neurotransmitter receptors e.g. potentiating $GABA_A$ and α1 glycine receptors and blocking NMDA and AMPA receptor (Hara *et al.*, 2002). Therefore urethane may have less impact on voltage-gated sodium channels localised at primary sensory neurones resulting in the higher spontaneous activity of PCX rats compared to control previously found (Cata *et al.*, 2006). Another potential contributor is the time point of characterisation. Numerous temporal changes occur in somatosensory system throughout the development and maintenance of pain behaviour in

the PCX model (Burgos *et al.*, 2012; Li *et al.*, 2014; Peters *et al.*, 2007b; Zhang *et al.*, 2012). In addition, when the pain behaviour reach a plateau, approximately 2-4 weeks post induction (Zhang *et al.*, 2012), GLAST was found to be significantly down regulated at day 14 but not day 28 post induction (Zhang *et al.*, 2012) suggesting that the mechanisms contributing pain behaviour in PCX model is dynamic over time resulting in the unique characteristics of the spinal neurones at each time points.

The characterisation of spinal neuronal responses under isoflurane anaesthesia in the current study is fundamental to the future interrogation of the PCX model using this anaesthetic agent for examples, studying whether a drug could prevent the functional switch of the neuronal populations.

5.5.2 PCX alters physiological properties of spinal WDR neurones

Major electrophysiological changes of spinal WDR neurones in the PCX model characterised in the current study are summarised in **Table 5.4**. Alongside the reduced Aβ and C-fibre threshold, facilitated responses of WDR neurones in the latency range of myelinated fibres (Aβ and Aδ) and the faster latency peak of unmyelinated fibre (C-fibre and PD) responses in PCX rats were evident. These data suggest there is an increase in either peripheral conduction velocity/input or a change in the excitability / inhibitory balance of the spinal neurones. PCX-induced reduction in the thresholds of Aβ and C fibre evoked responses are in agreement with a reduction in Aβ and C-fibre thresholds found in behavioural study of the PCX model using paw withdrawal to electrical stimulation (Kawakami *et al.*, 2012; Matsumoto *et al.*, 2006). The proposed mechanisms were PCX-mediated upregulation of voltage-gated calcium channel subunit α2δ-1 mRNA (Matsumoto *et al.*, 2006) and calcium channel sensitisation (Kawakami *et al.*, 2012) in DRGs.

Another study has shown that the PCX model significantly increased the cross-sectional area of C-fibres on day 27 (Flatters *et al.*, 2006). The enlarged C-fibre cross-sectional area may allow the more rapid propagation of action potential through peripheral C-fibres and result in the faster peak response in C-fibre-PD latency detected in the present study.

The correlations of electrical evoked responses in Aδ and C-fibre latencies and 15 g or 26 g mechanical evoked responses were found only in control but not PCX rats (**Figure 5.7**) suggesting the processing of nociceptive information is altered in PCX model. The loss of such correlation in PCX rats may be caused by 2 extreme neuronal populations that were different from control (as indicated in the green and orange boxes for the low and high responsive neurones, respectively, in **Figure 5.7**). In PCX rats, the neurones displaying an extreme low or high response to both mechanical and electrical stimuli were absent or less than control rats. These support that the PCX model alters physiological properties of the pain pathway.

Table 5.4 Major electrophysiological changes of spinal WDR neuronal characteristics in the PCX model.

Electrophysiological measure	Major finding
Response threshold	
Aβ	↓
C-fibre	↓
Averaged evoked responses	
Electrical	↑ responses in Aβ-Aδ latency ↓Time to peak response in C-fibre-PD latency
Mechanical	Likely to reduce ~ 50% versus baseline ↓ for 15 g evoked responses
Cold	⇔
Neuronal subsets	↑ Proportion of neurones displaying • SA • AR • 8gPD • AR+8gPD • SA+AR+8gPD
Other findings	C-fibre thresholds correlated with day 28 PWT Absence in correlations of noxious electrical (Aδ and C fibre latencies) and noxious mechanical (15 and 26 g) evoked responses

Spinal WDR neurones were characterised under isoflurane at 28-32 days following PCX induction.
⇔ no changed, ↓ significantly decreased, ↑ significantly increased compared to control
8gPD= post-discharge following 8g von Frey filament presentation, AR=acetone responsive, NA= not applicable, PD=post discharge, SA=spontaneous activity

Several spinal mechanisms could be implicated in PCX-induced WDR neuronal hyperexcitability. Transmission between presynaptic primary sensory fibre terminals and post synaptic dorsal horn neurones can be enhanced by several mechanisms. The PCX model was found to increase GluN2A subunits and PKC dependent phosphorylated GluN1 protein levels (Xie *et al.*, 2016), but did not change post-synaptic NMDA receptor activity. Upregulation of a voltage-gated calcium channel auxiliary subunit $\alpha_2\delta$-1 mRNA in spinal cord previously found in PCX model (Gauchan *et al.*, 2009), could enhance the channel activity. PCX down-regulates neuronal glutamate reuptake transporter EAAC-1 (Cata *et al.*, 2006), which may result in an increase in synaptic glutamate availability. These events can promote pronociceptive neurotransmitter release e.g. glutamate, SP (Chiba *et al.*, 2016) and CGRP (Pittman *et al.*, 2014) and activation of post-synaptic receptors, all of which will result in hyperexcitability. Dysregulation of ion channels in peripheral nerve e.g. TRPV3, HCN, Kv1.2, Kv1.3, Nav1.7 in the paclitaxel model (Zhang *et al.*, 2014) leading to an increase in peripheral input also an enhanced release of those neurotransmitters and sensitisation of the spinal dorsal horn.

The slight reduction in mechanical-evoked responses in PCX treated rats did not match the robust mechanical allodynia indicated in the behavioural assessment. This is probably due to a decrease in sensory input coupled with an increase in spinal excitability which is common to models of neuropathic pain e.g. sciatic nerve injury (Chapman *et al.*, 1998) and diabetic neuropathy models (Byrne *et al.*, 2015).

PCX induces structural and functional changes in spinal cord contributing to a hypernociceptive state (Cata *et al.*, 2006; Xie *et al.*, 2016; Zhang *et al.*, 2012). I have identified a functional switch of the responses of subsets of WDR neurones in the dorsal horn, with a larger number exhibiting spontaneous activity, increased acetone

responsiveness and post-discharge following low intensity mechanical stimuli and a more convergence in stimulus processing (summarised in **Table 5.4**). Recent research has shown that a subset of polymodal nociceptors in DRGs are unmasked following intraplantar injection of PGE2 (Emery *et al.*, 2016). In addition, an *in vivo* patch-clamp study in a lumbar radicular pain model reveals that the proportion of substantia gelatinosa neurones responding to nociceptive and non-nociceptive stimuli (defined as multireceptive neurones) is higher (Terashima *et al.*, 2011) than control rats. Considering subsets of WDR neurones described in the current study, a significantly larger proportion of neurones in PCX rats displayed multiple properties, specifically (1) generating post discharge following 8g (innocuous mechanical stimulus) + acetone responsive or (2) generating post discharge following 8g + generating spontaneous activity + acetone responsive. These data, together with the previous findings, support that, the specificity of stimulus processing is impaired widely in pain pathway during pathological pain states.

5.5.3 Spinal AT-RvD1 inhibits evoked responses of WDR neurones in PCX rats

Targeting endogenous lipids has successfully shown the analgesic potential in alleviating pain in the PCX models. For example, antagonism of a receptor for proinflammatory lipid ceramide-sphingosine 1-phosphate (Janes *et al.*, 2014) and inhibiting the generation of the proinflammatory lipid 9,10-epoxy-12Z-octadecenoic acid derive from linoleic acid (Sisignano *et al.*, 2016) attenuated the development and maintenance of mechanical allodynia in the PCX model in rodents. Augmentation of anti-inflammatory lipids such as resolvins is another promising approach. Here I have examined, for the first time, the effects of AT-RVD1 on neuronal responses evoked by 3 different stimulus modalities,

electrical mechanical and non-noxious cold (acetone) in PCX rats compared to control.

Electrical evoked responses were generally unaffected by spinal administration of AT-RVD1 in PCX or control rats. Although, the higher dose of AT-RVD1 (150ng/50ul) had a small but significant effect on Aδ responses in control rats (12% inhibition). AT-RVD1 dose-dependently inhibited low intensity mechanical and cold-evoked responses in PCX rats. Mechanical-evoked responses in control rats were unaffected by AT-RvD1 at any doses. AT-RVD1 inhibition on cold-evoked responses was similar in both PCX and control. Morphine, as a positive control, produced a significant profound suppression on evoked responses from all stimulus modalities. Morphine-mediated inhibition of the input responses was however significantly diminished in PCX compared to control.

I previously demonstrated that AT-RVD1 inhibited electrical evoked responses in a model of acute overt inflammation but not in a chronic osteoarthritic pain model (Meesawatsom *et al.*, 2016). Using electrical stimulation may give an advantage to study the effects of treatments on responses driven by distinct fibre types, but does not replicate natural somatosensory stimuli. To increase the translational potential of this work, the current study also employed mechanical and cold stimuli.

The inhibition of AT-RvD1 on the mechanical-evoked responses was only observed in PCX rats, indicating that this compound has a selective effect in the pathological state, with minimal effects on normal physiological function. This result is consistent with my previous report whereby AT-RVD1 modestly affected electrical evoked responses in control rats only (Meesawatsom *et al.*, 2016). This finding suggests that there are specific molecular changes in resolvin system in the spinal cord in the PCX model, which underpin the selectively of AT-RvD1.

The differential effects of AT-RvD1 on the different stimulus modalities is not surprising. Electrical stimulus delivered via 2 stimulatory electrodes activates larger and less confined receptive fields, and triggers a standardised and synchronised neuronal response. On the contrary, mechanical stimuli delivered by von Frey filaments are applied to a confined area of the receptive field, generating a slower peak and then shallow curve of response. The intensity of neuronal response synchronisation is less than the electrical stimulation.

In the present study, effects of AT-RvD1 were compared to those of the potent analgesic morphine, also applied directly to the spinal cord. The magnitude of AT-RvD1 (15 and 150 ug)-mediated inhibition was comparable to that of morphine (1 ug) on 8 g-evoked responses (% inhibition AT-RvD1 both doses: 73 % versus morphine: 84%), but less than the effect of morphine for 10 g-evoked responses (% inhibition AT-RvD1 15 ug: 35% and 150 ng: 46% versus morphine: 84%). As the mechanical stimulus intensity increased to 15 and 26 g, the effects of AT-RvD1 was were lost. These suggest that AT-RvD1 favours in inhibiting responses evoked from innocuous mechanical stimuli and possibly allodynia in PCX model rather than the noxious mechanical stimuli.

Cold allodynia is an important feature of the pain experienced by patients with CIPNP (Seretny *et al.*, 2014). The mechanisms of cold allodynia in this particular model of CIPNP are not fully understood, but at least involve sensitisation of TRPV1, TRPA1, and TRPV4 (Hara *et al.*, 2013; Li *et al.*, 2015b; Materazzi *et al.*, 2012). We used the acetone test (Choi *et al.*, 1994; Leith *et al.*, 2010) in this study, both doses of AT-RvD1 produced a robust inhibition of acetone-evoked responses of WDR neurones in a dose-related fashion. The magnitude of effect (~80-90%) was comparable in both PCX and control rats. Comparison of these data and those obtained from mechanical stimulation suggest that there are differing mechanisms

underpinning these responses per se, and that in the case of the acetone-evoked response these are not specific to the PCX model. It is also worth noting that the dose of AT-RvD1 was calculated based on a previous study reporting the minimum effective dose to attenuate mechanical hypersensitivity in rats (Abdelmoaty *et al.*, 2013). It is therefore conceivable that the dose range employed was not appropriate (too high) to identify potential differences of the acetone mediated responses between the control and PCX rats. Another possibility to explain the effect of AT-RvD1 in normal rats is the low baseline response following acetone (**Figure 5.9**) which may give a larger effect size when calculating %inhibition.

Accumulating evidence indicates that TRPM8 may be a target for treating cold allodynia from CIPNP from cisplatin and oxaliplatin (Naziroglu *et al.*, 2017). However, the involvement of TRPM8 in the PCX model is less clear. Recent evidence has shown that 9,10-epoxy-12Z-octadecenoic acid) (9,10-EpOME) a pronociceptive lipid metabolite was elevated in the DRGs and contributed to the mechanical hypersensitivity and 9,10-EpOME sensitises TRPV1 but not TRPA1, TRPV4, or TRPM8 in sensory neurones (Sisignano *et al.*, 2016). RvD1/AT-RvD1 inhibited TRPA1, TRPV3 and TRPV4, but not TRPV1, TRPV2 and TRPM8 (Bang *et al.*, 2012; Bang *et al.*, 2010). Thus, the inhibition of TRPM8 sensitisation may not be a major mechanisms of AT-RvD1.

The time-course of the inhibitory effect of AT-RvD1 on mechanical and acetone evoked responses is in agreement with previous reports. AT-RvD1 mediated inhibition reached the maximum within 15-30 min post spinal cord administration and returned to baseline by 60 min, suggesting the short-lived action of AT-RvD1. Although AT-RvD1 is more stable than RvD1, collective results from our studies suggest that its duration of action is still limited.

This study investigated the acute inhibitory effect of AT-RvD1 on neuronal responses exclusively in spinal cord and from a single direct

administration following mechanical and cold hypersensitivity were established. It would be of interest to investigate the acute inhibitory effect of AT-RvD1 on pain behaviour in PCX model and determine whether it could have preventive effects or therapeutic effects on neuropathic pain behaviour. These future studies will provide a more comprehensive understanding of analgesic potential of AT-RvD1 and are fundamental for designing optimal therapeutic regimen.

Chapter 6 INVESTIGATING SPINAL EXPRESSION OF GENES RELEVANT TO RESOLVIN SYSTEM AND NEUROINFLAMMATION IN RAT PAIN MODELS

6.1 Introduction

The spinal cord is the first site of the central nervous system receiving sensory information from the peripheral nervous system. The spinal dorsal horn functions as a relay centre with the excitability of neurones modulated by inputs from several neural pathways, namely the ascending peripheral sensory fibres and the descending pathways from rostral ventromedial medulla (RVM). A number of analgesic targets present at the spinal level have been described (Yaksh *et al.*, 2017). It is well established that the spinal cord processing of sensory inputs is very complex, and subject to considerable modulatory control. Advances in the understanding of spinal nociceptive mechanisms lead to the identification of novel targets for analgesia.

Neuroinflammation plays a key role in several diseases affecting CNS function including pain. In other CNS diseases e.g. Alzheimer's diseases, brain trauma and spinal cord injury, neuroinflammation is induced by direct injury to the CNS (Wang *et al.*, 2002). Spinal neuroinflammation associated with pain is often driven by aberrant peripheral activity of primary sensory neurones (Ji *et al.*, 2014). It is established that nociceptive afferent barrage leads to the relatively quick up- and down-regulation of mRNAs for various enzymatic pathways in the spinal cord (Ji *et al.*, 2002; Okine *et al.*, 2012; Svensson *et al.*, 2003). These changes in mRNA expression likely promote neuroinflammation, nociceptive responses and drive hyperexcitability, or in some cases act to counteract these events. Previous studies have shown that alterations in spinal mRNA expression often persist following acute injury (Yukhananov *et al.*, 2008), and can be temporally evolving in the case of chronic pain states (Huang *et al.*, 2017; Rodriguez Parkitna *et al.*, 2006).

Previous studies have shown that changes in spinal mRNA expression associated with pain are heterogeneous depending on the pain model induced, and time point measured. For example, the relative

abundance of intercellular adhesion molecule 1 (ICAM-1), calcitonin gene related peptide (CGRP), tissue inhibitor of metalloproteinase 1 (TIMP-1) and chemokine-like receptor 1 (Cmklr1 or ChemR23) was increased at day 14 in chronic constriction injury (CCI) model of neuropathic pain, but not complete Freund's adjuvant (CFA)-induced hindpaw inflammatory pain (Rodriguez Parkitna *et al.*, 2006). Changes in the mRNA expression of a particular gene have been found to be associated with pain behaviour and drug-mediated analgesia e.g. nerve injury and streptozotocin models of neuropathic pain induced dorsal root ganglion and/or spinal cord α2δ-1 calcium channel subunit up-regulation where the mechanical hypersensitivity was gabapentin sensitive (Luo *et al.*, 2002). Such upregulation and anti-allodynic effects were absent in the vincristine model of chemotherapy induced neuropathic pain (Luo *et al.*, 2002). These data suggest there are injury type-specific alterations in mRNA expression in pain pathway, which may predict the effect (s) of analgesics.

Work in the previous chapters demonstrated that AT-RvD1 exhibited differential inhibitory effects on spinal nociceptive processing in models of acute inflammatory (**Chapter 3**), chronic arthritic (**Chapter 4**) and chronic neuropathic pain (**Chapter 5**). Following carrageenan induced acute overt inflammation, AT-RvD1 significantly inhibited electrical-evoked responses of WDR neurones. The effects of AT-RvD1 on electrical-evoked responses was milder in the MIA and PCX model of chronic pain, but were still evident for mechanical and cold evoked responses in the PCX model. Alterations in the spinal resolvin system and neuroinflammation have been previously reported in carrageenan (Abdelmoaty *et al.*, 2013; Meesawatsom *et al.*, 2016), MIA (Huang *et al.*, 2017; Sagar *et al.*, 2011) and PCX (Sisignano *et al.*, 2016) models such as, 15-LOX, FLAP, CYP2J4 and ChemR23. It is feasible, therefore, that distinct spinal mRNA expression profile of resolvin and neuroinflammatory mRNA in these

pain models may underpin the differential inhibitory effects of AT-RvD1.

TaqMan® Array Micro Fluidic Cards or TaqMan® Low-Density Array (TLDA) has been widely used for microarray screening of mRNA expression. The principle of using TaqMan® TLDA is similar to classical Taqman® quantitative polymerase chain reaction (qPCR) with additional advantages i.e. requiring small amount of cDNA samples and simultaneously screening a number of genes (up to 384 genes) in a single run. Given the complexity of resolvin system and also neuroinflammation, TLDA is, therefore, suitable for studying potential changes in a number of genes involved in these process in pain models.

This chapter investigated the distinct profile of spinal mRNA expression relevant to the resolvin system and neuroinflammation in 3 rat pain models using TLDA. Given the relative novelty of applying these methods in spinal cord tissue results were analysed by 3 different methods of relative quantification.

6.2 Study hypothesis and objectives

This chapter is a question-based study, therefore had no hypothesis.

The objectives of this study were to;

- compare different methods in analysing TLDA data including, $\Delta\Delta C_T$ using single reference gene, ΔC_T using single reference gene, and ΔC_T using multiple reference genes.
- investigate changes in spinal mRNA expression in the carrageenan, MIA or paclitaxel pain models in the rat, compared to their respective controls using TLDA.

6.3 Methods

6.3.1 Animals and tissue preparation methods

Pain models were induced in rats, fresh spinal cords were collected and extracted to obtain RNA similar to the detail methods in Chapter 3. Briefly, Male Sprague-Dawley rats were divided into 6 groups (n=6-7/ group, total 40) and injected with either intraplantar carrageenan, intra-articular MIA, intraperitoneal PCX or their appropriate vehicle controls (detailed in **Chapter 2 Section 2.2**). Pain behaviour in all models was assessed using von Frey filaments and weight bearing asymmetry was also assessed in the carrageenan and MIA models as only unilateral limb injury was induced (detailed in **Chapter 2 Section 2.3**). After the last time point of pain assessment (30 h post carrageenan or 28 days post either MIA or PCX), rats were sacrificed and fresh ipsilateral dorsal quadrants of lumbar enlargement (L4-6) spinal cords were collected, immediately frozen on dry ice and stored at -80°C until use (detailed in **Chapter 2 Section 2.7**).

Total RNA was extracted from ~50 mg tissue using Trizol® reagent and Direct-Zol® RNA MiniPrep kit. RNA quantity and quality were checked using NanoDrop 2000 spectrophotometer (detailed in **Chapter 2 Section 2.7**). The concentration of extracted RNA samples was normalised to 20 ng/ul in HPLC water. The diluted samples were reverse transcribed to complementary DNA (cDNA) using SuperScript III reverse transcriptase (Invitrogen, U.K.) according to the manufacturer's instructions. cDNA products from duplicate reverse transcription were then pooled. Quantification of β-actin mRNA expression using classical Taqman qPCR showed that all samples had C_T values approximately 23-27 cycles (**Table 6.1**), confirming that the starting RNA material was properly reverse transcribed to cDNA. C_T values from control wells without RNA templates or without the reverse transcriptase enzyme were below detection limit indicating no exogenous RNA contamination in the experiment.

Table 6.1 Ct values of Actb (β-actin) from ipsilateral spinal dorsal horns from 3 rat pain models quantified by classical Taqman quantitative polymerase chain reaction. CAR= carrageenan, PCX=paclitaxel, MIA=monosodium iodoacetate, NTC= no RNA template control, NEC= no reverse transcriptase enzyme control.

Batch1		Batch2	
Sample ID	Ct	Sample ID	Ct
NTC 1	Undetermined	NTC 2	Undetermined
NEC 1	Undetermined	NEC 2	Undetermined
CAR 5	22.79991	CAR 11	25.64137
CAR 6	23.42851	CAR 12	25.6134
CAR 7	23.41852	CAR 13	26.07075
CAR 8	23.77382	CAR 14	26.64518
CAR 9	22.6028	CAR 15	26.47548
CAR 10	23.14967	CAR 16	26.38732
PCX 5	24.29598	CAR 17	26.49282
PCX 6	23.03079	PCX 14	28.7646
PCX 7	25.05927	PCX 15	27.14704
PCX 8	23.61431	PCX 16	26.83328
PCX 9	23.41962	PCX 1L	26.53563
PCX 10	23.20111	PCX 2L	28.13943
PCX 11	27.77756	PCX 3L	27.83137
PCX 13	22.04281	MIA 11	26.00159
MIA 5	23.68811	MIA12	27.12724
MIA 6	23.01911	MIA13	27.18672
MIA 7	23.89324	MIA14	25.85669
MIA 8	24.81514	MIA15	28.54598
MIA 9	24.58413	MIA16	27.22945
MIA 10	23.47969	MIA17	25.71498

6.3.2 Relative quantification of spinal mRNA expression using TLDA

TLDA is a 384-well microfluidic card preload with TaqMan® Gene Expression Assay components, including forward and reverse primers and probes. Ninety-six genes were carefully selected and assigned to Format 96a of TLDA cards (Applied Biosystems, New York, USA) containing 8 loading ports accommodating 4 unique samples (2 ports needed per sample). Genes of interest were grouped into 8 clusters, (1) resolvin systems, (2) pro-inflammatory cascades, (3) anti-inflammatory cascades, (4) glial markers, (5) markers for central sensitization, (6) chemokines and (7) chemokine receptors and (8) reference genes. The complete list of genes, synonyms, protein products and ABI assay IDs are shown in **Table 6.2**.

The mRNA expression levels of all gene was expected to be moderate, therefore a concentration of 1-2 ng/ul cDNA (converted from starting RNA concentration) was loaded. To obtain 1.5 ng/ul final concentration (200 ul), cDNA samples (23ul) were gently mixed with HPLC water (77 ul) and TaqMan® Universal Mastermix II, with Uracil N-glycosylase (UNG) (Applied Biosystems, USA) (100 ul). Diluted cDNA samples were loaded into 2 separate ports (100 ul each) of the array cards equilibrated for at least 15 min at room temperature. Loaded cards were centrifuged twice at 1,200 rpm for 1 min at room temperature and sealed with TaqMan® Array Micro Fluidic Card Sealer (Applied Biosystems, USA). To quantify mRNA expression, the sealed cards were loaded into ABI PRISM 7900 HT Sequence Detection System (Applied Biosystems, USA) controlled by Sequence Detection System (SDS) software version 2.1. The cards were incubated with the following PCR cycling conditions; 2 min at 50°C, 10 min at 95°C and 40 cycles of 30 sec at 97°C and 1 min at 59.7°C. The quantitative endpoint of the method is the threshold

cycle (C_T, between 0-40) which the fluorescence of the reporter dye reaches the placed threshold. The numerical value is inversely related to the amount amplicon amplified.

Table 6.2 Complete list of selected target and reference genes for TLDA study.

Gene name	***Other gene name***	**Protein name**	**Relevant function**	**ABI assay ID**
Resolvin system				
Fpr2	*Fpr-rs2;Fprl1*	formyl peptide receptor 2 (FPR2/ALX or ALX receptor)	Receptor for RvD1, LXA4 and their aspirin triggered versions (Ye *et al.*, 2009)	Rn03037051_gH
Cmklr1	*Chemr23*	chemokine-like receptor 1 or ChemR23	Receptor for RvE1 and aspirin triggered RvE1(Arita *et al.*, 2005a)	Rn00573616_s1
Ltb4r	*Ltb4r1*	leukotriene B4 receptor or BLT-1	Receptor for RvE1 (acts as an antagonists(Arita *et al.*, 2007))	Rn00572209_s1
Gpr18	-	G protein-coupled receptor 18 (Gpr18)	Receptor for RvD2 (Chiang *et al.*, 2015)	Rn01493247_m1
Ptgs2	*COX-2;Cox2*	prostaglandin-endoperoxide synthase 2; cycloocxygenase-2 (COX-2)	PGE_2 generating enzyme, down regulated by 17-R-HDHA, a precursor for AT-RvD1 (Lima-Garcia *et al.*, 2011)	Rn00568225_m1
Alox15	*12-LOX;15-LOX;Alox12;Alox12l*	arachidonate 15-lipoxygenase (15-LOX); 15-LOX (15-lipoxygenase or 12/15-lipoxygenase)	Synthetic enzyme for RvD1 (Hong *et al.*, 2003; Lehmann *et al.*, 2015)	Rn00578743_m1
Alox5	*LOX5A*	arachidonate 5-lipoxygenase; 5-LOX (5-lipoxygenase)	Synthetic enzyme for RvD1 (Hong *et al.*, 2003; Lehmann *et al.*, 2015) and RvE1(Oh *et al.*, 2011)	Rn00563172_m1
Alox5ap	-	arachidonate 5-lipoxygenase activating protein; FLAP (5-lipoxygenase activating protein)	Activating protein for 5-LOX. Lipoxin and resolvin biosynthesis is dependent on FLAP expression (Lehmann *et al.*, 2015).	Rn00568506_m1
Cyp2c7	*Cyp2c39*	cytochrome P450, family 2, subfamily c, polypeptide 7;Cytochrome P450, family 2, subfamily c, polypeptide 7-like	Homolog of human CYP2C8, involves in the synthesis of anti-inflammatory lipid possibly including RvE1 synthesis (Arita *et al.*, 2005b)	Rn01529602_mH
Cyp2j4	*CYP2J2*	cytochrome P450, family 2, subfamily j, polypeptide 4; also known as CYP2J4	Involves in the synthesis of anti-inflammatory lipid possibly including RvE1 synthesis (Arita *et al.*, 2005b)	Rn00576482_m1
Lta4h	-	leukotriene A4 hydrolase (LTA4H)	Synthetic enzyme for RvE1 (last step following 5-LOX) (Oh *et al.*, 2011) Synthetic enzyme for LTB4 (pro-inflammatory) localised at nuclear membrane and requires 5-LOX mediated activation. Hypothesised that inhibited by RvD1 (Fredman *et al.*, 2014)	Rn01503878_m1
Ptgr1	*Dig1;Ltb4dh*	prostaglandin reductase 1 (PTGR1); leukotriene B4 12-hydroxydehydrogenase (LTB4DH)	Degradation enzyme for LXA4 (Clish *et al.*, 2000) RvD1 (Sun *et al.*, 2007) and RvE1 (Arita *et al.*, 2006)	Rn00593950_m1
Hpgd	-	hydroxyprostaglandin dehydrogenase 15 (NAD) (HPGD); 15-PGDH (15-hydroxyprostaglandin dehydrogenase)	Degradation enzyme for LXA4 (Clish *et al.*, 2000) RvD1 (Sun *et al.*, 2007) and RvE1 (Arita *et al.*, 2006)	Rn00577775_m1
Cyp2e1	*Cyp2e*	cytochrome P450, family 2, subfamily e, polypeptide 1 (CYP2E1)	Degradation enzyme for RvE1 (proposed) (Hong *et al.*, 2008)	Rn00580624_m1
Cyp4f4	-	cytochrome P450, family 4, subfamily f, polypeptide 4 (CYP4F4)	Homolog of human CYP4F8, degradation enzyme for RvE1 (proposed) (Hong *et al.*, 2008)	Rn01408362_g1
Ptges	*Pges*	prostaglandin E synthase; microsomal prostaglandin E synthase-1 (mPGS-1)	PGE2 generating enzyme, upregulated in spinal cord in carrageenan model (Guay *et al.*, 2004)	Rn00572047_m1

Gene name	*Other gene name*	Protein name	Relevant function	ABI assay ID
Pro-inflammatory cascades				
Nfkb1	*EBP-1;NF-kB*	nuclear factor of kappa light polypeptide gene enhancer in B-cells 1; nuclear factor kappa B subunit 1 (NF-κB subunit 1); p50	p50 subunit of NF-κB	Rn01399583_m1
Rela	*NFkB*	v-rel avian reticuloendotheliosis viral oncogene homolog A; RELA proto-oncogene, NF-κB subunit p65	p65 subunit of NF-κB, upregulated in acute incisional pain (Yang *et al.*, 2015), radicular pain (Liu *et al.*, 2016a). Spinal expression reduced by RvD1(Liu *et al.*, 2016a)	Rn01502266_m1
Chuk	*Ikbka;Ikka*	conserved helix-loop-helix ubiquitous kinase; inhibitor of nuclear factor kappa-B kinase alpha (IKKα)	Catalytic subunit of NF-κB essential modulator (NEMO), inhibition of IKKα attenuates pain behaviour and spinal expression of p65, COX-12, IL-1 and TNF(Tegeder *et al.*, 2004)	Rn01444501_m1
Nfkbia	*RL/IF-1*	nuclear factor of kappa light polypeptide gene enhancer in B-cells inhibitor, alpha; NF-κB inhibitor alpha (IκBα)	Inhibitor of p50-RelA NF-κB complex	Rn01473657_g1
Otulin	*Fam105b*	OTU deubiquitinase with linear linkage specificity or ubiquitin thioesterase otulin	Thiol-dependent ubiquitin-specific protease, plays roles in controlling inflammation, promotes proteasomal degradation of IKK complex	Rn00573991_m1
Tlr4	-	toll-like receptor 4 (TLR4)	A pathogen-associated molecular pattern receptor predominantly expressed by microglia, upregulated within 4 hr after CFA (Raghavendra *et al.*, 2004)	Rn00569848_m1
Cd14	-	Monocyte differentiation antigen CD14	Co-receptor for TLR	Rn00572656_g1
Myd88	-	myeloid differentiation primary response 88 (MyD88)	Downstream signalling molecule for TLR-4 and IL-1R	Rn01640049_m1
Traf3	-	Tnf receptor-associated factor 3 (TRAF3)	Signalling protein of TLR4, capable to induce IL-10 mRNA expression and a negative regulator of IL-17	Rn01429852_m1
Traf6	-	TNF receptor-associated factor 6 (TRAF6); E3 ubiquitin protein ligase	Signalling protein of cytokine receptors e.g. TLR4, IL-1and IL-17. mRNA Upregulated in spinal cord of SNL rats (Lu *et al.*, 2014)	Rn01512911_m1
Tnf	*RATTNF;TNF-alpha;Tnfa*	tumor necrosis factor;tumor necrosis factor-alpha (TNF-α)	Proinflammatory cytokine Spinal mRNA expression reduced by ALX receptor activation(Wang *et al.*, 2014b)	Rn00562055_m1
Tnfrsf1a	*TNFR-1;Tnfr1*	tumor necrosis factor receptor superfamily, member 1a (TNFR1)	Receptor for TNF-α	Rn01492348_m1
Tnfrsf1b	*Tnfr2*	tumor necrosis factor receptor superfamily, member 1b (TNFR2)	Receptor for TNF-α	Rn00709830_m1
Il1b	-	interleukin 1 beta (IL-1β)	Proinflammatory cytokine Spinal mRNA expression reduced by ALX receptor activation(Wang *et al.*, 2014b)	Rn00580432_m1
Il1r1	-	interleukin 1 receptor, type I (IL-1β receptor)	Receptor for IL-1β	Rn00565482_m1
Irak1	*RGD1563841*	interleukin-1 receptor-associated kinase 1 (IRAK) Checked mRNA changeable(Li *et al.*, 2011)	Target for ALX receptor mediated miR-146b	Rn01193545_m1
Casp1	*Ice;Il1bc*	caspase 1	Cleaves ProIL-1β to active IL-1β	Rn00562724_m1
Mmp2	-	matrix metallopeptidase 2	Protease from astrocytes converts pro-IL-1β and fractalkine to active forms	Rn01538170_m1

Gene name	***Other gene name***	**Protein name**	**Relevant function**	**ABI assay ID**
Mmp9	-	matrix metallopeptidase 9	Protease from microglia and pro-IL-1β and fractalkine to active forms	Rn00579162_m1
Timp1	*TIMP-1;Timp*	TIMP metallopeptidase inhibitor 1	Tissue inhibitor of MMP-9	Rn01430873_g1
Timp2	-	TIMP metallopeptidase inhibitor 2	Tissue inhibitor of MMP-2	Rn00573232_m1
Il6	*ILg6;Ifnb2*	interleukin 6 (IL-6)	Proinflammatory cytokine Spinal mRNA expression reduced by ALX receptor activation (Wang *et al.*, 2014b)	Rn99999011_m1
Il6r	*IL6R1;Il6ra*	interleukin 6 receptor, ligand binding subunit	Receptor for IL-6	Rn01495381_m1
Jak2	-	Janus kinase 2 (Jak2)	IL-6 signalling protein, mRNA level increased in CCI model (Xue *et al.*, 2014)	Rn00676341_m1
Stat1	*DD6G4-4*	signal transducer and activator of transcription 1 (STAT-1)	IL-6 signalling protein	Rn00583505_m1
Stat3	-	signal transducer and activator of transcription 3 (STAT-3); acute-phase response factor)	IL-6 signalling protein, mRNA level increased in CCI model (Xue *et al.*, 2014)	Rn00680715_m1
Socs1	*Cish1;Socs-1*	suppressor of cytokine signaling 1 (SOCS-1)	Suppressor of signalling from various cytokine receptors e.g. IL-6 receptor, TLR4, IFN-γ receptor (Yoshimura *et al.*, 2007)	Rn00595838_s1
Socs2	*Cish2;Socs-2*	suppressor of cytokine signaling 2 (SOCS-2)	Neuron specific SOCS involving with nerve growth factor dependent neurite outgrowth and increased TrkA receptor surface localization in dorsal root ganglion neurons(Uren *et al.*, 2014). Spinal mRNA upregulated in CCI model (Wang *et al.*, 2014b). Shown to be crucial for the anti-inflammatory activity of lipoxins (Machado *et al.*, 2006)	Rn00589521_m1
Socs3	*Cish3;Socs-3;Ssi-3*	suppressor of cytokine signaling 3 (SOCS-3)	Suppressor of IL-6 signalling. Spinal mRNA upregulated in CCI model and even more increased after i.t. aspirin-triggerd LXA_4 (Wang *et al.*, 2014b)	Rn00585674_s1
Nlrp1a	*Nalp1;Nlrp1*	NOD-like receptor family, pyrin domain containing 1A (NLRP1)	Inflammasome associated protein for caspase-1 activation, inhibited by ATL(Li *et al.*, 2013)	Rn01467482_m1
Nlrp3	*Cias1*	NOD-like receptor family, pyrin domain containing 3 (NLRP3)	Inflammasome associated protein for caspase-1 activation	Rn04244620_m1
Pdcd4	*Dug*	programmed cell death 4	Inhibitor of apoptosis, inhibited by miR-21	Rn00573954_m1
Cd40lg	*Cd40l;Tnfsf5*	CD40 ligand (CD40L)	Target for ALX receptor mediated miR208a	Rn00584362_m1
Il8	*Nap1, Cxcl8*	similar to Nef associated protein 1; IL-8 or C-X-C motif chemokine ligand 8 (CXCL8)	Proinflammatory cytokine	Rn01437056_m1
Il17a	*CTLA-8;IL-17;IL-17A;Il17*	interleukin 17A (IL-17A)	Proinflammatory cytokine	Rn01757168_m1
Anti-inflammatory cascades				
Il4	*Il4e12*	interleukin 4 (IL-4)	Anti-inflammatory cytokine	Rn99999010_m1
Gata3	-	GATA binding protein 3 *(GATA3)*	Transcription protein for IL-4	Rn00484683_m1
Il10	*IL10X*	interleukin 10 (IL-10)	Anti-inflammatory cytokine	Rn00563409_m1
Il13	-	interleukin 13 (IL-13)	Anti-inflammatory cytokine	Rn00587615_m1
Tgfb1	*Tgfb*	transforming growth factor, beta 1 (TGF-β1)	Anti-inflammatory cytokine	Rn00572010_m1

Gene name	***Other gene name***	**Protein name**	**Relevant function**	**ABI assay ID**
Ppara	*PPAR*	peroxisome proliferator activated receptor alpha (PPAR-α)	Nuclear transcription factor, a target for anti-inflammatory lipid mediators such as OEA, PEA and LXA4. PPAR-α by activation OEA has analgesic effect in various (LoVerme *et al.*, 2006)	Rn00566193_m1
Ppard	*Pparb*	peroxisome proliferator-activated receptor delta (PPAR-δ)		Rn00565707_m1
Pparg	-	peroxisome proliferator-activated receptor gamma (PPAR-γ)	Nuclear transcription factor, a target for anti-inflammatory lipid mediators such as 12- and 15-(S)HETE. RvD1 is essential for PPAR-γ mediated analgesia in a rat model of diabetes(Saito *et al.*, 2015)	Rn00440945_m1
Kcnip3	*Csen;Dream;rKChIP3*	Kv channel interacting protein 3; calsenilin; downstream regulatory element-antagonist modulator (DREAM)	Transcription-repressor supresses inflammation	Rn00583484_m1
Glia markers				
Itgam	*Cd11b*	integrin subunit alpha M	Microglia activation	Rn00709342_m1
Aif1	*BART-1;Bart1;iba1;mrf-1*	allograft inflammatory factor 1; ionised calcium-binding adaptor molecule 1 or allograft inflammatory factor 1 (IbA1)	Microglia activation	Rn00574125_g1
Arg1	-	arginase 1 (Arg1)	Marker for alternatively activated anti-inflammatory microglia (M2), elevated after spinal cord injury in rats(Chen *et al.*, 2015)	Rn00691090_m1
Cd163	-	CD163 molecule	Marker for alternatively activated anti-inflammatory microglia (M2), elevated after spinal cord injury in rats(Chen *et al.*, 2015)	Rn01492519_m1
Chi3l3	*Chi3l4;Chil3;rYM1olf*	chitinase 3-like 3 (Chi3l3) or Ym1	Marker for alternatively activated anti-inflammatory microglia (M2) (Cherry *et al.*, 2014)	Rn01523660_g1
Trem2	-	triggering receptor expressed on myeloid cells 2 (Trem2)	Macrophage marker, upregulated in peripheral nerves after sciatic nerve axotomy (Ydens *et al.*, 2012)	Rn01512170_m1
Retnla	*Himf*	resistin like alpha (*Retnla*) or Fizz1	Marker for alternatively activated anti-inflammatory microglia (M2) (Cherry *et al.*, 2014)	Rn00584229_m1
Gfap	-	glial fibrillary acidic protein (GFAP)	Astrocyte activation	Rn01253033_m1
S100b	*S100P*	S100 calcium binding protein B	Astrocyte activation	Rn04219408_m1
Markers for central sensitisation				
Grin2b	*GluN2B*	glutamate receptor, ionotropic, N-methyl D-aspartate 2B; glutamate ionotropic receptor NMDA type subunit (GluN2B)	Glutamatergic receptor involves in spinal pain transmission in pathological condition (Gu *et al.*, 2010)	Rn00680474_m1
Gria1	*GluA1;gluR-A*	glutamate receptor, ionotropic, AMPA 1, glutamate ionotropic receptor AMPA type subunit 1 (GluR1)	Glutamatergic receptor involves in spinal pain transmission in pathological condition (Larsson *et al.*, 2008). mRNA level increased in RVM from 24 h post CFA injection onward(Guan *et al.*, 2003)	Rn00709588_m1
Slc1a2	*Eaat2;Glt;Glt-1*	solute carrier family 1 (glial high affinity glutamate transporter), member 2; glutamate transporter1 (GLT1)	Glutamate transporter predominantly expressed by microglia, uptaking glutamate from synaptic cleft. Spinal mRNA expression upregulated in CCI and SNI model (Mirzaei *et al.*, 2010)	Rn00691548_m1

Gene name	***Other gene name***	**Protein name**	**Relevant function**	**ABI assay ID**
Slc1a3	*EAAT1;GLAST;GLAST-1;GluT-1*	solute carrier family 1 (glial high affinity glutamate transporter), member 3; glutamate-aspatate transporter (GLAST)	Glutamate transporter predominantly expressed by microglia, uptaking glutamate from synaptic cleft. Spinal mRNA expression upregulated in CCI and SNI model (Mirzaei *et al.*, 2010)	Rn01402419_g1
Nos2	*Nos2a;iNos*	nitric oxide synthase 2; inducible nitric oxide synthase (iNOS)	Inducible isoform of nitric oxide, reduced expression by RvD1	Rn00561646_m1
P2rx7	-	purinergic receptor P2X, ligand-gated ion channel, 7 (P2X7)	ATP-gated ion channels activated resulting in spinal microglia activation and the release of IL-1β contributing to hypernociception in CIA model(Nieto *et al.*, 2016) Spinal mRNA expression upregulated in SNI from day 3 onward(Kobayashi *et al.*, 2011)	Rn00570451_m1
Chemokines and chemokine receptors				
Cx3cl1	*Cx3c;Scyd1*	chemokine (C-X3-C motif) ligand 1	Released from neurones, binds to CXCR1 in microglia, Induces the activation of microglia and promotes neuropathic pain, cancer pain and inflammatory pain (Ji *et al.*, 2014)	Rn00593186_m1
Cxcl1	*CINC-1;Gro1*	chemokine (C-X-C motif) ligand 1	Released from astrocytes binds to CXCR2 in neurones. Maintains central sensitization and neuropathic pain (Ji *et al.*, 2014)	Rn00578225_m1
Cxcl6	*Cxcl5*	chemokine (C-X-C motif) ligand 6	Upregulated in skin after UVB-induced pain (Dawes *et al.*, 2013b)	Rn00573587_g1
Ccl2	*MCP-1;Scya2;Sigje*	chemokine (C-C motif) ligand 2	Released from neurones and astrocytes, binds to CCR2 in microglia and neurones (Ji *et al.*, 2014) Induces activation of microglia and neuropathic pain and Maintains central sensitization and neuropathic pain (Ji *et al.*, 2014)	Rn00580555_m1
Ccl7	-	chemokine (C-C motif) ligand 7	Released from astrocytes binds to CCR2 in microglia Maintains activation of microglia and neuropathic pain (Ji *et al.*, 2014)	Rn01467286_m1
Ccl21	*Ccl21b*	chemokine (C-C motif) ligand 21	Released from neurones, binds to CXCR3 in microglia, Induces activation of microglia and neuropathic pain (Ji *et al.*, 2014)	Rn01764651_g1
Cxcl13	-	chemokine (C-X-C motif) ligand 13	Spinal mRNA expression upregulated in SNL model from day 1 onward. Binds to CXCR5 and activates astrocyte in IN SNL model(Jiang *et al.*, 2016)	Rn01450028_m1
Cx3cr1	*Rbs11*	chemokine (C-X3-C motif) receptor 1	Receptor for CX3CL1. Spinal mRNA expression upregulated in rat model of spinal cord injury (day 35)(Detloff *et al.*, 2008)	Rn02134446_s1
Ctss	-	cathepsin S *Checked mRNA changeable*	Protease released from microglia cleaves membrane bound fractalkine to free form. Increased mRNA level in CCI and PNL models *(Barclay et al., 2007)*	Rn00569036_m1
Cxcr1	*Il8ra*	chemokine (C-X-C motif) receptor 1	Receptor for CXCL1, 5, 6 and 8	Rn00570857_s1
Cxcr2	*Cmkar2;Il8rb*	chemokine (C-X-C motif) receptor 2	Receptor for CXCL1, 2, 3, 5, 6, 7 and 8	Rn02130551_s1
Ccr1	-	chemokine (C-C motif) receptor 1	Receptor for CCL3, 5, 7, 9, 13, 14, 15, 16, 23	Rn00571950_s1
Ccr2	-	chemokine (C-C motif) receptor 2	Receptor for CCL2 and CCL7 and also CCL8, 12, 13, 14, 16	Rn01637698_s1
Ccr3	*Cmkbr3*	chemokine (C-C motif) receptor 3	Receptor for CCL3, 4, 5, 8, 11 14, 16	Rn02134292_s1
Ccr7	-	chemokine (C-C motif) receptor 7	Receptor for CCL21 and also CCL19	Rn02758813_s1
Cxcr5	*Blr1;NLR*	chemokine (C-X-C motif) receptor 5	Receptor for CXCR13. Spinal mRNA expression upregulated in SNL model from day 1 onward. (Jiang *et al.*, 2016)	Rn02132880_s1

Gene name	***Other gene name***	**Protein name**	**Relevant function**	**ABI assay ID**
Reference genes				
Gapdh	*BARS-38;Gapd*	glyceraldehyde-3-phosphate dehydrogenase	Commonly used reference gene	Rn01749022_g1
Actb	*Actx*	actin, beta (β-actin)	Commonly used reference gene, validated for normalization of mRNA expression in qPCR experiments in the spinal cord of CFA rats (may combine with Mapk6) (Walder *et al.*, 2014)	Rn00667869_m1
Mapk6	*ERK3*	mitogen-activated protein kinase 6	The most stable reference gene validated for normalization of mRNA expression in qPCR experiments in the spinal cord of CFA rats (may combine with Actb or Hprt1) (Walder *et al.*, 2014)	Rn00581152_m1
Hprt1	*Hgprtase;Hprt*	hypoxanthine phosphoribosyltransferase 1	Reference gene validated for normalization of mRNA expression in qPCR experiments in the spinal cord of CFA rats (may combine with Mapk6) (Walder *et al.*, 2014)	Rn01527840_m1
18s rRNA	*18s rRNA*	-	Commonly used reference gene Manufacturer's mandatory	Hs99999901_s1

6.3.3 Statistical analyses and interpretation of data from TLDA

6.3.3.1 Selecting reference genes

C_T values of 6 reference genes were first analysed to determine whether they were normally distributed across groups using Kolmogorov-Smirnov tests. Real time amplification plots and analyses of the normal distribution are shown in **Figure 6.1 and Table 6.3**. Ct values of Actb, Gapdh and Mapk6 were normally distributed in all groups regardless of the pain models. Expression stability of selected references genes calculated by a Visual Basic Application (VBA) for Microsoft Excel - termed geNorm (Vandesompele *et al.*, 2002) and expressed as M values which is inversely related to the stability. Actb and MAPK6 had the lowest M value (**Table 6.4**) and were therefore identified as the best performance genes that are stably expressed in all subgroup analyses including, acute pain (carrageenan), chronic (MIA and PCX) models or all models. C_T values of Actb and MAPK6 were also consistent across groups as shown in **Figure 6.2**.

Figure 6.1 Real time amplification plot of selected reference genes form ipsilateral spinal cord samples following carrageenan, MIA or PCX treatment and their respective controls. Changes from background of fluorescence of the reporter dye versus cycle number (0-40) detected by ABI Prism® 7900 Sequence Detection System. n=6-7 /group, total = 40.

Actb (β-actin)

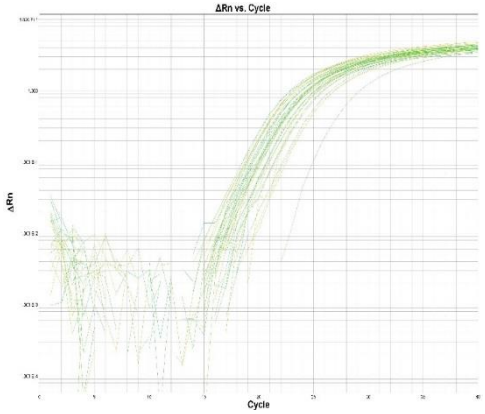

Gapdh

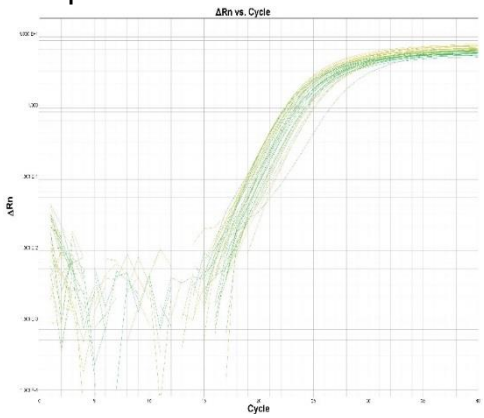

Hprt1

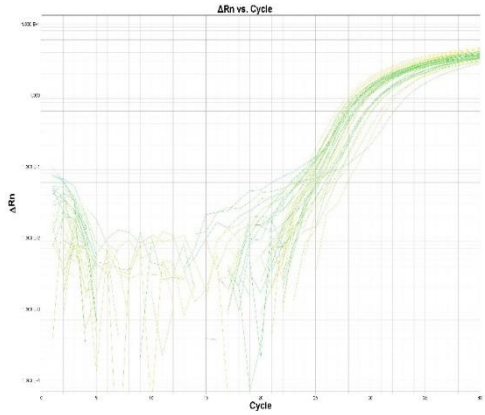

Mapk6

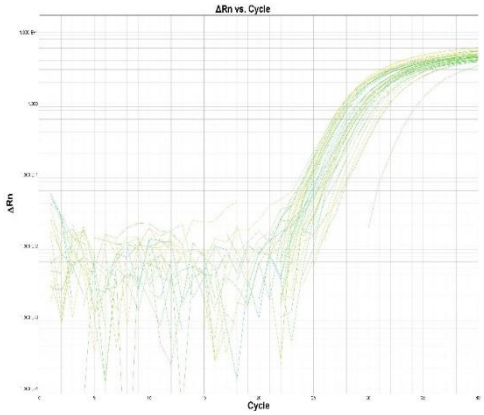

18s

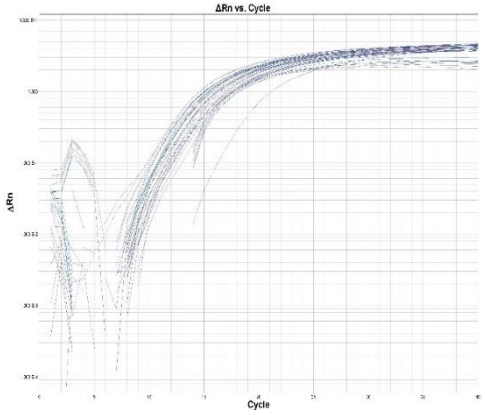

Table 6.3 Analyses of the normal distribution of selected reference genes across all samples used in TLDA. Ct vales of Actb, Gapdh and Mapk6 were normally distributed in all groups.

Genes	Groups	n	Min	25% Percentile	Median	75% Percentile	Max	Mean	S.D.	S.E.M.	Lower 95% CI of mean	Upper 95% CI of mean	KS normality test	
													KSdistance	P value
Actb	**CAR**	6	19.47	19.84	20.76	21.77	22.34	20.81	1.05	0.4287	19.71	21.92	0.1227	>0.10
	Control	7	19.55	20.49	20.86	21.74	23.08	21.08	1.1	0.4159	20.07	22.1	0.2163	>0.10
	MIA	7	19.93	20.94	21.17	22.56	23.35	21.61	1.187	0.4486	20.51	22.71	0.216	>0.10
	Control	6	19.93	19.95	21.12	21.92	22.05	21.01	0.9153	0.3737	20.05	21.97	0.2084	>0.10
	PCX	7	20.24	20.33	21.02	21.7	21.98	21.04	0.68	0.2776	20.32	21.75	0.1728	>0.10
	Control	7	19.82	19.92	20.5	21.93	23.33	20.99	1.278	0.4832	19.81	22.17	0.2209	>0.10
Gapdh	**CAR**	6	19.88	19.92	20.88	21.43	21.67	20.77	0.7312	0.2985	20	21.53	0.2053	>0.10
	Control	7	19.95	20.23	20.86	21.63	21.95	20.93	0.7245	0.2738	20.26	21.6	0.1186	>0.10
	MIA	7	19.99	20.36	20.96	21.86	22.62	21.15	0.9552	0.361	20.27	22.04	0.1783	>0.10
	Control	6	19.96	19.97	20.39	21.04	21.6	20.53	0.6223	0.2541	19.87	21.18	0.2198	>0.10
	PCX	7	20.18	20.49	21.02	22.36	23.83	21.42	1.266	0.4787	20.25	22.59	0.2736	>0.10
	Control	7	19.9	20.04	20.26	21.97	22.57	20.84	1.057	0.3994	19.87	21.82	0.2821	0.0974
Hprt1	**CAR**	6	24.69	25.07	25.97	26.81	26.95	25.92	0.9021	0.3683	24.98	26.87	0.174	>0.10
	Control	7	25.94	26.02	26.45	27.24	27.4	26.61	0.5734	0.2167	26.08	27.14	0.1848	>0.10
	MIA	7	25.63	26.21	26.75	28.17	28.52	27.11	1.15	0.4345	26.05	28.17	0.246	>0.10
	Control	6	25.4	25.53	26.24	27.14	27.44	26.32	0.8254	0.337	25.46	27.19	0.194	>0.10
	PCX	7	25.38	25.76	26.34	27.86	29.95	26.99	1.607	0.6074	25.5	28.47	0.2277	>0.10
	Control	7	25.13	25.95	25.98	27.76	29.16	26.56	1.392	0.5263	25.27	27.85	0.3678	**0.0048****
Mapk6	**CAR**	6	25.01	25.09	26.52	27.59	28.02	26.44	1.218	0.4971	25.16	27.72	0.1953	>0.10
	Control	7	25.57	25.76	26.66	27.76	29.3	26.84	1.323	0.5001	25.62	28.07	0.1926	>0.10
	MIA	7	25.19	25.58	27.15	28.85	28.95	27.24	1.481	0.5596	25.87	28.61	0.1543	>0.10
	Control	6	25.48	25.57	26.45	27.1	27.14	26.37	0.7725	0.3154	25.56	27.18	0.2716	>0.10
	PCX	7	25.69	25.97	27.12	27.85	31.98	27.52	2.128	0.8044	25.55	29.49	0.2963	0.06
	Control	7	24.99	25.27	25.77	27.48	28.95	26.42	1.411	0.5335	25.11	27.72	0.2483	>0.10
18s	**CAR**	6	14.3	14.41	14.58	15.32	17.34	14.98	1.163	0.4747	13.76	16.2	0.4485	**0.0004*** **
	Control	7	14.2	14.28	14.39	15.01	15.09	14.57	0.3604	0.1362	14.23	14.9	0.2555	>0.10
	MIA	7	14.12	14.34	14.72	14.93	15.34	14.66	0.4187	0.1583	14.27	15.05	0.198	>0.10
	Control	6	14.12	14.24	14.51	14.69	14.98	14.5	0.2964	0.121	14.19	14.81	0.2078	>0.10
	PCX	7	14.3	14.3	14.57	14.64	17.34	14.89	1.093	0.4131	13.87	15.9	0.4448	**0.0001*** **
	Control	7	14.16	14.2	14.36	14.66	14.95	14.45	0.2826	0.1068	14.18	14.71	0.1849	>0.10

Table 6.4 Expression stability of selected references genes calculated by geNorm software.

	Actb	Gapdh	Hprt1	Mapk6	18s
Acute pain model					
Carrageenan and control (n=13)	0.022	0.028	0.040	0.022	0.070
Chronic pain models					
Combined MIA, PCX and their controls (n=27)	0.022	0.033	0.032	0.022	0.047
All models					
Combined carrageenan, MIA, PCX and their controls (n=40)	0.022	0.032	0.035	0.022	0.056

Expression stability values were calculated and expressed as M values using geNorm Microsoft Excel Add-in. Actb and Mapk6 had the lowest M values; therefore, were identified as best performance genes stably expressed in all subgroup analyses including, acute pain (carrageenan), chronic (MIA and PCX) models or all models.

Figure 6.2 Ct values of Actb and mapk6 quantified by TLDA were comparable across all pain models. n=6-7/group. One-way ANOVA were used for comparing the means.

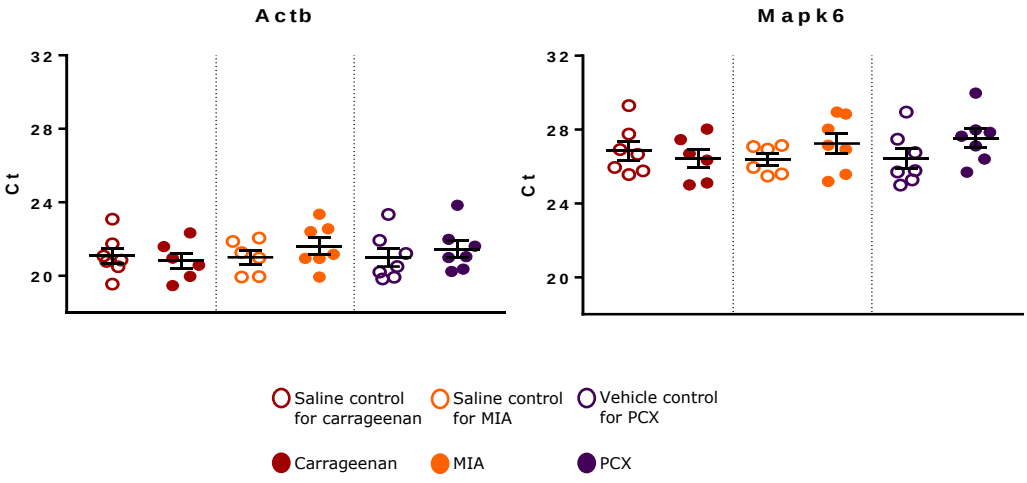

6.3.3.2 Analyses of relative expression levels

mRNA expression levels were calculated using the comparative C_T method (Schmittgen *et al.*, 2008). Data were analysed by 3 different methods:

- *Method 1 ΔC_T with multiple reference genes*: Geometric means of pooled C_T of Actb and Mapk6 was used to normalise data. Expression levels in each group were calculated by the following formula (Schmittgen *et al.*, 2008);

  Expression level = $2^{-(C_T \text{ Target}-C_T \text{ Reference})}$

  C_T target = C_T of target genes

  C_T Reference = geometric mean of Actb and Mapk6 C_T

- *Method 2 ΔC_T with single reference gene*: Expression levels were calculated in a similar to Method 1 except data were normalised using geometric means of Actb C_T.

- *Method 3 $\Delta\Delta C_T$ with single reference gene*: Results were expressed as fold change (Livak *et al.*, 2001; Mallinson *et al.*, 2015; Schmittgen *et al.*, 2008) (either carrageenan, MIA or PCX) to the appropriate saline/vehicle control which were calculated from the formula below. Geometric means of C_T of a single reference gene, Actb, were used to normalise the data;

  Fold change in treatment group= $2^{-(\Delta\text{Treatment})-(\Delta\text{Control})}$

  ΔTreatment = C_T of target gene in treatment group - C_T of reference gene (Actb) in treatment group

  ΔControl = C_T of target gene in saline/vehicle control group – geometric mean of C_T of reference gene (Actb) in control group

In order to express fold change in the control groups, geometric means of C_T of a reference gene, Actb, in saline/vehicle control group was used to normalise the data as in the following formula. This gave geometric means of the fold change in control group close to 1.

Fold change in control group= $2^{-(\Delta Control)- (Geo\ mean\ Control)}$

ΔControl = C_T of target gene in saline/vehicle control group – of C_T of reference gene (Actb) of saline/vehicle control

Geo mean Control = geometric mean of C_T of reference gene (Actb) of each control group

Heatmap presentation of the fold change in mRNA expression (only those identified as being significant above) was constructed using GraphPad Prism 7 software (GraphPad Software, Inc, USA). The fold change (**FC**) of mRNA of a particular gene was calculated by dividing the median expression level in a treatment group by the median of the respective control. A ±1.5 fold change was considered as baseline variation. Changes >±1.5 fold were categorised as modest (1.5-2 fold), moderate (2-4 fold) and prominent (>4 fold) and colour coded.

6.4 Results

6.4.1 Pain behaviour

Pain behaviour was assessed throughout the course of the study, up to 24 hr in the carrageenan model and 28 days in MIA and PCX models (**Figure 6.3**). Consistent with previous studies in this thesis, rats that received either intra-plantar carrageenan (**Figure 6.3A** and **B**), intra-articular MIA (**Figure 6.3C** and **D**) or intraperitoneal PCX (**Figure 6.3E**) developed robust pain behaviour.

At 24 h post carrageenan injection, carrageenan rats (n=6) developed significantly lower PWTs (3.2±0.71 g versus 16.7±2.54 g, $p<0.01$) and had weight bearing asymmetry (23.6±13.26% versus 0.27±2.82, $p<0.001$) compared to control rats (n=7). All carrageenan injected rats had paw oedema which was absent in the control (saline injected) rats. The paw circumference of the carrageenan-injected rats was significantly ($p<0.0001$) higher (28.8 ± 0.65 mm) than control rats (23.4±0.61 mm).

Similarly, 28 days post intra-articular injection of MIA (n=6), rats had a significantly lower PWT (MIA: 4.3±0.52 g; saline: 18.8±2.55 g, $p<0.05$) and weight bearing asymmetry (MIA: 26.7±2.72%; saline:-1.40±1.68, $p<0.0001$) compared to control rats (n=7). Post mortem macroscopic scoring of knee joints confirmed that all MIA rats, but not saline injected rats had chondropathy (macroscopic score MIA: 17±10; saline: 0±0, $p<0.01$).

The PCX model was associated with a significant mechanical hypersensitivity of the ipsilateral paw, compared to vehicle control (PCX: 6.0±1.10 g; control: 19.4±2.70 g, $p<0.0001$, n=7 per group). The mechanical hypersensitivity was maintained until day 28 post model induction (PCX: 4.4±0.98; vehicle: 19.2±4.18 g, $p<0.0001$).

Figure 6.3 Carrageenan, MIA and PCX evoked pain behaviour. Pain behaviour measured at baseline and following either; (**A**) 8 h post intraplantar carrageenan (n=7) or saline (n=6); (**B**) 28 days post intraarticular MIA (n=6) or saline (n=7) or (**C**) 28 days post intraperitoneal PCX (n=7) or vehicle (n=7). *p<0.05, **p<0.01, ***p<0.001, ****p<0.0001, two-way ANOVA with Sidak post hoc tests.

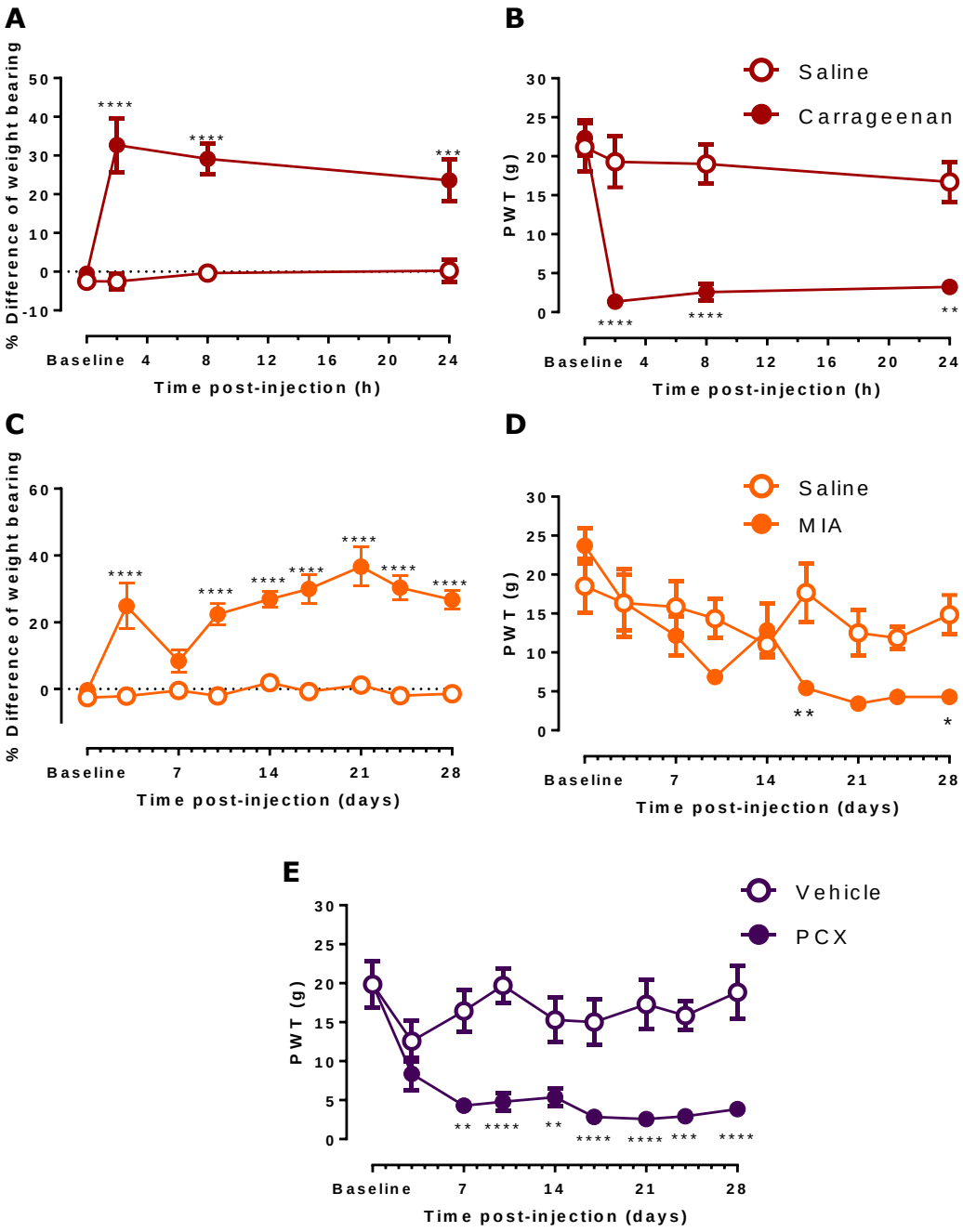

6.4.2 ΔCT with multiple reference genes was chosen to analyse the TDLA data

mRNA expression levels of each gene in the treatment groups were compared with the respective controls according to the pain models using Mann-Whitney U tests. Each method gave a different number of genes that were significantly changed, summarised in **Tables 6.5-6.7**. Method 1 detected 18 genes that were significantly altered (**Table 6.3**). Method 2 and 3 possess a similarity, using a single reference gene, Actb, for normalisation but expressing data as ΔC_T or $\Delta\Delta C_T$ gave distinct significant results. Using Method 2, only 9 significant genes (**Table 6.4**) were detected whereas Method 2 detected more than 30 significant genes (**Table 6.5**). Importantly, all methods of analysis consistently found some genes to be significantly altered: Fpr2 (carrageenan); Ptgr1 (carrageenan); Pparg (PCX); Cxcr1 (PCX); Ccr1 (PCX).

Following consideration of the outcomes of the different methods, method 1 (ΔCT with multiple reference genes) was chosen to analyse the TDLA data further in this chapter. Complete results for all 91 genes of interest are shown in **Figures 6.4-6.9**. Heatmap presentation of all 91 genes is shown in **Figure 6.11** and of those which were significantly altered is shown in **Figure 6.12**.

Table 6.5 Summary of significant changes in mRNA expression in rat ipsilateral spinal dorsal horns following either carrageenan MIA or PCX treatment calculated using ΔCT method and normalised by Actb-Mapk6 geometric means.

Cluster	Genes	Carrageenan		MIA		Paclitaxel	
Resolvin Receptor	Fpr2	↓9.9	#				
	Ltb4r	↓2.4	#				
Resolvin synthetic enzyme	Alox5ap					↑3.2	#
	Cyp2j4					↑3.4	##
Resolvin degradation enzyme	Ptgr1	↑2.2	#			↑2.8	#
	Hpgd			↑2.6	#		
Pro-inflammatory cascades	Tlr4					↑3.0	#
	Nlrp1a					↑2.7	#
	Tnfrsf1a					↑2.0	##
	Tnfrsf1b					↑2.8	#
	Soc2					↑4.6	##
Anti-inflammatory cascades	Pparg					↑3.7	##
Central sensitisation	Grin2b					↑2.1	#
Chemokine	Cxcl6					↑2.6	#
Chemokine receptors	Cxcr1					↑9.7	##
	Cxcr5					↑4.2	#
	Ccr1					↑7.8	#
	CX3cr1					↑2.4	#

Expressed as fold change of ΔCT vs saline/vehicle) $^{\#}p<0.05$, $^{\#\#}$ $p<0.01$ Mann-Whitney U Test when compared raw C_T values of each treatment versus its control, n=5-7/group.

Table 6.6 Summary of significant changes in mRNA expression in rat ipsilateral spinal dorsal horns following either carrageenan MIA or PCX treatment calculating using ΔCT method and normalised by Actb geometric means.

Cluster	Genes	Carrageenan	MIA	Paclitaxel
Resolvin system	Fpr2	↓8.8 #		
	Alox15		↓2.4 #	
	Alox5ap	↑4.6 #		
	Ptgr1	↑2.8 #		
	Hpgd			↓2.6 ##
Anti-inflammatory cascades	Pparg			↑2.0 #
Glial markers	Arg1			↓2.9 #
Chemokine receptors	Cxcr1			↑2.2 #
	Ccr1			↑5.5 #

Expressed as fold change of ΔCT vs saline/vehicle) $^{\#}p<0.05$, $^{\#\#}$ $p<0.01$ Mann-Whitney U Test when compared raw C_T values of each treatment versus its control, n=5-7/group

Table 6.7 Summary of significant changes in mRNA expression in rat ipsilateral spinal dorsal horns following either carrageenan MIA or PCX treatment calculated using ΔΔCT method and normalised by Actb geometric means.

Cluster	Genes	Carrageenan		MIA		Paclitaxel	
Resolvin system	Fpr2	↓7.7	#				
Resolvin synthetic enzyme	Alox15	↓1.7					
	Alox5ap	↑2.8	##				
	Cyp2j4			↑2.0	#	↑1.9	#
Resolvin degradation enzyme	Ptgr1	↑2.3	#			↑1.7	#
	Cyp4f4	↑2.5	#				
Pro-inflammatory signalling	Il1b	↑4.5	##				
	Mmp2			↑1.9	#		
	Il6r			↑2.6	#		
	Tnfrsf1a					↑1.5	#
	Tnfrsf1b					↑1.7	#
	Tlr4	↓2.6	##				
	Traf3	↑1.4	#				
	Irak1			↓1.2	##		
	Rela			↑1.3	##		
	Chuk	↑2.1	##				
	Nlrp1a					↑2.8	##
	Nlrp3	↓3.0	##				
Anti-inflammatory signalling	Socs2					↑3.0	##
	Nfkbia			↓1.3	#	↑1.5	##
	Pparg					↑2.7	##
	Otulin	↑1.5	#			↑4.0	#
Glial markers	Itgam	↑2.1	##			↑1.5	##
	Arg1					↓2.9	##
	Cd163	↓1.9	#				
Markers for central sensitisation	Grin2b					↑2.1	##
	Gria1					↓1.5	#
	Slc1a3			↓1.4	#	↓1.3	#
Chemokines	Cxcl6	↑2.6	#			↑3.1	#
	Ctss	↑1.4	##				
Chemokine receptors	Cxcr1					↑6.7	#
	Ccr1					↑7.9	#
	Ccr2					↑4.5	#
	Cx3cr1					↑1.6	##

Expressed as fold changed of ΔΔCT vs saline/vehicle) $^{\#}p<0.05$, $^{\#\#}p<0.01$ Mann-Whitney U Test when compared raw C_T values of each treatment versus its control, n=5-7/group.

6.4.3 Global changes: overview

Global changes in mRNA expression of all mRNA in the spinal cord samples from carrageenan, MIA and PCX model are shown as a heatmap in **Figure 6.11**. The carrageenan and PCX models were associated with changes in a number of mRNA that were moderately or prominently altered in the ipsilateral dorsal horn of the spinal cord. In the carrageenan model mRNA of some key mRNA were upregulated (Ptgr1, Myd88, Pparg, etc.) whereas others were downregulated (Fpr2, Nlrp3). In the PCX model the majority of mRNAs altered were upregulated (i.e. Cmklr1, Prgr1, Cyp2e1, Timp1). Interestingly, there were moderate or prominent changes in several mRNAs in chemokine and chemokine clusters in the PCX model. The carrageenan and PCX models were generally associated with altered mRNA expression in most of the clusters selected, this was less so for the the MIA model.

6.4.4 Resolvin system

Of 16 mRNAs screened, the carrageenan and PCX models were associated with changes in slightly different subsets of the resolvin system relevant mRNAs in the spinal cord. The relative expression of 2 resolvin receptors, Fpr2 and Ltb4r mRNA (**Figures 6.4A** and **C** and **6.12A**), was significantly down regulated in the carrageenan model compared to saline control (Fpr2 FC-9.9, $p<0.05$ and Ltb4r FC -2.4, $p<0.05$). However in the MIA and PCX models, the expression of these resolvin receptor mRNAs in the spinal cord were comparable to their respective controls. No significant changes in ChemR23 and Gpr18 expression in the spinal cord were evident in either carrageenan, MIA or the PCX model when compared to their controls.

Two mRNAs involved in resolvin synthesis (from 7 screened) were significantly altered in the pain models, Alox5ap and Cyp2j2 (**Figures 6.4H** and **I** and **6.12A**). Alox5ap tended to an increase (FC 1.9) in the carrageenan model compared to saline control, but did not reach

significance. In the PCX model there was a significant increase in Alox5ap (FC 3.2, $p<0.05$) and Cyp2j4 (FC 3.4, $p<0.01$) expression in the spinal cord, compared to control. Ptgs2 (Cox2), Alox15, Alox5, and Lta4h expression levels were not significantly changed in the spinal cord in any of the models. Expression of Cyp2c7 was below detection limit.

Two mRNAs encoding enzymes involved in resolvin metabolism (from 4 screened) were altered in the pain models (**Figures 6.2K** and **L** and **6.12A**). In the carrageenan and PCX models Ptgr1 expression (FC 2.2, $p<0.05$ and FC 2.8, $p<0.05$, respectively) was significantly increased, but not in the MIA model. There was however another mRNA in this cluster, Hpgd, which was significantly increased (FC 2.6, $p<0.05$) in the MIA model, compared to saline control. Expression levels of Cyp2e1 in MIA model and Cyp4f4 in carrageenan model were not robust. Cyp2e1 was prominently upregulated in carrageenan (FC 4.0) and PCX (FC 14.6) models, but due to variability in these changes statistical significance was not reached.

Figure 6.4 Changes in mRNA expression levels of resolvin receptors in rat ipsilateral spinal dorsal horns following either carrageenan MIA or PCX treatment compared to their controls. $^{\#}p<0.05$, $^{\#\#}p<0.01$ versus control, Mann-Whitney U Test, n=5-7/group.

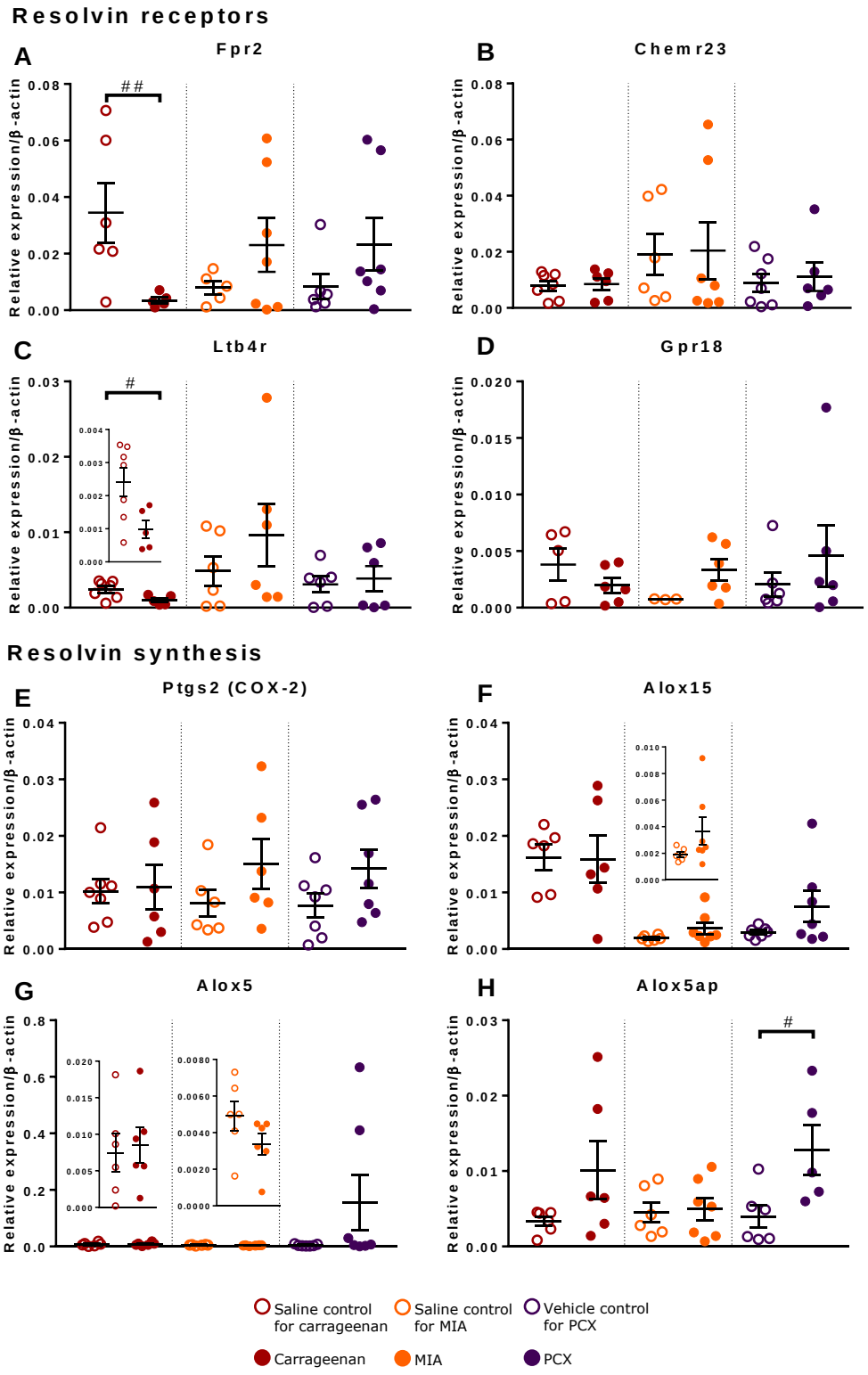

Figure 6.4 continue – Resolvin system

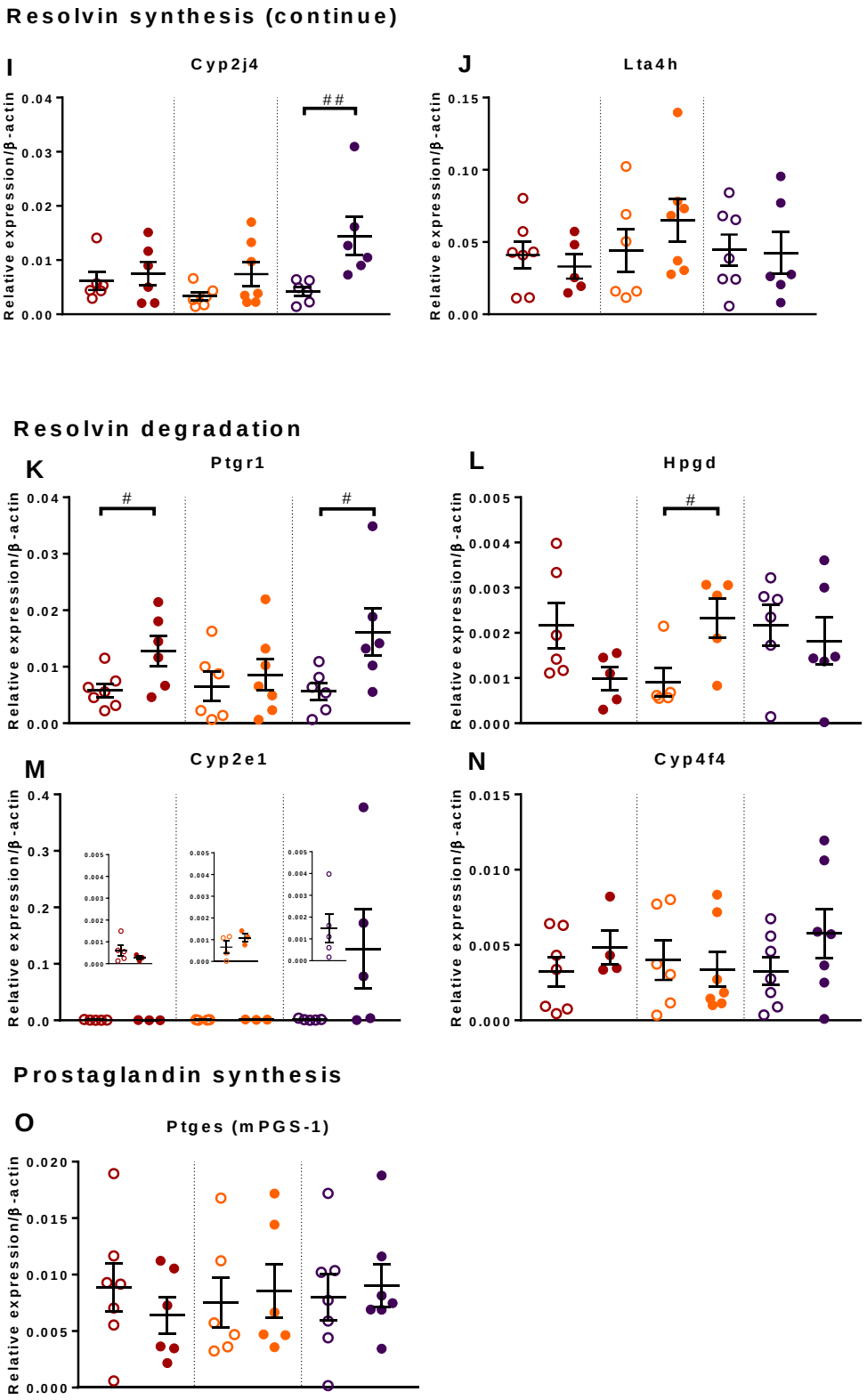

6.4.5 Pro-inflammatory cascades

The impact of the models of pain on the spinal expression of pro-inflammatory signalling pathways was studied (**Figure 6.5**). In the PCX model the expression levels of 5 mRNAs (Tlr4, Tnfrsf1a, Tnfrst1b and Nlrp1a and Socs2) were significantly elevated (**Figures 6.5 F, L, M, AB and AD** and **6.12B**). The Tlr4 mRNA was significantly increased in the ipsilateral dorsal horn of the spinal cord of PCX rats (FC 3, $p<0.05$) (**Figures 6.4F** and **6.12B**). Non-significant changes in other mRNAs essential for TLR4 signal transduction, including, a co-receptors (Cd14) and adapter proteins (Myd88, Traf3 and Traf6) were also evident in the PCX model (**Figure 6.12** TLR4 panel).

Two mRNAs for inflammasomes screened were elevated in the PCX model, Nlrp1a and Nlrp3. However, only Nlrp1a reached the significance (FC 2.7, $p<0.05$) (**Figures 6.5AD** and **6.12B**).

mRNAs for 2 TNF-α receptors were significantly higher in the PCX model compared to control, Tnfrsf1a (FC 2.0, $p<0.01$) and Tnfrsf1b (FC 2.8, $p<0.05$) (**Figures 6.5 L**-**M** and **6.12B**). Unfortunately, the data for Tnf, the mRNA for TNF-α, was not sufficiently robust to allow data analysis (**Figure 6.12 TNF-α panel**).

Eight mRNAs in the IL-6 pro-inflammatory cascade including IL-6 itself, receptor and intracellular adaptor proteins were examined. Socs2 (a suppressor of cytokine signalling) expression was significantly increased (FC 4.6, $p<0.01$) in the PCX model, compared to control (Figure 6.3E and Figure 6.5B). Other mRNAs in this cascade (Il6, Il6r, Jak2, Stat1, Stat3, Socs1 and Socs3) were not significantly altered (**Figure 6.12** IL-6 panel).

No significant changes were found in other pro-inflammatory cascades including NF-κB (Nfkb1, Rela, Chuk, Nfkbia and Otulin), PDCD, IL-1β (Il1b, Il1r1, Irak1, Casp1, Mmp2, Mmp9, Timp1 and Timp2), IL-8 and IL-17 in any of the pain models. Similar to the

resolvin mRNAs, the largest upregulation of pro-inflammatory mRNAs was in the PCX model. Changes in the carrageenan model were on the whole moderate. In the MIA model, there was a moderate downregulation in Casp1 (FC -3.1) and a moderate upregulation in Mmp2 (FC 2.1), but statistical differences were not detected.

Figure 6.5 Changes in mRNA expression levels of pro-inflammatory cascade in rat ipsilateral spinal dorsal horns following either carrageenan MIA or PCX treatment compared to their controls. $^{\#}p<0.05$, $^{\#\#}p<0.01$ versus corresponding saline/vehicle, Mann-Whitney U Test, n=5-7/group, ns=not significant.

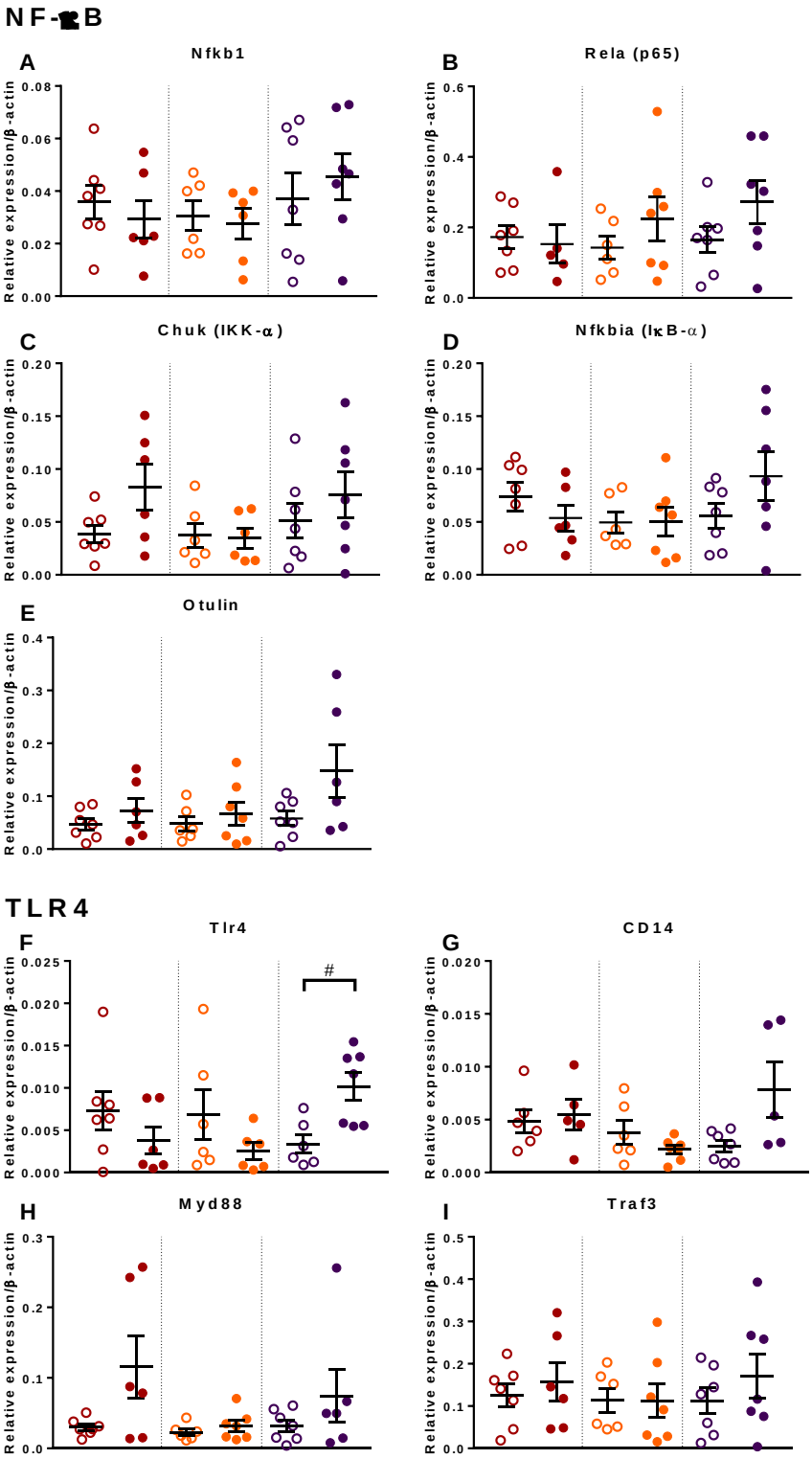

Figure 6.5 continue - Pro-inflammatory cascades

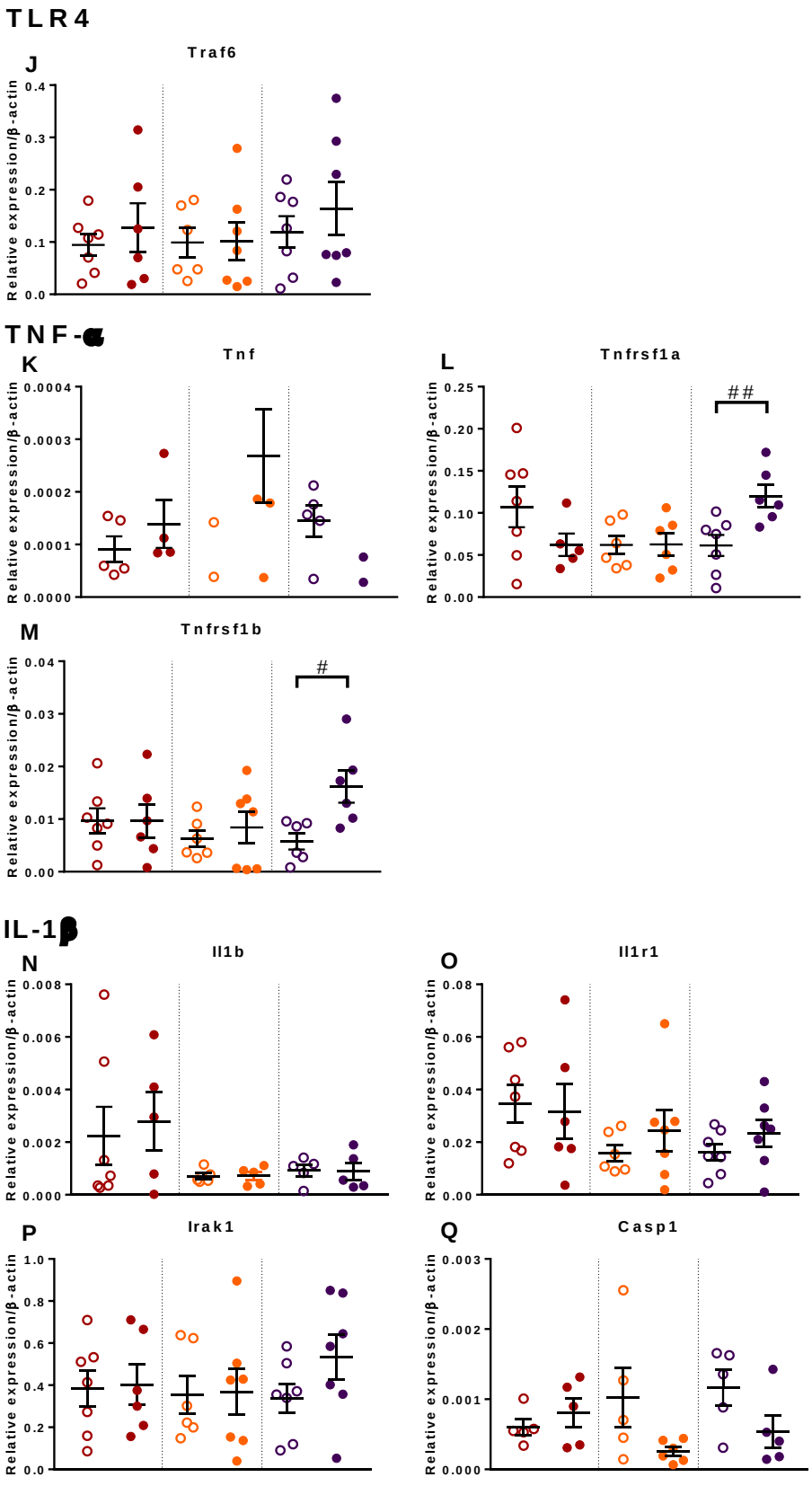

Figure 6.5 continue - Pro-inflammatory cascades

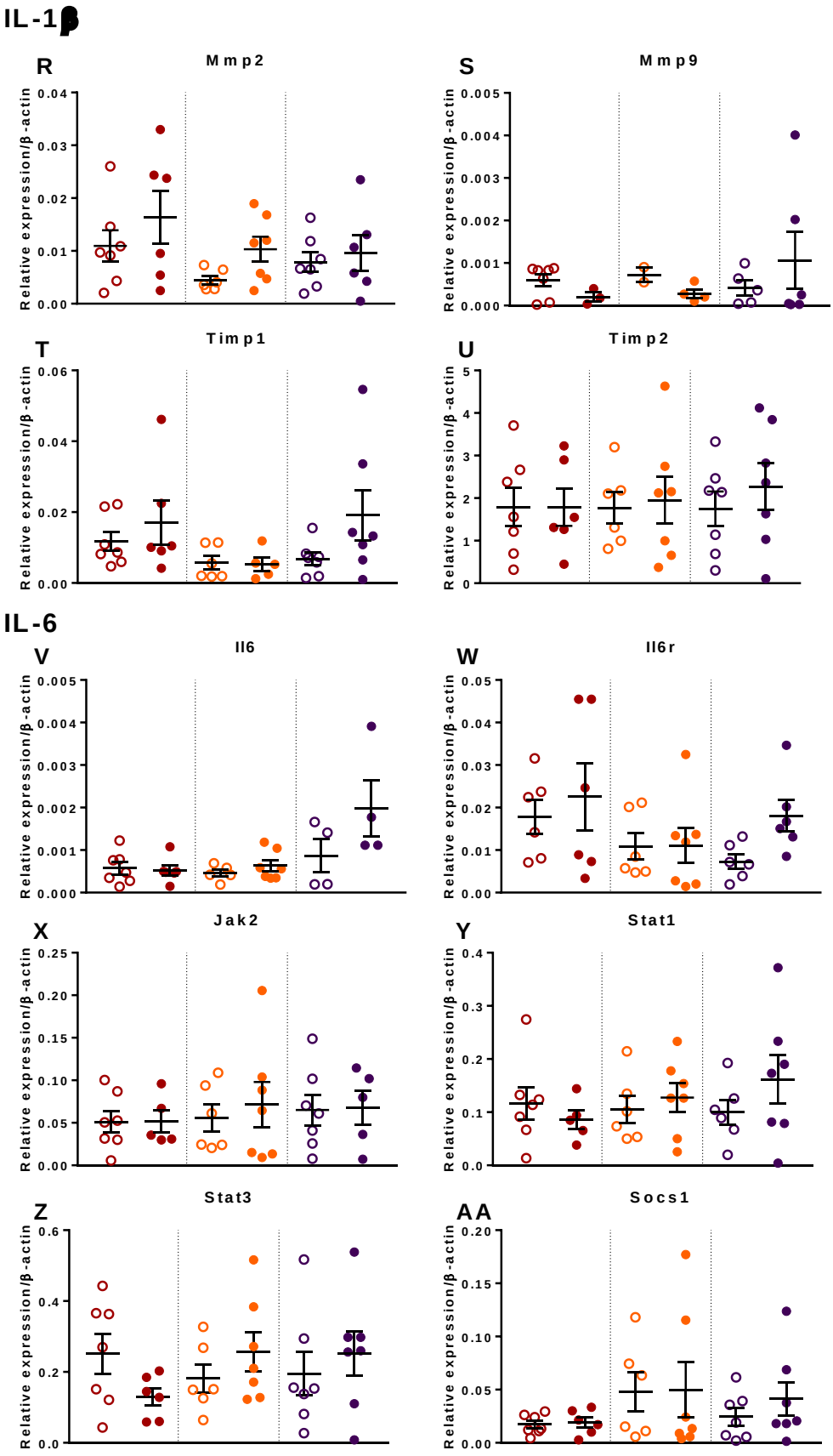

Figure 6.5 continue - Pro-inflammatory cascades

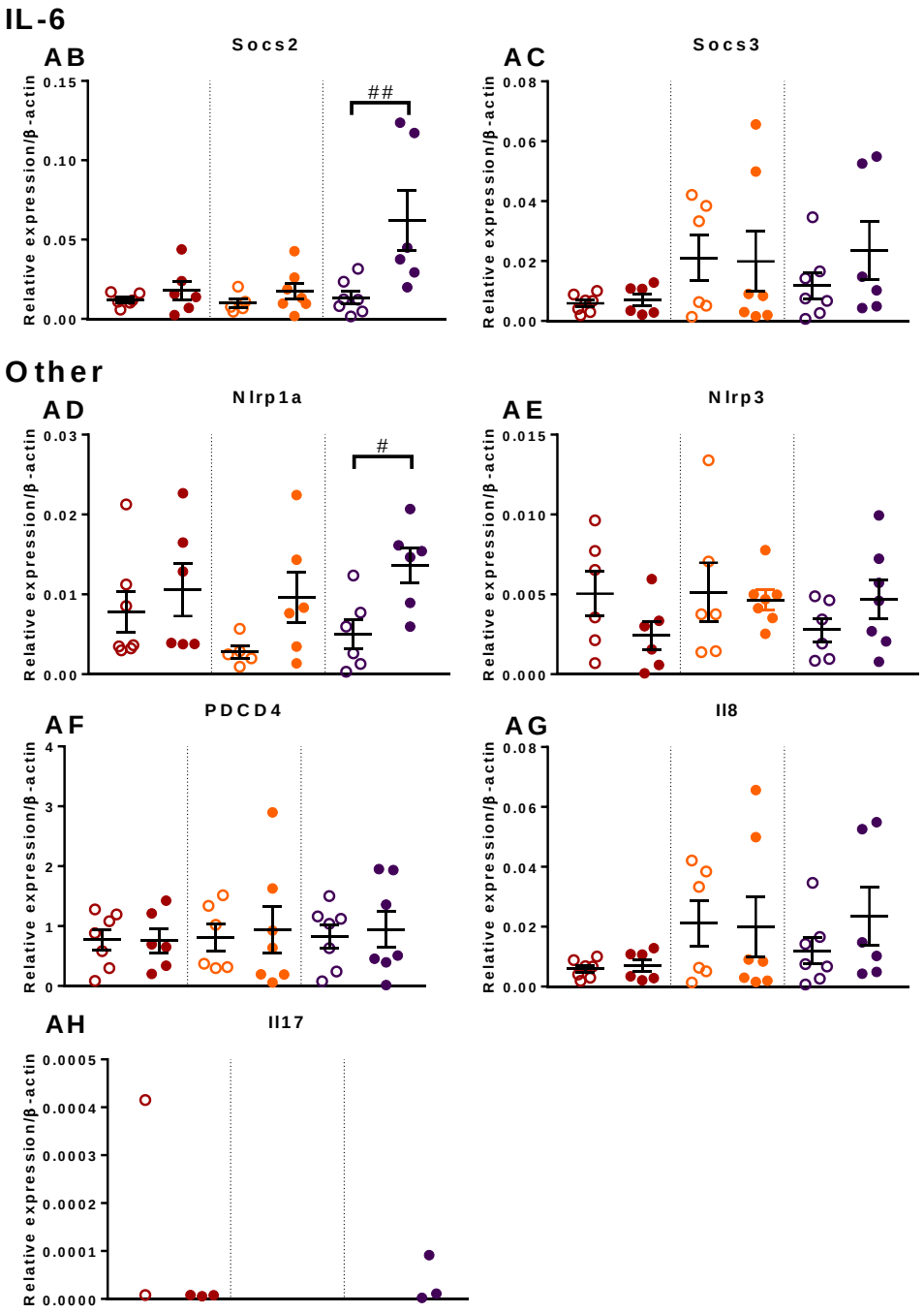

6.4.6 Anti-inflammatory cascades

The mRNA for anti-inflammatory cascades were investigated (**Figures 6.6**). PPAR-gamma (Pparg) mRNA was consistently upregulated across the 3 models of pain, to varying degrees. The highest magnitude of change was in PCX model (FC 3.7, $p<0.01$) (**Figures 6.6H** and **6.12B**). Expression levels of GATA (a transcription factor for IL-4), Tgfb, Ppara, Ppard, Otulin and Kcnip3 were not significantly altered in any of the models. The expression levels of the mRNAs for IL-4, IL-10 and IL-13 (Il4, Il10 and Il13) were not quantifiable due to the levels were below the detection limit.

Figure 6.6 Changes in mRNA expression levels of anti-inflammatory cascades in rat ipsilateral spinal dorsal horns following either carrageenan MIA or PCX treatment compared to their controls. ##p<0.01 versus saline/vehicle, Mann-Whitney U Test, n=5-7/group.

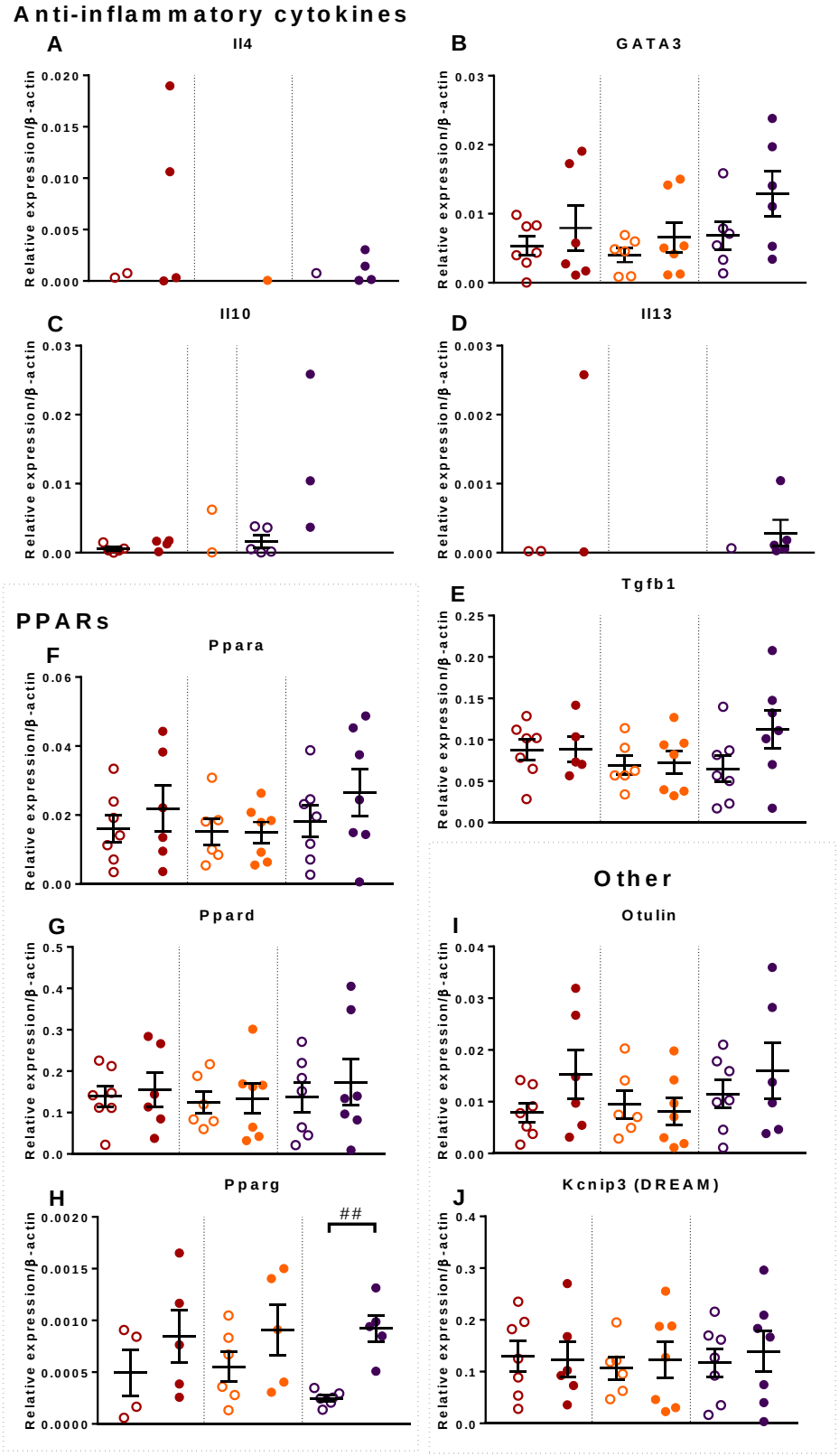

6.4.7 Glial markers

mRNAs of markers for microglia populations and astrocytes were investigated (**Figure 6.7**). None of the makers for activated microglia (Itgam, and Aif1 or Iba1), alternatively activated microglia (Arg1, Cd163 and Trem2) or astrocytes (Gfap and s100b) were significantly altered in any of the pain models studied. The spinal abundance of Itgam, Chi3l3 and Retnla was below the detection limit.

Figure 6.7 Changes in mRNA expression levels of glial markers in rat ipsilateral spinal dorsal horns following carrageenan MIA or PCX treatment. n=5-7/group.

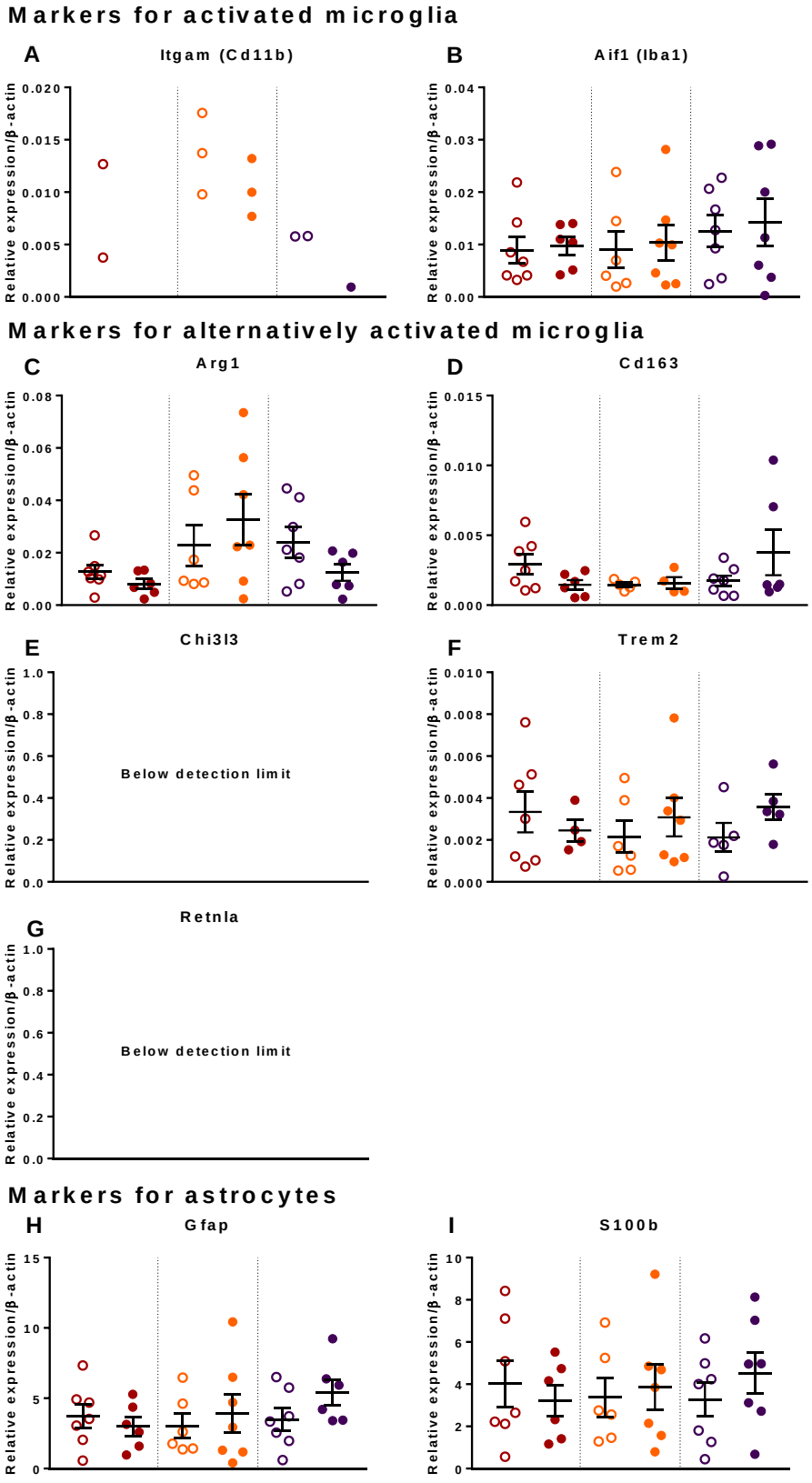

6.4.8 Markers for central sensitisation

Investigation of mRNAs for central sensitisation (**Figures 6.8A**) revealed that the only significant mRNA changed in this cluster was Grin2b (GluN2B receptor) in the PCX model (FC 2.1, $p<0.05$) (**Figures 6.8A** and **6.12B**). Other glutamatergic mRNAs studied, Gria (GluR1 receptor), Slc1a2 (glutamate transporter 1) and Slc1a3 (glutamate/aspartate transporter GLAST-1) and P2x7 mRNAs were not significantly altered in either carrageenan, MIA or PCX model.

Figure 6.8 Changes in mRNA expression levels of markers for central sensitisation in rat ipsilateral spinal dorsal horns following carrageenan MIA or PCX treatment. #p<0.05 versus saline/vehicle, Mann-Whitney U Test, n=5-7/group.

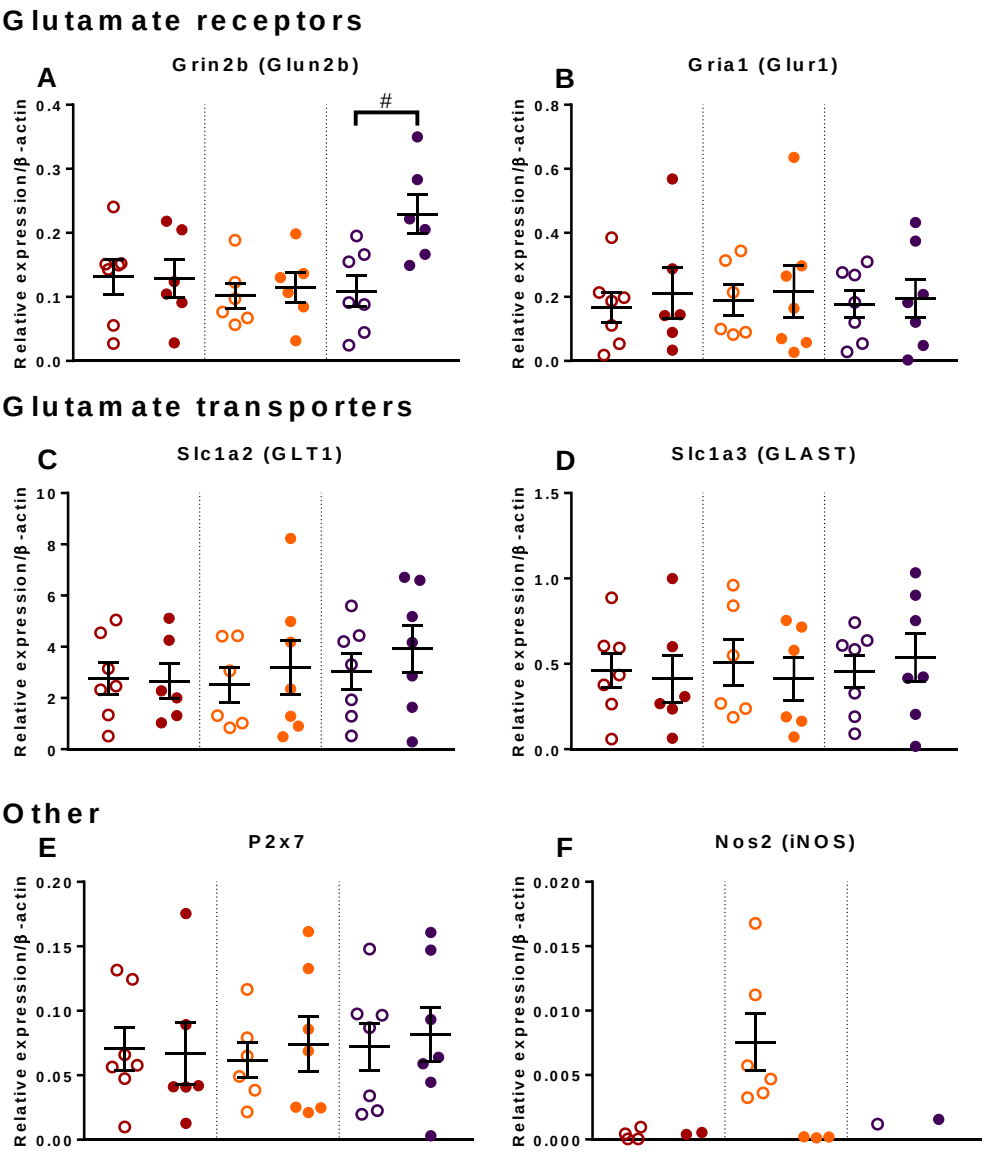

6.4.9 Chemokines and chemokine receptors

Results of the mRNA expression of chemokines and chemokine receptors are showin in **Figures 6.9** and **6.10,** respectively. Similar to the other clusters, the PCX model had the predominance of changes in mRNA expression for this cluster. There was a significant increase in the expression of the chemokine Cxcl6 (FC 2.6, $p<0.05$) in the PCX model (**Figures 6.9C** and **6.12C**). There were a greater number of significant changes in the chemokine receptor mRNAs. The significant up-regulated chemokine receptor mRNAs in the PCX model, ordered by magnitude, were Cxcr1 (FC 9.7, $p<0.01$), Cxcr5 (FC 4.2, $p<0.05$), Ccr1 (FC 7.8, $p<0.05$) and Cx3cr1 (FC 2.4, $p<0.05$) (**Figures 6.10 A, C, D** and **H and 6.12C**). Other chemokines (Cxcl13, Ccl2, Ccl7, Ccl23, Cx3cl1), CX3CL1 activating protein (Ctss) and chemokine receptors (Cxcr2, Ccr2, CCr3, Ccr7) were not significantly altered.

Figure 6.9 Changes in mRNA expression levels of chemokines in rat ipsilateral spinal dorsal horns following carrageenan MIA or PCX treatment. #p<0.05 versus saline/vehicle, Mann-Whitney U Test, n=5-7/group.

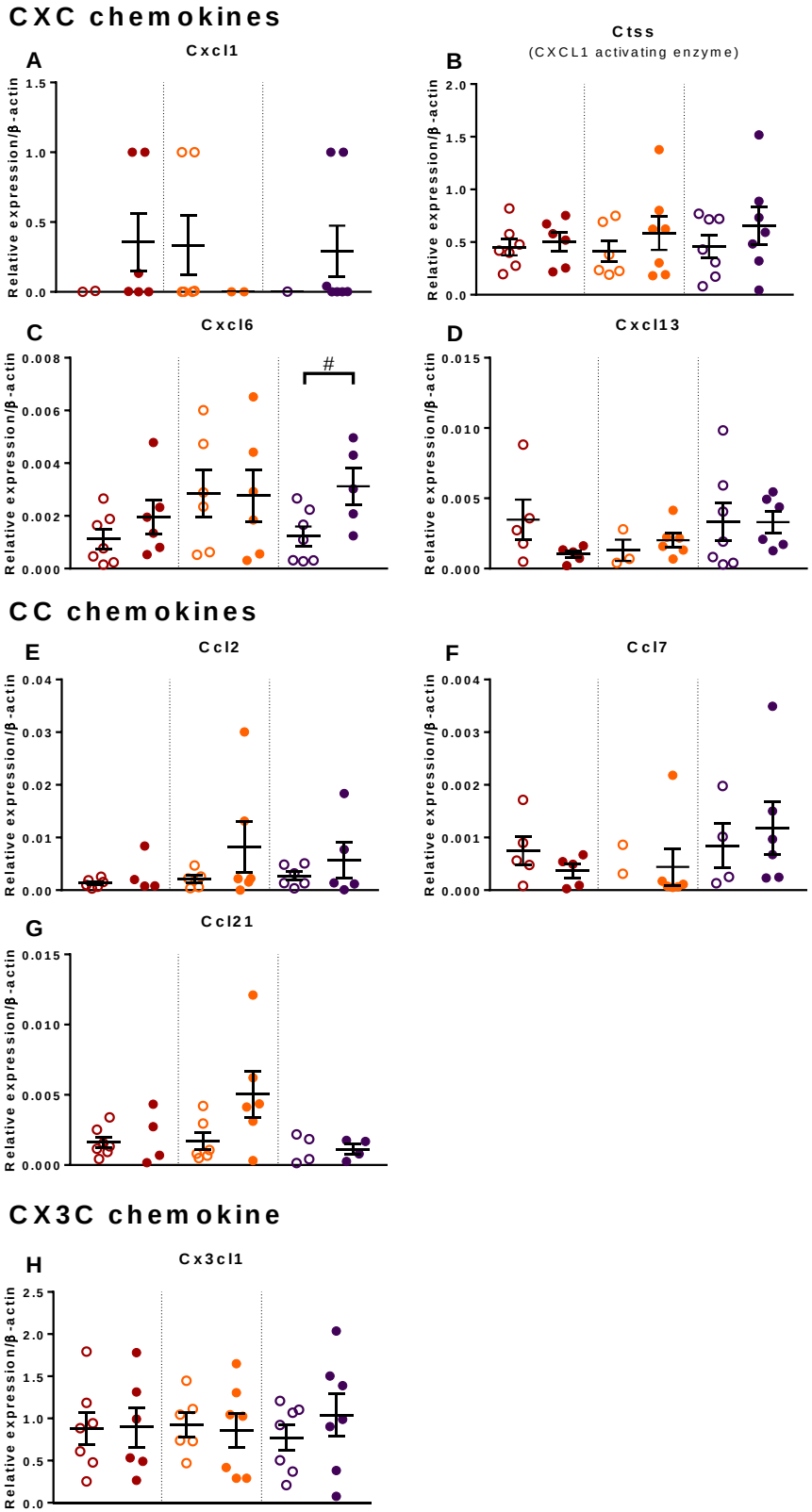

Figure 6.10 Changes in mRNA expression levels of chemokine receptors in rat ipsilateral spinal dorsal horns following carrageenan MIA or PCX treatment. #p<0.05, ##p<0.01 versus saline/vehicle, Mann-Whitney U Test, n=5-7/group.

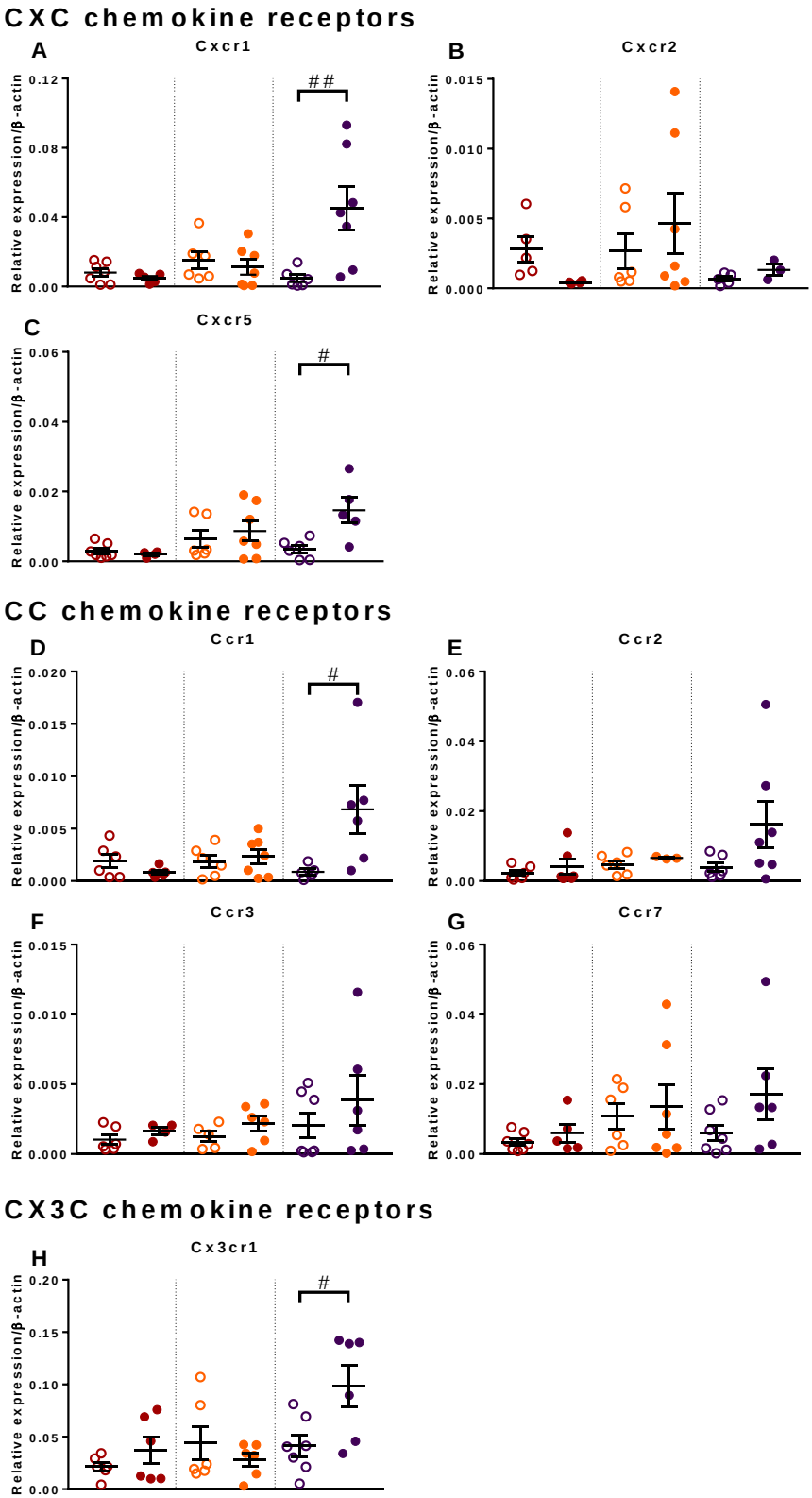

Figure 6.11 Comparison of mRNA expression profile in rat ipsilateral spinal dorsal horns following either carrageenan MIA or PCX treatment. Each cell represents the fold change of a particular mRNA in the treatment group (carrageenan (CAR), MIA or PCX) relative to the respective control. $^{\#}p<0.05$, $^{\#\#}p<0.01$ Mann-Whitney U Test when compared raw C_T values of each treatment versus its control (as shown in Figures 6.4-6.10), n=5-7/group. NA=not applicable.

Figure 6.11 - continue

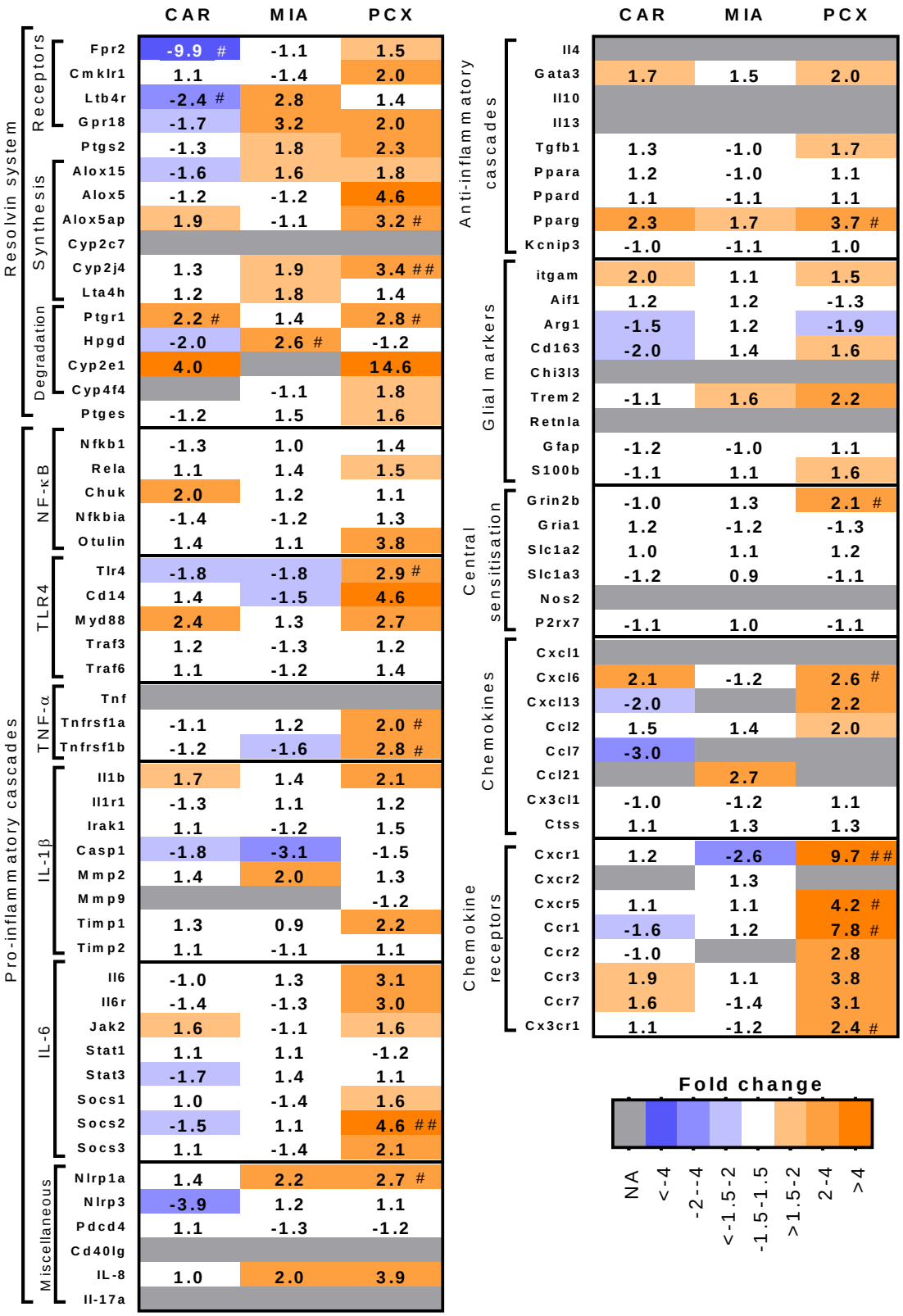

Figure 6.5 Heatmap comparing significant changes in mRNA expression levels in rat ipsilateral spinal dorsal horns in carrageenan, MIA and PCX models. The fold change of a particular mRNA was calculated by dividing the median of expression level in a treatment group by the median of respective control. A ± 1.5 fold change was considered as baseline variation. Changes >±1.5 fold were categorised as modest (1.5-2 fold), moderate (2-4 fold) and prominent (>4 fold). $^{\#}p<0.05$, $^{\#\#}p<0.01$ Mann-Whitney U Test when compared raw C_T values of each treatment versus its control (as shown in Figures 6.4-6.10), n=5-7/group. CAR=carrageenan.

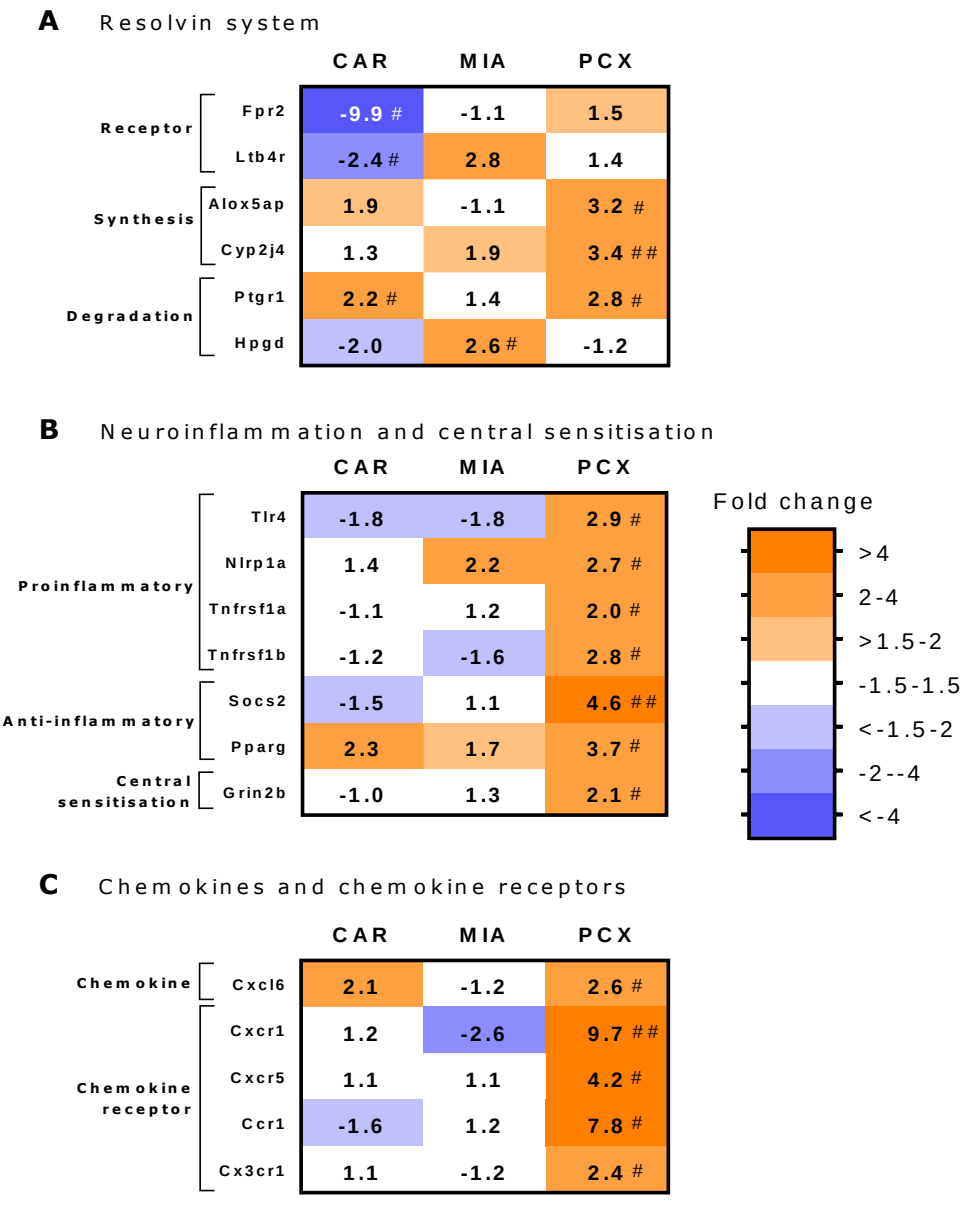

6.5 Discussion

The present study investigated alterations in spinal mRNA expression in 3 well-characterised pain models, mimicking acute (carrageenan model) and chronic pain mechanisms (MIA and PCX models) in the rat. Profiling of spinal mRNA expression using TLDA was performed on ipsilateral dorsal horns of the spinal cord in rats with established pain behaviour, compared to their controls. This work demonstrates, for the first time, unique spinal changes in a subset of mRNAs relevant to the resolvin system and neuroinflammation. The findings of this work are discussed in 3 main themes: 1) the consistent significance results from different methods of analysing TLDA data, and the distinct spinal expression profile of mRNAs in the spinal cord relevant to 2) the resolvin system and 3) neuroinflammation, in the 3 models of pain.

6.5.1 Methods of analysing TLDA data affect the significant mRNAs found

Several methods have been developed to present the mRNA expression levels of target genes relative to reference gene (s) (Schmittgen *et al.*, 2008; Vandesompele *et al.*, 2002). Either single, or multiple, reference genes can be used to normalise the data. Since this is the first time we have undertaken this type of study using spinal cord tissue it was important to investigate whether the type of method used to analyse the microarray data could affect the conclusion drawn from studies. Herein data are predominantly normalised to Actb as it was consistently expressed across groups and this provided comparability to the data presented in Chapter 3. Expressing changes in mRNA expression data by the $\Delta\Delta C_T$ (Method 3) was originally developed to compare mRNA expression levels in one or more treatment group, relative to their relevant control groups (Livak *et al.*, 2001). Relative mRNA expression quantification using ΔCT method (Method 1 and 2) is relatively simpler than $\Delta\Delta C_T$. Raw C_T

data from the treatment and control groups are calculated directly. However, geometric means from one or more reference genes may be used depending on the stability of potential reference genes or approach of the laboratory.

In the current study, I compared the expression levels in different models of pain to the respective saline/vehicle control, with the goal of comparing changes in expression between the models (fold changes). To enable this, the geometric mean of mRNA expression of a reference gene (Actb) of each control group were used to normalise the individual data in the group. Thus, the relative mRNA expression levels in saline/vehicle control groups were expressed. Although this method allowed comparison between the models, it is probably less stringent as virtual geometric means of mRNA expression of a reference gene required for normalisation in the control group and the data were normalised twice. This is evidenced by the identification of several mRNAs which had small fold changes, which are considered as mild (<2 fold change) or within baseline variation (±1.5 fold change), but were identified as being significant. mRNAs identified were: carrageenan model, Traf 3 (FC 1.4, $p<0.05$); PCX model, Tnfrsf1a (FC 1.5, $p<0.05$), Tnfrsf1b (FC 1.7, $p<0.05$); MIA model; Irak1 -1.2 (FC 1.5, $p<0.05$).

Analysis of the data using the ΔC_T with Actb alone as a reference gene detected a more limited number of mRNAs with significant changes in the expression, compared to $\Delta\Delta C_T$ method. However, inspection of the method revealed that some mRNAs that had higher fold expression changes, for example, Alox5ap and Cyp2j4 (2-4 fold changes) in the PCX model and Socs2 and Cxcr5 (>4 fold change) in PCX model were not identified as significant.

Previous evidence indicates that normalisation errors can occur when using a single reference gene (Vandesompele *et al.*, 2002) especially where numerous genes are studied, and that this error is reduced by using multiple reference genes. In this thesis Actb and Mapk6 were

the best performing reference genes in the dorsal horn, in agreement with a previous report (Walder *et al.*, 2014). On this basis ΔC_T with Actb and Mapk6 as reference genes (Method 1) was selected to perform a comprehensive analysis of the TLDA data. On the whole only data which reached significance is reported in this chapter. Where a pattern of change in a mRNA cluster was evident a non-significant fold change was considered, as previously reported for the interpretation of microarray data (Dalman *et al.*, 2012).

6.5.2 Distinct changes of resolvin system in pain models

The resolvin system is intricate involving a number of different receptors and enzymes. **Table 6.8** and **Figure 6.13** summarise the mRNAs involved in the resolvin pathway that were significantly altered in the carrageenan, MIA and PCX models.

Alterations in D- and E- series resolvin pathways in the ipsilateral spinal dorsal horn following each pain model induction were unique, suggesting distinct alterations of D- and E- series resolvin pathways (**Figure 6.8**). In the carrageenan model the expression of mRNAs relevant to the D- (Fpr2) and E- series (Ltb4r and Ptgr1) resolvin pathways were altered, suggesting generalised changes in spinal D- and E-series resolvin systems following the overt inflammation. The PCX model was predominantly associated with changes in the E-series resolvins, as indicated by significant changes in expression of Alox5ap, Cyp2j4 and Ptgr1. With lesser extent, the increase in Alox5ap in the PCX model also suggests some changes in the D-series pathway. The change in the spinal resolvin system induced by MIA model was limited to only Hpgd in the D-series pathway (significantly increased).

There were some clear differences between the carrageenan and PCX model and the respective controls-for example there was a significant down-regulation in the expression of the resolvin receptor mRNAs in

the carrageenan model. In the PCX model there was no change in the expression of the mRNAs for the receptors, but there was an upregulation of the mRNAs involved in the synthesis and degradation enzymes for the resolvins. Most of the changes in resolvin mRNAs in the MIA model were limited, suggesting the plasticity of spinal resolvin system is relatively less in this model than in carrageenan and PCX models.

The mRNAs encoding the resolvin receptors FPR2/ALX receptor (a target for resolvin D1 and aspirin-triggered resolvin D1) and LTB-1 receptor (a target for RvE1 as an antagonist) were significantly down regulated in the spinal cord 24 hours after induction of carrageenan inflammation. The decreased expression of Fpr2 expression is not consistent with the unaltered Fpr2 mRNA expression (Meesawatsom *et al.*, 2016) in spinal cords from carrageenan treated rat at the similar time point (24-30 h). Equally it is not in line with previous reports showing unaltered FPR2 protein immunoreactivity (Abdelmoaty *et al.*, 2013). An in vivo investigation in HEK293 cells revealed the FPR2 receptor mediated calcium flux was reduced post a 5-min incubation with annexin A1 10 nM (Bena *et al.*, 2012), providing evidence of receptor desensitisation under these conditions. Despite the prominent downregulation of Fpr2 in the carrageenan model, spinal administration of AT-RvD1 resulted in a robust inhibition of spinal nociceptive processing in this model, suggesting that this receptor system remained functional or that AT-RvD1 also acts via another receptor. In the present study, expression of Cmklr1 (encoding ChemR23 a receptor for RvE1) was not significantly altered in the carrageenan or the MIA models. This is not in line with the significant increase in Cmklr1 in previous reports from our group in carrageenan (30 h post induction) (Meesawatsom *et al.*, 2016) and MIA (35 days post induction) (Huang *et al.*, 2017) models.

It is clear from the work in this thesis and previous studies that the findings from different approaches to study mRNA expression vary.

We cannot rule out the impact of different primer and probe sets used in classical qPCR to quantify the mRNA expression versus those used for the current TLDA study, however we would expect the TLDA method to be less sensitive than the classical qPCR approach. It is feasible that inter-batch variability of rats, or the robustness of the models is a factor, however the models selected are widely used and replicated and pain behaviour and other features of the models were replicated between the studies in this thesis.

Resolvin E1 has been shown to be an antagonist at the BLT-1 receptor (Arita *et al.*, 2007), which is encoded by the Ltb4r. Herein I report a significant downregulation of Ltb4r in the spinal cord in the carrageenan model. BLT-1 receptor is expressed in both the peripheral and central nervous systems and a role of BLT-1 in modulating nociceptive sensitivity has been reported (Zinn *et al.*, 2017). Dorsal root ganglion neurones express BLT-1, and its ligand leukotriene B4 sensitises TRPV1, potentially contributing to pain hypersensitivity (Zinn *et al.*, 2017). BLT-1 activation also enhances NMDA-mediated spontaneous excitatory postsynaptic currents (sEPSCs) in spinal cord slices from the spared nerve injury (SNI) model in rats (Kiyoyuki *et al.*, 2015). These data suggest a pronociceptive role of BLT-1. It is conceivable that the spinal Ltb4r down regulation may counteract spinal excitability during acute overt inflammation. Functional contribution of altered Ltb4r in spinal nociceptive processing in these models could be investigated in the future using a selective antagonist such as U-75302 (Okubo *et al.*, 2010).

Resolvin synthesis involves a number of enzymes which sequentially catalyse the biosynthetic generation of D-series resolvins from docosahexaenoic acid (DHA) and E-series resolvins from eicosapentaenoic acid (EPA) including, COX-2, 15-LOX, 5-LOX, FLAP and LTA4H (**Figure 6.8**). A cell-based study investigating the contribution of FLAP in pro-resolving lipid mediator synthesis

reported that resovin D1 and also lipoxin A1 levels in polymorphonuclear leukocytes are dependent on FLAP activity (Lehmann *et al.*, 2015), suggesting the crucial role of FLAP. Alox5ap (encodes FLAP) expression in the spinal cord was elevated in the PCX model, but not the MIA model. Using the TLDA approach, a nonsignificant 1.9 fold elevation of Alox5ap was seen in carrageenan model, which is consistent with the significant 1.2 fold elevation previously identified by qPCR in carrageenan model (Meesawatsom *et al.*, 2016). Since AT-RvD1 inhibited spinal nociceptive processing in both models of pain, my data suggests a potential role of FLAP in the action of AT-RvD1 in carrageenan and PCX models. Future research probing the contribution of FLAP in spinal pain processing could be investigated using MK-866, a specific FLAP inhibitor (Lehmann *et al.*, 2015).

There are 2 major enzymes proposed responsible for inactivating resolvins (Arita *et al.*, 2006; Sun *et al.*, 2007), LTB4DH (encoded by Ptgr1) and HPGD (encoded by Hpgd) (**Figure 6.8**). HPGD metabolises both D- and E -series resolvins where as LTB4DH metabolises only E-series resolvins. Herein, the reported significant moderate up-regulation of Ptgr1 in the carrageenan and PCX models, and the increase in Hpgd in the MIA model suggests that E-series resolvin metabolism is predominantly altered in carrageenan and PCX models whereas D-series resolvin metabolism is predominantly altered in MIA model. The increase in the expression of mRNAs responsible for the catabolism of the resolvins supports the evidence that there is increased flux through this pathway in these models. Indeed, the minimal effects of exogenous administration of AT-RvD1 applied directly to the spinal cord on evoked spinal neuronal responses in MIA model may reflect the upregulation of Hpgd which rapidly degrades AT-RvD1. On the contrary, LTB4DH does not metabolise AT-RvD1 which may account for the sustained inhibitory effects of spinal AT-RvD1 on evoked spinal neuronal responses in carrageenan and PCX models. Since LTB4DH and HPGD are essential

for terminating other proalgesic eicosanoids such as PGE_2 and LTA_4 (Tai *et al.*, 2002), interrogating the functional effects of LTB4DH and HPGD inhibition on resolvin synthesis and spinal nociceptive processing or pain behaviour *in vivo* is not easily achievable.

CYPs are a large family of enzymes metabolising xenobiotics and also endogenous lipids (Haining *et al.*, 2007). CYPs are responsible for the synthesis and metabolism of a wide variety of endogenous lipids e.g. hydroxyeicosatrienoic acids (HETEs), dihydroxyeicosatrienoic acids (DHETs), epoxyeicosatrienoic acids (EETs), hydroperoxyeicosatetraenoic acids (HPETEs) and epoxyoctadacamonoenoic acids (EpOMEs) (Gilroy *et al.*, 2016; Wong *et al.*, 2014). Many CYP isoforms are expressed in neurones in pain pathways (Ruparel *et al.*, 2012; Sisignano *et al.*, 2016). The analysis of some CYP mRNAs in the present study was led by previous reports of plastic changes in CYP expression in rat trigeminal ganglia following complete Freund's adjuvant (CFA) injection into vibrissal pads, and the proposed roles of these enzymes in resolvin synthesis and degradation (Arita *et al.*, 2006; Sun *et al.*, 2007). Although resolvin metabolism via CYPs is proposed to be a minor pathway under normal conditions, many CYPs are inducible which may exaggerate their impact upon this pathway. Four CYP mRNAs were selected, CYP2J4 and CYP2C7 potentially responsible for resolvin synthesis and CYP4F8 and CYP2E1 potentially responsible for resolvin degradation. The increase in spinal Cyp2j4 expression in PCX model is consistent with a recent report showing an increase in Cyp2j6 (a mouse homologue of rat Cyp2j4) expression in dorsal root ganglia (DRGs) from PCX mice (Sisignano *et al.*, 2016). A recent investigation of the role of Cyp2j4 mediated generation of a lipid-derived from linoleic acid, 9,10-epoxy-12Z-octadecenoic acid (9,10-EpOME) (Sisignano *et al.*, 2016) provided evidence that CYP2J4 induction may be pro-nociceptive. Specifically, 9,10-EpOME sensitised TRPV1 mediated calcium influx in primary DRG culture, and potentiated CGRP release and excitatory postsynaptic potentials

in spinal cord slices; in vivo hind paw injection of 9,10-EpOME in naïve mice caused a reduction in hind paw thermal and mechanical thresholds (Sisignano *et al.*, 2016). The link between function of CYP2J6 and pain has also been studied, as intraperitoneal injection of telmisartan attenuated 9,10-EpOME level in DRGs and plasma as well as thermal and mechanical hypersensitivity in PCX mice (Sisignano *et al.*, 2016). These data suggest that CYP2J4 plays a significant role in another proalgesic lipid family, countering the theory that Cyp2j4 induction could enhance resolvin synthesis and mediate analgesia.

Table 6.8 Summary of significant mRNA expression changes in resolvin pathways in the ipsilateral spinal dorsal horn following either carrageenan, MIA or PCX treatment.

Clusters	mRNAs	Carrageenan		MIA		Paclitaxel	
Resolvin receptors	Fpr2	↓9.9	#				
	Ltb4r	↓2.4	#				
Resolvin synthetic enzymes	Alox5ap					↑3.2	#
	Cyp2j4					↑3.4	##
Resolvin degradation enzymes	Ptgr1	↑2.2	#			↑2.8	#
	Hpgd			↑2.6	#		

$^{\#}p<0.05$, $^{\#\#}p<0.01$ Mann-Whitney U Test when compared raw C_T values of each treatment versus its control (as shown in Figure 6.3-6.5), expressed as fold change versus control, n=5-7/group.

Figure 6.13 Summary of significant mRNA expression changes in resolvin pathways in the ipsilateral spinal dorsal horn following either carrageenan, MIA or PCX treatment.

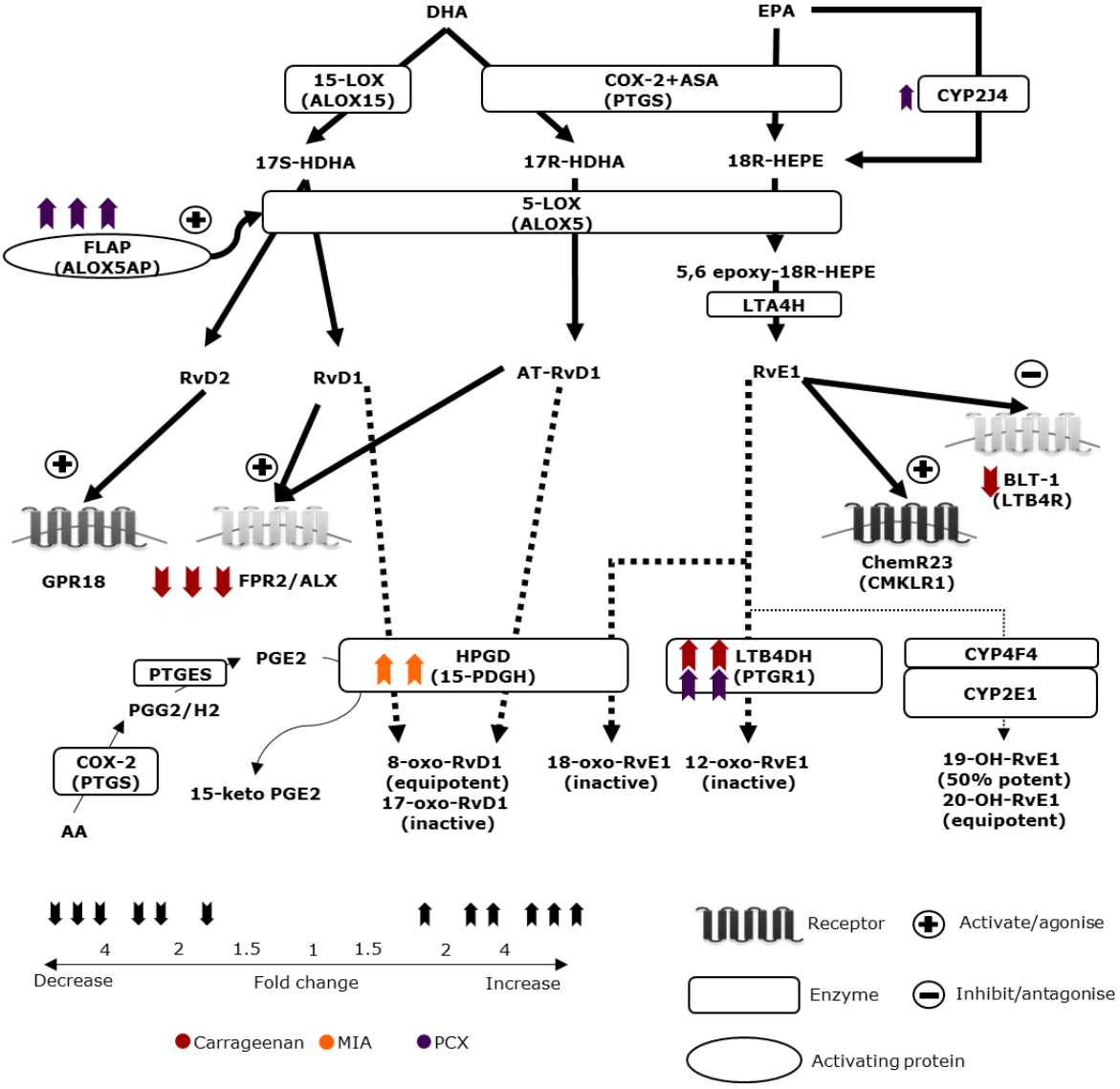

6.5.3 Profound spinal neuroinflammation in the PCX model is associated with central sensitisation

A number of pro-inflammatory mRNAs, Tlr4, inflammasome Nlrp1a and TNF-α receptors Tnfrsf1a and Tnfrsf1b, anti-inflammatory mRNAs Socs2 and Pparg and an mRNA representing central sensitisation Grin2b, were up-regulated in the PCX model (summarised in **Table 6.9**). The expression of many chemokines and chemokine receptors were also altered.

TLR4 and TNF-α signalling have well established the roles in promoting spinal nociceptive hyperexcitability (Grace *et al.*, 2014; Ren *et al.*, 2010; Uceyler *et al.*, 2009). In the spinal cord, TLR4 has been localised to astrocytes, but not with either microglia or neurones (Li *et al.*, 2014). TLR4 has been reported having both peripheral and central changes which were associated with pain behaviour in PCX model (Li *et al.*, 2014; Yan *et al.*, 2015). Previous studies have shown the immediate upregulation of TLR4 in DRGs and spinal cord post PCX-induction (Li *et al.*, 2014; Yan *et al.*, 2015). The upregulated TLR4 in spinal cord was maintained for at least 21 days (Li *et al.*, 2014). The finding of elevated spinal TLR4 mRNA in the present study is in agreement with previously reported (Li *et al.*, 2014).

Previously TNFR1 and TNFR2 (encoded by Tnfrsf1a and Tnfrsf1b) were reported to mediate mechanical and cold allodynia in a model of neuropathic pain (George *et al.*, 2005; Vogel *et al.*, 2006). In my study mechanical and cold allodynia was associated with upregulated Tnfrsf1a and Tnfrsf1b in the PCX model, suggesting that TNFR1 or TNFR2 may contribute to neuropathic pain behaviour following both surgical and chemotherapy induced nerve injury.

IL-1β is a potent inducer of inflammation and pain. Proteolytic activation of IL-1β is under the control of several molecules i.e. matrix metalloproteinases (MMPs), tissue inhibitors of matrix

metalloproteinase (TIMPs), and large multiprotein signalling complex, termed inflammasomes (Guo *et al.*, 2015). Activation of inflammasomes results in the cleavage of caspase-1, which subsequently induces downstream initiation of several potent pro-inflammatory cascades including IL-1β. Here, I did not find any significant changes in IL-1β cascade component expression (i.e. IL-1β itself, IL-1β activating enzymes, receptor and effector proteins) but there was a significant elevation of the inflammasome mRNA Nlrp1a in PCX model. Nlrp1a may be more important than Nlrp3 in spinal pain processing as previously it was reported to be significantly upregulated in the CCI model (Li *et al.*, 2013). Targeting NLRP1 signalling using aspirin-triggered-15-epi-lipoxin A4 (ATL), has been shown to attenuate pain behaviour in CCI model (Li *et al.*, 2013). Since sharing a common target (FPR2/ALX receptor) with ATL, AT-RvD1 would also inhibit NLRP1 signalling.

Overall, spinal neuroinflammation associated with the PCX model included major pro-inflammatory pathways, TLR-4, TNF-α, IL1β and IL-6. These pro-inflammatory pathways have been postulated as having key roles in increasing NMDA receptor excitability via phosphorylation, and sensitising pain pathways (Calvo *et al.*, 2012; Latremoliere *et al.*, 2009). In the PCX model Grin2B (encoding the Glun2B (NR2B) subunit of NMDA receptor) was significantly upregulated in in the spinal cord. Previously, NR2B subunit-containing NMDA receptors have been shown to have a crucial role in spinal sensitisation in pathological pain states (Gogas, 2006; Latremoliere *et al.*, 2009; Qu *et al.*, 2009). Overall my data support the co-occurrence of profound spinal neuroinflammation and sensitisation in PCX model.

Table 6.9 Summary of significant mRNA expression changes of mRNAs relevant to neuroinflammation and central sensitisation in the ipsilateral spinal dorsal horn following PCX treatment.

Cluster	Pathway	MRNAs	Paclitaxel	
Pro-inflammatory cascades	TLR4	Tlr4	↑3.0	#
	IL-1αβ	Nlrp1a	↑2.7	#
	TNF-α	Tnfrsf1a	↑2.0	##
		Tnfrsf1b	↑2.8	#
Anti-inflammatory cascades	IL-6	Soc2	↑4.6	##
	PPAR-γ	Pparg	↑3.7	##
Central sensitisation	Glutamate receptor	Grin2b	↑2.1	#

$^{\#}p<0.05$, $^{\#\#}p<0.01$ Mann-Whitney U Test when compared raw C_T values of each treatment versus its control (as shown in Figure 6.5-6.8), expressed as fold change versus control, n=5-7/group.

6.5.4 PCX-induced neuropathic pain is associated with a dramatic shift in spinal mRNA expression of multiple chemokine families

Chemokines are a large family of small proteins similar to cytokines but possess chemotactic activities; more than 50 chemokine ligands and 19 functional receptors have been described to date (Bachelerie *et al.*, 2014). The roles of chemokines in pain have been widely investigated (Dawes *et al.*, 2013b; Ji *et al.*, 2014; White *et al.*, 2005), nevertheless, alterations in chemokine systems in acute and chronic pain are still largely unknown.

The present study has demonstrated profound changes of multiple chemokines in the chemotherapy-induced neuropathic pain model (summarised in **Table 6.10** and **Figure 6.14**) which were not evident in the acute inflammatory and chronic arthritic model. The PCX model induced a significant upregulation of chemokine Cxcl6 and had even more profound effects on chemokine receptor expression (Cxcr1, Cxcr5 and Ccr1 Cx3cr1).

Promiscuity is an important characteristic of the chemokine system, one chemokine is capable of binding to more than one receptor and vice versa (Bachelerie *et al.*, 2014). This phenomenon is particularly described in CXC and CC chemokine families (Bachelerie *et al.*, 2014), for example CXCR1 recognises CXCL5, CXCL6 and CXCL8, and CCR1 recognises at least 10 chemokines. Prior evidence using a specific antibody targeting CCL2 in chronic constriction injury model (Thacker *et al.*, 2009) or CCL3 in PCX model (Ochi-ishi *et al.*, 2014) demonstrated only a partial reversal of mechanical allodynia suggesting that targeting a single chemokine may produce partial pain relief. In addition to the significant upregulation of Ccr1, expression levels of other CC receptor, including, Ccr2, Ccr3 and Ccr7 were concurrently increased >2 fold (although not statistical significant) in PCX model (**Figure 6.11**). Receptors encoded by all those mRNAs possess some degree of amino acid homology, bind to

many chemokines and probably act in concert. Given the promiscuous properties and the upregulation of multiple chemokine receptors support the theory that targeting a single chemokine axis would produce limited analgesia.

For the CXC family chemokines, there was a simultaneous upregulation of chemokine Cxcl6 (2.6 fold) and its receptor Cxcr1 (9.7 fold) in PCX model (**Figure 6.14**). The high magnitude of Cxcr1 upregulation suggests the pivotal contribution of this receptor in spinal pain processing in this model. Activation of CXCR1/2 has been reported to sensitise pain pathway both in peripheral (Brandolini *et al.*, 2017; Lopes *et al.*, 2016; Wigerblad *et al.*, 2016) and central (Lopes *et al.*, 2016) levels. Here I reported for the first time a significant increase in spinal CXCR1 mRNA in PCX model. As CXCR1 not only recognises CXCL6 but also CXCL5 and CXCL8, exploring the sources, changes and contribution of these molecules in PCX model is of interest for future research. Differently, Cxcr5 was found to be increased but not its ligand Cxcl13 (**Figure 6.14**) suggesting the co-upregulation of a chemokine and the paired receptor is not a common change in the CXC chemokine family.

Spinal Ccr1 expression in PCX rats was previously reported to be unaltered from day 1- 7 post PCX induction and then slightly increased (1.5-2 fold) on day 14 (Ochi-ishi *et al.*, 2014). The present study detected a prominent increase (7.8 fold) in Ccr1 at day 28 post PCX induction. The marked increase of Ccr1 at the later timepoint (day28) found here is suggestive of a temporal change in Ccr1 over the course of PCX-induced neuropathic pain.

Fractalkine (CX3CL1) is a unique chemokine controlling neurone-glial interactions. In spinal dorsal horn, membrane bound CX3CL1 is cleaved free from the neuronal membrane by cathepsin S and diffuses to activate its specific receptor CX3CR1 located at neighbouring microglia (Clark *et al.*, 2009). It is well-established that spinal CX3CL1 mediated CX3CR1 activation induces hypersensitivity

to both thermal and mechanical stimuli in animal models of neuropathic pain (Clark *et al.*, 2007; Clark *et al.*, 2009; Verge *et al.*, 2004). The finding on significant upregulation of Cx3cr1 (2.4 fold) but not Cx3cl1 in PCX model is in agreement with previous reports in CCI models (Verge *et al.*, 2004) suggesting the plasticity of this receptor, but not the ligand, is common in neuropathic pain state among several causes.

Beside the neuroinflammatory mRNAs discussed, PCX-induced mechanical hypersensitivity is clearly associated with a profound upregulation of multiple chemokine/chemokine receptor mRNA generalised in all chemokine families screened in the ipsilateral spinal dorsal horn. In addition, PCX models seems to have a greater influence on chemokine receptor mRNAs than the ligands. Therefore analgesics targeting at chemokine receptors may have more translation potential than targeting chemokines in this particular model.

Table 6.10 Summary of significant mRNA expression changes of chemokine and chemokine receptor mRNAs in the ipsilateral spinal dorsal horn following PCX treatment.

Cluster	mRNAs	Paclitaxel	
Chemokine	Cxcl6	↑2.6	#
Chemokine receptors	Cxcr1	↑9.7	##
	Cxcr5	↑4.2	#
	Ccr1	↑7.8	#
	Cx3cr1	↑2.4	#

$^{\#}p<0.05$, $^{\#\#}p<0.01$ Mann-Whitney U Test when compared raw C_T values of each treatment versus its control (as shown in Figure 6.3-6.5), expressed as fold change versus control, n=5-7/group.

Figure 6.14 Complete networks of relevant chemokine-chemokine receptors and summary of significant mRNA expression changes of chemokines and chemokine receptors in the ipsilateral spinal dorsal horn following PCX treatment. mRNAs of interest in TLDA study are indicated in red. ⬆⬆ and ⬆⬆ indicate the mRNAs identified as being significantly increased 2-4 fold and > 4 fold, respectively compared raw C_T values of each treatment versus its control (as shown in Figure 6.3-6.5), n=5-7/group.

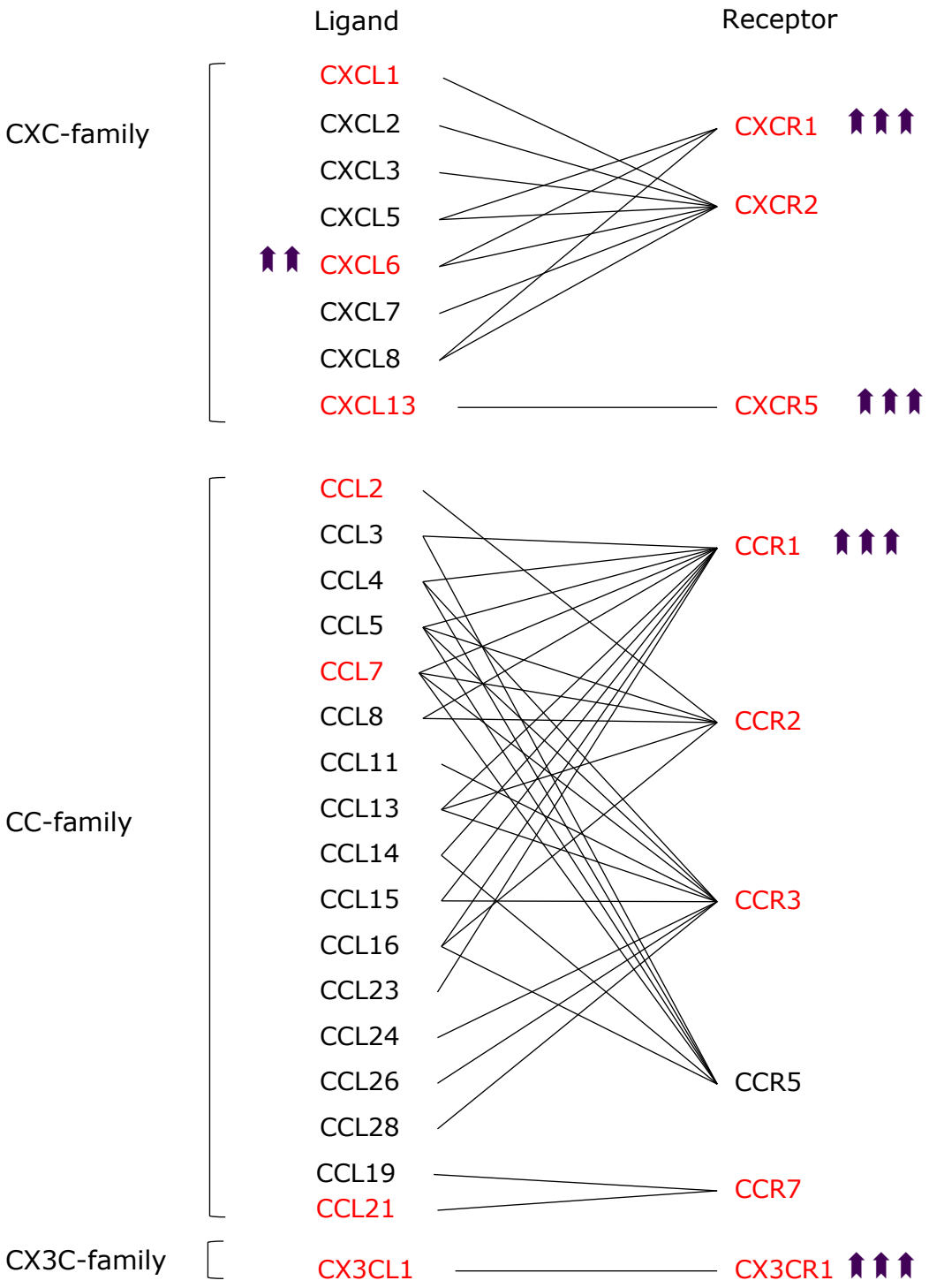

6.5.5 Anti-inflammatory roles of SOCS2 and PPAR-γ in PCX model

The current study demonstrated the significant upregulation of Socs2 (4.6 fold) and Pparg (3.7 fold) in the spinal cord in the PCX model. Known functions of suppressor of cytokine signalling-2 (SOCS2) and peroxisome proliferator-activated receptor gamma (PPAR-γ) include anti-inflammatory effects. Spinal Socs2 was reported to be upregulated in CCI model (Wang *et al.*, 2014b) similarly to the results described in the PCX model. PPAR-γ is a nuclear receptor initially described as a regulator of glucose metabolism, insulin sensitivity and adipocyte differentiation (Spiegelman, 1998). Activation of PPAR-γ is known to suppress pro-inflammatory TLR4 signalling (Pascual *et al.*, 2005b), TNFα (Wen *et al.*, 2010) and expression of CCL2-CCR2 in microglial (Kim *et al.*, 2012) and astrocyte (Lee *et al.*, 2008) culture.

Despite the mRNAs for Socs2 and Pparg being significantly upregulated in the spinal cord, mechanical sensitivity was still evident in PCX model. This suggests that the mechanisms counteracting spinal neuroinflammation are enhanced in PCX-induced neuropathic pain, but not sufficient to surmount the pro-inflammatory mechanisms leading to central sensitisation and the manifestation of aberrant pain behaviour.

Previous work suggests that SOCS2 and PPAR-γ may be essential for the anti-inflammatory/analgesic action of SPMs as the anti-inflammatory action of lipoxin A4 are SOCS2 dependent (Machado *et al.*, 2006). RvD1 does not directly activate PPARs (Krishnamoorthy *et al.*, 2010) however PPAR-γ agonist mediated analgesia has been previously reported to be RvD1 dependent (Saito *et al.*, 2015) suggesting a link between resolvin system and PPAR-γ. Findings in this thesis on the upregulation of Socs2, Pparg and also Alox5ap concurrent with the AT-RvD1 inhibition on spinal nociceptive

processing in PCX model suggest there may be an interaction between the resolvin system and SOCS2 and PPAR-γ anti-inflammatory signalling in spinal cord in the chemotherapy-induced neuropathic pain.

6.5.6 Site of the input and area of the spinal cord in the MIA study

Since the changes in the mRNA expression in the MIA study are minimal, the model may cause minimal spinal neuroinflammation per se, as discussed earlier. However, the spinal cord region collected may be another possible factor. The spinal cord samples used in the studies were collected using the same techniques by isolating the lumbar enlargement. This region receives the input from both the knee and the hindpaw. However, the receptive field from the knee is relatively small when compared to the paw. Previous work has shown the areas of the spinal cord receiving the input from the knee are slightly higher than the paw and mainly at L3-L4 (Neugebauer *et al.*, 1996; Sagar *et al.*, 2015; Salo *et al.*, 1997). Therefore, the peripheral nociceptive barrage originated from the knee is likely to impact mainly on L3-L4 region and may contribute to the primary hyperalgesia. Collecting the whole lumbar enlargement region may include areas that receive low input and dilute the mRNA expression results.

Chapter 7 GENERAL DISCUSSION

A novel genus of specialised pro-resolving lipid mediators (SPMs) including the E- and D-series resolvins, their aspirin-triggered versions, and the protectins and maresin have been recently identified (Arita *et al.*, 2006; Marcheselli *et al.*, 2010; Serhan *et al.*, 2002). The therapeutic potential of SPMs has been investigated in many inflammatory conditions, such as sepsis (Spite *et al.*, 2009), inflammatory arthritis (Norling *et al.*, 2016), periodontitis (Hasturk *et al.*, 2006), lung fibrosis (Hsiao *et al.*, 2015). RX-10045, an analogue of resolvin D1, is the most developed agent targeting this system, and entering Phase II clinical trial to be approved as a topical drug for treating dry eye disease (Hesselink *et al.*, 2016).

SPMs possess some interesting pharmacological characteristics. Firstly, SPMs act via specific G-protein coupled receptors (Piomelli *et al.*, 2014; Serhan *et al.*, 2008b) in nanomolar concentrations (Ji *et al.*, 2011; Xu *et al.*, 2010). Syntheses, action, and enzymatic inactivation, of SPMs are stereoselective (Hong *et al.*, 2008; Sun *et al.*, 2007). Unlike many current anti-inflammatory drugs, SPMs are not immunosuppressive (Dinarello, 2010). The SPM system, particularly the resolvin system, comprises of a series of enzymes catalysing sequential reactions for SPM synthesis and metabolism (Serhan *et al.*, 2008a). Given the potent anti-inflammatory action of SPMs, it is not surprising that SPMs also have analgesic potential. Therefore, the challenges ahead are to identify whether the resolvin system is altered in pathological pain, and if these novel systems can be harnessed to identify novel targets for analgesics. To start to address these questions, the combination of behavioural, electrophysiological and RNA microarray approaches have been applied in this thesis to investigate the alterations in resolvin system at the spinal level in acute and chronic pain models driven by different mechanisms (carrageenan model of acute inflammatory pain, monosodium iodoacetate (MIA) model of pain from osteoarthritis (OA) and paclitaxel (PCX) model of chemotherapy-induced neuropathic pain). Augmentation of the resolvin system

using spinally applied AT-RvD1 was tested in the pain models to pharmacologically probe whether it possesses a selective action, and to probe the existence of spinal plasticity of the resolvin system in pathological pain states. Spinally applied AT-RvD1 had distinct inhibitory effects on evoked responses of spinal WDR neurones in the different models, indicating the heterogeneous nature of the role of resolvin system among pain models.

7.1 Summary of key findings

A comparison of the effects of spinally applied AT-RvD1 on evoked responses of spinal WDR neurones in the carrageenan, MIA and PCX models revealed differential inhibitory effects of AT-RvD1 on spinal WDRs neurones in the carrageenan model, versus the MIA and PCX models (**Table 7.1**). AT-RvD1 had inhibitory effects on electrical-evoked responses in the carrageenan model and on mechanical and cold evoked responses in the PCX model. However, AT-RvD1 had only minimal effects on electrical-evoked responses in the MIA model.

Previous behavioural studies have shown the potential inhibitory effects of AT-RvD1 and RvD1 following intrathecal injection on mechanical hypersensitivity (summarised in **Chapter 1 Table 1.7**). Most previous studies used AT-RvD1 and RvD1 at very low concentrations (nanogram range), indicating AT-RvD1 and RvD1 are very potent. Their anitinociceptive effects of these compounds are broadly comparable in preclinical pain models from different aetiologies. However, work in this thesis suggests that AT-RvD1 differentially inhibits spinal nociceptive processing between pain models.

There are some properties of AT-RvD1 that has been observed consistently across pain models investigated in this thesis. Firstly, AT-RvD1 had minimal effects on electrical-evoked WDR neuronal responses in control rats in carrageenan, MIA and PCX studies. These data suggest AT-RvD1 has minimal effects upon physiological pain

processing. Previous behavioural studies have shown that AT-RvD1 and RvD1 have no significant effects on the duration of licking or flinching mechanical threshold in control rats (Bang *et al.*, 2012; Bang *et al.*, 2010; Quan-Xin *et al.*, 2012). My data ascertain that the AT-RvD1 mediated inhibition on spinal nociceptive processing has a selectivity window. This selective inhibition produced by AT-RvD1 is a desirable property of a novel analgesic. Lastly, as shown in carrageenan and PCX studies, the inhibition of the evoked responses of the WDR neurones following a single spinal dose of AT-RvD1 has a quick onset (15-30 min) but short duration (<60 min).

Initial spinal gene expression performed in the carrageenan model indicated that the expression of the resolvin genes were altered in this model, an increase in chemerin receptor 23 (ChemR23 or Cmklr1), 5-lipoxygenase activating proteins (FLAP or Alox5AP) and a decrease in 15- lipoxygenase (15-LOX or Alox15) were identified. Finally TaqMan® Low Density Arrays (TLDA) was used to quantify expression levels of 96 genes to advance the understanding of the potential changes in the resolvin system and neuroinflammatory signals in spinal cord in the pain models. This gene card analysis revealed unique differences in the resolvin system and neuroinflammatory circuits between the pain models (summarised in **Table 7.2**). Each pain model induces unique changes in the spinal resolvin systems (**Table 7.2A**). In the carrageenan model the expression of genes relevant to the D- (Fpr2, Alox15, Apx5ap) and E- series (Apx5ap Ltb4r, Cmklr1 and Ptgr1) resolvin pathways were altered, suggesting generalised changes in spinal D- and E-series resolvin systems following the overt hindpaw inflammation. The PCX model was predominantly associated with changes in the E-series resolvins, as indicated by significant changes in expression of Alox5ap, Cyp2j4 and Ptgr1. The changes induced by MIA model were limited to only Hpgd, part of the D-series pathway.

The three models of pain studied all had some degree of upregulation of the genes underlying the degradation of the resolvins, Hpgd and Ptgr1. The selective inhibitory effects of AT-RvD1 seen in the carrageenan and PCX models were associated with pathway specific changes in the gene expression of enzymes known to mediate the generation of the resolvins (Lehmann *et al.*, 2015), the upregulation of 5-lipoxygenase activating protein (FLAP) in these 2 models (**Table 7.2A**).

PCX-model is associated with profound spinal neuroinflammation

This thesis demonstrates an association of the PCX model and the broad up-regulation of genes with well-established proinflammatory/pronociceptive signalling systems, TLR4 (Tlr4), IL-1β (Nlrp1a) and TNF-α (Tnfrsf1a and Tnfrsf1b) in the spinal cord (**Table 7.2B**). This thesis also reports the upregulation of multiple chemokine signalling pathways in the PCX models. Such changes are generalised in all three main families of chemokines CXC (Cxcl6, Cxcr1, Cxcr5), CCR (Ccr1) and CX3C (Cx3cr1)(**Table 7.32B**). Even though, the anti-inflammatory Soc2 and PPAR-γ genes were upregulated in the dorsal horn of the spinal cord in the PCX model, these failed to counteract the upregulated proinflmmatory signallings (based on the pain phenotype).

The up-regulation of the proinflammatory mRNAs in the spinal cord in the PCX model are in accordance with a significant upregulation of Grin2b, which encodes the GluN2B (NR2B) subunit of NMDA receptor. The NR2B subunit has a relatively restricted distribution in the superficial spinal dorsal horn (Laurie *et al.*, 1997). Activation of NMDA receptors in the spinal cord has an established pivotal role in central sensitisation (Dickenson *et al.*, 1987; Qu *et al.*, 2009). The upregulation of Grin2b likely contributes to central sensitisation in the PCX model. All these changes may contribute to the physiological

switch in the response profile of spinal WDR neurones in PCX rats identified in this thesis: reduced threshold for Aβ and C-fibre responses; greater proportion of neurones displaying multiple properties defined by the increase in spontaneous activity; acetone responsiveness; post-discharge following 8 g (low intensity) mechanical stimulation (detailed in **Chapter 5 Table 5.4**). The PCX model-associated neuronal response switch demonstrated herein is an indication of robust spinal sensitisation which may be driven in part by profound changes in neuroinflammatoty signallings.

Table 7.1 Summary of the effects of spinally applied AT-RvD1 and morphine on spinal WDR neuronal responses evoked by various stimulus modalities in pain models in the rat.

	Acute inflammatory pain (30 h post intraplantar carrageenan)	**Chronic joint pain (28 days post Intra-articular MIA)**	**Chronic neuropathic pain (28 days post intraperitoneal paclitaxel)**
Major mechanisms of nociceptive barrage	Overt peripheral inflammation	Low grade peripheral inflammation	Peripheral nerve inflammation and dysfunction
AT-RvD1 doses tested (ng/50 ul)	15	15, 150	15 and 150
Effects of AT-RvD1			
■ Electrical	Aδ, C-fibre, input and wind-up; 30-50% inhibition	Aδ; 14% inhibition by 150 ug on	Aδ; 15% inhibition by 150 ng
■ Mechanical	NA	NA	8 g; ~73% inhibition by both doses 10 g; 35 % and 46% inhibition by 15 and by 150 ug, respectively)
■ Cold	NA	NA	68 and 82 % inhibition by 15 and 150 ug, respectively

NA=not available

Table 7.2 Comparison of changes in mRNA expression in the ipsilateral spinal dorsal horn of the spinal cord in the carrageenan, MIA or PCX models.

A mRNAs forming the resolvin pathways

Cluster	mRNAs	Carrageenan		MIA		Paclitaxel	
Resolvin receptors							
■ RvD1 and AT-RvD1 receptor	Fpr2	↓9.9	#				
■ RvE1 receptor	Ltb4r	↓2.4	#				
	Cmklr1	↑1.3[a]	#				
Resolvin synthetic enzymes							
■ D-series	Alox15	↓1.7[a]	#				
■ D-and E series	Alox5ap	↑1.2[a]	#			↑3.2	#
■ E series	Cyp2j4					↑3.4	##
Resolvin degradation enzymes							
■ D-series	Hpgd			↑2.6	#		
■ E-series	Ptgr1	↑2.2	#			↑2.8	#

B mRNAs involving neuroinflammation and central sensitisation

Clusters	mRNAs	Carrageenan		MIA		Paclitaxel	
Pro-inflammatory cascades							
■ TLR4	Tlr4					↑3.0	#
■ IL-1β	Nlrp1a					↑2.7	#
■ TNF-α	Tnfrsf1a					↑2.0	##
	Tnfrsf1b					↑2.8	#
Anti-inflammatory cascades							
■ Anti-IL-6	Soc2					↑4.6	##
■ PPAR-γ	Pparg					↑3.7	##
Central sensitisation							
■ Glutamate receptor	Grin2b					↑2.1	#
Pro-inflammatory chemokine	Cxcl6					↑2.6	#
Pro-inflammatory chemokine receptors	Cxcr1					↑9.7	##
	Cxcr5					↑4.2	#
	Ccr1					↑7.8	#
	Cx3cr1					↑2.4	#

All mRNAs reported here were significantly altered, #p<0.05, ##p<0.01 Mann-Whitney U Test when compared the expression level versus the respective control, expressed as fold change versus control, n=5-7/group

[a] Data from classical TaqMan® quantitative polymerase chain reaction

7.3 Potential underlying mechanisms of the differential inhibition of AT-RvD1 in pain models

Clearly, the results from my electrophysiological studies indicate the differential effects of AT-RvD1 on evoked spinal WDR neuronal responses in the different pain models. The TLDA results also revealed that upregulated FLAP mRNA in resolvin synthetic pathway may be a possible mechanism underpinning the differential inhibition by AT-RvD1. This finding needs to be confirmed at the protein level, before the therapeutic potential of these targets are further explored.

Previously, intrathecal injection of AT-RvD1 (at the same concentration as in this thesis) attenuated pain behaviour in carrageenan model (Abdelmoaty *et al.*, 2013). Therefore, it is not surprising that AT-RvD1 potently inhibited the responses of spinal neurones in the carrageenan model. The robust inhibition of neuronal responses by low dose AT-RvD1 (15 ng) suggests that AT-RvD1 is very potent and the spinal cord is a major site of action of AT-RvD1-mediated analgesia in inflammatory pain. Carrageenan is known to cause overt peripheral inflammation and many proinflammatory mediators are released at the site of injection e.g. prostaglandin E2 (Guay *et al.*, 2004), IL-1β, IL-6, TNF-α, etc. (Annamalai *et al.*, 2017). These mediators can activate the nociceptors and generate aberrant barrage which induces acute neuroinflammation and plastic changes of the resolvin system in the ipsilateral spinal cord as clearly shown in the current study (**Table 7.2A**). The gene card analysis reveals that Alox5ap is upregulated in the spinal cord in the carrageenan and PCX models, but not in the MIA model. Since D-series biosynthesis is dependent on FLAP activity (Lehmann *et al.*, 2015), upregulated FLAP mRNA in these 2 models may result in an increase in levels of the endogenous resolvins in the dorsal horn. Thus, the exogenous AT-RvD1 given in this study may

augment the effects of those endogenous resolvins in the carrageenan and PCX models. In addition, upregulated FLAP and the subsequent increased synthesis of the resolvins may lead to the down regulation of FPR2/ALX receptors in the carrageenan model.

The limited inhibitory effects of AT-RvD1 on electrically evoked responses in both the MIA and PCX model, compared to the carrageenan model, may be due to several reasons depending on the pain models. Carrageenan, MIA and PCX model are different in the features of the nociceptive hypersensitivity. In carrageenan model, considered as inflammatory pain, numerous proinflammatory/pronociceptive mediators are released at the site of the inflammation which activate/sensitise the nociceptors. Thus, the nociceptive barrage is mainly driven by the overt peripheral inflammation. This is followed by the nociceptive sensitisation at the spinal level. Since it is a model of acute inflammation, the nociceptive hypersensitivity is likely to resolve over time as the inflammation resolves. TLDA results suggesting the plasticity of the spinal resolvin system may indicate that the system is altered to interact with the inflammation at the spinal level. The inhibitory effects of AT-RvD1 was therefore seen.

MIA and PCX are models for chronic pain. MIA and PCX-treated rats developed a similar degree of mechanical hypersensitivity, however the mechanisms underlying nociceptive hypersensitivity are different. In the MIA model, when OA pathology developed, there is inflammation in the affected joint, although the inflammation is relatively low grade but chronic. It may create continuous nociceptive barrage to the spinal cord and induce the activation of spinal microglia and subsequently astrocytes (Sagar *et al.*, 2011). However, the spinal inflammatory component and the plasticity of the resolvin system in the MIA model is less evident as demonstrated in the gene card study. This may lead to the modest effects of AT-RvD1 in inhibiting the spinal nociceptive processing in this model. PCX model

is associated with profound changes in peripheral nerves, DRGs and spinal dorsal horn. A high degree of peripheral nerve inflammation and dysfunction (e.g. dysregulation of ion channels and mitochondria)(Sisignano *et al.*, 2014) is likely to be the main origin of peripheral nociceptive barrage. These events are likely to create robust and continuous nociceptive input to the spinal dorsal horn and trigger microglia and astrocyte activation which are greater than those in the MIA model. The gene card results reveals that the spinal resolvin and neuroinflammation is widely altered in PCX model.

Spinal mRNA expression changes in the PCX model are far greater than in the carrageenan or MIA model (**Table 7.2B**). The PCX model was associated with profound changes in spinal neuroinflammatory pathways and an upregulation of Grin2b, indicating central sensitisation (**Table 7.2B**). Thus, the extent of the multiple excitatory pathways activated in the spinal cord is greater in the PCX model which may account for the reduced ability of AT-RvD1 to elicit a robust inhibition of electrically-evoked responses of WDR neurones, compared to the carrageenan model. However, AT-RvD1 still clearly exerts a robust inhibition on low intensity mechanical and cold evoked responses of WDR neurones in the PCX model- indicating that the receptor system is functional. These data also illustrate that the resolvin system can modulate the spinal processing of low intensity mechanical and cold sensations.

At the level of the spinal cord the MIA model had far less evidence for a pro-inflammatory phenotype at the level of the spinal cord, compared to the PCX model. The significant upregulation of Hpgd mRNA (encode 15-hydroxyprostaglandin dehydrogenase (15-HPGD)) in the spinal cord of MIA rats may be a major mechanism contributing to the minimal effects of AT-RvD1 on the electrical evoked responses in this model. 15-HPGD is a major enzyme responsible for inactivation of AT-RvD1 (Orr *et al.*, 2015; Sun *et al.*, 2007). Recent evidence suggests the presence of 15-HPGD in activated spinal

astrocytes (Miyagishi *et al.*, 2017). Thus the upregulated 15- HPGD mRNA in the MIA model may underpin a greater inactivation of the exogenous AT-RvD1 applied onto the spinal cord, and minimal effects of AT-RvD1 on evoked responses of spinal neurones in MIA model.

Anatomical studies have shown that FPR2/ALX receptor, the main target of AT-RvD1, is normally expressed in several structures in spinal dorsal horn, mainly astrocytes, and to a lesser extent in neurones under control conditions (Hu *et al.*, 2012). FPR2/ALX receptor is also express by DRGs (Pei *et al.*, 2011), and therefore may be present on the pre-synaptic terminals of the afferent fibres. The current study is not able to differentiate whether the AT-RvD1 mediated effects on WDR neuronal responses are mediated by pre- or post-synaptic receptors. It is possible that FPR2/ALX is expressed by myelinated fibres, or the spinal neurones processing innocuous low-intensity mechanical and cold stimuli, as suggested by the results from the PCX study. Another possibility is AT-RvD1 may act on the surrounding glia cells and reduce their pronociceptive mediator release e.g. TNF-α and IL-1β (Abdelmoaty *et al.*, 2013) which in turn attenuates post-synaptic neuronal hyperexcitability. Further studies are required to elucidate further the laminar and fibre sites of action of FPR2/ALX in the spinal cord and whether this is altered in models of chronic pain.

7.4 Comparison of AT-RvD1 and morphine

Morphine was employed as a gold standard analgesic for the MIA and PCX models of chronic pain in this thesis. Although AT-RvD1 and morphine have different target G-protein coupled receptors, they both utilise Gi for signal transduction (Alexander *et al.*, 2015; Ye *et al.*, 2009). Activation of Gi-coupled receptors inhibits adenylate cyclase, reduces intracellular cyclic AMP and protein kinase A (PKA) activity. By these mechanisms, morphine can directly hyperpolarise membrane potential by opening potassium channels and inhibits

neurotransmitter release by inhibiting voltage-gated calcium channels. Morphine suppresses nociceptive processing at the level of the WDR neurone in sham / naive rats (Suzuki *et al.*, 1999). By contrast, AT-RvD1 did not alter normal physiological nociceptive responses of WDR neurones in sham or naïve rats. These data, plus behavioural data, suggest that AT-RvD1 inhibits sensitised ion channel responses and pain behaviour selectively in pathological states (Bang *et al.*, 2012; Bang *et al.*, 2010; Quan-Xin *et al.*, 2012). Therefore, D-series resolvin-induced analgesia appears to be selective to persistent pain states, possibly by inhibiting hyperexcitability rather than directly suppressing physiological nociceptive neuronal excitability.

Unlike morphine, which the pharmacokinetics and adverse effects have been well-documented (Smith, 2009), pharmacokinetic parameters of AT-RvD1 and its analogues such as plasma half-life remain to be investigated. In addition the main site of metabolism of AT-RvD1 needs to be clarified. 15-PDGH, a major AT-RvD1 inactivation enzyme, is highly expressed in gastrointestinal tract (Yan *et al.*, 2004), liver and kidney (Yu *et al.*, 2014) which are the tissues potentially affecting pharmacokinetics. Potential ALX/FPR2 receptor mediated adverse effects and toxicity are unknown, especially following long-term activation. Since the receptor is mainly expressed by immune cells, one would expect any adverse effects to be seen mainly in the immune system. However AT-RvD1 and other SPMs are believed not to be immunosuppressive (Dinarello, 2010). Lastly, it is well established that opioids are associated with receptor desensitisation and tolerance especially at high doses or after long term treatment in chronic pain conditions (Williams *et al.*, 2013). *In vitro* studies revealed that FPR2/ALX receptor mediated calcium flux in HEK293 cells was reduced following a 5-min incubation with annexin A1 10 nM (Bena et al., 2012), suggesting that the FPR2/ALX receptor is capable of desensitisation. However, this may be less significant *in vivo* since a more recent pain behavioural study in rats

has shown sustained analgesic effects of repeated intraperitoneal injection of a precursor of AT-RvD1 (Huang *et al.*, 2017). Further work is required to fully characterise the potential importance of FPR2/ALX receptor desensitisation *in vivo*.

7.5 Reduced morphine sensitivity in chronic pain models

The inhibitory effects of morphine against some electrical evoked responses was reduced in the PCX model compared to sham controls, which is consistent with diminished morphine sensitivity in some previous studies (Kohno *et al.*, 2005; Yamamoto *et al.*, 2008; Zhu *et al.*, 2017). Reductions in μ (mu) receptor expression and μ receptor-mediated inhibition of C-fibre responses have been proposed to underlie the diminished sensitivity of models associated with nerve injury to opioids (Kohno *et al.*, 2005; Yamamoto *et al.*, 2008; Zhu *et al.*, 2017). A recent anatomical study reported that μ receptors are expressed by around 15% of large diameter DRG neurones (Weibel *et al.*, 2013) suggesting that some Aβ fibres express μ receptor. μ receptor down regulation in the PCX model may contribute to the reduced inhibitory effects of morphine on C-fibre mediated input in the PCX model.

7.6 Limitations

In this thesis, the effects of AT-RvD1 following application to the spinal cord on evoked responses of the WDR neurones was studied. There are of course other cells types in the dorsal horn for example, nociceptive-specific (NS) neurones in the superficial lamina (I-II) which receive inputs from with Aδ- and C-fibres, and proprioceptive neurones which receive input exclusively from Aβ-fibres in lamina (III-V). Evoked responses of NS neurones are more sensitive than WDR neurones to the suppressive effects of anaesthetic doses needed for these types of experiments (Barter *et al.*, 2009). Since

WDR neurones also receive input from NS neurones, the anaesthetic suppression of responses of NS neurones could affect the responses of WDR neurones. It is feasible that AT-RvD1 had direct effects on NS neurones, as well as non-neuronal cells microglia and astrocytes, which contribute to the full manifestation of antinociceptive effects *in vivo*. Despite this limitation, the electrophysiological findings from this thesis that AT-RvD1 inhibited evoked responses of WDR neurones in the carrageenan model replicates the alleviation of mechanical hypersensitivity behaviour by AT-RvD1 in this previously reported (Abdelmoaty *et al.*, 2013).

I investigated the alteration mRNA expression in the ipsilateral spinal cord using TLDA. The lack of more detailed spatial resolution of the changes in mRNA expression, even the dorsal quadrant was isolated, is another limitation of this thesis. For example, Ctss (encodes cathepsin S) expression was unaltered in any models studied in this thesis. However a previous anatomical study revealed that cathepsin S protein immunoreactivity was increased exclusively in microglia located at the mediolateral part of the ipsilateral dorsal horn following partial ligation of the sciatic nerve (PNL) (Clark *et al.*, 2007). Since, RNA samples in the current study were prepared from the ipsilateral dorsal quadrant, the sensitivity to detect focal changes may be compromised. Immunohistochemistry could be employed to detect focal changes in the dorsal horn in response to pathological pain. Another limitation of quantifying mRNA expression is it may not correlate with the level or activity of a particular protein. The activities of some proteins are regulated by post-translational modification such as proteolytic activation and phosphorylation. A good example derived from this thesis (TLDA data) are IL-1β cascade component mRNA expression whereby only Nlrp1 was altered. The proteolytic cleavage of inactive pro-IL-1β to active IL-1β is controlled by several regulatory enzymes: NLRP1 inflammasome; caspase 1; matrix metalloproteinase (MMP) 2 and 9; tissue inhibitor of metallopeptidase (TIMP) 1 and 2 (Parks *et al.*, 2004; Zhang *et al.*,

2016a). No significant alteration in mRNA of these genes were found in any models studied herein. Studies of the changes in the protein levels and/or activities of these molecules may provide better insight in the actual changes of these signalling pathways, rather than only studying the mRNA levels. In addition, some proteins are activated or have a gain of function by phosphorylation, such as NF-κB (Christian *et al.*, 2016), JAK2 (Robertson *et al.*, 2009) and NR2B subunit of NMDA receptor (Chen *et al.*, 2007). I have collected protein pellets obtained during the RNA extraction. In the future these samples can be used to investigate potential changes in protein levels using other techniques e.g. Western blot, enzyme-linked immunosorbent assay (ELISA) or protein microarray. This would enable us to correlate the RNA and protein relationship, investigate post-translational modification and achieve a better understanding these complex changes.

In the TLDA study genes were selected for those encoding key pro-inflammatory cytokines, chemokines and other molecules essential in the actions of those mediators. However, there are many other mechanisms underlying the spinal sensitisation in chronic pain models beyond the candidate genes screen here. For instance, spinal sensitisation in the MIA model can be induced by the increased neuronal phosphorylated mitogen-activated protein kinase 1 (MAPK1) (Lee *et al.*, 2011), substance P (SP) and calcitonin gene-related peptide (CGRP) (Otis *et al.*, 2016). In the PCX model upregulation of ceramide-sphingosine 1-phosphate (S1P) signalling (Janes *et al.*, 2014) and bradykinin B1 receptor (Costa *et al.*, 2011) also play roles. In addition, the MIA and PCX model are associated with astrocyte activation (Sagar *et al.*, 2011; Zhang *et al.*, 2012). Activated astrocytes produce numerous pro-inflammatory mediators most of which have been well-documented in mediating sensitised pain behaviour in many chronic pain models (Ji *et al.*, 2013; Mika *et al.*, 2013; Milligan *et al.*, 2009).

7.7 Future directions

The work in this thesis forms the foundations for future studies investigating the pharmacology of AT-RvD1 in pain processing. Behavioural studies evaluating the effects of single intrathecal injection of AT-RvD1 could confirm whether the effects of AT-RvD1 on neuronal responses also alter pain behaviour the MIA model and the PCX model. In addition, it is important to identify whether repeated administration AT-RvD1 in the PCX model could prevent or reverse on mechanical, cold allodynia, and the physiological switch of spinal WDR neurons and altered gene expression in the dorsal horn.

The relatively short duration of AT-RvD1 leads to challenges in extending AT-RvD1 action. This disadvantage could be improved by using AT-RvD1 analogues which are more resistant to 15-HPGD-mediated inactivation e.g. benzo-diacetylenic-17R-RvD1-methyl ester (BDA-RvD1) which has been recently synthesised (Orr *et al.*, 2015). BDA-RvD1 was reported to activate the same target receptor (FPR2/ALX), have similar potency to RvD1 in inhibiting lung neutrophil infiltration but have a complete resistance to 15-HPGD (Orr *et al.*, 2015). This may allow a more sustained analgesic effect over time, and the less frequent dosing regimen. In addition, this strategy is promising in the MIA model since it directly counteracts the upregulated 15-HPGD and will possibly increase AT-RvD1 availability and allow more robust inhibition of evoked responses of spinal WDR neurones.

FLAP is proposed to be crucial for the spinal action of AT-RvD1 in the carrageenan and PCX models where AT-RvD1 elicits inhibitory effects on the evoked neuronal responses. FLAP possesses a complicated function whereby it is capable of facilitating the synthesis of pro- or anti-inflammatory lipids, depending on FLAP cellular localisation; perinuclear FLAP preferentially produces anti-inflammatory lipid

lipoxins whereas cytosolic FLAP preferentially produces pro-inflammatory lipid leukotriene A4 (Norris *et al.*, 2014). It is also of relevance whether these events occur in spinal glia, which are activated in chronic pain states (Ji *et al.*, 2013; Milligan *et al.*, 2009), and how this may potentially alter resolvin levels. A behavioural correlation of with FLAP expression/ activity and the subcellular distribution would consolidate understanding in this area.

Simultaneous profiling of resolvins and other DHA and EPA –derived SMPs in spinal tissue using lipidomic analysis (Valdes *et al.*, 2017; Wong *et al.*, 2014) would provide the correlation between the changes in resolvin genes and the levels of those lipids. This would reveal overall flux of these lipid pathways and identify the major pathways to be thoroughly investigated.

Since AT-RvD1 inhibits low intensity mechanical and cold allodynia the PCX model, the FPR2/ALX receptor distribution on primary sensory fibre subtypes, and the contribution of the receptor in this model needs to be investigated. TRPV1, TRPV4 and TRPA1 are associated with PCX-induced mechanical and cold hypersensitivity (Chen *et al.*, 2011). A-fibre expressing TLR-5 (Xu *et al.*, 2015) may involve sensitisation to low intensity mechanical stimuli. Co-localisation of resolvin receptors and these other targets using immunohistochemistry would advance understanding the putative involvement of these channels. To differentiate the potential effects of AT-RvD1 at pre- versus post-synaptic sites in the spinal cord, patch clamp recoding of spinal neurones could be performed (Fioravante *et al.*, 2011).

Conclusion

In conclusion, this thesis demonstrates the differential inhibition of AT-RvD1 on spinal nociceptive processing in different models of pain. Spinal administration of AT-RvD1 produced rapid and robust inhibition of evoked responses of spinal WDR neurones in vivo following acute carrageenan-induced overt peripheral inflammation and PCX-induced peripheral neuropathy, suggesting spinal cord is a major site of action of AT-RvD1. On the contrary, the AT-RvD1-mediated inhibition on the evoked neuronal responses in the MIA-induced arthritis was very limited. The inhibitory effects of AT-RvD1 was evident in acute inflammatory pain and chronic neuropathic pain models. Finally, the inhibition of AT-RvD1 in pain model may be underpinned by unique spinal changes of resolvin system, especially the increase in FLAP mRNA expression in the carrageenan and PCX models which is not seen in the MIA model. These data provide for the first time the evidence of heterogeneous spinal alteration of the resolvin system in different type of pain and supports further investigation of AT-RvD1 as a novel analgesic.

REFERENCES

Abdelmoaty S, Wigerblad G, Bas DB, Codeluppi S, Fernandez-Zafra T, El-Awady el S*, et al.* (2013). Spinal actions of lipoxin A4 and 17(R)-resolvin D1 attenuate inflammation-induced mechanical hypersensitivity and spinal TNF release. *PloS one* **8**(9)**:** e75543.

Ahmadi S, Lippross S, Neuhuber WL, Zeilhofer HU (2002). PGE(2) selectively blocks inhibitory glycinergic neurotransmission onto rat superficial dorsal horn neurons. *Nature neuroscience* **5**(1)**:** 34-40.

Alexander SP, Davenport AP, Kelly E, Marrion N, Peters JA, Benson HE*, et al.* (2015). The Concise Guide to PHARMACOLOGY 2015/16: G protein-coupled receptors. *British journal of pharmacology* **172**(24)**:** 5744-5869.

Alexander SP, Striessnig J, Kelly E, Marrion NV, Peters JA, Faccenda E*, et al.* (2017). THE CONCISE GUIDE TO PHARMACOLOGY 2017/18: Voltage-gated ion channels. *British journal of pharmacology* **174 Suppl 1:** S160-S194.

Alvarez FJ, Morris HR, Priestley JV (1991). Sub-populations of smaller diameter trigeminal primary afferent neurons defined by expression of calcitonin gene-related peptide and the cell surface oligosaccharide recognized by monoclonal antibody LA4. *Journal of neurocytology* **20**(9)**:** 716-731.

Annamalai P, Thangam EB (2017). Local and Systemic Profiles of Inflammatory Cytokines in Carrageenan-induced Paw Inflammation in Rats. *Immunological investigations* **46**(3)**:** 274-283.

Arendt-Nielsen L, Nie H, Laursen MB, Laursen BS, Madeleine P, Simonsen OH*, et al.* (2010). Sensitization in patients with painful knee osteoarthritis. *Pain* **149**(3)**:** 573-581.

Ariel A, Serhan CN (2007). Resolvins and protectins in the termination program of acute inflammation. *Trends in immunology* **28**(4)**:** 176-183.

Arita M, Bianchini F, Aliberti J, Sher A, Chiang N, Hong S*, et al.* (2005a). Stereochemical assignment, antiinflammatory properties, and receptor for the omega-3 lipid mediator resolvin E1. *The Journal of experimental medicine* **201**(5)**:** 713-722.

Arita M, Clish CB, Serhan CN (2005b). The contributions of aspirin and microbial oxygenase to the biosynthesis of anti-inflammatory resolvins: novel oxygenase products from omega-3 polyunsaturated fatty acids. *Biochemical and biophysical research communications* **338**(1)**:** 149-157.

Arita M, Oh SF, Chonan T, Hong S, Elangovan S, Sun YP*, et al.* (2006). Metabolic inactivation of resolvin E1 and stabilization of its anti-inflammatory actions. *The Journal of biological chemistry* **281**(32)**:** 22847-22854.

Arita M, Ohira T, Sun YP, Elangovan S, Chiang N, Serhan CN (2007). Resolvin E1 selectively interacts with leukotriene B4 receptor BLT1 and ChemR23 to regulate inflammation. *Journal of immunology* **178**(6)**:** 3912-3917.

Arnardottir HH, Dalli J, Norling LV, Colas RA, Perretti M, Serhan CN (2016). Resolvin D3 Is Dysregulated in Arthritis and Reduces Arthritic Inflammation. *Journal of immunology* **197**(6)**:** 2362-2368.

Ashraf S, Mapp PI, Burston J, Bennett AJ, Chapman V, Walsh DA (2014). Augmented pain behavioural responses to intra-articular injection of nerve growth factor in two animal models of osteoarthritis. *Annals of the rheumatic diseases* **73**(9)**:** 1710-1718.

Babbin BA, Lee WY, Parkos CA, Winfree LM, Akyildiz A, Perretti M*, et al.* (2006). Annexin I regulates SKCO-15 cell invasion by signaling through formyl peptide receptors. *The Journal of biological chemistry* **281**(28)**:** 19588-19599.

Bachelerie F, Ben-Baruch A, Burkhardt AM, Combadiere C, Farber JM, Graham GJ*, et al.* (2014). International Union of Basic and Clinical Pharmacology. [corrected]. LXXXIX. Update on the extended family of chemokine receptors and introducing a new nomenclature for atypical chemokine receptors. *Pharmacological reviews* **66**(1)**:** 1-79.

Back M, Powell WS, Dahlen SE, Drazen JM, Evans JF, Serhan CN*, et al.* (2014). Update on leukotriene, lipoxin and oxoeicosanoid receptors: IUPHAR Review 7. *British journal of pharmacology* **171**(15)**:** 3551-3574.

Bang S, Yoo S, Yang TJ, Cho H, Hwang SW (2012). 17(R)-resolvin D1 specifically inhibits transient receptor potential ion channel vanilloid 3 leading to peripheral antinociception. *British journal of pharmacology* **165**(3)**:** 683-692.

Bang S, Yoo S, Yang TJ, Cho H, Kim YG, Hwang SW (2010). Resolvin D1 attenuates activation of sensory transient receptor potential channels leading to multiple anti-nociception. *British journal of pharmacology* **161**(3)**:** 707-720.

Bannenberg GL, Chiang N, Ariel A, Arita M, Tjonahen E, Gotlinger KH*, et al.* (2005). Molecular circuits of resolution: formation and actions of resolvins and protectins. *Journal of immunology* **174**(7)**:** 4345-4355.

Bannister K, Dickenson AH (2017). The plasticity of descending controls in pain: translational probing. *The Journal of physiology* **595**(13)**:** 4159-4166.

Bannuru RR, Schmid CH, Kent DM, Vaysbrot EE, Wong JB, McAlindon TE (2015). Comparative effectiveness of pharmacologic interventions for knee osteoarthritis: a systematic review and network meta-analysis. *Annals of internal medicine* **162**(1)**:** 46-54.

Barclay J, Clark AK, Ganju P, Gentry C, Patel S, Wotherspoon G*, et al.* (2007). Role of the cysteine protease cathepsin S in neuropathic hyperalgesia. *Pain* **130**(3)**:** 225-234.

Barter LS, Carstens EE, Jinks SL, Antognini JF (2009). Rat dorsal horn nociceptive-specific neurons are more sensitive than wide dynamic range neurons to depression by immobilizing doses of volatile anesthetics: an effect partially reversed by the opioid receptor antagonist naloxone. *Anesthesia and analgesia* **109**(2)**:** 641-647.

Bauer CS, Nieto-Rostro M, Rahman W, Tran-Van-Minh A, Ferron L, Douglas L*, et al.* (2009). The increased trafficking of the calcium channel subunit alpha2delta-1 to presynaptic terminals in neuropathic pain is inhibited by the alpha2delta ligand pregabalin. *The Journal of neuroscience : the official journal of the Society for Neuroscience* **29**(13)**:** 4076-4088.

Bautista DM, Movahed P, Hinman A, Axelsson HE, Sterner O, Hogestatt ED*, et al.* (2005). Pungent products from garlic activate the sensory ion channel TRPA1. *Proceedings of the National Academy of Sciences of the United States of America* **102**(34)**:** 12248-12252.

Bazan NG (2001). COX-2 as a multifunctional neuronal modulator. *Nature medicine* **7**(4)**:** 414-415.

Becker C, Hammerle-Fickinger A, Riedmaier I, Pfaffl MW (2010). mRNA and microRNA quality control for RT-qPCR analysis. *Methods* **50**(4)**:** 237-243.

Beggs S (2009). Microglia and trophic factors in neuropathic pain. In: Malcangio M (ed)^(eds). *Synaptic Plasticity in Pain*, edn: Springer. p^pp 439-453.

Beggs S, Salter MW (2013). Microglia: Critical mediators of pain after peripheral nerve injury. In: McMahon SB, Koltzenburg M, Tracey I, Turk DC (ed)^(eds). *Wall & Melzack's Textbook of Pain*, 6th edn: Elsevier Saunders. p^pp 68-76.

Beiche F, Scheuerer S, Brune K, Geisslinger G, Goppelt-Struebe M (1996). Up-regulation of cyclooxygenase-2 mRNA in the rat spinal cord following peripheral inflammation. *FEBS letters* **390**(2)**:** 165-169.

Bena S, Brancaleone V, Wang JM, Perretti M, Flower RJ (2012). Annexin A1 interaction with the FPR2/ALX receptor: identification of distinct domains and downstream associated signaling. *The Journal of biological chemistry* **287**(29)**:** 24690-24697.

Benabdoune H, Rondon EP, Shi Q, Fernandes J, Ranger P, Fahmi H*, et al.* (2016). The role of resolvin D1 in the regulation of inflammatory and catabolic mediators in osteoarthritis. *Inflammation research : official journal of the European Histamine Research Society ... [et al.]* **65**(8)**:** 635-645.

Bennett GJ, Liu GK, Xiao WH, Jin HW, Siau C (2011). Terminal arbor degeneration--a novel lesion produced by the antineoplastic agent paclitaxel. *The European journal of neuroscience* **33**(9)**:** 1667-1676.

Berta T, Park CK, Xu ZZ, Xie RG, Liu T, Lu N*, et al.* (2014). Extracellular caspase-6 drives murine inflammatory pain via microglial TNF-alpha secretion. *The Journal of clinical investigation* **124**(3)**:** 1173-1186.

Biber K, Tsuda M, Tozaki-Saitoh H, Tsukamoto K, Toyomitsu E, Masuda T*, et al.* (2011). Neuronal CCL21 up-regulates microglia P2X4 expression and initiates neuropathic pain development. *The EMBO journal* **30**(9)**:** 1864-1873.

Bonnington JK, McNaughton PA (2003). Signalling pathways involved in the sensitisation of mouse nociceptive neurones by nerve growth factor. *The Journal of physiology* **551**(Pt 2)**:** 433-446.

Bove SE, Calcaterra SL, Brooker RM, Huber CM, Guzman RE, Juneau PL*, et al.* (2003). Weight bearing as a measure of disease progression and efficacy of anti-inflammatory compounds in a model of monosodium iodoacetate-induced osteoarthritis. *Osteoarthritis and cartilage / OARS, Osteoarthritis Research Society* **11**(11)**:** 821-830.

Boyette-Davis J, Xin W, Zhang H, Dougherty PM (2011). Intraepidermal nerve fiber loss corresponds to the development of taxol-induced hyperalgesia and can be prevented by treatment with minocycline. *Pain* **152**(2)**:** 308-313.

Braddock M, Quinn A (2004). Targeting IL-1 in inflammatory disease: new opportunities for therapeutic intervention. *Nature reviews. Drug discovery* **3**(4)**:** 330-339.

Brandolini L, Benedetti E, Ruffini PA, Russo R, Cristiano L, Antonosante A*, et al.* (2017). CXCR1/2 pathways in paclitaxel-induced neuropathic pain. *Oncotarget* **8**(14)**:** 23188-23201.

Brater DC, Harris C, Redfern JS, Gertz BJ (2001). Renal effects of COX-2-selective inhibitors. *American journal of nephrology* **21**(1)**:** 1-15.

Braz JM, Nassar MA, Wood JN, Basbaum AI (2005). Parallel "pain" pathways arise from subpopulations of primary afferent nociceptor. *Neuron* **47**(6)**:** 787-793.

Breivik H, Collett B, Ventafridda V, Cohen R, Gallacher D (2006). Survey of chronic pain in Europe: prevalence, impact on daily life, and treatment. *European journal of pain* **10**(4)**:** 287-333.

Bullock DC, Palmer AR, Rees A (1988). Compact and easy-to-use tungsten-in-glass microelectrode manufacturing workstation. *Medical & biological engineering & computing* **26**(6)**:** 669-672.

Burgos E, Gomez-Nicola D, Pascual D, Martin MI, Nieto-Sampedro M, Goicoechea C (2012). Cannabinoid agonist WIN 55,212-2 prevents the development of paclitaxel-induced peripheral neuropathy in rats. Possible involvement of spinal glial cells. *European journal of pharmacology* **682**(1-3)**:** 62-72.

Burnstock G (2008). Purinergic signalling and disorders of the central nervous system. *Nature reviews. Drug discovery* **7**(7)**:** 575-590.

Burston JJ, Sagar DR, Shao P, Bai M, King E, Brailsford L*, et al.* (2013). Cannabinoid CB2 receptors regulate central sensitization and pain responses associated with osteoarthritis of the knee joint. *PloS one* **8**(11)**:** e80440.

Busserolles J, Tsantoulas C, Eschalier A, Lopez Garcia JA (2016). Potassium channels in neuropathic pain: advances, challenges, and emerging ideas. *Pain* **157 Suppl 1:** S7-14.

Byrne FM, Cheetham S, Vickers S, Chapman V (2015). Characterisation of pain responses in the high fat diet/streptozotocin model of diabetes and the analgesic effects of antidiabetic treatments. *Journal of diabetes research* **2015:** 752481.

Calvo M, Dawes JM, Bennett DL (2012). The role of the immune system in the generation of neuropathic pain. *Lancet neurology* **11**(7)**:** 629-642.

Cata JP, Weng HR, Chen JH, Dougherty PM (2006). Altered discharges of spinal wide dynamic range neurons and down-regulation of glutamate transporter expression in rats with paclitaxel-induced hyperalgesia. *Neuroscience* **138**(1)**:** 329-338.

Cata JP, Weng HR, Dougherty PM (2008). The effects of thalidomide and minocycline on taxol-induced hyperalgesia in rats. *Brain research* **1229:** 100-110.

Caterina MJ, Rosen TA, Tominaga M, Brake AJ, Julius D (1999). A capsaicin-receptor homologue with a high threshold for noxious heat. *Nature* **398**(6726)**:** 436-441.

Caterina MJ, Schumacher MA, Tominaga M, Rosen TA, Levine JD, Julius D (1997). The capsaicin receptor: a heat-activated ion channel in the pain pathway. *Nature* **389**(6653)**:** 816-824.

Catterall WA, Perez-Reyes E, Snutch TP, Striessnig J (2005). International Union of Pharmacology. XLVIII. Nomenclature and structure-function relationships of voltage-gated calcium channels. *Pharmacological reviews* **57**(4)**:** 411-425.

Chai S, Li M, Lan J, Xiong ZG, Saugstad JA, Simon RP (2007). A kinase-anchoring protein 150 and calcineurin are involved in regulation of acid-sensing ion channels ASIC1a and ASIC2a. *The Journal of biological chemistry* **282**(31)**:** 22668-22677.

Chaplan SR, Bach FW, Pogrel JW, Chung JM, Yaksh TL (1994). Quantitative assessment of tactile allodynia in the rat paw. *Journal of neuroscience methods* **53**(1)**:** 55-63.

Chapman V, Suzuki R, Dickenson AH (1998). Electrophysiological characterization of spinal neuronal response properties in anaesthetized rats after ligation of spinal nerves L5-L6. *The Journal of physiology* **507 (Pt 3):** 881-894.

Chen BS, Roche KW (2007). Regulation of NMDA receptors by phosphorylation. *Neuropharmacology* **53**(3)**:** 362-368.

Chen W, Walwyn W, Ennes HS, Kim H, McRoberts JA, Marvizon JC (2014). BDNF released during neuropathic pain potentiates NMDA receptors in primary afferent terminals. *The European journal of neuroscience* **39**(9)**:** 1439-1454.

Chen Y, Yang C, Wang ZJ (2011). Proteinase-activated receptor 2 sensitizes transient receptor potential vanilloid 1, transient receptor potential vanilloid 4, and transient receptor potential ankyrin 1 in paclitaxel-induced neuropathic pain. *Neuroscience* **193:** 440-451.

Chen YJ, Zhu H, Zhang N, Shen L, Wang R, Zhou JS*, et al.* (2015). Temporal kinetics of macrophage polarization in the injured rat spinal cord. *Journal of neuroscience research* **93**(10)**:** 1526-1533.

Cherry JD, Olschowka JA, O'Banion MK (2014). Neuroinflammation and M2 microglia: the good, the bad, and the inflamed. *Journal of neuroinflammation* **11:** 98.

Chiang N, Dalli J, Colas RA, Serhan CN (2015). Identification of resolvin D2 receptor mediating resolution of infections and organ protection. *The Journal of experimental medicine* **212**(8)**:** 1203-1217.

Chiang N, Serhan CN (2017). Structural elucidation and physiologic functions of specialized pro-resolving mediators and their receptors. *Molecular aspects of medicine* **58:** 114-129.

Chiang N, Serhan CN, Dahlen SE, Drazen JM, Hay DW, Rovati GE*, et al.* (2006). The lipoxin receptor ALX: potent ligand-specific and stereoselective actions in vivo. *Pharmacological reviews* **58**(3)**:** 463-487.

Chiba T, Oka Y, Kambe T, Koizumi N, Abe K, Kawakami K*, et al.* (2016). Paclitaxel-induced peripheral neuropathy increases substance P release in rat spinal cord. *European journal of pharmacology* **770:** 46-51.

Choi Y, Yoon YW, Na HS, Kim SH, Chung JM (1994). Behavioral signs of ongoing pain and cold allodynia in a rat model of neuropathic pain. *Pain* **59**(3)**:** 369-376.

Christian F, Smith EL, Carmody RJ (2016). The Regulation of NF-kappaB Subunits by Phosphorylation. *Cells* **5**(1).

Clapham DE, Runnels LW, Strubing C (2001). The trp ion channel family. *Nature reviews. Neuroscience* **2**(6)**:** 387-396.

Clark AK, Staniland AA, Marchand F, Kaan TK, McMahon SB, Malcangio M (2010). P2X7-dependent release of interleukin-1beta and nociception in the spinal cord following lipopolysaccharide. *The Journal of neuroscience : the official journal of the Society for Neuroscience* **30**(2)**:** 573-582.

Clark AK, Yip PK, Grist J, Gentry C, Staniland AA, Marchand F*, et al.* (2007). Inhibition of spinal microglial cathepsin S for the reversal of neuropathic pain. *Proceedings of the National Academy of Sciences of the United States of America* **104**(25)**:** 10655-10660.

Clark AK, Yip PK, Malcangio M (2009). The liberation of fractalkine in the dorsal horn requires microglial cathepsin S. *The Journal of neuroscience : the official journal of the Society for Neuroscience* **29**(21)**:** 6945-6954.

Clish CB, Levy BD, Chiang N, Tai HH, Serhan CN (2000). Oxidoreductases in lipoxin A4 metabolic inactivation: a novel role for 15-onoprostaglandin 13-reductase/leukotriene B4 12-hydroxydehydrogenase in inflammation. *The Journal of biological chemistry* **275**(33)**:** 25372-25380.

Colburn RW, Lubin ML, Stone DJ, Jr., Wang Y, Lawrence D, D'Andrea MR*, et al.* (2007). Attenuated cold sensitivity in TRPM8 null mice. *Neuron* **54**(3)**:** 379-386.

Collins JG, Kendig JJ, Mason P (1995). Anesthetic actions within the spinal cord: contributions to the state of general anesthesia. *Trends Neurosci* **18**(12)**:** 549-553.

Cook AJ, Woolf CJ, Wall PD, McMahon SB (1987). Dynamic receptive field plasticity in rat spinal cord dorsal horn following C-primary afferent input. *Nature* **325**(7000)**:** 151-153.

Costa R, Motta EM, Dutra RC, Manjavachi MN, Bento AF, Malinsky FR*, et al.* (2011). Anti-nociceptive effect of kinin B(1) and B(2) receptor antagonists on peripheral neuropathy induced by paclitaxel in mice. *British journal of pharmacology* **164**(2b)**:** 681-693.

Coull JA, Beggs S, Boudreau D, Boivin D, Tsuda M, Inoue K*, et al.* (2005). BDNF from microglia causes the shift in neuronal anion gradient underlying neuropathic pain. *Nature* **438**(7070)**:** 1017-1021.

Cox JJ, Reimann F, Nicholas AK, Thornton G, Roberts E, Springell K*, et al.* (2006). An SCN9A channelopathy causes congenital inability to experience pain. *Nature* **444**(7121)**:** 894-898.

Creamer P, Lethbridge-Cejku M, Hochberg MC (2000). Factors associated with functional impairment in symptomatic knee osteoarthritis. *Rheumatology (Oxford, England)* **39**(5)**:** 490-496.

Cuellar JM, Dutton RC, Antognini JF, Carstens E (2005). Differential effects of halothane and isoflurane on lumbar dorsal horn neuronal windup and excitability. *British journal of anaesthesia* **94**(5)**:** 617-625.

da Costa BR, Reichenbach S, Keller N, Nartey L, Wandel S, Juni P*, et al.* (2016). Effectiveness of non-steroidal anti-inflammatory drugs for the treatment of pain in knee and hip osteoarthritis: a network meta-analysis. *Lancet* **387**(10033)**:** 2093-2105.

Dalman MR, Deeter A, Nimishakavi G, Duan Z-H (2012). Fold change and p-value cutoffs significantly alter microarray interpretations. *BMC Bioinformatics* **13**(2)**:** S11.

Damazo AS, Yona S, Flower RJ, Perretti M, Oliani SM (2006). Spatial and temporal profiles for anti-inflammatory gene expression in leukocytes during a resolving model of peritonitis. *Journal of immunology* **176**(7)**:** 4410-4418.

Dawes JM, Anderson DA, Bennett DLH, Bevan S, McMahon SB (2013a). Inflammatory mediators and modulators of pain. In: McMahon SB, Koltzenburg M, Tracey I, Turk DC (ed)^(eds). *Wall & Melzack's Textbook of Pain*, 6th edn: Elsevier/Saunders. p^pp 48-76.

Dawes JM, McMahon SB (2013b). Chemokines as peripheral pain mediators. *Neuroscience letters* **557 Pt A:** 1-8.

Day AR, Pinon D, Muthukumaraswamy N, Freer RJ (1980). Synthesis of several chemotactic peptide antagonists. *Peptides* **1**(4)**:** 289-291.

de Oliveira C, Garami A, Lehto SG, Pakai E, Tekus V, Pohoczky K*, et al.* (2014). Transient receptor potential channel ankyrin-1 is not a cold sensor for autonomic thermoregulation in rodents. *The Journal of neuroscience : the official journal of the Society for Neuroscience* **34**(13)**:** 4445-4452.

Deng L, Guindon J, Cornett BL, Makriyannis A, Mackie K, Hohmann AG (2015). Chronic cannabinoid receptor 2 activation reverses paclitaxel neuropathy without tolerance or cannabinoid receptor 1-dependent withdrawal. *Biological psychiatry* **77**(5)**:** 475-487.

Derry S, Conaghan P, Da Silva JA, Wiffen PJ, Moore RA (2016). Topical NSAIDs for chronic musculoskeletal pain in adults. *The Cochrane database of systematic reviews* **4:** CD007400.

Detloff MR, Fisher LC, McGaughy V, Longbrake EE, Popovich PG, Basso DM (2008). Remote activation of microglia and pro-inflammatory cytokines predict the onset and severity of below-level neuropathic pain after spinal cord injury in rats. *Exp Neurol* **212**(2)**:** 337-347.

Dhaka A, Murray AN, Mathur J, Earley TJ, Petrus MJ, Patapoutian A (2007). TRPM8 is required for cold sensation in mice. *Neuron* **54**(3)**:** 371-378.

Dickenson AH, Brigitte LK (2013). Opioids: Basic mechanisms. In: McMahon SB, Koltzenburg M, Tracey I, Turk DC (ed)^(eds). *Wall & Melzack's Textbook of Pain*, 6th edn: Elsevier/Saunders. p^pp 413-428.

Dickenson AH, Sullivan AF (1987). Evidence for a role of the NMDA receptor in the frequency dependent potentiation of deep rat dorsal horn nociceptive neurones following C fibre stimulation. *Neuropharmacology* **26**(8)**:** 1235-1238.

Dinarello CA (2010). Anti-inflammatory Agents: Present and Future. *Cell* **140**(6)**:** 935-950.

Djouhri L, Fang X, Okuse K, Wood JN, Berry CM, Lawson SN (2003a). The TTX-resistant sodium channel Nav1.8 (SNS/PN3): expression and correlation with membrane properties in rat nociceptive primary afferent neurons. *The Journal of physiology* **550**(Pt 3)**:** 739-752.

Djouhri L, Lawson SN (2004). Abeta-fiber nociceptive primary afferent neurons: a review of incidence and properties in relation to other afferent A-fiber neurons in mammals. *Brain research. Brain research reviews* **46**(2)**:** 131-145.

Djouhri L, Newton R, Levinson SR, Berry CM, Carruthers B, Lawson SN (2003b). Sensory and electrophysiological properties of guinea-pig sensory neurones expressing Nav 1.7 (PN1) Na+ channel alpha subunit protein. *The Journal of physiology* **546**(Pt 2)**:** 565-576.

Dominick KL, Ahern FM, Gold CH, Heller DA (2004). Health-related quality of life and health service use among older adults with osteoarthritis. *Arthritis and rheumatism* **51**(3)**:** 326-331.

Donnelly-Roberts D, McGaraughty S, Shieh CC, Honore P, Jarvis MF (2008). Painful purinergic receptors. *The Journal of pharmacology and experimental therapeutics* **324**(2)**:** 409-415.

Dostrovsky JO, Craig AD (2013). Ascending projection system. In: McMahon SB, Koltzenburg M, Tracey I, Turk DC (ed)^(eds). *Wall & Melzack's Textbook of Pain*, 6th edn: Elsevier/Saunders. p^pp 182-197.

Dougherty PM, Cata JP, Cordella JV, Burton A, Weng HR (2004). Taxol-induced sensory disturbance is characterized by preferential impairment of myelinated fiber function in cancer patients. *Pain* **109**(1-2)**:** 132-142.

Egawa D, Itoh T, Akiyama Y, Saito T, Yamamoto K (2016). 17-OxoDHA Is a PPARalpha/gamma Dual Covalent Modifier and Agonist. *ACS chemical biology* **11**(9)**:** 2447-2455.

Emery EC, Luiz AP, Sikandar S, Magnusdottir R, Dong XZ, Wood JN (2016). In vivo characterization of distinct modality-specific subsets of somatosensory neurons using GCaMP. *Sci Adv* **2**(11).

Erhuma A, Salter AM, Sculley DV, Langley-Evans SC, Bennett AJ (2007). Prenatal exposure to a low-protein diet programs disordered regulation of lipid metabolism in the aging rat. *American journal of physiology. Endocrinology and metabolism* **292**(6)**:** E1702-1714.

Fagni L, Chavis P, Ango F, Bockaert J (2000). Complex interactions between mGluRs, intracellular Ca2+ stores and ion channels in neurons. *Trends Neurosci* **23**(2)**:** 80-88.

Fang X, Djouhri L, Black JA, Dib-Hajj SD, Waxman SG, Lawson SN (2002). The Presence and Role of the Tetrodotoxin-Resistant Sodium Channel Nav1.9 (NaN) in Nociceptive Primary Afferent Neurons. *The Journal of Neuroscience* **22**(17)**:** 7425.

Ferreira-Gomes J, Adaes S, Sousa RM, Mendonca M, Castro-Lopes JM (2012). Dose-dependent expression of neuronal injury markers during experimental osteoarthritis induced by monoiodoacetate in the rat. *Molecular pain* **8:** 50.

Field MJ, Cox PJ, Stott E, Melrose H, Offord J, Su TZ*, et al.* (2006). Identification of the alpha2-delta-1 subunit of voltage-dependent calcium channels as a molecular target for pain mediating the analgesic actions of pregabalin. *Proceedings of the National Academy of Sciences of the United States of America* **103**(46)**:** 17537-17542.

Finn A, Angeby Moller K, Gustafsson C, Abdelmoaty S, Nordahl G, Ferm M*, et al.* (2014). Influence of model and matrix on cytokine profile in rat and human. *Rheumatology (Oxford, England)* **53**(12)**:** 2297-2305.

Fioravante D, Regehr WG (2011). Short-term forms of presynaptic plasticity. *Current opinion in neurobiology* **21**(2)**:** 269-274.

Flatters SJ, Bennett GJ (2004). Ethosuximide reverses paclitaxel- and vincristine-induced painful peripheral neuropathy. *Pain* **109**(1-2)**:** 150-161.

Flatters SJ, Bennett GJ (2006). Studies of peripheral sensory nerves in paclitaxel-induced painful peripheral neuropathy: evidence for mitochondrial dysfunction. *Pain* **122**(3)**:** 245-257.

Fredman G, Ozcan L, Spolitu S, Hellmann J, Spite M, Backs J*, et al.* (2014). Resolvin D1 limits 5-lipoxygenase nuclear localization and leukotriene B4 synthesis by inhibiting a calcium-activated kinase pathway. *Proceedings of the National Academy of Sciences of the United States of America* **111**(40)**:** 14530-14535.

Gao BN, Sekido Y, Maximov A, Saad M, Forgacs E, Latif F*, et al.* (2000). Functional properties of a new voltage-dependent calcium channel alpha(2)delta auxiliary subunit gene (CACNA2D2). *Journal of Biological Chemistry* **275**(16)**:** 12237-12242.

Gao YJ, Zhang L, Samad OA, Suter MR, Yasuhiko K, Xu ZZ*, et al.* (2009). JNK-induced MCP-1 production in spinal cord astrocytes contributes to central

sensitization and neuropathic pain. *The Journal of neuroscience : the official journal of the Society for Neuroscience* **29**(13)**:** 4096-4108.

Gauchan P, Andoh T, Ikeda K, Fujita M, Sasaki A, Kato A*, et al.* (2009). Mechanical allodynia induced by paclitaxel, oxaliplatin and vincristine: different effectiveness of gabapentin and different expression of voltage-dependent calcium channel alpha(2)delta-1 subunit. *Biological & pharmaceutical bulletin* **32**(4)**:** 732-734.

Gegelashvili G, Bjerrum OJ (2014). High-affinity glutamate transporters in chronic pain: an emerging therapeutic target. *Journal of neurochemistry* **131**(6)**:** 712-730.

George A, Buehl A, Sommer C (2005). Tumor necrosis factor receptor 1 and 2 proteins are differentially regulated during Wallerian degeneration of mouse sciatic nerve. *Exp Neurol* **192**(1)**:** 163-166.

Gilroy DW, Colville-Nash PR, Willis D, Chivers J, Paul-Clark MJ, Willoughby DA (1999). Inducible cyclooxygenase may have anti-inflammatory properties. *Nature medicine* **5**(6)**:** 698-701.

Gilroy DW, Edin ML, De Maeyer RP, Bystrom J, Newson J, Lih FB*, et al.* (2016). CYP450-derived oxylipins mediate inflammatory resolution. *Proceedings of the National Academy of Sciences of the United States of America* **113**(23)**:** E3240-3249.

Giulietti A, Overbergh L, Valckx D, Decallonne B, Bouillon R, Mathieu C (2001). An overview of real-time quantitative PCR: applications to quantify cytokine gene expression. *Methods* **25**(4)**:** 386-401.

Gogas KR (2006). Glutamate-based therapeutic approaches: NR2B receptor antagonists. *Current opinion in pharmacology* **6**(1)**:** 68-74.

Gold MS, Levine JD, Correa AM (1998). Modulation of TTX-R INa by PKC and PKA and their role in PGE2-induced sensitization of rat sensory neurons in vitro. *The Journal of neuroscience : the official journal of the Society for Neuroscience* **18**(24)**:** 10345-10355.

Grace PM, Hutchinson MR, Maier SF, Watkins LR (2014). Pathological pain and the neuroimmune interface. *Nature reviews. Immunology*.

Gregus AM, Doolen S, Dumlao DS, Buczynski MW, Takasusuki T, Fitzsimmons BL*, et al.* (2012). Spinal 12-lipoxygenase-derived hepoxilin A3 contributes to inflammatory hyperalgesia via activation of TRPV1 and TRPA1 receptors. *Proceedings of the National Academy of Sciences of the United States of America* **109**(17)**:** 6721-6726.

Groneberg DA, Serowka F, Peckenschneider N, Artuc M, Grutzkau A, Fischer A*, et al.* (2005). Gene expression and regulation of nerve growth factor in atopic dermatitis mast cells and the human mast cell line-1. *Journal of neuroimmunology* **161**(1-2)**:** 87-92.

Grossin L, Etienne S, Gaborit N, Pinzano A, Cournil-Henrionnet C, Gerard C*, et al.* (2004). Induction of heat shock protein 70 (Hsp70) by proteasome inhibitor MG 132 protects articular chondrocytes from cellular death in vitro and in vivo. *Biorheology* **41**(3-4)**:** 521-534.

Gu X, Zhang J, Ma Z, Wang J, Zhou X, Jin Y*, et al.* (2010). The role of N-methyl-D-aspartate receptor subunit NR2B in spinal cord in cancer pain. *European journal of pain* **14**(5)**:** 496-502.

Guan Y, Guo W, Zou SP, Dubner R, Ren K (2003). Inflammation-induced upregulation of AMPA receptor subunit expression in brain stem pain modulatory circuitry. *Pain* **104**(1-2)**:** 401-413.

Guay J, Bateman K, Gordon R, Mancini J, Riendeau D (2004). Carrageenan-induced paw edema in rat elicits a predominant prostaglandin E2 (PGE2) response in the central nervous system associated with the induction of microsomal PGE2 synthase-1. *The Journal of biological chemistry* **279**(23)**:** 24866-24872.

Guingamp C, Gegout-Pottie P, Philippe L, Terlain B, Netter P, Gillet P (1997). Mono-iodoacetate-induced experimental osteoarthritis: a dose-response study of loss of mobility, morphology, and biochemistry. *Arthritis and rheumatism* **40**(9)**:** 1670-1679.

Guo H, Callaway JB, Ting JPY (2015). Inflammasomes: mechanism of action, role in disease, and therapeutics. *Nature medicine* **21**(7)**:** 677-687.

Guo W, Wang H, Watanabe M, Shimizu K, Zou S, LaGraize SC*, et al.* (2007). Glial-cytokine-neuronal interactions underlying the mechanisms of persistent pain. *The Journal of neuroscience : the official journal of the Society for Neuroscience* **27**(22)**:** 6006-6018.

Gutman GA, Chandy KG, Adelman JP, Aiyar J, Bayliss DA, Clapham DE*, et al.* (2003). International Union of Pharmacology. XLI. Compendium of voltage-gated ion channels: potassium channels. *Pharmacological reviews* **55**(4)**:** 583-586.

Guzman RE, Evans MG, Bove S, Morenko B, Kilgore K (2003). Mono-iodoacetate-induced histologic changes in subchondral bone and articular cartilage of rat femorotibial joints: an animal model of osteoarthritis. *Toxicologic pathology* **31**(6)**:** 619-624.

Haining RL, Nichols-Haining M (2007). Cytochrome P450-catalyzed pathways in human brain: metabolism meets pharmacology or old drugs with new mechanism of action? *Pharmacology & therapeutics* **113**(3)**:** 537-545.

Hains BC, Waxman SG (2006). Activated microglia contribute to the maintenance of chronic pain after spinal cord injury. *The Journal of neuroscience : the official journal of the Society for Neuroscience* **26**(16)**:** 4308-4317.

Hamilton SG, Warburton J, Bhattacharjee A, Ward J, McMahon SB (2000). ATP in human skin elicits a dose-related pain response which is potentiated under conditions of hyperalgesia. *Brain : a journal of neurology* **123 (Pt 6):** 1238-1246.

Hara K, Harris RA (2002). The anesthetic mechanism of urethane: the effects on neurotransmitter-gated ion channels. *Anesthesia and analgesia* **94**(2)**:** 313-318, table of contents.

Hara T, Chiba T, Abe K, Makabe A, Ikeno S, Kawakami K*, et al.* (2013). Effect of paclitaxel on transient receptor potential vanilloid 1 in rat dorsal root ganglion. *Pain* **154**(6)**:** 882-889.

Hargreaves K, Dubner R, Brown F, Flores C, Joris J (1988). A new and sensitive method for measuring thermal nociception in cutaneous hyperalgesia. *Pain* **32**(1)**:** 77-88.

Hasturk H, Kantarci A, Ohira T, Arita M, Ebrahimi N, Chiang N*, et al.* (2006). RvE1 protects from local inflammation and osteoclast- mediated bone destruction in periodontitis. *FASEB journal : official publication of the Federation of American Societies for Experimental Biology* **20**(2)**:** 401-403.

Hay CH, Trevethick MA, Wheeldon A, Bowers JS, de Belleroche JS (1997). The potential role of spinal cord cyclooxygenase-2 in the development of Freund's complete adjuvant-induced changes in hyperalgesia and allodynia. *Neuroscience* **78**(3)**:** 843-850.

Hayhoe RP, Kamal AM, Solito E, Flower RJ, Cooper D, Perretti M (2006). Annexin 1 and its bioactive peptide inhibit neutrophil-endothelium interactions under flow: indication of distinct receptor involvement. *Blood* **107**(5)**:** 2123-2130.

Haywood AR, Hathway GJ, Chapman V (2018). Differential contributions of peripheral and central mechanisms to pain in a rodent model of osteoarthritis. *Scientific reports* **8**(1)**:** 7122.

Hefti FF, Rosenthal A, Walicke PA, Wyatt S, Vergara G, Shelton DL*, et al.* (2006). Novel class of pain drugs based on antagonism of NGF. *Trends Pharmacol Sci* **27**(2)**:** 85-91.

Heinricher MM, Field HL (2013). Central nervous system mechanisms of pain modulation. In: McMahon SB, Koltzenburg M, Tracey I, Turk DC (ed)^(eds). *Wall & Melzack's Textbook of Pain*, 6th edn: Elsevier/Saunders. p^pp 129-142.

Herold KF, Nau C, Ouyang W, Hemmings HC, Jr. (2009). Isoflurane inhibits the tetrodotoxin-resistant voltage-gated sodium channel Nav1.8. *Anesthesiology* **111**(3)**:** 591-599.

Hershman DL, Lacchetti C, Dworkin RH, Lavoie Smith EM, Bleeker J, Cavaletti G*, et al.* (2014). Prevention and management of chemotherapy-induced peripheral neuropathy in survivors of adult cancers: American Society of Clinical Oncology clinical practice guideline. *Journal of clinical oncology : official journal of the American Society of Clinical Oncology* **32**(18)**:** 1941-1967.

Hesselink JM, Chiosi F, Costagliola C (2016). Resolvins and aliamides: lipid autacoids in ophthalmology - what promise do they hold? *Drug design, development and therapy* **10:** 3133-3141.

Hill CL, Hunter DJ, Niu J, Clancy M, Guermazi A, Genant H*, et al.* (2007). Synovitis detected on magnetic resonance imaging and its relation to pain and cartilage loss in knee osteoarthritis. *Annals of the rheumatic diseases* **66**(12)**:** 1599-1603.

Hirsch S, Dickenson A, Corradini L (2014). Anesthesia influences neuronal activity and drug effectiveness in neuropathic rats. *Pain* **155**(12)**:** 2583-2590.

Hong S, Gronert K, Devchand PR, Moussignac RL, Serhan CN (2003). Novel docosatrienes and 17S-resolvins generated from docosahexaenoic acid in murine brain, human blood, and glial cells. Autacoids in anti-inflammation. *The Journal of biological chemistry* **278**(17)**:** 14677-14687.

Hong S, Lu Y, Yang R, Gotlinger KH, Petasis NA, Serhan CN (2007). Resolvin D1, protectin D1, and related docosahexaenoic acid-derived products: Analysis via electrospray/low energy tandem mass spectrometry based on spectra and fragmentation mechanisms. *Journal of the American Society for Mass Spectrometry* **18**(1)**:** 128-144.

Hong S, Porter TF, Lu Y, Oh SF, Pillai PS, Serhan CN (2008). Resolvin E1 metabolome in local inactivation during inflammation-resolution. *Journal of immunology* **180**(5)**:** 3512-3519.

Hosl K, Reinold H, Harvey RJ, Muller U, Narumiya S, Zeilhofer HU (2006). Spinal prostaglandin E receptors of the EP2 subtype and the glycine receptor alpha3 subunit, which mediate central inflammatory hyperalgesia, do not contribute to pain after peripheral nerve injury or formalin injection. *Pain* **126**(1-3)**:** 46-53.

Hsiao HM, Thatcher TH, Colas RA, Serhan CN, Phipps RP, Sime PJ (2015). Resolvin D1 Reduces Emphysema and Chronic Inflammation. *The American journal of pathology* **185**(12)**:** 3189-3201.

Hsieh MT, Donaldson LF, Lumb BM (2015). Differential contributions of A- and C-nociceptors to primary and secondary inflammatory hypersensitivity in the rat. *Pain* **156**(6)**:** 1074-1083.

Hu S, Mao-Ying QL, Wang J, Wang ZF, Mi WL, Wang XW*, et al.* (2012). Lipoxins and aspirin-triggered lipoxin alleviate bone cancer pain in association with suppressing expression of spinal proinflammatory cytokines. *Journal of neuroinflammation* **9:** 278.

Huang J, Burston JJ, Li L, Ashraf S, Mapp PI, Bennett AJ*, et al.* (2017). Targeting the D Series Resolvin Receptor System for the Treatment of Osteoarthritis Pain. *Arthritis & rheumatology* **69**(5)**:** 996-1008.

Huang L, Wang CF, Serhan CN, Strichartz G (2011). Enduring prevention and transient reduction of postoperative pain by intrathecal resolvin D1. *Pain* **152**(3)**:** 557-565.

Hulse R, Wynick D, Donaldson LF (2010). Intact cutaneous C fibre afferent properties in mechanical and cold neuropathic allodynia. *European journal of pain* **14**(6)**:** 565 e561-565 e510.

Hunt SP, Mantyh PW (2001). The molecular dynamics of pain control. *Nature reviews. Neuroscience* **2**(2)**:** 83-91.

IASP (1979). Pain terms: a list with definitions and notes on usage. Recommended by the IASP Subcommittee on Taxonomy. *Pain* **6**(3)**:** 249.

IASP (1994). Part III: Pain terms, a current list with definitions and notes on usage. In: Merskey H, Bogduk N (ed)^(eds). *Classification of Chronic Pain*, 2nd edn: IASP Press. p^pp.

Ikeda H, Heinke B, Ruscheweyh R, Sandkuhler J (2003). Synaptic plasticity in spinal lamina I projection neurons that mediate hyperalgesia. *Science* **299**(5610)**:** 1237-1240.

Imai S, Ikegami D, Yamashita A, Shimizu T, Narita M, Niikura K*, et al.* (2013). Epigenetic transcriptional activation of monocyte chemotactic protein 3 contributes to long-lasting neuropathic pain. *Brain : a journal of neurology* **136**(Pt 3)**:** 828-843.

Ivanavicius SP, Ball AD, Heapy CG, Westwood FR, Murray F, Read SJ (2007). Structural pathology in a rodent model of osteoarthritis is associated with neuropathic pain: Increased expression of ATF-3 and pharmacological characterisation. *Pain* **128**(3)**:** 272-282.

Jackson T, Thomas S, Stabile V, Han X, Shotwell M, McQueen K (2015). Prevalence of chronic pain in low-income and middle-income countries: a systematic review and meta-analysis. *Lancet* **385 Suppl 2:** S10.

Janes K, Little JW, Li C, Bryant L, Chen C, Chen Z*, et al.* (2014). The development and maintenance of paclitaxel-induced neuropathic pain require activation of the sphingosine 1-phosphate receptor subtype 1. *The Journal of biological chemistry* **289**(30)**:** 21082-21097.

Jara JH, Singh BB, Floden AM, Combs CK (2007). Tumor necrosis factor alpha stimulates NMDA receptor activity in mouse cortical neurons resulting in ERK-dependent death. *Journal of neurochemistry* **100**(5)**:** 1407-1420.

Jhaveri MD, Richardson D, Robinson I, Garle MJ, Patel A, Sun Y*, et al.* (2008). Inhibition of fatty acid amide hydrolase and cyclooxygenase-2 increases levels of endocannabinoid related molecules and produces analgesia via peroxisome

proliferator-activated receptor-alpha in a model of inflammatory pain. *Neuropharmacology* **55**(1)**:** 85-93.

Ji R-R, Berta T, Nedergaard M (2013). Glia and pain: Is chronic pain a gliopathy? *PAIN*® **154, Supplement 1**(0)**:** S10-S28.

Ji R-R, Kohno T, Moore KA, Woolf CJ (2003). Central sensitization and LTP: do pain and memory share similar mechanisms? *Trends in Neurosciences* **26**(12)**:** 696-705.

Ji RR, Befort K, Brenner GJ, Woolf CJ (2002). ERK MAP kinase activation in superficial spinal cord neurons induces prodynorphin and NK-1 upregulation and contributes to persistent inflammatory pain hypersensitivity. *The Journal of neuroscience : the official journal of the Society for Neuroscience* **22**(2)**:** 478-485.

Ji RR, Xu ZZ, Gao YJ (2014). Emerging targets in neuroinflammation-driven chronic pain. *Nature reviews. Drug discovery* **13**(7)**:** 533-548.

Ji RR, Xu ZZ, Strichartz G, Serhan CN (2011). Emerging roles of resolvins in the resolution of inflammation and pain. *Trends Neurosci* **34**(11)**:** 599-609.

Jiang BC, Cao DL, Zhang X, Zhang ZJ, He LN, Li CH*, et al.* (2016). CXCL13 drives spinal astrocyte activation and neuropathic pain via CXCR5. *The Journal of clinical investigation* **126**(2)**:** 745-761.

Jin HW, Flatters SJ, Xiao WH, Mulhern HL, Bennett GJ (2008). Prevention of paclitaxel-evoked painful peripheral neuropathy by acetyl-L-carnitine: effects on axonal mitochondria, sensory nerve fiber terminal arbors, and cutaneous Langerhans cells. *Exp Neurol* **210**(1)**:** 229-237.

Jin SX, Zhuang ZY, Woolf CJ, Ji RR (2003). p38 mitogen-activated protein kinase is activated after a spinal nerve ligation in spinal cord microglia and dorsal root ganglion neurons and contributes to the generation of neuropathic pain. *The Journal of neuroscience : the official journal of the Society for Neuroscience* **23**(10)**:** 4017-4022.

Jinks SL, Antognini JF, Dutton RC, Carstens E, Eger EI, 2nd (2004). Isoflurane depresses windup of C fiber-evoked limb withdrawal with variable effects on nociceptive lumbar spinal neurons in rats. *Anesthesia and analgesia* **99**(5)**:** 1413-1419; table of contents.

Jordan MA, Wilson L (2004). Microtubules as a target for anticancer drugs. *Nature reviews. Cancer* **4**(4)**:** 253-265.

Ju G, Hokfelt T, Brodin E, Fahrenkrug J, Fischer JA, Frey P*, et al.* (1987). Primary sensory neurons of the rat showing calcitonin gene-related peptide immunoreactivity and their relation to substance P-, somatostatin-, galanin-, vasoactive intestinal polypeptide- and cholecystokinin-immunoreactive ganglion cells. *Cell and tissue research* **247**(2)**:** 417-431.

Kapoor M, Martel-Pelletier J, Lajeunesse D, Pelletier JP, Fahmi H (2011). Role of proinflammatory cytokines in the pathophysiology of osteoarthritis. *Nature reviews. Rheumatology* **7**(1)**:** 33-42.

Kashiba H, Uchida Y, Senba E (2001). Difference in binding by isolectin B4 to trkA and c-ret mRNA-expressing neurons in rat sensory ganglia. *Brain research. Molecular brain research* **95**(1-2)**:** 18-26.

Kawakami K, Chiba T, Katagiri N, Saduka M, Abe K, Utsunomiya I*, et al.* (2012). Paclitaxel increases high voltage-dependent calcium channel current in dorsal root ganglion neurons of the rat. *Journal of pharmacological sciences* **120**(3)**:** 187-195.

Kawamata M, Narimatsu E, Kozuka Y, Takahashi T, Sugino S, Niiya T*, et al.* (2005). Effects of halothane and isoflurane on hyperexcitability of spinal dorsal horn neurons after incision in the rat. *Anesthesiology* **102**(1)**:** 165-174.

Kawasaki Y, Zhang L, Cheng JK, Ji RR (2008). Cytokine mechanisms of central sensitization: distinct and overlapping role of interleukin-1beta, interleukin-6, and tumor necrosis factor-alpha in regulating synaptic and neuronal activity in the superficial spinal cord. *The Journal of neuroscience : the official journal of the Society for Neuroscience* **28**(20)**:** 5189-5194.

Kearney PM, Baigent C, Godwin J, Halls H, Emberson JR, Patrono C (2006). Do selective cyclo-oxygenase-2 inhibitors and traditional non-steroidal anti-inflammatory drugs increase the risk of atherothrombosis? Meta-analysis of randomised trials. *BMJ (Clinical research ed.)* **332**(7553)**:** 1302-1308.

Kelly S, Dobson KL, Harris J (2013). Spinal nociceptive reflexes are sensitized in the monosodium iodoacetate model of osteoarthritis pain in the rat. *Osteoarthritis and Cartilage* **21**(9)**:** 1327-1335.

Kelly S, Dunham JP, Murray F, Read S, Donaldson LF, Lawson SN (2012). Spontaneous firing in C-fibers and increased mechanical sensitivity in A-fibers of knee joint-associated mechanoreceptive primary afferent neurones during MIA-induced osteoarthritis in the rat. *Osteoarthritis and cartilage / OARS, Osteoarthritis Research Society* **20**(4)**:** 305-313.

Kilkenny C, Browne WJ, Cuthill IC, Emerson M, Altman DG (2012). Improving bioscience research reporting: the ARRIVE guidelines for reporting animal research. *Osteoarthritis and cartilage / OARS, Osteoarthritis Research Society* **20**(4)**:** 256-260.

Kim SE, Lee EO, Yang JH, Kang JH, Suh YH, Chong YH (2012). 15-deoxy-Delta(1)(2),(1)(4) -prostaglandin J(2) inhibits human immunodeficiency virus-1 tat-induced monocyte chemoattractant protein-1/CCL2 production by blocking the extracellular signal-regulated kinase-1/2 signaling pathway independently of peroxisome proliferator-activated receptor-gamma and heme oxygenase-1 in rat hippocampal slices. *Journal of neuroscience research* **90**(9)**:** 1732-1742.

Kiyoyuki Y, Taniguchi W, Okubo M, Yamanaka H, Kobayashi K, Nishio N*, et al.* (2015). Leukotriene enhances NMDA-induced inward currents in dorsal horn neurons of the rat spinal cord after peripheral nerve injury. *Molecular pain* **11:** 53.

Knowlton WM, Palkar R, Lippoldt EK, McCoy DD, Baluch F, Chen J*, et al.* (2013). A sensory-labeled line for cold: TRPM8-expressing sensory neurons define the cellular basis for cold, cold pain, and cooling-mediated analgesia. *The Journal of neuroscience : the official journal of the Society for Neuroscience* **33**(7)**:** 2837-2848.

Ko MH, Hu ME, Hsieh YL, Lan CT, Tseng TJ (2014). Peptidergic intraepidermal nerve fibers in the skin contribute to the neuropathic pain in paclitaxel-induced peripheral neuropathy. *Neuropeptides* **48**(3)**:** 109-117.

Kobayashi K, Fukuoka T, Obata K, Yamanaka H, Dai Y, Tokunaga A*, et al.* (2005). Distinct expression of TRPM8, TRPA1, and TRPV1 mRNAs in rat primary afferent neurons with adelta/c-fibers and colocalization with trk receptors. *The Journal of comparative neurology* **493**(4)**:** 596-606.

Kobayashi K, Takahashi E, Miyagawa Y, Yamanaka H, Noguchi K (2011). Induction of the P2X7 receptor in spinal microglia in a neuropathic pain model. *Neuroscience letters* **504**(1)**:** 57-61.

Kohno T, Ji RR, Ito N, Allchorne AJ, Befort K, Karchewski LA*, et al.* (2005). Peripheral axonal injury results in reduced mu opioid receptor pre- and post-synaptic action in the spinal cord. *Pain* **117**(1-2)**:** 77-87.

Krishnamoorthy S, Recchiuti A, Chiang N, Fredman G, Serhan CN (2012). Resolvin D1 receptor stereoselectivity and regulation of inflammation and proresolving microRNAs. *The American journal of pathology* **180**(5)**:** 2018-2027.

Krishnamoorthy S, Recchiuti A, Chiang N, Yacoubian S, Lee CH, Yang R*, et al.* (2010). Resolvin D1 binds human phagocytes with evidence for proresolving receptors. *Proceedings of the National Academy of Sciences of the United States of America* **107**(4)**:** 1660-1665.

Kuner R, Flor H (2017). Structural plasticity and reorganisation in chronic pain. *Nature reviews. Neuroscience* **18**(1)**:** 20-30.

Kwan KY, Allchorne AJ, Vollrath MA, Christensen AP, Zhang DS, Woolf CJ*, et al.* (2006). TRPA1 contributes to cold, mechanical, and chemical nociception but is not essential for hair-cell transduction. *Neuron* **50**(2)**:** 277-289.

Lappin SC, Randall AD, Gunthorpe MJ, Morisset V (2006). TRPV1 antagonist, SB-366791, inhibits glutamatergic synaptic transmission in rat spinal dorsal horn following peripheral inflammation. *European journal of pharmacology* **540**(1-3)**:** 73-81.

Lardner A (2001). The effects of extracellular pH on immune function. *Journal of leukocyte biology* **69**(4)**:** 522-530.

Larsson M, Broman J (2008). Translocation of GluR1-containing AMPA receptors to a spinal nociceptive synapse during acute noxious stimulation. *The Journal of neuroscience : the official journal of the Society for Neuroscience* **28**(28)**:** 7084-7090.

Latremoliere A, Woolf CJ (2009). Central sensitization: a generator of pain hypersensitivity by central neural plasticity. *The journal of pain : official journal of the American Pain Society* **10**(9)**:** 895-926.

Laurie DJ, Bartke I, Schoepfer R, Naujoks K, Seeburg PH (1997). Regional, developmental and interspecies expression of the four NMDAR2 subunits, examined using monoclonal antibodies. *Mol Brain Res* **51**(1-2)**:** 23-32.

Lawson SN, Harper AA, Harper EI, Garson JA, Anderton BH (1984). A monoclonal antibody against neurofilament protein specifically labels a subpopulation of rat sensory neurones. *The Journal of comparative neurology* **228**(2)**:** 263-272.

Ledeboer A, Breve JJ, Wierinckx A, van der Jagt S, Bristow AF, Leysen JE*, et al.* (2002). Expression and regulation of interleukin-10 and interleukin-10 receptor in rat astroglial and microglial cells. *The European journal of neuroscience* **16**(7)**:** 1175-1185.

Ledeboer A, Jekich BM, Sloane EM, Mahoney JH, Langer SJ, Milligan ED*, et al.* (2007). Intrathecal interleukin-10 gene therapy attenuates paclitaxel-induced mechanical allodynia and proinflammatory cytokine expression in dorsal root ganglia in rats. *Brain, behavior, and immunity* **21**(5)**:** 686-698.

Ledeboer A, Wierinckx A, Bol JG, Floris S, Renardel de Lavalette C, De Vries HE*, et al.* (2003). Regional and temporal expression patterns of interleukin-10, interleukin-10 receptor and adhesion molecules in the rat spinal cord during chronic relapsing EAE. *Journal of neuroimmunology* **136**(1-2)**:** 94-103.

Lee JH, Woo JH, Woo SU, Kim KS, Park SM, Joe EH*, et al.* (2008). The 15-deoxy-delta 12,14-prostaglandin J2 suppresses monocyte chemoattractant protein-1 expression in IFN-gamma-stimulated astrocytes through induction of MAPK phosphatase-1. *Journal of immunology* **181**(12)**:** 8642-8649.

Lee Y, Pai M, Brederson JD, Wilcox D, Hsieh G, Jarvis MF*, et al.* (2011). Monosodium iodoacetate-induced joint pain is associated with increased phosphorylation of mitogen activated protein kinases in the rat spinal cord. *Molecular pain* **7**.

Lehmann C, Homann J, Ball AK, Blocher R, Kleinschmidt TK, Basavarajappa D*, et al.* (2015). Lipoxin and resolvin biosynthesis is dependent on 5-lipoxygenase activating protein. *FASEB journal : official publication of the Federation of American Societies for Experimental Biology* **29**(12)**:** 5029-5043.

Leith JL, Koutsikou S, Lumb BM, Apps R (2010). Spinal processing of noxious and innocuous cold information: differential modulation by the periaqueductal gray. *The Journal of neuroscience : the official journal of the Society for Neuroscience* **30**(14)**:** 4933-4942.

Leon A, Buriani A, Dal Toso R, Fabris M, Romanello S, Aloe L*, et al.* (1994). Mast cells synthesize, store, and release nerve growth factor. *Proceedings of the National Academy of Sciences of the United States of America* **91**(9)**:** 3739-3743.

Levy BD, Clish CB, Schmidt B, Gronert K, Serhan CN (2001). Lipid mediator class switching during acute inflammation: signals in resolution. *Nature immunology* **2**(7)**:** 612-619.

Li D, Huang ZZ, Ling YZ, Wei JY, Cui Y, Zhang XZ*, et al.* (2015a). Up-regulation of CX3CL1 via Nuclear Factor-kappaB-dependent Histone Acetylation Is Involved in Paclitaxel-induced Peripheral Neuropathy. *Anesthesiology* **122**(5)**:** 1142-1151.

Li Q, Tian Y, Wang ZF, Liu SB, Mi WL, Ma HJ*, et al.* (2013). Involvement of the spinal NALP1 inflammasome in neuropathic pain and aspirin-triggered-15-epi-lipoxin A4 induced analgesia. *Neuroscience* **254:** 230-240.

Li Y, Adamek P, Zhang H, Tatsui CE, Rhines LD, Mrozkova P*, et al.* (2015b). The Cancer Chemotherapeutic Paclitaxel Increases Human and Rodent Sensory Neuron Responses to TRPV1 by Activation of TLR4. *The Journal of neuroscience : the official journal of the Society for Neuroscience* **35**(39)**:** 13487-13500.

Li Y, Zhang H, Zhang H, Kosturakis AK, Jawad AB, Dougherty PM (2014). Toll-like receptor 4 signaling contributes to Paclitaxel-induced peripheral neuropathy. *The journal of pain : official journal of the American Pain Society* **15**(7)**:** 712-725.

Li YY, Cui JG, Dua P, Pogue AI, Bhattacharjee S, Lukiw WJ (2011). Differential expression of miRNA-146a-regulated inflammatory genes in human primary neural, astroglial and microglial cells. *Neuroscience letters* **499**(2)**:** 109-113.

Lima-Garcia JF, Dutra RC, da Silva K, Motta EM, Campos MM, Calixto JB (2011). The precursor of resolvin D series and aspirin-triggered resolvin D1 display anti-hyperalgesic properties in adjuvant-induced arthritis in rats. *British journal of pharmacology* **164**(2)**:** 278-293.

Lingueglia E (2007). Acid-sensing ion channels in sensory perception. *The Journal of biological chemistry* **282**(24)**:** 17325-17329.

Liu CC, Lu N, Cui Y, Yang T, Zhao ZQ, Xin WJ*, et al.* (2010). Prevention of paclitaxel-induced allodynia by minocycline: Effect on loss of peripheral nerve fibers and infiltration of macrophages in rats. *Molecular pain* **6:** 76.

Liu X, Sandkuhler J (1997). Characterization of long-term potentiation of C-fiber-evoked potentials in spinal dorsal horn of adult rat: essential role of NK1 and NK2 receptors. *Journal of neurophysiology* **78**(4)**:** 1973-1982.

Liu Y, Zhou D, Long FW, Chen KL, Yang HW, Lv ZY*, et al.* (2016a). Resolvin D1 protects against inflammation in experimental acute pancreatitis and associated lung injury. *American journal of physiology. Gastrointestinal and liver physiology* **310**(5)**:** G303-309.

Liu ZH, Miao GS, Wang JN, Yang CX, Fu ZJ, Sun T (2016b). Resolvin D1 Inhibits Mechanical Hypersensitivity in Sciatica by Modulating the Expression of Nuclear Factor-kappaB, Phospho-extracellular Signal-regulated Kinase, and Pro- and Antiinflammatory Cytokines in the Spinal Cord and Dorsal Root Ganglion. *Anesthesiology* **124**(4)**:** 934-944.

Livak KJ, Schmittgen TD (2001). Analysis of relative gene expression data using real-time quantitative PCR and the 2(-Delta Delta C(T)) Method. *Methods* **25**(4)**:** 402-408.

Loeser RF, Goldring SR, Scanzello CR, Goldring MB (2012). Osteoarthritis: a disease of the joint as an organ. *Arthritis and rheumatism* **64**(6)**:** 1697-1707.

Lopes AH, Brandolini L, Aramini A, Bianchini G, Silva RL, Zaperlon AC*, et al.* (2016). DF2755A, a novel non-competitive allosteric inhibitor of CXCR1/2, reduces inflammatory and post-operative pain. *Pharmacological research* **103:** 69-79.

Lories RJ, Luyten FP (2011). The bone-cartilage unit in osteoarthritis. *Nature reviews. Rheumatology* **7**(1)**:** 43-49.

LoVerme J, Russo R, La Rana G, Fu J, Farthing J, Mattace-Raso G*, et al.* (2006). Rapid broad-spectrum analgesia through activation of peroxisome proliferator-activated receptor-alpha. *The Journal of pharmacology and experimental therapeutics* **319**(3)**:** 1051-1061.

Lu Y, Jiang BC, Cao DL, Zhang ZJ, Zhang X, Ji RR*, et al.* (2014). TRAF6 upregulation in spinal astrocytes maintains neuropathic pain by integrating TNF-alpha and IL-1beta signaling. *Pain* **155**(12)**:** 2618-2629.

Luo C, Kuner T, Kuner R (2014). Synaptic plasticity in pathological pain. *Trends Neurosci* **37**(6)**:** 343-355.

Luo ZD, Calcutt NA, Higuera ES, Valder CR, Song YH, Svensson CI*, et al.* (2002). Injury type-specific calcium channel alpha 2 delta-1 subunit up-regulation in rat neuropathic pain models correlates with antiallodynic effects of gabapentin. *The Journal of pharmacology and experimental therapeutics* **303**(3)**:** 1199-1205.

Machado FS, Johndrow JE, Esper L, Dias A, Bafica A, Serhan CN*, et al.* (2006). Anti-inflammatory actions of lipoxin A4 and aspirin-triggered lipoxin are SOCS-2 dependent. *Nature medicine* **12**(3)**:** 330-334.

Mallinson JE, Marimuthu K, Murton A, Selby A, Smith K, Constantin-Teodosiu D*, et al.* (2015). Statin myalgia is not associated with reduced muscle strength, mass or protein turnover in older male volunteers, but is allied with a slowing of time to peak power output, insulin resistance and differential muscle mRNA expression. *The Journal of physiology* **593**(5)**:** 1239-1257.

Marchand F, Perretti M, McMahon SB (2005). Role of the immune system in chronic pain. *Nature reviews. Neuroscience* **6**(7)**:** 521-532.

Marcheselli VL, Mukherjee PK, Arita M, Hong S, Antony R, Sheets K*, et al.* (2010). Neuroprotectin D1/protectin D1 stereoselective and specific binding with human

retinal pigment epithelial cells and neutrophils. *Prostaglandins, leukotrienes, and essential fatty acids* **82**(1)**:** 27-34.

Martini AC, Berta T, Forner S, Chen G, Bento AF, Ji RR*, et al.* (2016). Lipoxin A4 inhibits microglial activation and reduces neuroinflammation and neuropathic pain after spinal cord hemisection. *Journal of neuroinflammation* **13**(1)**:** 75.

Materazzi S, Fusi C, Benemei S, Pedretti P, Patacchini R, Nilius B*, et al.* (2012). TRPA1 and TRPV4 mediate paclitaxel-induced peripheral neuropathy in mice via a glutathione-sensitive mechanism. *Pflugers Archiv : European journal of physiology* **463**(4)**:** 561-569.

Matsumoto M, Inoue M, Hald A, Xie WJ, Ueda H (2006). Inhibition of paclitaxel-induced A-fiber hypersensitization by gabapentin. *Journal of Pharmacology and Experimental Therapeutics* **318**(2)**:** 735-740.

McAlindon TE, Cooper C, Kirwan JR, Dieppe PA (1993). Determinants of disability in osteoarthritis of the knee. *Annals of the rheumatic diseases* **52**(4)**:** 258-262.

McCarthy PW, Lawson SN (1989). Cell type and conduction velocity of rat primary sensory neurons with substance P-like immunoreactivity. *Neuroscience* **28**(3)**:** 745-753.

Meents JE, Fischer MJ, McNaughton PA (2017). Sensitization of TRPA1 by Protein Kinase A. *PloS one* **12**(1)**:** e0170097.

Meesawatsom P, Burston J, Hathway G, Bennett A, Chapman V (2016). Inhibitory effects of aspirin-triggered resolvin D1 on spinal nociceptive processing in rat pain models. *Journal of neuroinflammation* **13**(1)**:** 233.

Meller ST, Gebhart GF (1993). Nitric oxide (NO) and nociceptive processing in the spinal cord. *Pain* **52**(2)**:** 127-136.

Mendell LM (1966). Physiological properties of unmyelinated fiber projection to the spinal cord. *Exp Neurol* **16**(3)**:** 316-332.

Michael GJ, Priestley JV (1999). Differential expression of the mRNA for the vanilloid receptor subtype 1 in cells of the adult rat dorsal root and nodose ganglia and its downregulation by axotomy. *The Journal of neuroscience : the official journal of the Society for Neuroscience* **19**(5)**:** 1844-1854.

Mika J, Zychowska M, Popiolek-Barczyk K, Rojewska E, Przewlocka B (2013). Importance of glial activation in neuropathic pain. *European journal of pharmacology* **716**(1-3)**:** 106-119.

Milligan ED, Watkins LR (2009). Pathological and protective roles of glia in chronic pain. *Nature reviews. Neuroscience* **10**(1)**:** 23-36.

Mirzaei V, Manaheji H, Maghsoudi N, Zaringhalam J (2010). Comparison of changes in mRNA expression of spinal glutamate transporters following induction of two neuropathic pain models. *Spinal cord* **48**(11)**:** 791-797.

Miyagishi H, Kosuge Y, Takano A, Endo M, Nango H, Yamagata-Murayama S*, et al.* (2017). Increased Expression of 15-Hydroxyprostaglandin Dehydrogenase in Spinal Astrocytes During Disease Progression in a Model of Amyotrophic Lateral Sclerosis. *Cellular and molecular neurobiology* **37**(3)**:** 445-452.

Momin A, Wood JN (2008). Sensory neuron voltage-gated sodium channels as analgesic drug targets. *Current opinion in neurobiology* **18**(4)**:** 383-388.

Mori T, Kanbara T, Harumiya M, Iwase Y, Masumoto A, Komiya S*, et al.* (2014). Establishment of opioid-induced rewarding effects under oxaliplatin- and Paclitaxel-induced neuropathy in rats. *Journal of pharmacological sciences* **126**(1)**:** 47-55.

Moriyama T, Higashi T, Togashi K, Iida T, Segi E, Sugimoto Y*, et al.* (2005). Sensitization of TRPV1 by EP1 and IP reveals peripheral nociceptive mechanism of prostaglandins. *Molecular pain* **1:** 3.

Morris CJ (2003). Carrageenan-induced paw edema in the rat and mouse. *Methods in molecular biology* **225:** 115-121.

Motsko SP, Rascati KL, Busti AJ, Wilson JP, Barner JC, Lawson KA*, et al.* (2006). Temporal relationship between use of NSAIDs, including selective COX-2 inhibitors, and cardiovascular risk. *Drug safety : an international journal of medical toxicology and drug experience* **29**(7)**:** 621-632.

Naziroglu M, Braidy N (2017). Thermo-Sensitive TRP Channels: Novel Targets for Treating Chemotherapy-Induced Peripheral Pain. *Frontiers in physiology* **8:** 1040.

Neugebauer V, Vanegas H, Nebe J, Rumenapp P, Schaible HG (1996). Effects of N- and L-type calcium channel antagonists on the responses of nociceptive spinal cord neurons to mechanical stimulation of the normal and the inflamed knee joint. *Journal of neurophysiology* **76**(6)**:** 3740-3749.

Nieto FR, Clark AK, Grist J, Hathway GJ, Chapman V, Malcangio M (2016). Neuron-immune mechanisms contribute to pain in early stages of arthritis. *Journal of neuroinflammation* **13**(1)**:** 96.

Nolan T, Hands RE, Bustin SA (2006). Quantification of mRNA using real-time RT-PCR. *Nat. Protocols* **1**(3)**:** 1559-1582.

Norling LV, Headland SE, Dalli J, Arnardottir HH, Haworth O, Jones HR*, et al.* (2016). Proresolving and cartilage-protective actions of resolvin D1 in inflammatory arthritis. *JCI insight* **1**(5)**:** e85922.

Norling LV, Perretti M (2013). The role of omega-3 derived resolvins in arthritis. *Current opinion in pharmacology* **13**(3)**:** 476-481.

Norris PC, Gosselin D, Reichart D, Glass CK, Dennis EA (2014). Phospholipase A2 regulates eicosanoid class switching during inflammasome activation. *Proceedings of the National Academy of Sciences of the United States of America* **111**(35)**:** 12746-12751.

Nwosu LN, Mapp PI, Chapman V, Walsh DA (2016). Relationship between structural pathology and pain behaviour in a model of osteoarthritis (OA). *Osteoarthritis and Cartilage* **24**(11)**:** 1910-1917.

Ochi-ishi R, Nagata K, Inoue T, Tozaki-Saitoh H, Tsuda M, Inoue K (2014). Involvement of the chemokine CCL3 and the purinoceptor P2X7 in the spinal cord in paclitaxel-induced mechanical allodynia. *Molecular pain* **10:** 53.

Oh SF, Pillai PS, Recchiuti A, Yang R, Serhan CN (2011). Pro-resolving actions and stereoselective biosynthesis of 18S E-series resolvins in human leukocytes and murine inflammation. *The Journal of clinical investigation* **121**(2)**:** 569-581.

Okine BN, Norris LM, Woodhams S, Burston J, Patel A, Alexander SP*, et al.* (2012). Lack of effect of chronic pre-treatment with the FAAH inhibitor URB597 on inflammatory pain behaviour: evidence for plastic changes in the endocannabinoid system. *British journal of pharmacology* **167**(3)**:** 627-640.

Okubo M, Yamanaka H, Kobayashi K, Noguchi K (2010). Leukotriene synthases and the receptors induced by peripheral nerve injury in the spinal cord contribute to the generation of neuropathic pain. *Glia* **58**(5)**:** 599-610.

Orita S, Ishikawa T, Miyagi M, Ochiai N, Inoue G, Eguchi Y*, et al.* (2012). Percutaneously absorbed NSAIDs attenuate local production of proinflammatory cytokines and suppress the expression of c-Fos in the spinal cord of a rodent model of knee osteoarthritis. *Journal of orthopaedic science : official journal of the Japanese Orthopaedic Association* **17**(1)**:** 77-86.

Orita S, Ishikawa T, Miyagi M, Ochiai N, Inoue G, Eguchi Y*, et al.* (2011). Pain-related sensory innervation in monoiodoacetate-induced osteoarthritis in rat knees that gradually develops neuronal injury in addition to inflammatory pain. *BMC musculoskeletal disorders* **12**.

Orr SK, Colas RA, Dalli J, Chiang N, Serhan CN (2015). Proresolving actions of a new resolvin D1 analog mimetic qualifies as an immunoresolvent. *American journal of physiology. Lung cellular and molecular physiology* **308**(9)**:** L904-911.

Orser BA, Canning KJ, Macdonald JF (2002). Mechanisms of general anesthesia. *Current opinion in anaesthesiology* **15**(4)**:** 427-433.

Otis C, Gervais J, Guillot M, Gervais JA, Gauvin D, Pethel C*, et al.* (2016). Concurrent validity of different functional and neuroproteomic pain assessment methods in the rat osteoarthritis monosodium iodoacetate (MIA) model. *Arthritis research & therapy* **18:** 150.

Paoletti P, Bellone C, Zhou Q (2013). NMDA receptor subunit diversity: impact on receptor properties, synaptic plasticity and disease. *Nature reviews. Neuroscience* **14**(6)**:** 383-400.

Park CK, Xu ZZ, Liu T, Lu N, Serhan CN, Ji RR (2011). Resolvin D2 is a potent endogenous inhibitor for transient receptor potential subtype V1/A1, inflammatory pain, and spinal cord synaptic plasticity in mice: distinct roles of resolvin D1, D2, and E1. *The Journal of neuroscience : the official journal of the Society for Neuroscience* **31**(50)**:** 18433-18438.

Park J, Luo ZD (2010). Calcium channel functions in pain processing. *Channels* **4**(6)**:** 510-517.

Parks WC, Wilson CL, Lopez-Boado YS (2004). Matrix metalloproteinases as modulators of inflammation and innate immunity. *Nature Reviews Immunology* **4**(8)**:** 617-629.

Pascual D, Goicoechea C, Suardiaz M, Martin MI (2005a). A cannabinoid agonist, WIN 55,212-2, reduces neuropathic nociception induced by paclitaxel in rats. *Pain* **118**(1-2)**:** 23-34.

Pascual G, Fong AL, Ogawa S, Gamliel A, Li AC, Perissi V*, et al.* (2005b). A SUMOylation-dependent pathway mediates transrepression of inflammatory response genes by PPAR-gamma. *Nature* **437**(7059)**:** 759-763.

Patapoutian A, Tate S, Woolf CJ (2009). Transient receptor potential channels: targeting pain at the source. *Nature reviews. Drug discovery* **8**(1)**:** 55-68.

Patel R, Bauer CS, Nieto-Rostro M, Margas W, Ferron L, Chaggar K*, et al.* (2013). alpha2delta-1 gene deletion affects somatosensory neuron function and delays mechanical hypersensitivity in response to peripheral nerve damage. *The Journal of neuroscience : the official journal of the Society for Neuroscience* **33**(42)**:** 16412-16426.

Pei L, Zhang J, Zhao F, Su T, Wei H, Tian J*, et al.* (2011). Annexin 1 exerts anti-nociceptive effects after peripheral inflammatory pain through formyl-peptide-receptor-like 1 in rat dorsal root ganglion. *British journal of anaesthesia* **107**(6)**:** 948-958.

Peier AM, Moqrich A, Hergarden AC, Reeve AJ, Andersson DA, Story GM*, et al.* (2002). A TRP channel that senses cold stimuli and menthol. *Cell* **108**(5)**:** 705-715.

Peters CM, Jimenez-Andrade JM, Jonas BM, Sevcik MA, Koewler NJ, Ghilardi JR*, et al.* (2007a). Intravenous paclitaxel administration in the rat induces a peripheral sensory neuropathy characterized by macrophage infiltration and injury to sensory neurons and their supporting cells. *Exp Neurol* **203**(1)**:** 42-54.

Peters CM, Jimenez-Andrade JM, Kuskowski MA, Ghilardi JR, Mantyh PW (2007b). An evolving cellular pathology occurs in dorsal root ganglia, peripheral nerve and spinal cord following intravenous administration of paclitaxel in the rat. *Brain research* **1168:** 46-59.

Piomelli D, Sasso O (2014). Peripheral gating of pain signals by endogenous lipid mediators. *Nature neuroscience* **17**(2)**:** 164-174.

Pittman SK, Gracias NG, Vasko MR, Fehrenbacher JC (2014). Paclitaxel alters the evoked release of calcitonin gene-related peptide from rat sensory neurons in culture. *Exp Neurol* **253:** 146-153.

Polgar E, Hughes DI, Riddell JS, Maxwell DJ, Puskar Z, Todd AJ (2003). Selective loss of spinal GABAergic or glycinergic neurons is not necessary for development of thermal hyperalgesia in the chronic constriction injury model of neuropathic pain. *Pain* **104**(1-2)**:** 229-239.

Polomano RC, Mannes AJ, Clark US, Bennett GJ (2001). A painful peripheral neuropathy in the rat produced by the chemotherapeutic drug, paclitaxel. *Pain* **94**(3)**:** 293-304.

Pomonis JD, Boulet JM, Gottshall SL, Phillips S, Sellers R, Bunton T*, et al.* (2005). Development and pharmacological characterization of a rat model of osteoarthritis pain. *Pain* **114**(3)**:** 339-346.

Priestley JV (2009). Trophic factors and their receptors in pain pathways. In: Malcangio M (ed)^(eds). *Synaptic Plasticity in Pain*, edn: Springer. p^pp 21-45.

Proudfoot CJ, Garry EM, Cottrell DF, Rosie R, Anderson H, Robertson DC*, et al.* (2006). Analgesia mediated by the TRPM8 cold receptor in chronic neuropathic pain. *Current biology : CB* **16**(16)**:** 1591-1605.

Qu XX, Cai J, Li MJ, Chi YN, Liao FF, Liu FY*, et al.* (2009). Role of the spinal cord NR2B-containing NMDA receptors in the development of neuropathic pain. *Exp Neurol* **215**(2)**:** 298-307.

Quan-Xin F, Fan F, Xiang-Ying F, Shu-Jun L, Shi-Qi W, Zhao-Xu L*, et al.* (2012). Resolvin D1 reverses chronic pancreatitis-induced mechanical allodynia, phosphorylation of NMDA receptors, and cytokines expression in the thoracic spinal dorsal horn. *BMC gastroenterology* **12:** 148.

Raghavendra V, Tanga FY, DeLeo JA (2004). Complete Freunds adjuvant-induced peripheral inflammation evokes glial activation and proinflammatory cytokine expression in the CNS. *The European journal of neuroscience* **20**(2)**:** 467-473.

Rahman W, Bauer CS, Bannister K, Vonsy JL, Dolphin AC, Dickenson AH (2009). Descending serotonergic facilitation and the antinociceptive effects of pregabalin in a rat model of osteoarthritic pain. *Molecular pain* **5:** 45.

Raja SN, Campbell JN, Meyer RA (1984). Evidence for different mechanisms of primary and secondary hyperalgesia following heat injury to the glabrous skin. *Brain : a journal of neurology* **107 (Pt 4):** 1179-1188.

Rang HP, Dale MM, Ritter JM, Flower RJ (2007). *Analgesic drugs*. 6th edn. Churchill Livingstone.

Recchiuti A, Serhan CN (2012). Pro-Resolving Lipid Mediators (SPMs) and Their Actions in Regulating miRNA in Novel Resolution Circuits in Inflammation. *Frontiers in immunology* **3:** 298.

Ren K, Dubner R (2010). Interactions between the immune and nervous systems in pain. *Nature medicine* **16**(11)**:** 1267-1276.

Rexed B (1952). The cytoarchitectonic organization of the spinal cord in the cat. *The Journal of comparative neurology* **96**(3)**:** 414-495.

Ringkamp M, Raja SM, Campbell JN, Meyer RA (2013). Peripheral mechanisms of cutaneous nociception. In: McMahon SB, Koltzenburg M, Tracey I, Turk DC (ed)^(eds). *Wall & Melzack's Textbook of Pain*, 6th edn: Elsevier/Saunders. p^pp.

Robertson SA, Koleva RI, Argetsinger LS, Carter-Su C, Marto JA, Feener EP*, et al.* (2009). Regulation of Jak2 function by phosphorylation of Tyr317 and Tyr637 during cytokine signaling. *Molecular and cellular biology* **29**(12)**:** 3367-3378.

Robinson WH, Lepus CM, Wang Q, Raghu H, Mao R, Lindstrom TM*, et al.* (2016). Low-grade inflammation as a key mediator of the pathogenesis of osteoarthritis. *Nature reviews. Rheumatology* **12**(10)**:** 580-592.

Rodriguez Parkitna J, Korostynski M, Kaminska-Chowaniec D, Obara I, Mika J, Przewlocka B*, et al.* (2006). Comparison of gene expression profiles in neuropathic and inflammatory pain. *Journal of physiology and pharmacology : an official journal of the Polish Physiological Society* **57**(3)**:** 401-414.

Romero-Sandoval A, Chai N, Nutile-McMenemy N, Deleo JA (2008). A comparison of spinal Iba1 and GFAP expression in rodent models of acute and chronic pain. *Brain research* **1219:** 116-126.

Rosemann T, Backenstrass M, Joest K, Rosemann A, Szecsenyi J, Laux G (2007). Predictors of depression in a sample of 1,021 primary care patients with osteoarthritis. *Arthritis and rheumatism* **57**(3)**:** 415-422.

Rothwell NJ, Luheshi GN (2000). Interleukin 1 in the brain: biology, pathology and therapeutic target. *Trends Neurosci* **23**(12)**:** 618-625.

Ruparel S, Henry MA, Akopian A, Patil M, Zeldin DC, Roman L*, et al.* (2012). Plasticity of cytochrome P450 isozyme expression in rat trigeminal ganglia neurons during inflammation. *Pain* **153**(10)**:** 2031-2039.

Rush AM, Dib-Hajj SD, Liu S, Cummins TR, Black JA, Waxman SG (2006). A single sodium channel mutation produces hyper- or hypoexcitability in different types of neurons. *Proceedings of the National Academy of Sciences of the United States of America* **103**(21)**:** 8245-8250.

Sagar DR, Burston JJ, Hathway GJ, Woodhams SG, Pearson RG, Bennett AJ*, et al.* (2011). The contribution of spinal glial cells to chronic pain behaviour in the monosodium iodoacetate model of osteoarthritic pain. *Molecular pain* **7:** 88.

Sagar DR, Nwosu L, Walsh DA, Chapman V (2015). Dissecting the contribution of knee joint NGF to spinal nociceptive sensitization in a model of OA pain in the rat.

Osteoarthritis and cartilage / OARS, Osteoarthritis Research Society **23**(6)**:** 906-913.

Sagar DR, Staniaszek LE, Okine BN, Woodhams S, Norris LM, Pearson RG*, et al.* (2010). Tonic modulation of spinal hyperexcitability by the endocannabinoid receptor system in a rat model of osteoarthritis pain. *Arthritis and rheumatism* **62**(12)**:** 3666-3676.

Saito T, Hasegawa-Moriyama M, Kurimoto T, Yamada T, Inada E, Kanmura Y (2015). Resolution of Inflammation by Resolvin D1 Is Essential for Peroxisome Proliferator-activated Receptor-gamma-mediated Analgesia during Postincisional Pain Development in Type 2 Diabetes. *Anesthesiology* **123**(6)**:** 1420-1434.

Salo PT, Theriault E (1997). Number, distribution and neuropeptide content of rat knee joint afferents. *Journal of anatomy* **190 (Pt 4):** 515-522.

Samad TA, Moore KA, Sapirstein A, Billet S, Allchorne A, Poole S*, et al.* (2001). Interleukin-1beta-mediated induction of Cox-2 in the CNS contributes to inflammatory pain hypersensitivity. *Nature* **410**(6827)**:** 471-475.

Samad TA, Sapirstein A, Woolf CJ (2002). Prostanoids and pain: unraveling mechanisms and revealing therapeutic targets. *Trends in molecular medicine* **8**(8)**:** 390-396.

Sandkuhler J (2013). Spinal cord plasticity and pain. In: McMahon SB, Koltzenburg M, Tracey I, Turk DC (ed)^(eds). *Wall & Melzack's Textbook of Pain*, 6th edn: Elsevier/Saunders. p^pp 94-110.

Schafers M, Geis C, Svensson CI, Luo ZD, Sommer C (2003). Selective increase of tumour necrosis factor-alpha in injured and spared myelinated primary afferents after chronic constrictive injury of rat sciatic nerve. *The European journal of neuroscience* **17**(4)**:** 791-804.

Schaible HG, Ebersberger A, Natura G (2011). Update on peripheral mechanisms of pain: beyond prostaglandins and cytokines. *Arthritis research & therapy* **13**(2)**:** 210.

Schmittgen TD, Livak KJ (2008). Analyzing real-time PCR data by the comparative C(T) method. *Nature protocols* **3**(6)**:** 1101-1108.

Schuelert N, McDougall JJ (2009). Grading of monosodium iodoacetate-induced osteoarthritis reveals a concentration-dependent sensitization of nociceptors in the knee joint of the rat. *Neuroscience letters* **465**(2)**:** 184-188.

Schwab JM, Chiang N, Arita M, Serhan CN (2007). Resolvin E1 and protectin D1 activate inflammation-resolution programmes. *Nature* **447**(7146)**:** 869-874.

Seretny M, Currie GL, Sena ES, Ramnarine S, Grant R, MacLeod MR*, et al.* (2014). Incidence, prevalence, and predictors of chemotherapy-induced peripheral neuropathy: A systematic review and meta-analysis. *Pain* **155**(12)**:** 2461-2470.

Serhan CN (2014). Pro-resolving lipid mediators are leads for resolution physiology. *Nature* **510**(7503)**:** 92-101.

Serhan CN (2007). Resolution phase of inflammation: novel endogenous anti-inflammatory and proresolving lipid mediators and pathways. *Annual review of immunology* **25:** 101-137.

Serhan CN, Chiang N (2008a). Endogenous pro-resolving and anti-inflammatory lipid mediators: a new pharmacologic genus. *British journal of pharmacology* **153 Suppl 1:** S200-215.

Serhan CN, Chiang N, Van Dyke TE (2008b). Resolving inflammation: dual anti-inflammatory and pro-resolution lipid mediators. *Nature reviews. Immunology* **8**(5)**:** 349-361.

Serhan CN, Gotlinger K, Hong S, Arita M (2004). Resolvins, docosatrienes, and neuroprotectins, novel omega-3-derived mediators, and their aspirin-triggered endogenous epimers: an overview of their protective roles in catabasis. *Prostaglandins & other lipid mediators* **73**(3-4)**:** 155-172.

Serhan CN, Hong S, Gronert K, Colgan SP, Devchand PR, Mirick G*, et al.* (2002). Resolvins: a family of bioactive products of omega-3 fatty acid transformation circuits initiated by aspirin treatment that counter proinflammation signals. *The Journal of experimental medicine* **196**(8)**:** 1025-1037.

Serhan CN, Petasis NA (2011). Resolvins and protectins in inflammation resolution. *Chemical reviews* **111**(10)**:** 5922-5943.

Shiraishi M, Harris RA (2004). Effects of alcohols and anesthetics on recombinant voltage-gated Na+ channels. *The Journal of pharmacology and experimental therapeutics* **309**(3)**:** 987-994.

Siau C, Xiao W, Bennett GJ (2006). Paclitaxel- and vincristine-evoked painful peripheral neuropathies: loss of epidermal innervation and activation of Langerhans cells. *Exp Neurol* **201**(2)**:** 507-514.

Sisignano M, Angioni C, Park CK, Meyer Dos Santos S, Jordan H, Kuzikov M*, et al.* (2016). Targeting CYP2J to reduce paclitaxel-induced peripheral neuropathic pain. *Proceedings of the National Academy of Sciences of the United States of America* **113**(44)**:** 12544-12549.

Sisignano M, Baron R, Scholich K, Geisslinger G (2014). Mechanism-based treatment for chemotherapy-induced peripheral neuropathic pain. *Nature reviews. Neurology* **10**(12)**:** 694-707.

Smith HS (2009). Opioid metabolism. *Mayo Clinic proceedings* **84**(7)**:** 613-624.

Sokolove J, Lepus CM (2013). Role of inflammation in the pathogenesis of osteoarthritis: latest findings and interpretations. *Therapeutic advances in musculoskeletal disease* **5**(2)**:** 77-94.

Sostres C, Gargallo CJ, Lanas A (2013). Nonsteroidal anti-inflammatory drugs and upper and lower gastrointestinal mucosal damage. *Arthritis research & therapy* **15 Suppl 3:** S3.

Spiegelman BM (1998). PPAR-gamma: Adipogenic regulator and thiazolidinedione receptor. *Diabetes* **47**(4)**:** 507-514.

Spite M, Norling LV, Summers L, Yang R, Cooper D, Petasis NA*, et al.* (2009). Resolvin D2 is a potent regulator of leukocytes and controls microbial sepsis. *Nature* **461**(7268)**:** 1287-U1125.

Stanfa LC, Dickenson AH (2004). In vivo electrophysiology of dorsal-horn neurons. *Methods in molecular medicine* **99:** 139-153.

Stanfa LC, Sullivan AF, Dickenson AH (1992). Alterations in neuronal excitability and the potency of spinal mu, delta and kappa opioids after carrageenan-induced inflammation. *Pain* **50**(3)**:** 345-354.

Staniaszek LE An Investigation of Pain Mechanisms in a Model of Osteoarthritis: Modulation by the Endocannabinoid Receptor System. PhD, University of Nottingham, 2010.

Staniaszek LE, Norris LM, Kendall DA, Barrett DA, Chapman V (2010). Effects of COX-2 inhibition on spinal nociception: the role of endocannabinoids. *British journal of pharmacology* **160**(3)**:** 669-676.

Stellwagen D, Beattie EC, Seo JY, Malenka RC (2005). Differential regulation of AMPA receptor and GABA receptor trafficking by tumor necrosis factor-alpha. *The Journal of neuroscience : the official journal of the Society for Neuroscience* **25**(12)**:** 3219-3228.

Stenfeldt AL, Karlsson J, Wenneras C, Bylund J, Fu H, Dahlgren C (2007). Cyclosporin H, Boc-MLF and Boc-FLFLF are antagonists that preferentially inhibit activity triggered through the formyl peptide receptor. *Inflammation* **30**(6)**:** 224-229.

Story GM, Peier AM, Reeve AJ, Eid SR, Mosbacher J, Hricik TR*, et al.* (2003). ANKTM1, a TRP-like channel expressed in nociceptive neurons, is activated by cold temperatures. *Cell* **112**(6)**:** 819-829.

Su L, Wang C, Yu YH, Ren YY, Xie KL, Wang GL (2011). Role of TRPM8 in dorsal root ganglion in nerve injury-induced chronic pain. *BMC neuroscience* **12:** 120.

Sun JL, Xiao C, Lu B, Zhang J, Yuan XZ, Chen W*, et al.* (2013). CX3CL1/CX3CR1 regulates nerve injury-induced pain hypersensitivity through the ERK5 signaling pathway. *Journal of neuroscience research* **91**(4)**:** 545-553.

Sun YP, Oh SF, Uddin J, Yang R, Gotlinger K, Campbell E*, et al.* (2007). Resolvin D1 and its aspirin-triggered 17R epimer. Stereochemical assignments, anti-inflammatory properties, and enzymatic inactivation. *The Journal of biological chemistry* **282**(13)**:** 9323-9334.

Sung B, Lim G, Mao J (2003). Altered expression and uptake activity of spinal glutamate transporters after nerve injury contribute to the pathogenesis of neuropathic pain in rats. *The Journal of neuroscience : the official journal of the Society for Neuroscience* **23**(7)**:** 2899-2910.

Suri S, Gill SE, de Camin SM, Wilson D, McWilliams DF, Walsh DA (2007). Neurovascular invasion at the osteochondral junction and in osteophytes in osteoarthritis. *Annals of the rheumatic diseases* **66**(11)**:** 1423-1428.

Suzuki R, Chapman V, Dickenson AH (1999). The effectiveness of spinal and systemic morphine on rat dorsal horn neuronal responses in the spinal nerve ligation model of neuropathic pain. *Pain* **80**(1-2)**:** 215-228.

Svensson CI, Marsala M, Westerlund A, Calcutt NA, Campana WM, Freshwater JD*, et al.* (2003). Activation of p38 mitogen-activated protein kinase in spinal microglia is a critical link in inflammation-induced spinal pain processing. *Journal of neurochemistry* **86**(6)**:** 1534-1544.

Svensson CI, Zattoni M, Serhan CN (2007). Lipoxins and aspirin-triggered lipoxin inhibit inflammatory pain processing. *The Journal of experimental medicine* **204**(2)**:** 245-252.

Tai H-H, Ensor CM, Tong M, Zhou H, Yan F (2002). Prostaglandin catabolizing enzymes. *Prostaglandins & other lipid mediators* **68:** 483-493.

Tamura S, Morikawa Y, Senba E (2005). TRPV2, a capsaicin receptor homologue, is expressed predominantly in the neurotrophin-3-dependent subpopulation of primary sensory neurons. *Neuroscience* **130**(1)**:** 223-228.

Tang NK, Wright KJ, Salkovskis PM (2007). Prevalence and correlates of clinical insomnia co-occurring with chronic back pain. *Journal of sleep research* **16**(1)**:** 85-95.

Tawfik VL, DeLeo JA (2009). The role of astrocytes in the modulation of pain. In: Malcangio M (ed)^(eds). *Synaptic Plasticity in Pain*, edn: Sptinger. p^pp 387-402.

Tegeder I, Niederberger E, Schmidt R, Kunz S, Guhring H, Ritzeler O*, et al.* (2004). Specific Inhibition of IkappaB kinase reduces hyperalgesia in inflammatory and neuropathic pain models in rats. *The Journal of neuroscience : the official journal of the Society for Neuroscience* **24**(7)**:** 1637-1645.

Terashima Y, Kawamata M, Takebayashi T, Tanaka S, Tanimoto K, Yamashita T (2011). Changes in synaptic transmission of substantia gelatinosa neurons in a rat model of lumbar radicular pain revealed by in vivo patch-clamp recording. *Pain* **152**(5)**:** 1024-1032.

Thacker MA, Clark AK, Bishop T, Grist J, Yip PK, Moon LD*, et al.* (2009). CCL2 is a key mediator of microglia activation in neuropathic pain states. *European journal of pain* **13**(3)**:** 263-272.

Thakur M, Rahman W, Hobbs C, Dickenson AH, Bennett DL (2012). Characterisation of a peripheral neuropathic component of the rat monoiodoacetate model of osteoarthritis. *PloS one* **7**(3)**:** e33730.

Todd AJ, Koerber HR (2013). Neuroanatomical substrates of spinnal nociception. In: McMahon SB, Koltzenburg M, Tracey I, Turk DC (ed)^(eds). *Wall & Melzack's Textbook of Pain*, 6th edn: Elsevier/Saunders. p^pp 77-93.

Todd AJ, Watt C, Spike RC, Sieghart W (1996). Colocalization of GABA, glycine, and their receptors at synapses in the rat spinal cord. *The Journal of neuroscience : the official journal of the Society for Neuroscience* **16**(3)**:** 974-982.

Tominaga M, Caterina MJ (2004). Thermosensation and pain. *Journal of neurobiology* **61**(1)**:** 3-12.

Tominaga M, Caterina MJ, Malmberg AB, Rosen TA, Gilbert H, Skinner K*, et al.* (1998). The cloned capsaicin receptor integrates multiple pain-producing stimuli. *Neuron* **21**(3)**:** 531-543.

Torebjork HE, Lundberg LE, LaMotte RH (1992). Central changes in processing of mechanoreceptive input in capsaicin-induced secondary hyperalgesia in humans. *The Journal of physiology* **448:** 765-780.

Tran-Van-Minh A, Dolphin AC (2010). The alpha2delta ligand gabapentin inhibits the Rab11-dependent recycling of the calcium channel subunit alpha2delta-2. *The Journal of neuroscience : the official journal of the Society for Neuroscience* **30**(38)**:** 12856-12867.

Trang T, McNaull B, Quirion R, Jhamandas K (2004). Involvement of spinal lipoxygenase metabolites in hyperalgesia and opioid tolerance. *European journal of pharmacology* **491**(1)**:** 21-30.

Treede RD, Meyer RA, Raja SN, Campbell JN (1995). Evidence for two different heat transduction mechanisms in nociceptive primary afferents innervating monkey skin. *The Journal of physiology* **483 (Pt 3):** 747-758.

Treede RD, Meyer RA, Raja SN, Campbell JN (1992). Peripheral and central mechanisms of cutaneous hyperalgesia. *Prog Neurobiol* **38**(4)**:** 397-421.

Tsantoulas C, McMahon SB (2014a). Opening paths to novel analgesics: the role of potassium channels in chronic pain. *Trends Neurosci* **37**(3)**:** 146-158.

Tsantoulas C, Zhu L, Shaifta Y, Grist J, Ward JP, Raouf R*, et al.* (2012). Sensory neuron downregulation of the Kv9.1 potassium channel subunit mediates neuropathic pain following nerve injury. *The Journal of neuroscience : the official journal of the Society for Neuroscience* **32**(48)**:** 17502-17513.

Tsantoulas C, Zhu L, Yip P, Grist J, Michael GJ, McMahon SB (2014b). Kv2 dysfunction after peripheral axotomy enhances sensory neuron responsiveness to sustained input. *Exp Neurol* **251:** 115-126.

Tsujino H, Kondo E, Fukuoka T, Dai Y, Tokunaga A, Miki K*, et al.* (2000). Activating transcription factor 3 (ATF3) induction by axotomy in sensory and motoneurons: A novel neuronal marker of nerve injury. *Molecular and cellular neurosciences* **15**(2)**:** 170-182.

Uceyler N, Schafers M, Sommer C (2009). Mode of action of cytokines on nociceptive neurons. *Experimental brain research* **196**(1)**:** 67-78.

Ugawa S, Ueda T, Yamamura H, Shimada S (2005). In situ hybridization evidence for the coexistence of ASIC and TRPV1 within rat single sensory neurons. *Brain research. Molecular brain research* **136**(1-2)**:** 125-133.

Urban L, Thompson SW, Dray A (1994). Modulation of spinal excitability: co-operation between neurokinin and excitatory amino acid neurotransmitters. *Trends Neurosci* **17**(10)**:** 432-438.

Urch CE, Dickenson AH (2003). In vivo single unit extracellular recordings from spinal cord neurones of rats. *Brain research. Brain research protocols* **12**(1)**:** 26-34.

Uren RT, Turbic A, Wong AW, Klein R, Murray SS, Turnley AM (2014). A novel role of suppressor of cytokine signaling-2 in the regulation of TrkA neurotrophin receptor biology. *Journal of neurochemistry* **129**(4)**:** 614-627.

Valdes AM, Ravipati S, Menni C, Abhishek A, Metrustry S, Harris J*, et al.* (2017). Association of the resolvin precursor 17-HDHA, but not D- or E- series resolvins, with heat pain sensitivity and osteoarthritis pain in humans. *Scientific reports* **7**(1)**:** 10748.

Van Steenwinckel J, Reaux-Le Goazigo A, Pommier B, Mauborgne A, Dansereau MA, Kitabgi P*, et al.* (2011). CCL2 released from neuronal synaptic vesicles in the spinal cord is a major mediator of local inflammation and pain after peripheral nerve injury. *The Journal of neuroscience : the official journal of the Society for Neuroscience* **31**(15)**:** 5865-5875.

Vandesompele J, De Preter K, Pattyn F, Poppe B, Van Roy N, De Paepe A*, et al.* (2002). Accurate normalization of real-time quantitative RT-PCR data by geometric averaging of multiple internal control genes. *Genome biology* **3**(7)**:** RESEARCH0034.

Vardeh D, Wang D, Costigan M, Lazarus M, Saper CB, Woolf CJ*, et al.* (2009). COX2 in CNS neural cells mediates mechanical inflammatory pain hypersensitivity in mice. *The Journal of clinical investigation* **119**(2)**:** 287-294.

Verge GM, Milligan ED, Maier SF, Watkins LR, Naeve GS, Foster AC (2004). Fractalkine (CX3CL1) and fractalkine receptor (CX3CR1) distribution in spinal cord and dorsal root ganglia under basal and neuropathic pain conditions. *The European journal of neuroscience* **20**(5)**:** 1150-1160.

Vogel C, Stallforth S, Sommer C (2006). Altered pain behavior and regeneration after nerve injury in TNF receptor deficient mice. *Journal of the peripheral nervous system : JPNS* **11**(4)**:** 294-303.

Walder RY, Wattiez AS, White SR, Marquez de Prado B, Hamity MV, Hammond DL (2014). Validation of four reference genes for quantitative mRNA expression studies in a rat model of inflammatory injury. *Molecular pain* **10:** 55.

Walther A, Riehemann K, Gerke V (2000). A novel ligand of the formyl peptide receptor: annexin I regulates neutrophil extravasation by interacting with the FPR. *Molecular cell* **5**(5)**:** 831-840.

Wang H, Sun H, Della Penna K, Benz RJ, Xu J, Gerhold DL*, et al.* (2002). Chronic neuropathic pain is accompanied by global changes in gene expression and shares pathobiology with neurodegenerative diseases. *Neuroscience* **114**(3)**:** 529-546.

Wang L, Yuan R, Yao C, Wu Q, Christelle M, Xie W*, et al.* (2014a). Effects of resolvin D1 on inflammatory responses and oxidative stress of lipopolysaccharide-induced acute lung injury in mice. *Chinese medical journal* **127**(5)**:** 803-809.

Wang S, Dai Y, Fukuoka T, Yamanaka H, Kobayashi K, Obata K*, et al.* (2008). Phospholipase C and protein kinase A mediate bradykinin sensitization of TRPA1: a molecular mechanism of inflammatory pain. *Brain : a journal of neurology* **131**(Pt 5)**:** 1241-1251.

Wang W, Gu J, Li YQ, Tao YX (2011). Are voltage-gated sodium channels on the dorsal root ganglion involved in the development of neuropathic pain? *Molecular pain* **7:** 16.

Wang ZF, Li Q, Liu SB, Mi WL, Hu S, Zhao J*, et al.* (2014b). Aspirin-triggered Lipoxin A4 attenuates mechanical allodynia in association with inhibiting spinal JAK2/STAT3 signaling in neuropathic pain in rats. *Neuroscience* **273:** 65-78.

Waxman SG, Zamponi GW (2014). Regulating excitability of peripheral afferents: emerging ion channel targets. *Nature neuroscience* **17**(2)**:** 153-163.

Weibel R, Reiss D, Karchewski L, Gardon O, Matifas A, Filliol D*, et al.* (2013). Mu opioid receptors on primary afferent nav1.8 neurons contribute to opiate-induced analgesia: insight from conditional knockout mice. *PloS one* **8**(9)**:** e74706.

Wemmie JA, Taugher RJ, Kreple CJ (2013). Acid-sensing ion channels in pain and disease. *Nature reviews. Neuroscience* **14**(7)**:** 461-471.

Wen X, Li Y, Liu Y (2010). Opposite action of peroxisome proliferator-activated receptor-gamma in regulating renal inflammation: functional switch by its ligand. *The Journal of biological chemistry* **285**(39)**:** 29981-29988.

West SJ, Bannister K, Dickenson AH, Bennett DL (2015). Circuitry and plasticity of the dorsal horn - Toward a better understanding of neuropathic pain. *Neuroscience*.

White FA, Bhangoo SK, Miller RJ (2005). Chemokines: integrators of pain and inflammation. *Nature reviews. Drug discovery* **4**(10)**:** 834-844.

Wigerblad G, Bas DB, Fernades-Cerqueira C, Krishnamurthy A, Nandakumar KS, Rogoz K*, et al.* (2016). Autoantibodies to citrullinated proteins induce joint pain independent of inflammation via a chemokine-dependent mechanism. *Annals of the rheumatic diseases* **75**(4)**:** 730-738.

Wigerblad G, Huie JR, Yin HZ, Leinders M, Pritchard RA, Koehrn FJ*, et al.* (2017). Inflammation-induced GluA1 trafficking and membrane insertion of Ca2+ permeable

AMPA receptors in dorsal horn neurons is dependent on spinal tumor necrosis factor, PI3 kinase and protein kinase A. *Exp Neurol* **293:** 144-158.

Williams JT, Ingram SL, Henderson G, Chavkin C, von Zastrow M, Schulz S*, et al.* (2013). Regulation of mu-opioid receptors: desensitization, phosphorylation, internalization, and tolerance. *Pharmacological reviews* **65**(1)**:** 223-254.

Wong A, Sagar DR, Ortori CA, Kendall DA, Chapman V, Barrett DA (2014). Simultaneous tissue profiling of eicosanoid and endocannabinoid lipid families in a rat model of osteoarthritis. *Journal of lipid research* **55**(9)**:** 1902-1913.

Wood JN, Boorman JP, Okuse K, Baker MD (2004). Voltage-gated sodium channels and pain pathways. *Journal of neurobiology* **61**(1)**:** 55-71.

Woolf AD, Pfleger B (2003). Burden of major musculoskeletal conditions. *Bulletin of the World Health Organization* **81**(9)**:** 646-656.

Woolf CJ (2011). Central sensitization: implications for the diagnosis and treatment of pain. *Pain* **152**(3 Suppl)**:** S2-15.

Xia Z, Xiao Y, Wu Y, Zhao B (2016). Sodium channel Nav1.7 expression is upregulated in the dorsal root ganglia in a rat model of paclitaxel-induced peripheral neuropathy. *SpringerPlus* **5**(1)**:** 1738.

Xiang Z, Bo X, Burnstock G (1998). Localization of ATP-gated P2X receptor immunoreactivity in rat sensory and sympathetic ganglia. *Neuroscience letters* **256**(2)**:** 105-108.

Xiao W, Boroujerdi A, Bennett GJ, Luo ZD (2007). Chemotherapy-evoked painful peripheral neuropathy: analgesic effects of gabapentin and effects on expression of the alpha-2-delta type-1 calcium channel subunit. *Neuroscience* **144**(2)**:** 714-720.

Xie JD, Chen SR, Chen H, Zeng WA, Pan HL (2016). Presynaptic N-Methyl-d-aspartate (NMDA) Receptor Activity Is Increased Through Protein Kinase C in Paclitaxel-induced Neuropathic Pain. *The Journal of biological chemistry* **291**(37)**:** 19364-19373.

Xing H, Chen M, Ling J, Tan W, Gu JG (2007). TRPM8 mechanism of cold allodynia after chronic nerve injury. *The Journal of neuroscience : the official journal of the Society for Neuroscience* **27**(50)**:** 13680-13690.

Xu JT, Xin WJ, Zang Y, Wu CY, Liu XG (2006). The role of tumor necrosis factor-alpha in the neuropathic pain induced by Lumbar 5 ventral root transection in rat. *Pain* **123**(3)**:** 306-321.

Xu M, Kim CJ, Neubert MJ, Heinricher MM (2007). NMDA receptor-mediated activation of medullary pro-nociceptive neurons is required for secondary thermal hyperalgesia. *Pain* **127**(3)**:** 253-262.

Xu ZZ, Berta T, Ji RR (2013). Resolvin E1 inhibits neuropathic pain and spinal cord microglial activation following peripheral nerve injury. *Journal of neuroimmune pharmacology : the official journal of the Society on NeuroImmune Pharmacology* **8**(1)**:** 37-41.

Xu ZZ, Kim YH, Bang S, Zhang Y, Berta T, Wang F*, et al.* (2015). Inhibition of mechanical allodynia in neuropathic pain by TLR5-mediated A-fiber blockade. *Nature medicine* **21**(11)**:** 1326-1331.

Xu ZZ, Zhang L, Liu T, Park JY, Berta T, Yang R*, et al.* (2010). Resolvins RvE1 and RvD1 attenuate inflammatory pain via central and peripheral actions. *Nature medicine* **16**(5)**:** 592-597, 591p following 597.

Xue ZJ, Shen L, Wang ZY, Hui SY, Huang YG, Ma C (2014). STAT3 inhibitor WP1066 as a novel therapeutic agent for bCCI neuropathic pain rats. *Brain research* **1583:** 79-88.

Yaksh TL, Fisher CJ, Hockman TM, Wiese AJ (2017). Current and Future Issues in the Development of Spinal Agents for the Management of Pain. *Current neuropharmacology* **15**(2)**:** 232-259.

Yamamoto J, Kawamata T, Niiyama Y, Omote K, Namiki A (2008). Down-regulation of mu opioid receptor expression within distinct subpopulations of dorsal root ganglion neurons in a murine model of bone cancer pain. *Neuroscience* **151**(3)**:** 843-853.

Yan M, Rerko RM, Platzer P, Dawson D, Willis J, Tong M*, et al.* (2004). 15-Hydroxyprostaglandin dehydrogenase, a COX-2 oncogene antagonist, is a TGF-beta-induced suppressor of human gastrointestinal cancers. *Proceedings of the National Academy of Sciences of the United States of America* **101**(50)**:** 17468-17473.

Yan X, Maixner DW, Yadav R, Gao M, Li P, Bartlett MG*, et al.* (2015). Paclitaxel induces acute pain via directly activating toll like receptor 4. *Molecular pain* **11:** 10.

Yang T, Yang P, Jiang LM, Zhou RY (2015). Activation of spinal NF-kappa B mediates pain behavior induced by plantar incision. *International journal of clinical and experimental medicine* **8**(6)**:** 9149-9155.

Yang Y, Wang Y, Li S, Xu Z, Li H, Ma L*, et al.* (2004). Mutations in SCN9A, encoding a sodium channel alpha subunit, in patients with primary erythermalgia. *Journal of medical genetics* **41**(3)**:** 171-174.

Ydens E, Cauwels A, Asselbergh B, Goethals S, Peeraer L, Lornet G*, et al.* (2012). Acute injury in the peripheral nervous system triggers an alternative macrophage response. *Journal of neuroinflammation* **9:** 176.

Ye RD, Boulay F, Wang JM, Dahlgren C, Gerard C, Parmentier M*, et al.* (2009). International Union of Basic and Clinical Pharmacology. LXXIII. Nomenclature for the formyl peptide receptor (FPR) family. *Pharmacological reviews* **61**(2)**:** 119-161.

Yeomans DC, Proudfit HK (1994). Characterization of the foot withdrawal response to noxious radiant heat in the rat. *Pain* **59**(1)**:** 85-94.

Yoshimura A, Naka T, Kubo M (2007). SOCS proteins, cytokine signalling and immune regulation. *Nature reviews. Immunology* **7**(6)**:** 454-465.

Yu Y, Fuscoe JC, Zhao C, Guo C, Jia M, Qing T*, et al.* (2014). A rat RNA-Seq transcriptomic BodyMap across 11 organs and 4 developmental stages. *Nature communications* **5:** 3230.

Yukhananov R, Kissin I (2008). Persistent changes in spinal cord gene expression after recovery from inflammatory hyperalgesia: a preliminary study on pain memory. *BMC neuroscience* **9:** 32.

Zhang H, Dougherty PM (2014). Enhanced excitability of primary sensory neurons and altered gene expression of neuronal ion channels in dorsal root ganglion in paclitaxel-induced peripheral neuropathy. *Anesthesiology* **120**(6)**:** 1463-1475.

Zhang H, Li F, Li WW, Stary C, Clark JD, Xu S*, et al.* (2016a). The inflammasome as a target for pain therapy. *British journal of anaesthesia* **117**(6)**:** 693-707.

Zhang H, Li Y, de Carvalho-Barbosa M, Kavelaars A, Heijnen CJ, Albrecht PJ*, et al.* (2016b). Dorsal Root Ganglion Infiltration by Macrophages Contributes to Paclitaxel

Chemotherapy-Induced Peripheral Neuropathy. *The journal of pain : official journal of the American Pain Society* **17**(7)**:** 775-786.

Zhang H, Yoon SY, Zhang H, Dougherty PM (2012). Evidence that spinal astrocytes but not microglia contribute to the pathogenesis of Paclitaxel-induced painful neuropathy. *The journal of pain : official journal of the American Pain Society* **13**(3)**:** 293-303.

Zhang L, Berta T, Xu ZZ, Liu T, Park JY, Ji RR (2011). TNF-alpha contributes to spinal cord synaptic plasticity and inflammatory pain: distinct role of TNF receptor subtypes 1 and 2. *Pain* **152**(2)**:** 419-427.

Zhang RX, Liu B, Wang L, Ren K, Qiao JT, Berman BM*, et al.* (2005). Spinal glial activation in a new rat model of bone cancer pain produced by prostate cancer cell inoculation of the tibia. *Pain* **118**(1-2)**:** 125-136.

Zhang RX, Ren K, Dubner R (2013a). Osteoarthritis pain mechanisms: basic studies in animal models. *Osteoarthritis and Cartilage* **21**(9)**:** 1308-1315.

Zhang W, Doherty M, Peat G, Bierma-Zeinstra MA, Arden NK, Bresnihan B*, et al.* (2010). EULAR evidence-based recommendations for the diagnosis of knee osteoarthritis. *Annals of the rheumatic diseases* **69**(3)**:** 483-489.

Zhang W, Jones A, Doherty M (2004). Does paracetamol (acetaminophen) reduce the pain of osteoarthritis? A meta-analysis of randomised controlled trials. *Annals of the rheumatic diseases* **63**(8)**:** 901-907.

Zhang W, Moskowitz RW, Nuki G, Abramson S, Altman RD, Arden N*, et al.* (2008). OARSI recommendations for the management of hip and knee osteoarthritis, Part II: OARSI evidence-based, expert consensus guidelines. *Osteoarthritis and Cartilage* **16**(2)**:** 137-162.

Zhang ZJ, Cao DL, Zhang X, Ji RR, Gao YJ (2013b). Chemokine contribution to neuropathic pain: respective induction of CXCL1 and CXCR2 in spinal cord astrocytes and neurons. *Pain* **154**(10)**:** 2185-2197.

Zheng FY, Xiao WH, Bennett GJ (2011). The Response of Spinal Microglia to Chemotherapy-Evoked Painful Peripheral Neuropathies Is Distinct from That Evoked by Traumatic Nerve Injuries. *Neuroscience* **176:** 447-454.

Zhou Y, Suzuki Y, Uchida K, Tominaga M (2013). Identification of a splice variant of mouse TRPA1 that regulates TRPA1 activity. *Nature communications* **4:** 2399.

Zhou Z, Peng X, Hao S, Fink DJ, Mata M (2008). HSV-mediated transfer of interleukin-10 reduces inflammatory pain through modulation of membrane tumor necrosis factor alpha in spinal cord microglia. *Gene therapy* **15**(3)**:** 183-190.

Zhu C, Tang J, Ding T, Chen L, Wang W, Mei XP*, et al.* (2017). Neuron-restrictive silencer factor-mediated downregulation of mu-opioid receptor contributes to the reduced morphine analgesia in bone cancer pain. *Pain* **158**(5)**:** 879-890.

Zhuang ZY, Gerner P, Woolf CJ, Ji RR (2005). ERK is sequentially activated in neurons, microglia, and astrocytes by spinal nerve ligation and contributes to mechanical allodynia in this neuropathic pain model. *Pain* **114**(1-2)**:** 149-159.

Zimmermann M (1983). Ethical guidelines for investigations of experimental pain in conscious animals. *Pain* **16**(2)**:** 109-110.

Zinn S, Sisignano M, Kern K, Pierre S, Tunaru S, Jordan H*, et al.* (2017). The leukotriene B4 receptors BLT1 and BLT2 form an antagonistic sensitizing system in

peripheral sensory neurons. *The Journal of biological chemistry* **292**(15)**:** 6123-6134.